The detection and characterisation of novel alkyl spin-adducts of PBN and its derivatives using capillary gas chromatography coupled to electron-ionisation mass spectrometry

Mudaser Zafar

Submitted in partial fulfilment of the requirements of the degree of Doctor of Philosophy

September 2021

Contents

List of Figures

List of Tables

Acknowledgements

This PhD would not have been possible without the support of many people and I am strongly indebted to each and every one of them. First and foremost, a big thankyou to my supervisor Dr Ian Podmore. Over the past 4 years you have been a source of ideas, encouragement, support, and guidance. I also pay my gratitude to academic staff and fellow PhD students for their support.

To my family and extended family my gratitude to you extends well beyond the time of this PhD. My mother and father who have stood by me and believed in me and I am forever indebted to you for giving me the opportunities and experiences that have made me who I am. My brother and sisters, I express my sincerest gratitude to you for your continuous and unparalleled love, help and support. My wife and two sons, Huzayfah and Hashim, who provide me with the inspiration to strive and work harder. I love you. This is for you all.

And above all, to the Almighty, I glorify and praise you for the blessings you have bestowed upon me.

Declaration

This thesis is the result of research carried under the supervision of Dr Ian Podmore at the school of environmental and life sciences at the university of Salford.

Except where acknowledged in the customary manner, the material presented in this thesis is to the best of my knowledge, original and has not been submitted in whole or part for a degree in any university

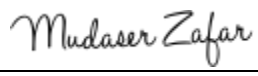

Mudaser Zafar

Abbreviations

4-HNE	4-hydroxynonenal
8-OH-dG	8-hydroxy-7,8-dihydro-2' deoxyguanosine
AD	Alzheimer's disease
CE	Capillary electrophoresis
CL	Chemiluminescence
ESR	Electron spin resonance
EI	Electron ionization
ERO-1	Endoplasmic reticulum oxidoreductin-1
FFA	Free fatty acids
GC	Gas chromatography
GPx	Glutathione peroxidase
GSH	Glutathione
HPLC-ED	High-performance liquid chromatography electro-chemical detection
HPLC-MS	High-performance liquid chromatography mass spectrometry
PBN	N-tert-butyl-a-phenyl nitrone
MDD	Major depressive disorder
MS	Mass spectrometry
m/z	Mass to charge ratio
CSP	Non-racemic chiral stationary phase
NAFLD	Non-alcoholic fatty liver disease
PMT	Photomultiplier tube
PUFAs	Polyunsaturated fatty acids
PDI	Protein disulphide isomerases
RNS	Reactive nitrogen species
ROS	Reactive oxygen species
RA	Rheumatoid arthritis
rt	Retention time (minutes)
SOD	Superoxide dismutase
tBu	Tertiary butyl

Abstract

Free radical induced oxidative stress has been reported to be involved in several diseases such as diabetes mellitus, neurodegenerative disorders, cardiovascular diseases (atherosclerosis and hypertension), respiratory diseases (asthma), cataract development, rheumatoid arthritis and in various cancers (colorectal, prostate, breast, lung, bladder cancers). Aldehydes are strong electrophilic compounds with terminal carbonyl groups making them highly reactive. Aldehydes may react with hydroxyl radicals forming radicals which, in turn, react with cellular components. Hydroxyl free radicals were generated by Fenton-based chemistry and reacted with aliphatic aldehydes to produce secondary radicals in the presence of the spin-trapping agent N-tert-butyl-a-phenylnitrone (PBN). Novel aldehyde related radicals were produced via Fenton chemistry and trapped using PBN to form stable adducts that could be analysed via the combined techniques of gas chromatography (GC) and mass spectrometry (MS). The significant findings of this work involve trapping various radicals such as propyl radicals, 2-methyl propyl radicals, butanal radicals (oxoallylic radicals), 2-methyl butanal radicals and methyl radicals in various conformations with PBN and its derivatives and elucidating the fragmentation patterns. The findings have been supported using deuterated isotopologues and PBN derivatives to aid in the understanding of the reaction mechanisms and structures.

1 Introduction

M: "Too many free radicals. That's your problem."

James Bond: "Free radicals, sir?"

M: "Yes. They're toxins that destroy the body and the brain. Caused by eating too much red meat and white bread, and too many dry martinis."

James Bond: "Then I shall cut out the white bread, sir."

Never Say Never Again (1983)

1.1 Free radicals

Free radicals can be described as any molecular species capable of independent existence that contain an unpaired electron in an atomic orbital (Lobo *et al*., 2010). The reactive species are either reactive oxygen species (ROS) or to a lesser extent reactive nitrogen species (RNS) and both groups can be subdivided into either radical or non-radical entities (Phaniendra *et al*., 2015). The sources can be exogenous as well as endogenous. Table 1.1 shows a list of possible reactive species formed during metabolism.

Free radicals play a profound role in many biochemical reactions and are generated in a wide variety of chemical and biological systems. The predominant method for formation of a free radical is through the homolytic cleavage of a covalent bond where one bonding electron is retained on each atomic of molecular fragment. Figure 1.1.1 shows how a radical is formed via homolytic cleavage. In a living organism, free radicals are the products of normal cellular metabolism. A free radical can be defined as an atom or molecule containing one or more unpaired electron in valency shell or outer orbit, which is capable of independent existence. This leads to it being unstable, short-lived, and highly reactive. The highly reactive nature leads to other compounds having their odd electrons removed to attain stability. Thus, the attacked molecule itself becomes a free radical after losing an electron, beginning a chain reaction cascade that eventually damages the cell (Phaniendra *et al*., 2015). To a physical organic chemist the naming of a free radical is typically derived by adding the *–yl* suffix to the corresponding even electron molecule for example, the removal of an electron from a hydroxide anion (HO^-) produces an oxygen centred hydroxyl radical ($HO^{\bullet}$), or the removal of an electron from the simplest carbon-centred molecule (methane) produces radical ($^{\bullet}CH_3$) (Lachlan, 2014).

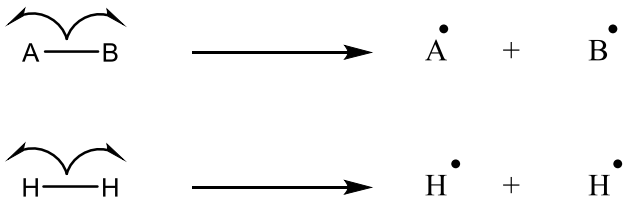

Figure 1.1.1 Homolytic cleavage of a bond is described using "fishhook" arrows which indicate the movement of a single electron. The homolysis of hydrogen (H_2) yield two hydrogen atom radicals.

Radical reactions have three stages which include initiation, propagation, and termination. Radical behaviour is dominated by their high reactivity and electron-deficient character and they often will react with the closest available atom, which can involve a reaction with σ bond or π bond. A very common

radical reaction is the abstraction of hydrogen from a C-H σ bond, producing a new radical species, leading to the propagation of the reaction (Figure 1.1.2, A). Another important reaction is the addition to a π bond forming a new C-C bond (Figure 1.1.2, B), and sometimes two radicals will "neutralise" one another by combining to form a new bond terminating the chain as the product of this reaction is no longer a radical (see Figure 1.1.2, C).

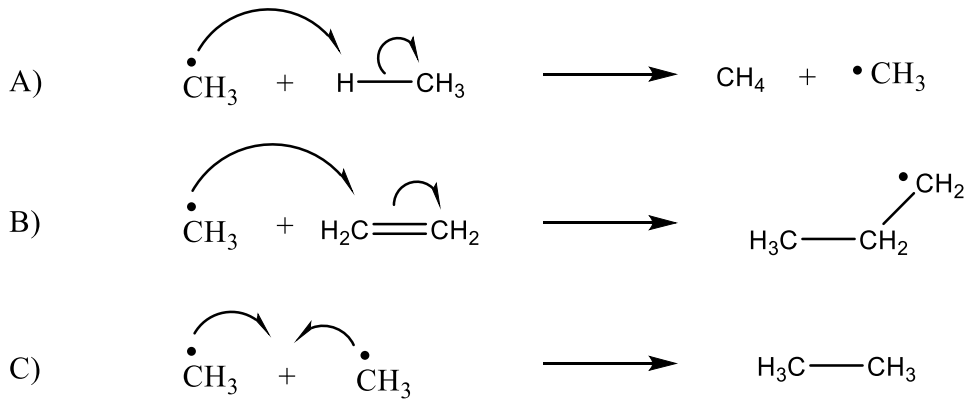

Figure 1.1.2 Radical reactions demonstrating A) breaking the C-H σ bond, B) adding to a π bond and C) terminating with another radical forming a new σ bond.

Reactive species are constantly generated in the human body. Some via accidents such as the leakage of electrons directly onto O_2 from the electron carriers of the mitochondrial electron transport chain generating superoxide $O_2^{\bullet-}$ and other via exposure of living organisms to ionising radiation splitting the O-H bond in water to form $OH^{\bullet}$ and $H^{\bullet}$. This can then lead to harmful consequences via the $OH^{\bullet}$ attacking proteins, DNA and lipids. $NO^{\bullet}$ was initially discovered in 1980 as a vasodilating substance secreted by the endothelium and is naturally synthesised by vascular endothelial cells and phagocytes. It helps regulate blood pressure and control inflammation and may be involved in killing microorganisms by macrophages (Halliwell, 2015).

Free radicals generate chain reactions which can lead to direct destruction of the cell membrane where, depending upon the location, it can lead to various conditions for example cirrhosis caused by hemochromatosis where free iron builds up and via the Fenton reaction can produce hydroxyl radicals. The Fenton system generates hydroxyl radicals which can be damaging to practically every type of biomolecule including carbohydrates, lipids, amino acids, and nucleic acids. This causes detrimental

effects to the constituents of the cell leading to organ failure and eventually death. Hydroxyl radicals have relatively short half-lives (10^{-16} s) making them very difficult to detect (Phaniendra *et al*., 2015).

Table 1.1 List of ROS and RNS produced during metabolism (adopted from Phaniendra *et al*., 2015)

Free Radical	**Symbol**
Reactive oxygen species -ROS	
Radicals	
Superoxide	$O_2^{\bullet-}$
Hydroxyl	$OH^{\bullet}$
Alkoxy radical	$RO^{\bullet}$
Peroxy radical	$ROO^{\bullet}$
Non radicals	
Hydrogen peroxide	H_2O_2
Singlet oxygen	$^1O_2$
Ozone	O_3
Organic peroxide	ROOH
Hypochrolous acid	HOCl
Hypobromous acid	HOBr
Reactive Nitrogen Species	
Radicals	
Nitric oxide	$NO^{\bullet}$
Nitrogen dioxide	$NO_2^{\bullet}$
Non radicals	
Peroxynitrite	$ONOO^-$
Nitrosyl cation	NO^+
Nitrosyl anion	NO^-
Dinitrogen trioxide	N_2O_3
Dinitrogen tetroxide	N_2O_4
Nitrous acid	HNO_2
Peroxynitrous acid	ONOOH
Nitryl chloride	NO_2Cl

1.2 Oxidative stress/nitrosative stress

The term oxidative stress is ambiguously defined however in essence is related to an excess of pro-oxidative factors and reactive oxygen species (ROS), over antioxidants. Carbohydrates, lipids, proteins, and DNA can all be oxidised and damaged as a result of this imbalance.

Oxidative stress can result from increased production of reactive species via the exposure of cells to increased levels of O_2 or to other toxins that are themselves reactive species ($NO^{\bullet}$) or metabolized generating a radical (paraquat) or via the overactivation of natural systems like the immune system. Oxidative stress can result from diminished levels of antioxidants for example the deficiency of dietary minerals (Zn^{2+},Mg^{2+},Fe^{2+},Cu^{2+}, Se) and antioxidants, a mutation affecting the activity of defence enzymes or glutathione peroxidase or toxins that deplete antioxidant levels (Halliwell and Whiteman, 2004). One important issue in free radical research is the need for accurate measurement, identification and quantification of oxidative stress (Calenic *et al*., 2015).

1.3 Sources of free radicals

ROS can be produced either endogenously or from exogenous sources. Endogenous sources of ROS can include different cellular organs such as mitochondria (cytochrome C oxidase, the electron transport chain), peroxisomes (peroxisomal oxidases) and endoplasmic reticulum, sites where oxygen consumption is high, iron ions, lipoxygenases, xanthine oxidase, cytochrome P450, cyclooxygenases, and NADPH oxidases. Many ROS are generated in the mitochondria on the electron transport chain where electrons are fed into NADH dehydrogenase (complex I) and ubiquinone cytochrome C reductase (complex II) and subsequently transferred to complex III and finally to cytochrome c oxidase (complex IV) forming water as the end-product, however leakage of electrons to O_2 prior to transfer to complex IV leads to the production of superoxide as by-product. The transfer of electrons in the electron transport chain to molecular oxygen leads to the formation of a superoxide radical and is direct result of metabolism meaning that the higher the level of metabolism the more superoxide is produced (Finkel and Holbrook, 2000). Superoxide is then converted into H_2O_2 by the enzymatic activity of mitochondrial superoxide dismutase (MnSOD), H_2O_2 is then detoxified by catalase and glutathione peroxidase. Other mitochondrial components that can also cause the formation of superoxide are glycerol phosphate dehydrogenase, α-ketoglutarate dehydrogenase and monoamino oxidase. Superoxide is not extremely reactive by itself and cannot attack DNA, nevertheless, it has been demonstrated *in vitro* that it favours the Fenton reaction by

reducing free ferric iron leading to production of hydroxyl radicals which can then damage any biomolecule (Valko *et al*., 2005)

Peroxisomes are a leading cause of ROS as species formed include H_2O_2, $O_2^{\bullet-}$ $OH^{\bullet}$ and $NO^{\bullet}$. it is commonly accepted that mitochondrial production of ROS is the main sources of ROS species in the cell however the endoplasmic reticulum and peroxisomes produce as much if not more ROS than mitochondria (Fransen *et al*., 2012). Mammalian peroxisomes play a key role in various metabolic pathways, including fatty acid α- and β-oxidation, phospholipid biosynthesis, glyoxylate metabolism, and amino acid catabolism. Peroxisomes contain various enzymes that produce H_2O_2 as part of their normal catalytic cycle. These enzymes include acetyl-CoA oxidases, urate oxidase, D-amino acid oxidase and xanthine oxidase, and are mainly flavoproteins. Peroxisomes contain two potential enzymatic sources of $O_2^{\bullet-}$ and $NO^{\bullet}$, namely xanthine oxidase and the inducible form of nitric oxide synthase. Xanthine oxidase is an enzyme that produces H_2O_2 and $O_2^{\bullet-}$ as by-products of its catalytic cycle. The inducible form of nitric oxide synthase (NOS2) is a homodimeric enzyme that catalyses the oxidation of L-arginine to $NO^{\bullet}$ and citrulline (Fransen *et al*., 2012). Currently, there is no solid evidence that mammalian peroxisomes contain enzymes that produce $^{\bullet}OH$ however, H_2O_2 inside peroxisomes may give rise to $^{\bullet}OH$ through the Fenton reaction (Rinnerthaler *et al*., 2015).

Oxygen radicals can be produced in the endoplasmic reticulum by the action of cytochrome P450 enzymes, protein disulphide isomerases (PDI) and endoplasmic reticulum oxidoreductin-1 (ERO-1). The protein PDI induces the formation of disulphide bonds in receptor proteins during the folding process and the isomerase gets reduced and regenerated by the ERO1. The reduced protein ERO1 then transfers the electron via the cofactor FAD to molecular oxygen finalising the process. It is important to note that incomplete transfer can lead to the production of superoxide (Benham *et al*., 2013).

The cytochrome P450 family of enzymes, found in the ER, is responsible for the detoxification of lipophilic compounds or xenobiotics, principally by increasing the water solubility of these substances. Electrons are transferred from NADPH to cytochrome P450 via cytochrome P450 reductase, finally leading to the hydroxylation of xenobiotics. A leaky transfer of electrons can result in the formation of oxygen radicals, especially superoxide(Benham *et al*., 2013).

Superoxide can be produced by the body as a defence mechanism to protect against invading micro-organisms. This is done on the membranes of cells the activity of NADPH oxidases. Electrons are passed on from NADPH over FAD and two b-type hemes to the final acceptor O_2, resulting in the formation of

superoxide. ROS can also be produced as a by-product of the arachidonic acid metabolism. The enzymes lipoxygenase and cyclooxygenase both use arachidonic acid as a substrate to synthesize the leukotrienes and prostaglandin H2, respectively. Both enzymes have the potential to produce superoxide in the presence of NADH or NADPH. The levels of arachidonic acid are relatively low in the skin, but increase in inflammatory skin diseases such as psoriasis, atopic dermatitis, and eventually aging (Das, 2006).

Exogenous sources of ROS production include UV and xenobiotics. UV irradiation can mediate damage via two different mechanisms; firstly, direct absorption of light by the cellular components, resulting in excited state formation and subsequent chemical reaction, or secondly photo-sensitisation mechanisms, where the light is absorbed by endogenous (or exogenous) sensitisers that are excited to their triplet states. The excited photosensitisers can induce cellular damage by two mechanisms; electron transfer and hydrogen abstraction processes producing free radicals (Type I) or energy transfer with O_2 to yield the reactive excited state, singlet oxygen (Type II) (Pattison and Davies, 2006).

Among xenobiotics and pollutants, polycyclic aromatic hydrocarbons (PAHs) are a class of mutagenic and tumorigenic environmental contaminants and are of special interest. These planar aromatic compounds are found in by-products of crude oil and coal and can be especially dangerous when combusted and volatilised. The compounds absorb light and reach a photo-activated or photo-excited states and can then go on to react with molecular oxygen, medium and co-existing chemicals to produce ROS and other reactive intermediates such as oxygenated PAHs. These intermediates induce lipid peroxidation and DNA oxidation (including DNA strand breakage, oxidation to 8-oxo-2-deoxyguanosine and DNA adducts) associated with age-related disease and cancer (Fu *et al*., 2012)

Noteworthy, H_2O_2 is not only toxic by its ability to form other ROS, like hydroxyl radicals through the Fenton reaction (see Figure 1.11.1) but H_2O_2 acting as a second messenger is involved in many biological processes including changes of morphology, proliferation, signalling (i.e. NF-κB), apoptosis, etc (Sies, 2017)

1.4 Free radical pathology

1.4.1 DNA oxidation

ROS have the potential to cause significant damage to biological macromolecules. The structure of DNA is highly prone to damage, and DNA damage is believed to occur at a rate of 1000 lesions/cell/day in humans, with oxidative DNA damage being particularly common. All four DNA nucleotide bases (and uracil) are

vulnerable to oxidative damage from ROS (see Figure 1.4.1), with more than 100 different forms of base damage identified as oxidative stress products (Cadet and Wagner, 2013). Both nuclear DNA and mitochondrial DNA (mtDNA) are affected by ROS.

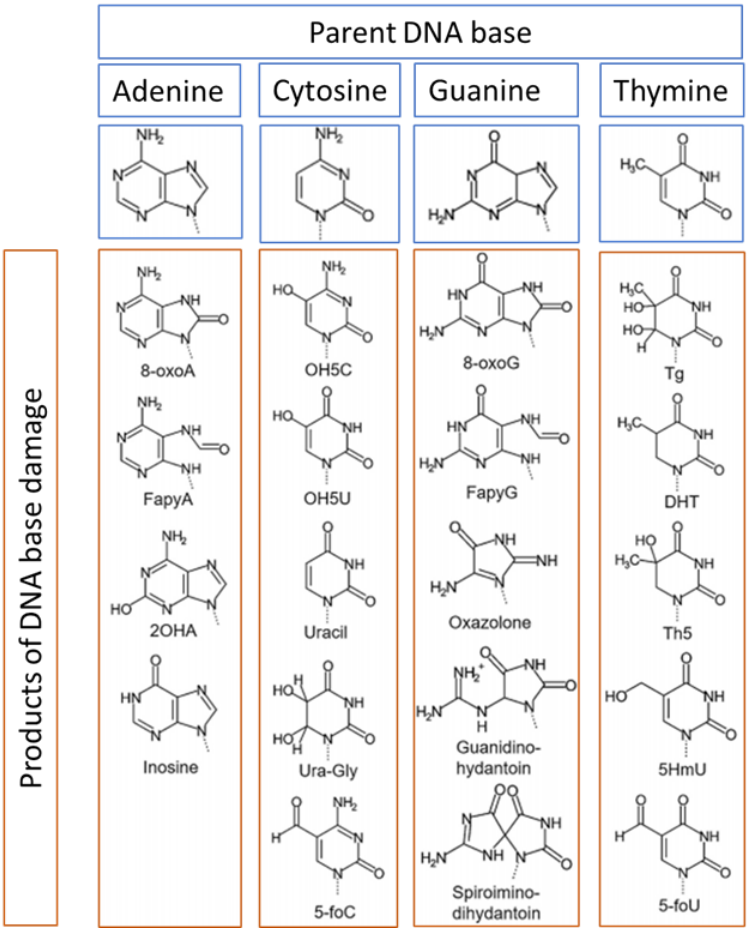

Figure 1.4.1 Biologically significant base lesions organized by parent base. All lesions are the result of oxidative damage, undergoing one or several ROS mediated attacks, and/or other damage related to oxidative stress (adopted from Whitaker *et al.*, 2017)

The hydroxyl radical has a pronounced role in ROS-induced DNA alterations. The radical reacts with DNA by the addition to double bonds of DNA bases and by removing a H atom from the methyl group of thymine and each of the C-H bonds of 2-deoxyribose (Cooke *et al*., 2003). When nucleotide base structure is altered due to oxidative damage, the base-pairing characteristics are usually altered as well, leading to either transition (purine to purine or pyrimidine to pyrimidine) or transversion (purine to pyrimidine or pyrimidine to purine) mutations.

Many oxidatively-modified base lesions are mutagenic (see Figure 1.4.1), regardless of whether they are produced *in situ* or arise due to misincorporation from the deoxynucleotide pool. The most studied of these lesions, that of 8-oxo-2'deoxyguanosine (8-OH-dG), arises by the introduction of an oxo group to the carbon at the C8 position and a hydrogen atom at the N7 position (Whitaker *et al*., 2017). 8-OH-dG is one of the most researched DNA lesions because of its stability and biological importance; in fact, 8-OH-dG studies account for the majority of what we know about how damaged DNA is handled and repaired.

1.4.2 Protein oxidation

Protein modification and subsequent aggregation, in addition to the denaturing of DNA and lipids, is a significant problem for cells. Protein oxidation and discernible unfolding have been demonstrated in human skin after only 30 minutes of UV exposure (Krutmann *et al*., 2021). Proteins can be modified directly or indirectly by ROS. Secondary by-products are a source of indirect attacks. The breakdown of the protein backbone that happens when previously oxidised glucose attaches to amino groups is an example of this. Direct ROS protein modifications are reported at the backbone, at amino-acid side chains or by the formation of carbonyls (Stadtman, 2006). Hydroxyl-radicals may by abstracting hydrogen atoms from the α-carbon of polypeptide chains, initiate backbone damage. This results in a series of chain reactions that eventually lead to the formation of alkoxyl derivatives resulting in spontaneous cleavage of the derivate itself. Several amino acid residues are more susceptible to oxidative modifications than others. Examples include histidine, leucine, methionine, and cysteine as well as phenylalanine, tyrosine, and tryptophan. Other modifications of amino acids such as proline, arginine, lysine and threonine form more stable products like carbonyl groups (such as aldehyde and ketones) (Rinnerthaler *et al*., 2015).

The process of protein oxidation can be divided into various stages according to the severity of modifications. At first, only slight oxidations take place leading to a marginally reduced enzyme activity of affected proteins or changes in thermostability. The next stage is marked by increased protein oxidation. Various protein modifications accumulate as a result of high levels of ROS or other sources of "protein modifiers" and the cell's incapacity to eliminate these damages. The chemically modified proteins completely lose their activity and unfold extensively. Proteins begin to cross-link and form tiny aggregates as they unfold. The proteins are then either degraded by the proteasome or refolded by heat shock proteins. The final stage of protein modification is marked by extensive oxidation of proteins, their complete unfolding and covalent crosslinking of several proteins (Valko *et al*., 2005; Rinnerthaler *et al*., 2015)

1.4.3 Lipid peroxidation

ROS molecules originating from different sources in the cell have the capacity to induce the lipid peroxidation process. The reaction of a ROS molecule with polyunsaturated fatty acids initiates this chain reaction. In the first stage, hydrogen atoms are removed from these lipids' methyl groups, resulting in the formation of a lipid radical. The following step involves a reaction with molecular oxygen, which produces a peroxyl radical. When this radical reacts with another polyunsaturated fatty acid, a lipid peroxide is formed, as well as a new radical, which propagates the chain reaction (Rinnerthaler *et al*., 2015). The most prominent product of lipid peroxidation is 4-hydroxynonenal (4-HNE). 4-HNE can modulate a number of signalling processes mainly through forming covalent adducts with nucleophilic functional groups in proteins, nucleic acids, and membrane lipids (Zhong and Yin, 2015). The degradation of hydroperoxide of ω-6 polyunsaturated fatty acids (PUFAs) at the sn-2 position of glycerophospholipids in cellular membranes is thought to be the source of 4-HNE. Thus, phospholipids on cytoplasm membranes containing linoleic acid (LA, 18:2, ω-6) and arachidonic acid (AA, 20:4,ω-6) are thought to be the main source of 4-HNE synthesis. Increased oxidative stress levels have been linked to a variety of cancer types, and 4-HNE is thought to be a key player in the mutagenic and carcinogenic effects of lipid peroxidation(Zhong and Yin, 2015). The formation of 4-HNE protein adducts in renal and colon cancer tissues has been linked to kidney and colon cancer growth and progression (Shoeb *et al*., 2014).

The major aldehyde product of lipid peroxidation besides 4-hydroxynonenal is malondialdehyde (MDA) MDA is mutagenic in bacterial and mammalian cells and carcinogenic in rats. MDA can react with DNA to form adducts to guanine, adenine and cytosine. (Valko *et al*., 2005).

1.4.4 Carbohydrate oxidation

Starch and cellulose are crucial polysaccharides of extreme biological importance as starch can be depolymerized into its building blocks such as monosaccharides, and cellulose is an important structural element of many living organisms such as plants. These polysaccharides can be attacked at the glycosidic bond depolymerising the molecule. It is also noteworthy that hydroxyl radicals can abstract a hydrogen from the C-H bond of a disaccharide generating a saccharide radical and water (Dai *et al*., 2017).

1.5 ROS associated disease

Here are brief examples of how selected diseases strictly related to oxidative stress, in which extensive detection and characterization of different oxidatively modified cellular components will contribute to understand the dysfunction mechanisms.

1.5.1 Free radicals and acute (adult) respiratory distress syndrome

Acute (adult) respiratory distress syndrome (ARDS) is a severe hypoxia caused by pulmonary oedema, characterized by diffuse inflammation in the lung parenchyma. Increased production of ROS/RNS combined with decreased antioxidant activity in the lung contributes to this pathology. ARDS is characterized by increased neutrophils, which generate $O_2^{\bullet-}$ oxidizing various lung proteins, such as surfactant protein A, inhibiting their functions (Dalle-Donne *et al*., 2005; Amann *et al*., 2014).

1.5.2 Free radicals and alzheimer's disease

Alzheimer's disease (AD) is the most common senile neurodegenerative disorder estimated to affect approximately 15 million people worldwide. AD is characterized by progressive loss of memory, language, and other cognitive functions accompanied by concomitant behavioural, emotional, and social deterioration, all leading to dementia. The neuro-pathological hallmarks of the brain of AD patients are numerous extracellular senile plaques containing amyloid-band neurofibrillary tangles (NFTs), which occur in pyramidal neurons of the cerebral cortex and hippocampus. Amyloid-β, the main constituent of senile plaques, induces oxidative stress, producing H_2O_2 and other ROS, which cause peroxidation of cell membranes and ultimately lead to cell death. Redox active iron present in AD brains is thought to catalyse hydroxyl radical formation (Dalle-Donne *et al*., 2005; Gogus and Smith, 2010).

1.5.3 Free radicals and cardiovascular diseases

Low density lipoproteins (LDL) in blood are composed of polyunsaturated fatty acids that are subject to oxidation by free radicals. The lipid components of LDLs have a major role in the formation of atherosclerosis. Continued blood vessel damage by oxidised lipids is presumed to be responsible via the formation of foam cells and plaques in vessels. The smooth cells and macrophages of blood vessels are known to release free radicals which affects lipid peroxidation (Lobo *et al*., 2010).

1.5.4 Free radicals and amyotrophic lateral sclerosis (Gehring's disease)

Amyotrophic lateral sclerosis (ALS), also known as Gehring's disease, is a fatal neurodegenerative disease that affects primarily motor neurons in the cerebral cortex, spinal cord, and brain stem. ALS eventually leads to death within 3–5 years from the onset of symptoms in most cases. Increased protein carbonyls have been found in brain tissues of both sporadic and familial ALS patients (Dalle-Donne *et al*., 2005).

1.5.5 Free radicals and diabetes mellitus

Diabetes mellitus is a very common chronic disease caused by the impaired production of insulin by pancreatic islet β-cells and/or by diminished tissue responses to insulin (Rösen *et al*., 2001). ROS/RNS make a significant contribution to the progression of diabetes and its complications. Elevated glucose levels are associated with increased production of ROS by several different mechanisms (Nishikawa *et al*., 2000). Oversupply of nutrients, including glucose and fatty acids, and the subsequent overstimulation of β cells, are believed to be an important contributor to insulin secretory failure in type 2 diabetes. Hypoxia has also recently been found to be implicated in β cell damage. Evidence points to a role for oxidative stress in both processes. Although ROS production results from mitochondrial respiration during glucose utilisation, the expression of antioxidant defence genes is relatively poor in β cells. (Gerber and Rutter, 2017)

1.5.6 Free radicals and rheumatoid arthritis

Rheumatoid arthritis (RA) is a systemic autoimmune disease characterized by chronic joint inflammation, especially in hands and legs, which eventually leads to cartilage destruction and subsequent bone erosion. Many studies suggest that ROS/RNS production at sites of inflammation may contribute to the development of RA. NADPH catalyses oxygen to form superoxide $O_2^{\bullet-}$ within the plasma membrane of activated polymorphonuclear leukocytes exposing the synovial cells to oxidative stress leading to degradation of the extracellular matrix (Dalle-Donne *et al*., 2005).

1.5.7 Free radicals and cancer

Cancer is one of the leading causes of death in humans (Phaniendra *et al*., 2015). Free radicals cause different types of chemical changes in DNA; thus, they could be mutagenic and involved in the etiology of cancer. Cancer cells display elevated levels of oxidative stress due to activation of oncogenes and loss of tumour suppressors and by altering the growth signals and gene expression cause continuous proliferation of cancer cells (Phaniendra *et al*., 2015). Oxidative stress-induced lipid peroxidation has been associated with human physiology and diseases including cancer. Overwhelming data suggest that reactive lipid mediators generated from this process, such as 4-hydroxynonenal (4-HNE), are biomarkers for oxidative stress and important players for mediating several signalling pathways. The biological effects of 4-HNE are primarily due to covalent modification of important biomolecules including proteins, DNA, and phospholipids containing amino group (Zhong and Yin, 2015).

1.5.8 Free radicals and aging

Oxidative stress plays a major role in the aging process. Extrinsic and intrinsic. Extrinsic aging is driven by oxidative stress caused by UV irradiation primarily on the skin. UV-irradiation especially leads to the genesis of ROS that are in turn main contributors to the aging of skin. This has led to the coining of the term “photoaging”. ROS production by UVA light induces different changes in the dermis and these seem to be mainly responsible for the process and progression of photoaging. UVB light does not have the capacity to penetrate to the deeper sections of the epidermis. Cellular chromophores absorb the UVA in turn affecting a whole host of functions and components such as urocanic acid, riboflavin, melanin, bilirubin, heme, porphyrin, and pterins (Rinnerthaler *et al*., 2015) These photosensitisers absorb photons/energy leading to a triplet state that can react with oxygen producing ROS such as superoxide, hydroxyl radicals, singlet oxygen or hydrogen peroxide.

1.5.9 Free radicals and the pathophysiology of non-alcoholic fatty liver disease (NAFLD)

Non-alcoholic fatty liver disease (NAFLD), or liver steatosis without alcohol usage, is a prevalent hepatic illness with a wide range of symptoms, ranging from simple triglyceride build up in hepatocytes without apparent liver damage to inflammation, necrosis, ballooning, and fibrosis (namely, non-alcoholic steatohepatitis) up to severe liver disease and eventually cirrhosis and/or hepatocellular carcinoma. Multiple factors (environmental and genetic) influence the pathophysiology of fatty liver and its progression, with oxidative stress likely serving as the principal initiator of hepatic and extrahepatic damage. The homeostasis of fat and energy in hepatic cells is regulated by mitochondrial activities, including beta-oxidation of free fatty acids (FFAs), electron transfer and production of ATP, and reactive oxygen species. Mitochondrial abnormalities disrupt the balance between prooxidant and antioxidant processes, resulting in an increase in nonmetabolized fatty acids in the cytosol as a result of fatty acid beta oxidation inhibition and the subsequent activation of ROS generation (Burns *et al*., 2018).

1.5.10 Free radicals and the role of oxidative stress in male infertility

Oxidative stress has been linked to male infertility, reduced sperm motility, sperm DNA damage, and an increased risk of spontaneous abortions and hereditary illnesses. Redox imbalance, poor sperm motility, and sperm DNA damage occur from increased ROS and lower antioxidant defence (Alahmar, 2019). As their cell membranes contain a high amount of unsaturated fatty acids, spermatozoa are particularly vulnerable to the negative effects of ROS. Peroxidation of lipids is aided by reactive oxygen species, resulting in an increase in intracellular oxidative burden. Lipid peroxidation, loss of membrane integrity

with increased permeability, reduced sperm motility, structural DNA damage, and apoptosis are all part of the chain of events (Schuppe *et al*., 2008).

1.5.11 Free radicals and the role of oxidative stress in depression

Reactive oxygen species (ROS) play an important function in cellular signalling as well as defence against invasive microbes. Excessive ROS production and antioxidative defence fatigue activate proinflammatory signalling, causing damage to critical macromolecules and cellular death. Cell necrosis occurs when cells fail to maintain redox equilibrium, resulting in the production of proinflammatory mediators. Because of its increased oxygen consumption, higher lipid content, and lower antioxidative defence, the brain is more prone to oxidative stress. Oxidative stress is a key contributor to neurodegeneration, and its role in the aetiology of major depressive disorder (MDD) has been proven beyond a shadow of a doubt. The pathophysiology of MDD has been linked to oxidative stress and proinflammatory signalling (Bhatt *et al*., 2020).

1.6 Aldehyde related disease

There is increasing evidence that aldehydes generated endogenously during the degradation process of biological molecules are involved in much of the pathophysiology associated with cardiovascular diseases such as atherosclerosis and the long-term complications of diabetes.

Major sources of reactive aldehydes *in vivo* are lipid peroxidation, glycation, and amino acid oxidation (Uchida, 2000). Aldehydes are strong electrophilic compounds with terminal carbonyl groups making them highly reactive and α,β-unsaturated aldehydes such as 4-hydroxy-2-nonenal (4-HNE) and acrolein contain another electrophile at the β-carbon (O'Brien *et al*., 2005). Aldehydes can react with cellular components in the vicinity of their origin however they are relatively stable, and have long half-lives compared to free radicals and this allows them to penetrate into the extracellular matrix, if their origin is intracellular and vice versa (LoPachin and Gavin, 2014). Some aldehydes play normal physiological roles however most are cytotoxic and carcinogenic. They are known to form adducts (Dalle-Donne *et al*., 2005) with various cellular targets such as glutathione thus affecting first line antioxidant defence, nuclear DNA, mitochondrial DNA, amino acid residues on proteins affecting function and lipids such as the lipid bilayer affecting processes such as nutrient transport across the membrane.

Michael-addition of these reactive aldehydes to the nucleophilic sidechain of cysteine, histidine and lysine amino acids incorporates these aldehydes into the peptide chain. The occurrence of the carbonyl moieties

may alter the conformation of the polypeptide chain, thus determining the partial or complete inactivation of a protein (Dalle-Donne *et al*., 2005).

In vivo, aldehydes are converted to acids and/or alcohols by oxidation and/or reduction. In humans, ALDHs (nicotinamide adenine dinucleotide) or NAD+ (nicotinamide adenine dinucleotide) oxidise a wide range of endogenous and exogenous aldehydes to their carboxylic acid equivalents. The ADH superfamily, AKR superfamily, and short-chain234 dehydrogenases/reductases superfamily are the human enzymes that reduce aldehydes (SDR). Aldehydes can also be oxidised by ADHs.

1.7 Volatile aldehyde adducts as biomarkers

Volatile organic compounds are a diverse group of organic carbon-based compounds which can be characterised by their retention time and boiling point (<=250C at standard room pressure) (WHO 1989). VOCs in the context of the human body are found in most biofluids such as breath, blood, urine, faeces and sweat emissions. These emissions can be isolated and the headspace analysed by various means (Schallschmidt *et al*., 2015; Schmidt and Podmore, 2015).

In recent years a body of evidence exists that suggests a relationship between volatile organic compounds released in the body and certain diseases such as cancer (Bartolazzi *et al*., 2010). It cannot be deduced with certainty whether this is because of altered body metabolism in disease or if they originate directly from cancer cells however it has been suggested that certain tumour cell lines possess a “fingerprint” profile of the volatiles released and that these cell lines can be characterised based on these profiles. The diagnosis of disease by analysing volatiles organic compounds is becoming popular due to the absolute non-invasivity of the method. The ultimate goal of these studies is to provide a non-invasive diagnostic technique that could improve early diagnosis capabilities (Bartolazzi *et al*., 2010; Lavra *et al*., 2015).

In a study by Phillips *et al*., (1999) over 20 VOCs, principally alkanes and benzene derivatives, were identified in the breath of patients with and without lung cancer. Samples of breath were collected by an automated breath collection apparatus and pumped through a sorbent trap, which contained activated carbon. The alveolar gradient of each breath VOC and the difference between breath and air was calculated and found that for stage 1 lung cancer, the VOCs had 100% sensitivity and 81.3% specificity and cross validation correctly predicted the diagnosis 71.7% of lung cancer patients and 66.7% of non-lung cancer patients. Similarly in a study by (De Lacy Costello et al., 2014) over 103 aldehydes were found in

the bodily fluids and breath of health humans including aliphatic, branched, unsaturated and aromatic aldehydes including ten specifically observed in breath.

In a study by (De Vietro *et al*., 2020) VOCs contained in exhaled breath were sampled in healthy and disease states of patients and analysed by GCMS and found levels of benzaldehyde, nonanal, benzene ethyl, benzene methyl, indole, octananoic acid and tetradecane were produced and a similar VOC pattern with different fingerprints could be elucidated. A positive correlation between exhaled VOCs could discriminate colorectal cancer patients from normal individuals.
In a study by (Phillips *et al*., 2003) patients with primary lung cancer had abnormal breath test findings that were consistent with accelerated catabolism of alkanes and monomethylated alkanes analysed via GCMS.

Aldehydes may be promising biomarkers and this identification is indispensable for future work on the biochemical sources of these compounds and their metabolic pathways.,

1.8 Exhaled breath offering a unique diagnostic possibility for analysing a range of biomarkers

Exhaled breath contains volatile substances that are formed and exhaled because of normal breathing and contain material from distal airways of the respiratory system. Exhaled breath can be used to monitor biomarkers of both endogenous and exogenous origin. Exhaled breath offers the unique possibility of non-invasive collection of material from the airways. In combination with modern MS instrumentation that is compatible with offline as well as online real-time analysis, exhaled breath sampling could offer analysis of a broad range of biomarkers including aldehydes, nitrogen dioxides, eicosanoids, adenosine and metabolites (Beck *et al*., 2016)

1.9 Aldehyde derived radicals

Radicals, such as acyl, hydrated acyl, alkyl and ketyl radicals, are some of the radicals that have been studied from aliphatic aldehyde oxidation chemistry. Photochemistry of aliphatic aldehyde is among the most familiar and studied; Photoreactions include autoxidation via homolysis of the bond hydrogen to carbonyl group or H-abstraction by other radicals leading to the formation of acyl radicals; primary σ-bond cleavage, forming alkyl and formyl radicals; radical-induced decarbonylation of aliphatic aldehydes yielding alkyl and acyl radicals. (Wang *et al*., 2005).

1.10 Antioxidants

Antioxidants are compounds that prevent oxidative damage by scavenging and reacting with free radicals before oxidative damage can occur. Antioxidants work by terminating the free radical chain reaction in 3 ways; 1, By scavenging active free radicals; 2, By repairing and clearing damage, and 3, by the reduction of hydroperoxides ($ROO^{\bullet}$) and H_2O_2 by suppression of active species production.

1.10.1 Non-enzymatic antioxidants- ascorbic acid, α-tocopherol, beta carotene, uric acid and CoQ_{10}

Ascorbic acid (Vitamin C) is one of the most prominent and abundant antioxidants consumed in food as it cannot be synthesised in humans, vitamins C is a water-soluble molecule and an electron donor. As an electron donor it can react with a free radical by donating its electron, becoming oxidized forming semidehydroascorbic acid resulting in a stable and comparatively unreactive molecule. Over and above the molecule can undergo further reactions to become dehydroascorbic acid or reduce back. (Alkadi, 2020).

α-tocopherol (vitamin E) is another remarkable molecule with antioxidant capability also consumed as foods originating from plant oils. Vitamin E is lipophilic and can be found in animal membranes. Vitamin E is highly important as it can stop free radicals particularly lipid peroxyl radicals by reducing them to hydroperoxide, and in the process losing a proton and transforming itself into a radical. Remarkably the α-tocopheroxyl radical is not significantly reactive and is subsequently detoxified downstream by vitamin C and glutathione (Niki, 2015).

Beta-carotene produced in plants and bacteria is the precursor molecule of retinol (vitamin A) and is also consumed in food. Vitamin A has a significant role in the human body forming retinal needed in the eye by combining with the protein opsin to form rhodopsin, a light absorbing molecule necessary for vision, additionally either scavenging radicals or inhibiting lipoxygenases (Sandmann, 2019) and other growth and developmental roles and as well as maintaining the immune system. Beta carotene itself is also antioxidant as it can react with the peroxyl radical adding it directly to its backbone forming resonance-stabilized carotenyl radicals that are decomposed downstream (Mordi *et al*., 2020).

Uric acid although not strictly classed as an antioxidant, with its powerful antioxidative activity, is thought to scavenge free radicals such as hydroxyl radicals, singlet oxygen, and oxo-heme oxidants and contribute to the total antioxidative capacity of plasma. Studies have indicated that uric acid provides a protective

role in red blood cells and nerve cells by providing an antioxidant defence and it has been linked with cell longevity (Song *et al*., 2019)

Coenzyme Q_{10} (CoQ_{10}) is an endogenous lipophilic quinone found in equilibrium between its oxidised (ubiquinone) and reduced (ubiquinol) forms. CoQ_{10} is known because of its contribution to the mitochondrial ETC where it exerts a pivotal role in mitochondrial bioenergetics since it acts as an electron carrier between complex I/II and complex III in the respiratory chain. Ubiquinone is reduced to ubisemiquinone and ubiquinol at complex I and II and oxidized back to ubiquinone at complex III. Furthermore, in its reduced form, ubiquinol is endowed with antioxidant properties by acting as a chain-breaker of peroxidative processes that occur in biological membranes (Marcheggiani *et al*., 2021).

1.10.2 The importance of superoxide dismutases, catalases, glutathione peroxidase, ferritin and peroxiredoxins in quenching ROS

Among the most prominent enzymes that can metabolise reactive oxygen species are the superoxide dismutases (SOD). These enzymes "dismutate" superoxide to hydrogen peroxide. There are three isoforms distinguished by localization, SOD1 is found in the cytosol and nucleus, SOD2 is found in the mitochondria to dismutate any superoxide originating from the ETC, and SOD3 which is found in the extracellular space coupled with Cu/Zn ions at its centre. In the first half-reaction the electron from the superoxide radical is transferred to the metal ion in the active centre thereby reducing it. The superoxide itself is oxidized to O_2. In the second half-reaction the reduced metal in the superoxide enzymes is re-oxidized by transferring the electron to superoxide resulting in the formation of hydrogen peroxide (Rinnerthaler *et al*., 2015).

A key enzyme that detoxifies hydrogen peroxide is catalase (CAT) that is localized in peroxisomes. This enzyme is made up of four identical polypeptide chains each containing a key heme group. The hydrogen peroxide reacts with the heme group leading to an oxoferryl porphyrin cation radical and a water molecule. This intermediate reacts immediately with another hydrogen peroxide producing water and molecular oxygen and regenerating the original heme group (Glorieux and Calderon, 2017).

Glutathione (GSH) is a tripeptide of glycine, cysteine and glutamic acid that is found in high concentrations intracellularly, being the most abundant low molecular mass thiol. A two-step procedure is used to make this peptide. The gamma-glutamyl cysteine synthetase performs the first step by conjugating glutamic acid and cysteine forming gamma-glutamyl cysteine. This compound containing cysteine with a sulfhydryl

group (SH) is responsible for the antioxidant activity of GSH. The glutathione synthetase performs the second step in the reaction by binding gamma-glutamyl cysteine with glycine by the enzyme glutathione synthetase, forming the tripeptide GSH.

Glutathione peroxidase (GPx) is an 80 kDa enzyme responsible for the removal of hydroperoxides formed in cells. Se- dependent GPx is capable of utilizing hydrogen peroxide (H_2O_2) and a variety of organic hydroperoxides as substrates. GPx is oxidised by reactants forming a dimer with another activated GPx via the formation of a disulphidic bond. The glutathione reductase, which consumes NADPH, can restore GPx in a reducing step. GPx not only detoxifies ROS but can also regenerate oxidized α-tocopherol and retinol. GSH is a cofactor for enzymatic reactions in addition to being an antioxidant. The glutathione peroxidase enzyme performs two functions: it converts hydrogen peroxide to water, and it prevents lipid peroxidation. The enzyme-bound selenium is oxidised by hydrogen peroxide or a lipid peroxide, in the first step, resulting in SeOH. In a subsequent stage, the enzyme combines with a thiol group in GPx, forming a selenyl-sulphide bond between the enzyme and glutathione. The enzyme is regenerated by a reaction with a second GPx, and a disulphide bond is produced

While iron is an essential nutrient, it is also toxic to cells. Due to the Fenton reactions potential to initiate a vicious cycle of ROS production in the cell, resulting in its death, free iron ions constitute a persistent threat to the cell. As a result, the cell must carefully contain the iron ions. The protein ferritin is responsible for iron storage. Iron stored in ferritin is redox inactive, which mitigates its toxic effects on cellular components. The protein consists of 24 subunits forming a sphere that surrounds the iron (see Figure 1.10.1). The iron is only stored in its Fe(III) form as ferrihydrite and upon its release it must be reduced to the Fe(II) form. Ferritin is primarily stored in the cytosol, although mitochondrial and nuclear forms are also known. The iron release is also dependent on lysosomal ferritin degradation (Asano *et al*., 2011)

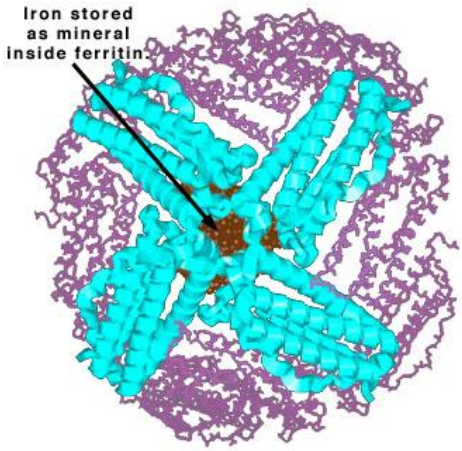

Figure 1.10.1 This is a three-dimensional representation showing ferritin, the iron-storage protein in the body. Ferritin has a spherical shape, and iron (brown) is stored as a mineral inside the sphere (adapted from (Asano *et al*., 2011)

The final class of enzymes and one of the most important enzyme systems that, together with SOD, CAT and GPx, act in the defence against oxidative stress is the ˙peroxiredoxin' (PRDX) family. PRDXs are a ubiquitously expressed family of small (22-27 kDa) non-seleno peroxidases that catalyse the peroxide reduction of H_2O_2, organic hydroperoxides and peroxynitrite. They have an important role in cell proliferation, differentiation, apoptosis, embryonic development, lipid metabolism, immunological response, and cellular homeostasis, among other physiological processes (Nicolussi *et al*., 2017). The catalytic activity of PRDXs is crucially dependent on a conserved peroxidatic cysteine residue contained within a universally conserved Pxxx(T/S)xxC active-site motif in the amino-terminal portion of the protein (Nelson *et al*., 2011). A peroxide substrate reacts with the conserved cysteine in the active centre of these enzymes leading to the formation of a sulphenic acid residue. This is followed by a reaction of the sulphenic acid with a second cysteine thereby forming an intra-molecular disulphide bond. The enzyme is then regenerated by a flavoprotein disulphide reductase such as the thioredoxin reductase There are many subgroups of PRDXs varying in their oligomerization states, conformational flexibility, and certain secondary structural elements. Put differently the mechanism of action varies dependent upon subtype. In typical 2-Cys PRDXs, the main peroxidatic cysteine residue reacts with the cysteine residue on an adjacent subunit of the dimer. In atypical 2-Cys PRDXs, the oxidized cysteine reacts with the cysteine residue located in the same molecule. In 1-Cys PRDXs, the main residue generates sulphenic acid and is regenerated directly through donation of an electron to the thiol form in presence of ascorbate (Nicolussi *et al*., 2017)

.

1.11 The Fenton reaction

The Fenton reaction is a specific example of the Haber-Weiss reaction. The Fenton reaction refers to the reaction between hydrogen peroxide and ferrous salts to produce a reactive species capable of oxidising a wide variety of organic substrates (Winterbourn, 1995). Iron has a pivotal role in oxidative stress by the formation of the hydroxyl radical via the Fenton reaction. Fe^{2+} is oxidised to Fe^{3+} by oxygen (O_2), O^{2-} is produced which subsequently reacts with a hydrogen ion (H^+) and H_2O_2 is produced. Then H_2O_2 reacts with Fe^{2+} and a hydroxyl radical ($^{\bullet}OH$) is produced by the Fenton reaction. More $^{\bullet}OH$ is produced by the reaction of hydrogen peroxide in the presence of Fe^{2+}/Fe^{3+} via the Haber-Weiss reaction (Das et al., 2015).

$$Fe^{2+} + H_2O_2 \longrightarrow Fe^{3+} + {}^{\bullet}OH + OH^-$$

Figure 1.11.1 The Fenton reaction was first described by H.J Fenton, (1894) and *it is described as the enhanced oxidative potential of H_2O_2, when iron (Fe) is used as a catalyst under acidic conditions*

1.12 Hydroxyl radical trapping and detection methods

Hydroxyl radicals can be detected using various analytical methods such as electron spin resonance (ESR), high-performance liquid chromatography electro-chemical detection (HPLC-ED), high-performance liquid chromatography mass spectrometry (HPLC-MS), GC-MS, capillary electrophoresis (CE) and chemiluminescence (CL) (Cheng *et al*., 2002).

ESR is a branch of absorption spectroscopy that measures the ESR spectrum of a spin adduct after spin trapping. ESR or electron paramagnetic resonance (EPR) is based on the fact that atoms, ions, molecules, or molecular fragments which have an odd number of electrons exhibit characteristic magnetic properties. Transitions can be induced between spin states by applying a magnetic field and then supplying electromagnetic energy, usually in the microwave range of frequencies. An electron has a spin and due to spin, there is a magnetic moment. Radiations with frequency in the microwave region (3 – 400 GHz range) is absorbed by paramagnetic substances to induce transitions between magnetic energy levels of electrons with unpaired spins. The resulting absorption spectra are described as electron spin resonance (ESR) or electron paramagnetic resonance (EPR)(Cheng *et al*., 2002)

HPLC-ED involves quantifying and identifying the hydroxylation products from the reaction of hydroxyl radicals with salicylate. It is based on the ability of hydroxyl radicals to attack the benzene rings of aromatic

molecules. Other applications of HPLC-ED in detecting hydroxyl radicals involves the formation of 8-hydroxy-7,8 dihydro-2'-deoxyguanosine (8-OH-dG), where the hydroxyl radicals react with DNA or 2-deoxyguanosine and can subsequently be separated and detected from 2'-deoxyguanosine by HPLC-ED (Catapano *et al*., 2019; Abuarrah *et al*., 2021).

HPLC-MS involves mass spectrometry that has been coupled with liquid chromatography for the analysis of samples that contain non-volatile constituents and converting the sample species into gaseous ions and separating them on based on mass to charge ratios. MS is by far the most powerful and widely used tool for the investigation of the structure of molecular species and the isotopic ratios of atoms in a sample species. In the application of HPLC–MS to determining species of hydroxyl radical, Vanhees *et al*., (2001). used the products of α-pinene and hydroxyl radical reaction to identify the oxidation products. HPLC measurements showed that semi-volatile products such as formaldehyde, acetaldehyde, acetone, campholenealdehyde and pinonaldehyde could be quantified as oxidation products for the α-pinene and $^{\bullet}$OH reaction.

Capillary electrophoresis is a powerful tool for the analysis of lipids, carbohydrates, nucleic acids, proteins and peptides. There are notable applications where it has been applied in studies related to hydroxyl radical detection in living systems. Cao *et al*., (2003) indirectly analysed hydroxyl radicals by their reaction with salicylic acid to produce 2,3-dihydroxy benzoic acid and 2,5-dihydroxy benzoic acid and Coolen *et al*., (1997) used antipyrine as an exogenous marker for the monitoring of oxidative damage caused by hydroxyl radicals. The ^{60}Co γ-radiation products of antipyrine were separated using micellar electrokinetic capillary electrophoresis in comparison to ESR and the results showed a significant correlation coefficient that this method could be used to detect hydroxyl radicals with significant accuracy.

Chemiluminescence (CL) refers to the phenomenon that generates light emission based on the molecules in a chemically generated excited state. Such emissions can be detected immediately by a photomultiplier tube (PMT) when the CL reactants are mixed. Li *et al*., (2019) applied the CL system on the principal mechanism that hydroxylated intermediates could be oxidized by persulphate in alkaline solution to form superoxide anion radicals and thus lead to an increase in the luminol CL. Finally, the proposed CL system was successfully applied in monitoring hydroxylated intermediates generated during persulphate-based advanced oxidation processes under different degradation conditions. Therefore, CL is a promising technique for monitoring the generation of intermediates with ultralow background, high sensitivity, fast

response, cheap instruments, and simple operation, without requiring sample pre-treatment (Li *et al*., 2019)

1.13 Spin trapping

There are many methods that can be used to detect free radicals; however, they are all limited in some way or form to how the information can be utilised. Electron paramagnetic resonance (EPR) is the only method where we can "see" the free radicals directly because it detects the presence of unpaired electrons, however it is limited as it can only detect unreactive free radicals at relatively high concentrations making it unsuitable for many applications *in vivo* (Halliwell and Whiteman, 2004). One way around this is to use spin traps that can form stable adducts with reactive species. Spin trapping is a technique that uses nitroso or nitrone compounds such as *N*-tert-butyl-α-phenyl nitrone (PBN) to trap hydroxyl radicals and form relatively stable nitroxide adducts that can be measured using various techniques such as GC-MS. The radicals that are trapped by PBN and the resulting adducts are stable enough for analysis and can be extracted using chloroform for subsequent analysis via GC-MS. Spin trapping is a powerful resource for quantifying the short-lived and unstable free radicals liberated in these reactions (Mantovani *et al*., 2018). Spin trapping was first introduced by Janzens group in 1968. N-tert-butyl-α-phenyl nitrone (PBN) and 5,5-dimethyl-1-pyrroline N-oxide (DMPO) (Khan *et al*., 2003) are well used spin traps, 1,1,3-trimethyl-isoindole N-oxide (TMINO), 5,5-diethylcarbonyl-1-pyrrolineN-oxide (DECPO) (Karoui *et al*., 2004) and N-2-(2-ethoxycarbonyl-pro-pyl)-a-phenylnitrone (EPPN) (Stolze *et al*., 2003) are relative newcomers that have been used to characterise adducts in *in vivo* animal studies however their greatest limitation is their application via EPR where any antioxidant activity can reduce the adducts and "silence" the signals (Halliwell and Whiteman, 2004). The addition of a nitrone is also still unreliable with this method as the nitroxide formed from the addition of the hydroxyl is unstable making measurements *in vivo* rather limited. Mass spectrometry coupled to a suitable chromatographic system (e.g. gas chromatography (GC)) offers an important alternative approach to measuring free radical spin adducts as it is possible to detect both paramagnetic and non-paramagnetic species (Mistry *et al*., 2008).

1.14 Nitrones

One technique that allows detection and identification of radicals in biological systems is the spin-trapping technique. Typically, either nitroso or nitrone compounds are used as trapping agents (as spin traps) because the addition of a radical results in the formation of a stable nitroxyl radical (or nitroxide, a spin adduct) see Figure 1.14.1. Nitrones were first recognised by Iwamura and Inamoto, (1967) in which

they found radical 1,3-addition to the carbon and oxygen atoms of the nitrone system and nitrones have since extensively been used for the detection and identification of free radical species in chemistry (Berliner, 2012).

Nitrones are preferred over nitroso compounds when conducting spin trapping studies, primarily due to the advantages that nitrones have. Nitroso compounds are sensitive to light and heat and decompose easily, they exist as dimers requiring UV irradiation for dissociation into the monomer form, they do not form stable adducts with oxygen-centred radicals, in contrast to nitrones and most hydrogen-atom adducts of nitroso compounds are unstable at ambient temperatures and disproportionate to the hydroxylamine derivative. In contrast, oxygen centred radical adducts and hydrogen-atom adducts of nitrones are relatively stable (Reeves Huie, 1987)

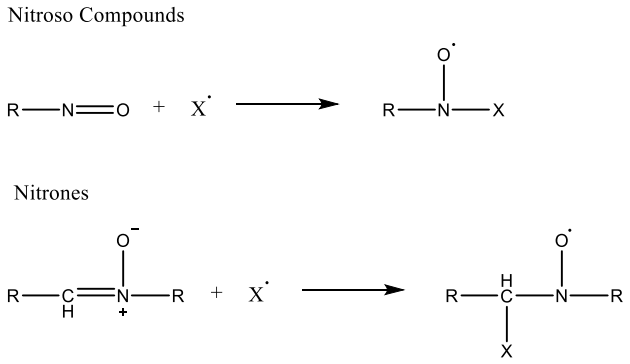

Figure 1.14.1 Nitroso and nitrones reacting with a radical species to form a stable nitroxide (spin adduct)

1.15 Nitroxides

Nitroxides are compounds that contain a stable free radical in the form of a nitroxyl group (>N–O•) with an unpaired electron (Lewandowski and Gwozdzinski, 2017). They are stable radicals, non-toxic, do not elicit an immunogenic effect and diffuse easily across cell membranes (Gariboldi *et al*., 2000) making them useful candidates for biological studies. Because the relatively stable nitroxide accumulates, spin trapping is an integrative method for measuring free radicals and is inherently more sensitive than procedures which detect only instantaneous or steady-state levels of free radicals. PBN; α-phenyl N-tert-butyl nitrone; DMPO 5,5-dimethylpyrroline N-oxide, DBNBS 3,5-dibromo-4- nitrosobenzenesulphonate are 3 commonly used spin traps due to their low toxicity

The redox reactions of nitroxide radicals have attracted much attention in the past few decades. One electron oxidation of nitroxide radicals gives the corresponding N-oxoammonium cation, and one electron reduction leads to the aminoxyl anion (see Figure 1.15.1).

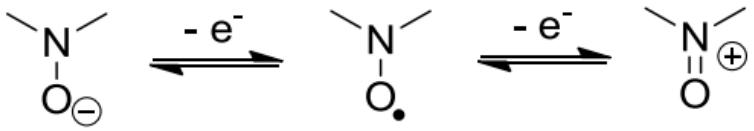

Figure 1.15.1 Redox reactions of nitroxide radicals

However, nitroxide radicals can, if presented the opportunity, decompose to the corresponding hydroxylamine and nitrone by the action of one or more α-hydrogens (see Figure 1.15.2).

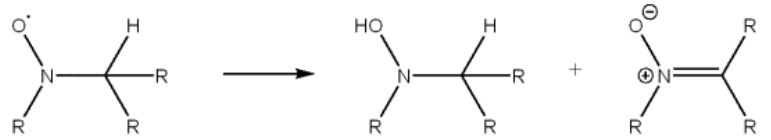

Figure 1.15.2 Decomposition of nitroxide radicals with one or more α-hydrogen atoms

1.16 Secondary spin trapping

Due to the difficulty associated with detecting short lived hydroxyl radicals, an indirect method to trap them is commonly employed. Secondary spin trapping involves utilising the hydroxyl radicals to react with a compound such as DMSO to form methyl radicals

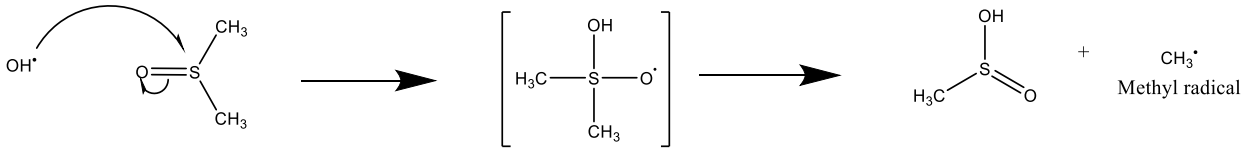

Figure 1.16.1 The hydroxyl radical attack of DMSO to produce methyl radicals (Jerzykiewicz *et al*., 2011)

Isotopically labelled DMSO produces deuterated methyl radicals ($^{\bullet}CD_3$) that can be used to confirm the identity of target molecules where the methyl is replaced with the deuterated analogue. The addition of methyl radicals to a molecule increases the molecular weight by 15 Da whereas the deuterated analogue increases it by 18 Da. Using these principles of comparing the mass spectra of normal against deuterated analogues, other organic molecules such as aldehydes may be utilised to generate secondary radicals for spin trap studies.

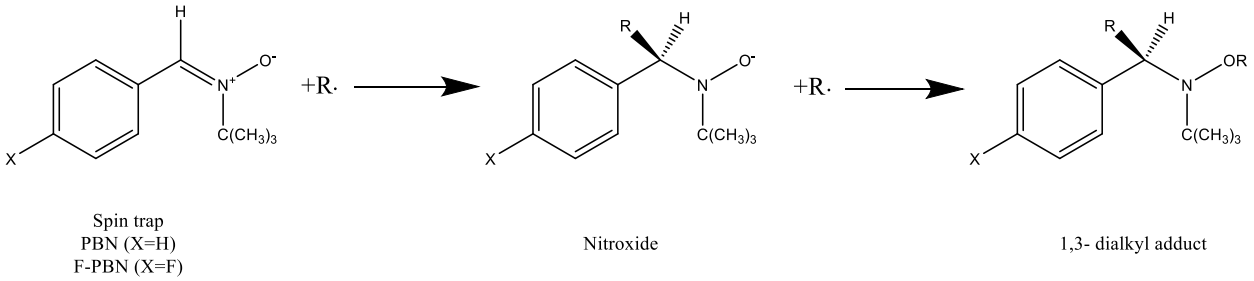

Figure 1.16.2 Addition of aldehyde-derived alkyl radicals on the spin trap (adapted from Manzoor, 2018).

1.17 Isomerism

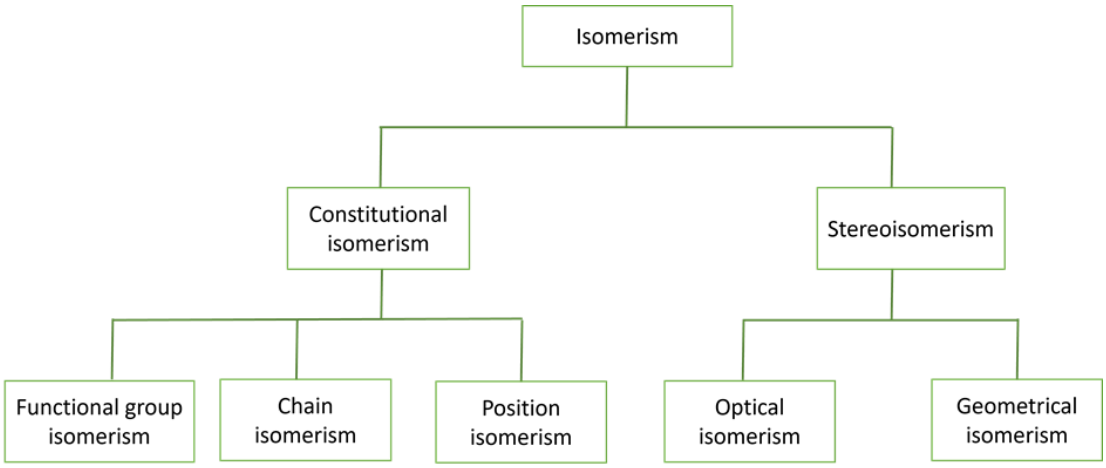

Figure 1.17.1 Isomerism diagram (adapted from Bulugahapitiya, (2020)

Isomers are compounds with the same molecular formulae but different structural formulae. (see Figure 1.17.1). Many different types of isomers are ubiquitous and play important roles in living organisms. Despite their early discovery, the actual analysis of isomers has been challenging and has confounded researchers. Using mass spectrometry (MS) to distinguish or identify isomers is an emerging topic and challenge for analytical chemists. For isomer identification/detection various approaches have been developed and applied since the early 1900s:spectroscopy (infra-red spectroscopy, Raman, NMR), X-ray crystallography, and optical rotation techniques especially for chiral compounds (circular dichroism and optical rotation dispersion) to name a few (Furuhashi and Okuda, 2017). The X-ray approach has the advantage of investigating not only structural differences between isomers but also conformational differences between compounds.

PBN exhibits geometric isomerism due to the double bond in the nitrone group where two possible configuration are possible (Reeves Huie, 1987). Ultraviolet spectral and NMR studies indicated that PBN exists in the stable trans form. The E (cis) form of this nitrone was formed when 2-tButyl-3-phenyloxazirane was treated with Boron trifluoride however complete isomerization to the Z (trans) form occurred within 24 hours in benzene solution (Hamer and Macaluso, 1964). The reason for this appears to be the presence of repulsive non-bonded steric interactions between the phenyl and N-alkyl groups in the E-form (see Figure 1.17.2), especially for the N-tert-alkyl groups, that are absent in the Z-form.

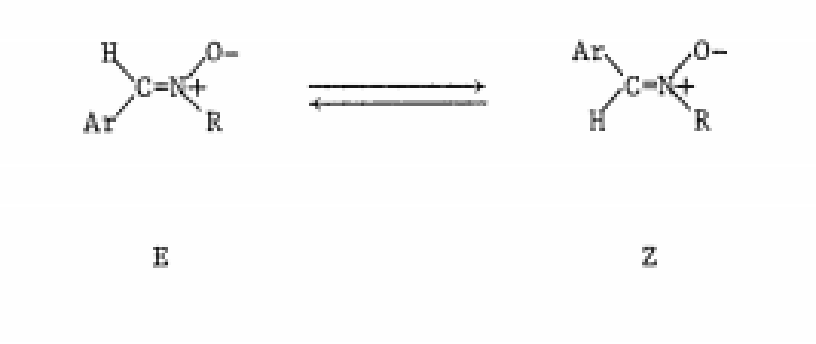

Figure 1.17.2 The two geometric isomers of PBN (from Reeves Huie, 1987)

One of the limitations of GC is its inability to separate enantiomers (non-superimposable mirror image molecules) since they have identical properties, they elute at the same time however diastereomers can be separated using GC as they have different chromatographic properties.

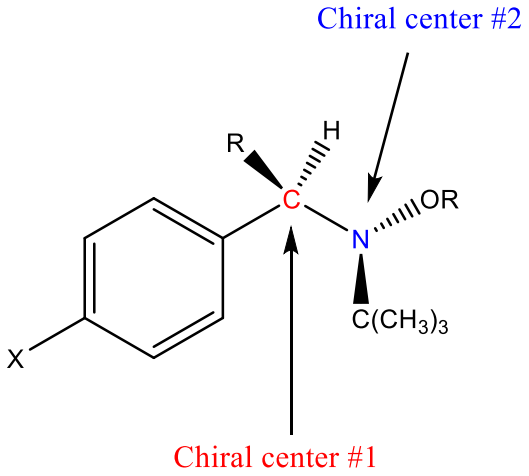

Figure 1.17.3 showing the chiral centres of PBN adducts

PBN when in the nitroxide form or di-adduct form exhibits optical isomerism and is a chiral compound with multiple stereogenic sites. The chirality (handedness) of enantiomeric molecules is caused by the presence of one or more chiral elements (chirality axis, chirality plane, or chirality centre, e.g., asymmetric carbon atom) in the structure(Evans and Kasprzyk-Hordern, 2014). The alpha carbon (see Figure 1.17.3,in red) when adducted to a species other than hydrogen is asymmetric due to 4 different species including hydrogen, the nitrogen, the phenyl group and the R group being investigated. The other chiral centre is the nitrogen (see Figure 1.17.3,in blue) which exhibits optical isomerism due to the alpha carbon, the oxygen, the tertiary butyl group and a lone pair of electrons on the nitrogen.

Today, considering the commercial availability, sensitivity and wide range of application, chromatographic separation coupled to mass spectrometry (i.e., GC-MS, CE-MS (capillary electrophoresis-mass spectrometry), LC-MS) is one of the best choices for isomer analysis for both identification and distinguishing isomers.

Certain isomers can produce different fragmentation patterns with MS. Nonetheless, some biologically important isomers (e.g., saccharides and lipids) remain difficult to separate chromatographically, and their fragmentation patterns can be quite similar or even identical. In the case of identical fragmentation patterns of co-eluted isomers, multidimensional separation techniques (i.e., GCxGC and LCxLC) are not conclusive. Although a retention time index must be developed, the identification as well as the possibility of another co-elution remain unclear.

One method to distinguish isomers is to use hydrogen-deuterium exchange to cause structural differences in isomers. This is done by replacing hydrogens in the analyte by adding deuterium and exchangeable hydrogen site is generated between functional groups of an analyte. For example, hydrogen in carboxylic acid can be replaced with a deuterium (Masson *et al*., 2019).

1.18 Aims and objectives

The primary aim of this study is the separation and mass spectrometric analysis of spin trapped aldehyde free radicals using N-tert butyl-α-phenyl nitrone (PBN) and its derivatives as spin trapping agents. Gas chromatography using solvent extraction via chloroform will be used to extract the compounds for analysis.

Fenton chemistry will be used to produce hydroxyl radicals that will react with butanal and 3-methyl butanal to produce secondary radicals. This is referred to as secondary spin trapping and may be used to confirm the presence of the primary radical (hydroxyl radical) as well as providing information about the radical adduct itself.

For traditional radical detection, EPR is the primary choice for detecting and analysing free radicals however it cannot detect all free radicals, as most radicals are too unstable, and provides limited structural information therefore it is necessary to trap the radicals in a stable form and analyse via GC-MS. Utilising single quadrupole GC-MS allows fragmentation of the molecule providing much more insight into the structural form of the molecules.

2 Materials and Methods section

2.1 Chemicals and reagents

2.1.1 Materials used for PBN and PBN derivative synthesis

Materials used to produce PBN and its derivatives were obtained as follows: 4-Fluorobenzaldehyde, Benzaldehyde, 2-methyl-2-nitropropane (Sigma-Aldrich®, Germany), Benzaldehyde-d_6 (CDN Isotopes, UK), Zinc (GPR, UK), Acetic acid (Acros Organics, Belgium), Ethanol and Diethyl ether for synthesis, Sodium bicarbonate and Sodium sulphate (Sigma-Aldrich®, UK).

2.1.2 Materials used for Fenton reactions

Potassium phosphate (K_2HPO_4), Ethylenediaminetetraacetic acid (EDTA) (Sigma-Aldrich®, Germany), Ammonium ferrous sulphate hexahydrate ($Fe(NH_4)_2(SO_4)_2.6H_2O$) (Fluka biochem, Germany), Ascorbic acid, Acetaldehyde, Propionaldehyde, Chloroform (Sigma-Aldrich®, UK), butanal, 2-Methylbutraldehyde, Valeraldehyde, Hexanal and Hydrogen peroxide 30% stabilized (H_2O_2) (Acros Organics, Belgium).

2.2 Synthesis of PBN derivatives

The synthesis method was adopted from Hinton et. al. (Hinton and Janzen, *1992*). The desired substituted benzaldehyde (10 mmoles), 2-methyl-2-nitropropane (20 mmoles), Zinc (30 mmoles) were placed in a round bottom flask along with 75ml of 95% ethanol. Acetic acid was added gradually (60 mmoles) whilst keeping the solution on ice. The solution was allowed to come to room temperature and continuously stirred for an additional 2 hours. The $Zn(OAc)_2$ was filtered out and the solution was concentrated on a rotary evaporator (Buchi, UK) leaving a clear solid. The solid was dissolved in diethyl ether (50 ml) and extracted with $NaHCO_3$ twice. The organic layer was dried with $MgSO_4$ and the ether was extracted and evaporated off. The resulting solid was recrystallized by allowing it to airdry. The structure was verified by MS analysis and the resulting identities are shown in Figure 2.2.1

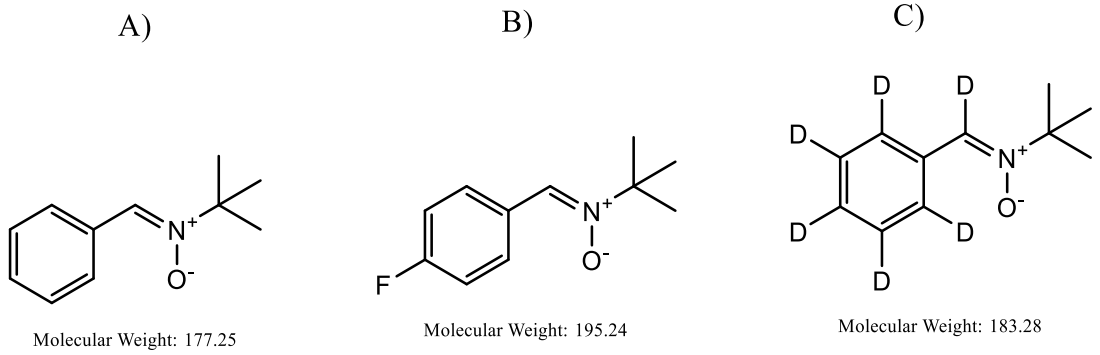

Figure 2.2.1 Structures of the PBN spin traps and derivatives; A) PBN, B) 4-FluoroPBN, and C) PBN-d_6

2.3 The Fenton reaction system

2.3.1 Reagent preparation

Stock solutions were prepared as follows: 100 mM Potassium buffer (pH 7.4), 11 mM EDTA, 100 mM spin trap, 3% H_2O_2, 100 mM Ascorbic acid, 10 mM Ammonium ferrous sulphate hexahydrate, 100 mM secondary radical source.

2.3.2 The Fenton system

The method used throughout the experiments for trapping the radicals via the PBN derivatives was a standard method. The final concentrations of stock solution used was standardised as follows (unless otherwise stated): 50 mM Potassium buffer (pH 7.4), 1.1 mM EDTA, 10 mM PBN, 0.3% H_2O_2, 10 mM Ascorbic acid, 1 mM Ammonium ferrous sulphate hexahydrate, 10 mM secondary radical source (aldehydes). The volumes and final concentration of the various reagents added are in Table 2.1 and the volumes of the secondary source of radicals are listed in Table 2.2

The sodium ascorbate reduces Fe(III) back to Fe(II) allowing for micromolar concentrations of iron to be used Ascorbic acid can act as both an iron chelator and an iron reductant. EDTA is an Fe-chelating agent and stimulates Fe-mediated oxygen radical generation as well as enhancing the autooxidation of Fe(II) (Valko *et al*., 2005)

Table 2.1 Table listing volumes of chemicals used and molar concentrations in the final reaction mix

Reagent	**Stock concentration (mM)**	**Added to reaction mix (ml)**	**Final concentration (mM)**
Potassium buffer	100	5	10
EDTA	11	1	1.1
PBN	100	1	10
F-PBN	100	1	10
D_6-PBN	100	1	10
H_2O_2	3%	1	0.30%
Ascorbic acid	100	1	10
Fe^{2+}	10	1	1
Secondary source	see Table 2.2	See Table 2.2	100

The table labelled Table 2.1 shows the concentrations of the chemicals used in the Fenton reaction. The appropriate spin trap was substituted dependent upon the reaction.

Table 2.2 Table listing volumes and final concentration of secondary sources of radicals

Secondary source	**Final molar concentration (mM)**	**Volume added (µl)**
Butanal	100	72
Butanal-2,2,-d_2	100	76
Butanal-2,2,3,3,4,4,4-d_7	100	86
3-methylbutanal	100	86
3-methylbutanal-2,2,-d_2	100	90
DMSO	100	78
DMSO--d_6	100	86

2.4 Extraction techniques- Direct chloroform extraction

The reaction was run for exactly 5 minutes before 1 ml of the reaction mix was aliquoted to 2 ml of chloroform and allowed to equilibrate for a further 2 minutes and finally 1µL was extracted from the organic phase and injected directly into the GC column.

2.5 Instrumentation

2.5.1 GC-MS

Gas chromatography (GC) and mass spectrometry (MS) is a technique combining the two techniques (GC-MS) by which complex mixtures can be separated, identified, and analysed according to their retention time, mass to charge ratio (*m/z*) and fragmentation pattern.

2.5.2 Gas chromatography

The main purpose of GC is to isolate the chemical of interest from other compounds in a sample mixture and introduce one compound at a time into the MS. Like most other chromatographic techniques, a mobile and a stationary phase are required for this technique. In GC, the mobile phase is composed of a sample and an inert carrier gas (helium, nitrogen, argon) and are passed together through a chromatographic column (stationary phase). The stationary phase consists of a packed column in which the packing or solid support itself acts as the stationary phase or is coated with the liquid stationary phase (high boiling point polymer) The majority of GC systems use capillary columns, where the stationary phase coats the walls of a small-diameter tube directly.

Each substance takes a different amount of time to pass through the column, which results in their separation into fractions. The factors that can influence the separation of these components are; vapor pressure, polarity of components versus the polarity of the stationary phase on the column; column temperature, carrier gas flow rate, column length and amount of material injected.

Highly soluble components need more time than poorly soluble components to be eluted from the liquid phase. The output detector can identify the foreign gas. Each substance can be detected upon its elution time and its amount determined from peak duration and intensity (Garcia-Alcega *et al*., 2017). Gas chromatography first becomes relevant when it can be used to replace physical instruments, for example, GC is a convenient, rapid, precise, and accurate alternative to distillation for measuring boiling points for hydrocarbon mixtures. GC is particularly relevant when hydrocarbon mixtures need to be separated into classes and subclasses such as: saturated hydrocarbons, cyclic alkanes, aromatics, components with heteroatoms, unsaturated alkanes, and combined structures (that cannot be classified in this list) containing aromatic rings. GC has many other applications such as determining the specific components in hydrocarbon mixtures such as such as benzene, toluene, ethyl benzene and xylenes (Schoenmakers *et al*., 2000). Combining GC with mass spectrometry is the most popular technique for analysing biomarkers due its sensitivity (ppb-ppt range)(Kim *et al*., 2016).

2.5.3 Mass spectrometry

The primary purpose of mass spectrometry (MS) is to determine the abundance of a specific mass of ions resulting from the fragmentation of either unlabelled or labelled compounds of interest. At its simplest, a

mass spectrometer is composed of three parts: an ion source for volatilising and ionising the analyte, one or multiple mass analysers and a detector. MS determines the ion-to-charge ratio *m/z*, which requires preliminary ionization of the substance to be detected. Various ionisation processes occur: electron impact; chemical and laser ionisation. The ions created are separated and identified. The separation is based on the difference between ion paths in a magnetic field and/or electrostatic field. The ions are subsequently identified via photomultipliers (Vaks *et al*., 2014).

2.5.4 Single quadrupole mass spectrometry

Single quadrupole mass spectrometry is a scanning mass analyser that uses the stability of ion trajectories in oscillating electrical fields to separate the ions based on their mass-to-charge (*m/z*) ratios. It is comprised of four rods arranged in parallel with a constant DC potential applied to each rod, one pair positive and the other negative, on opposing planes. An RF voltage is superimposed over the DC potential on each rod pair causing the ions to spiral as they transverse the quadrupole towards the detector, acting as a high and low pass filter.

2.5.5 Electron ionization

Electron ionization is a method in which excited electrons interact with gas phase and solid phase atoms to produce ions. Figure 2.5.1 describes how ionization "strips" analytes of electrons resulting in a molecular ion ($M^{+\bullet}$) (Davis and Frearson, 1987)

Figure 2.5.1 The electron ionization reaction. M is the analyte being ionized, e^- is the electron and $M^{+\bullet}$ is the resulting molecular ion

The diagram in Figure 2.5.2 shows the components of a gas chromatograph and quadrupole mass spectrometer. The carrier gas is usually helium, and as the sample is injected into the injection port it is volatilised and further heated during its passage through the GC column in the oven. Based upon the components of the sample it will be portioned between the mobile and stationary phase. As the sample exits the column it is ionised in an electron beam and concentrated by the quadrupole into an ion beam which is detected on a photomultiplier based upon the mass/charge ration of the molecule. This is then registered and sent to a computer for analysis .

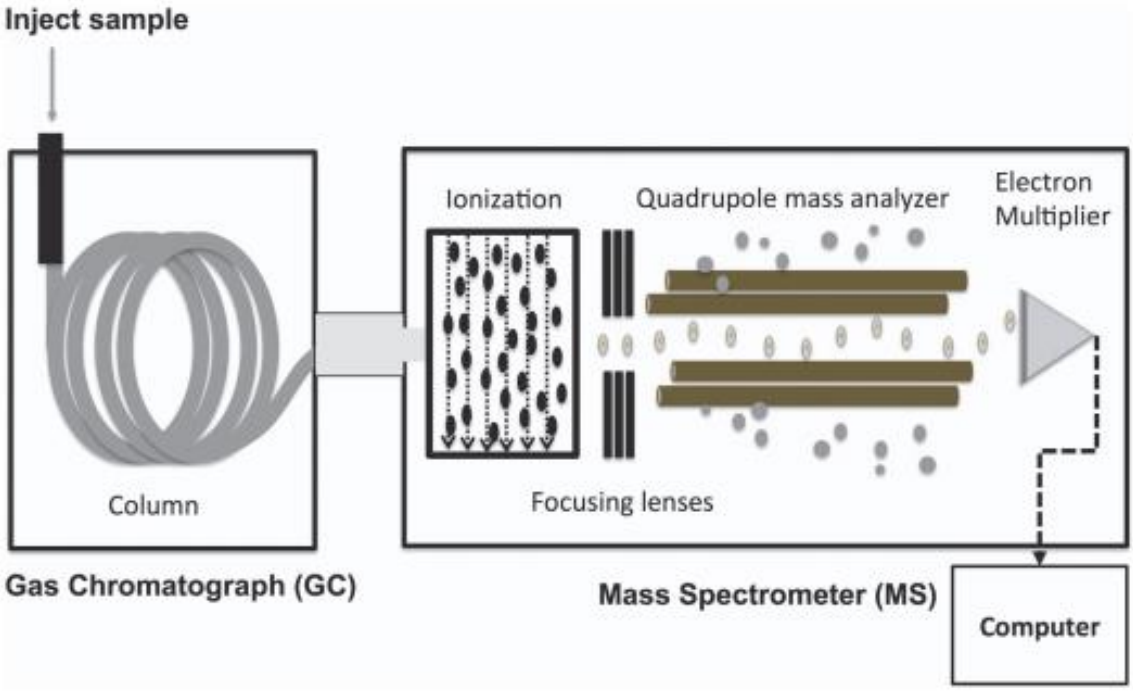

Figure 2.5.2 diagram depicting the major components and principles of GC-MS.

2.6 Instrumentation

2.6.1 GC-MS equipment

The instrument used was a Clarus© 580 (Perkin Elmer, UK) gas chromatograph coupled to a Clarus© SQ 8 S (Perkin Elmer, UK) mass spectrometer equipped with a Thames Restek Rxi-5ms 30m x 0.25mm, 0.25 µm capillary column using a polydimethylsiloxane stationary phase.

2.6.2 Method development

Free radicals were produced using Fenton chemistry as detailed earlier in this chapter. A series of experiments were carried out to validate the Fenton system (detailed in section 2.7). butanal, 3-methyl butanal and DMSO were used as secondary sources of free radicals for the development and validation of the Fenton system.

2.6.3 Method parameters

The GC setting were as follows: Inlet liner set to 250°C, injection port set to 200°C, Solvent delay set at 2 minutes, spitless injection, split 1:100 applied 1-minute post injection, initial column temperature set at 100°C for 2 mins and ramp increase set at 10°C/minute 300°C where it held for a further 2 minutes (total time for a run was 24 minutes). The MS settings were as follows: scan from 2 minutes post injection, scan range 50-500 *m/z,* photomultiplier set to 2000V voltage was used throughout, detector and ion source

were set to 250°C, total ion chromatograms were recorded and Turbomatrix© was used as the workstation. Helium was used as the carrier gas with a flow rate of 1mL/minute. 1 µL of sample was injected onto the column. The methods was optimised from studies carried out by Manzoor, (*2018)*

2.7 Control experiments

To validate the methods described a series of control experiments were carried out

2.7.1 The reaction mixture without the iron

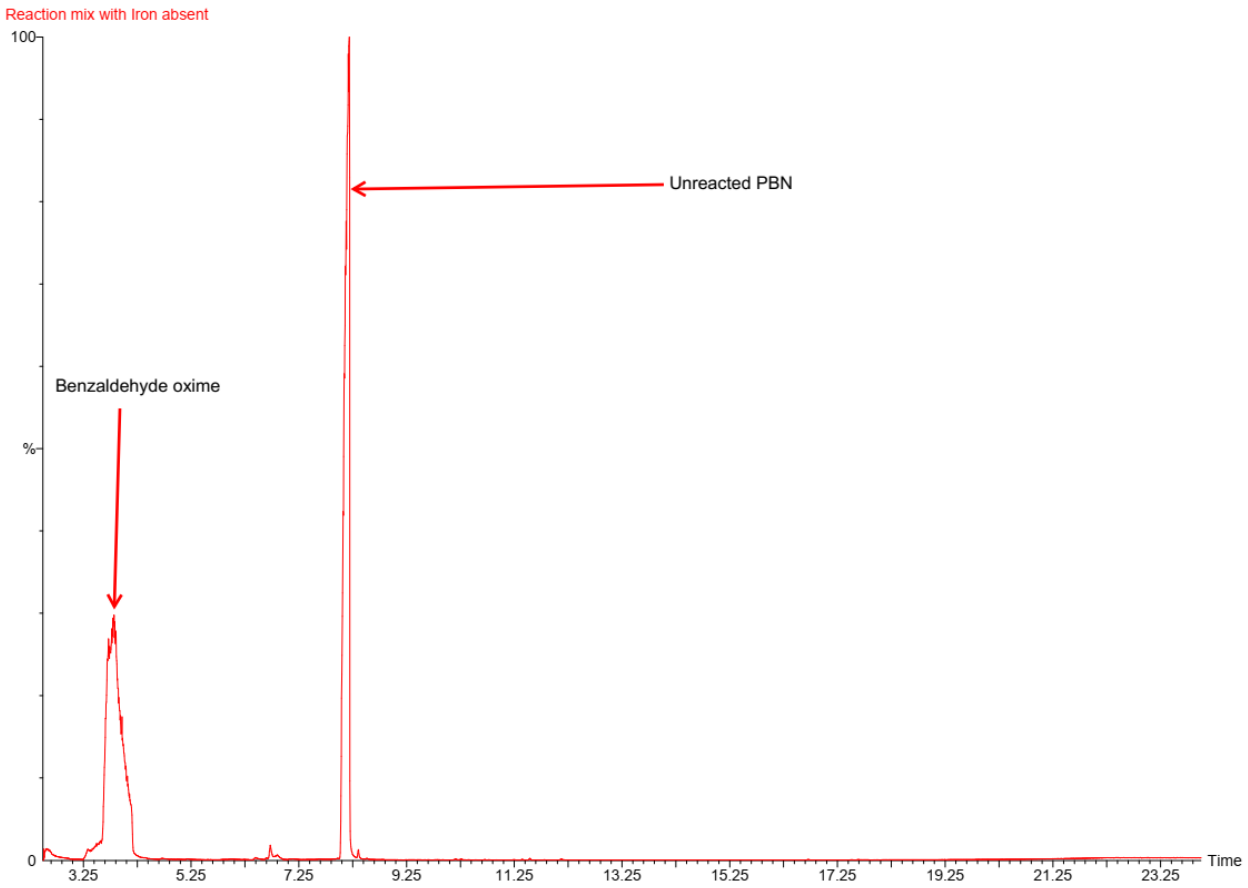

Figure 2.7.1 The total ion chromatogram obtained from the GC-MS analysis of the Fenton system with PBN in the absence of Fe^{2+} and EDTA

To confirm that the Fenton reaction is the source of the hydroxyl radicals and initiates the dissociation of hydrogen peroxide into hydroxyl radicals, the reaction was run without iron in the form of ammonium ferrous sulphate hexahydrate ($Fe(NH_4)_2(SO_4)_2.6H_2O$). Only 2 significant peaks derived from PBN. The peak at 6.72 minutes is discussed in the appendix.

2.7.2 The reaction mixture without H_2O_2

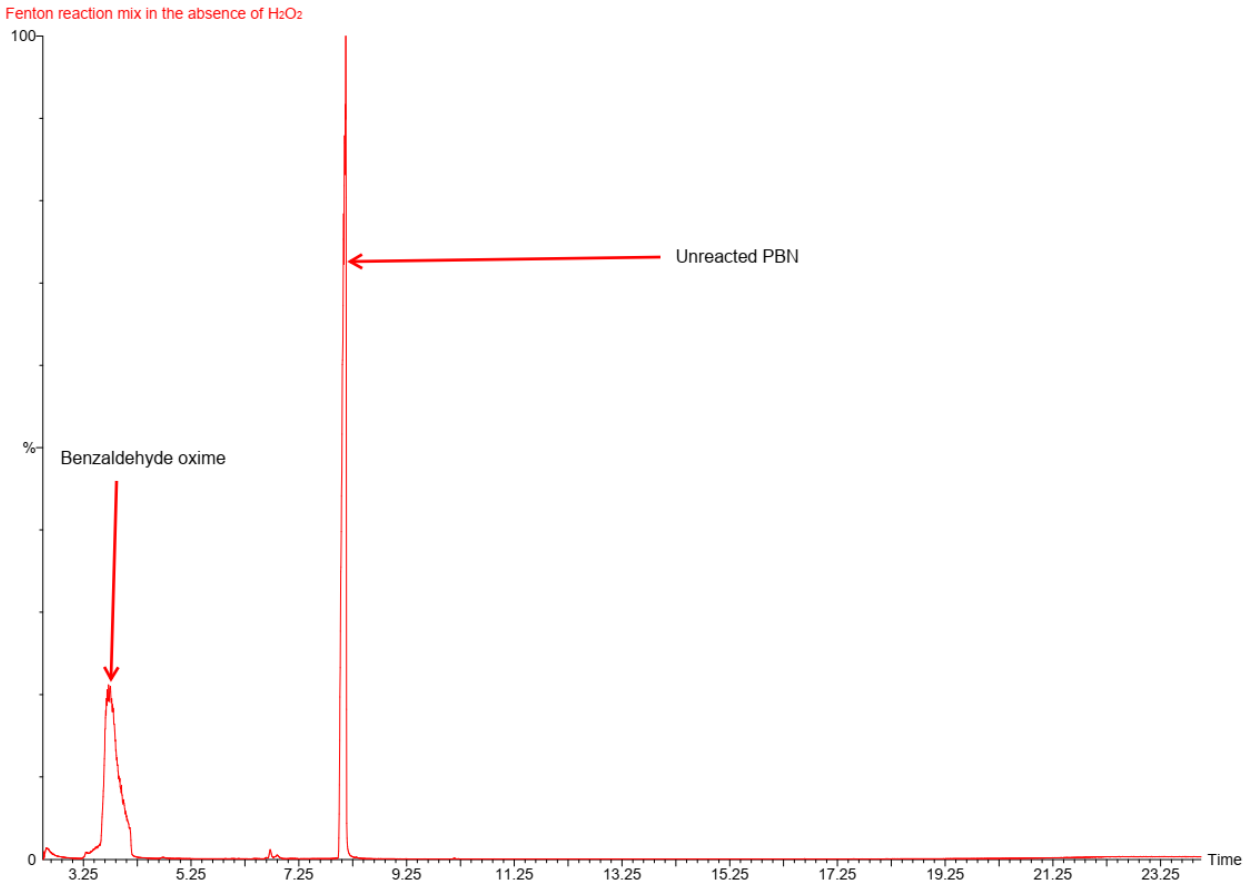

Figure 2.7.2The total ion chromatogram obtained from the GC-MS analysis of the Fenton system with PBN in the absence of H_2O_2

To confirm H_2O_2 is the source of the hydroxyl radicals, the Fenton reaction was run without hydrogen peroxide in the presence of PBN. The TIC shows no major peaks apart from the peak for unreacted PBN at 8.1 minutes and the peak at 3.6 minutes is a combination of multiple peaks for the benzaldehyde oxime/PBN hydroxylamine. It is ambiguous as to presence of the benzaldehyde oxime or whether it's a breakdown product due to the heat of the injector port and GC oven. It is clear the retention time is considerably less than PBN. There is also a small peak at 6.72 minutes (see section 4.13.1)

Chapter 3

3 Detection and analysis of hydroxyl radical products of N-tert-butyl-a-phenyl nitrone (PBN) and selected derivates using liquid injection gas chromatography-mass spectrometry

In this study, hydroxyl radicals were generated from Fenton chemistry. These hydroxyl radicals were then trapped by PBN and its derivatives to form stable adducts and sampled using liquid-liquid extraction with chloroform as a solvent. The extracted samples were subjected to GC/MS for detection and analysis. Numerous PBN radical adducts were identified and characterised and will be discussed in this following chapter.

3.1 Chromatograms of hydroxyl radical products of PBN and selected derivatives in the absence of a secondary source of free radicals

3.1.1 PBN

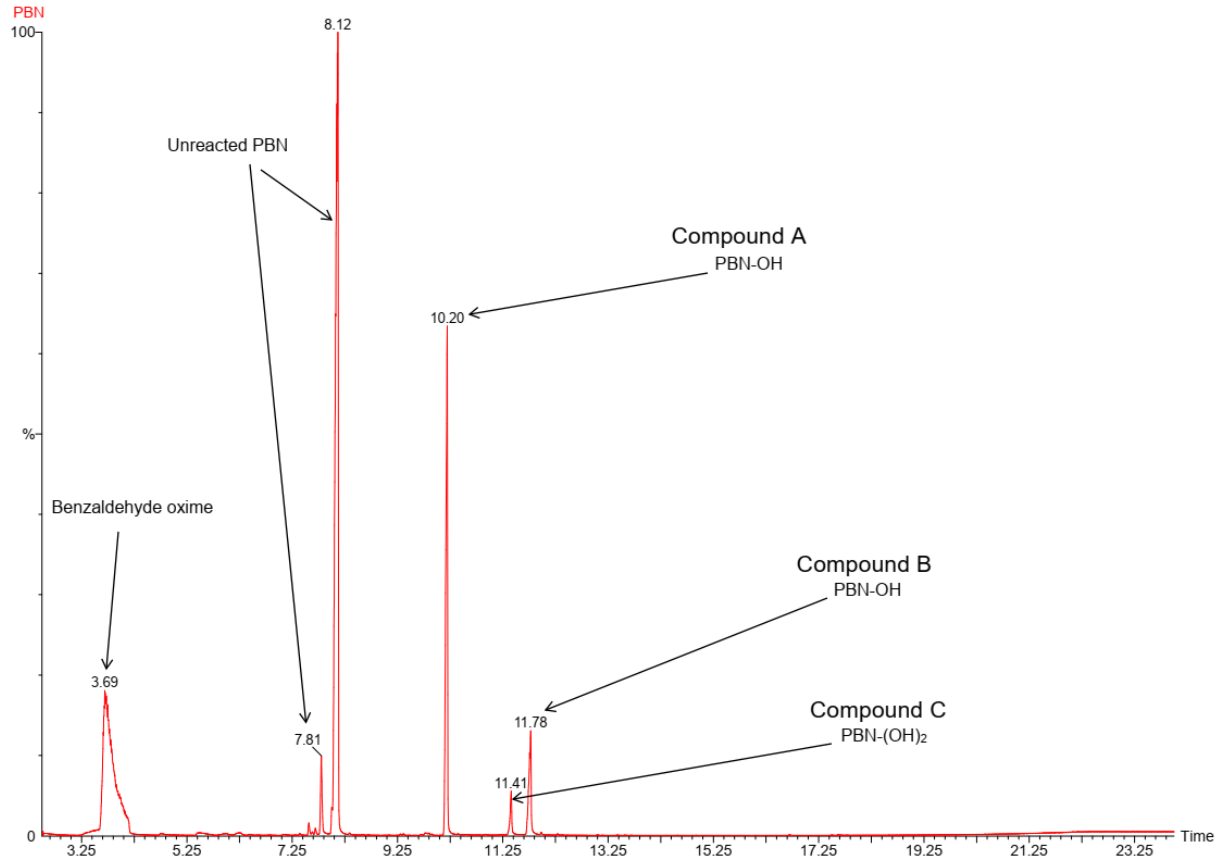

Figure 3.1.1 The total ion chromatogram obtained from the GC-MS analysis of the Fenton system with PBN in the absence of a secondary radical source.

The chromatogram in Figure 3.1.1 shows 6 peaks identified of which three may be assigned as PBN hydroxyl adducts, a mono hydroxyl adduct to the phenyl ring (ortho/meta) of the spin trap {PBN-OH; 10.2 minutes; Compound **A** (Figure 3.1.2)}; a second mono-hydroxyl adduct to the phenyl ring (para) of the spin trap; {PBN-OH; 11.78 minutes; Compound **B** (Figure 3.1.2)}; and a dihydroxyl adduct to the phenyl ring of the spin trap; {PBN-$(OH)_2$; 11.41 minutes; Compound **C** (Figure 3.1.2)}. Two of the peaks can be assigned to unreacted PBN (7.81 minutes and 8.12 minutes). The PBN seems to have eluted in two peaks with similar retention times. This is possibly due to the E and Z isomers having different retention times. The broad peak at 3.69 minutes is seen in control experiments in the absence of either Fe^{2+} or hydrogen peroxide (see appendix). It appears to consist of two overlapping peaks with one of the compounds having

an EI-MS spectral pattern consistent with benzaldehyde oxime. This compound has been observed previously by GC-MS when using PBN as a spin trap (Castro *et al*., 1997, 1998)

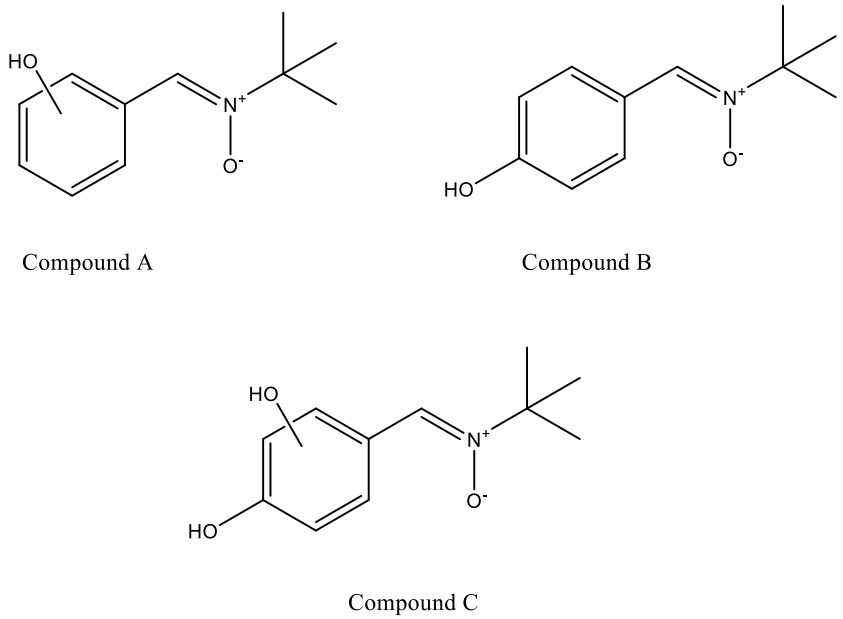

Compound A

Compound B

Compound C

Figure 3.1.2 The structures of compounds identified by GC-MS analysis of a Fenton-based reaction mixture containing PBN.

3.1.2 d_6-PBN

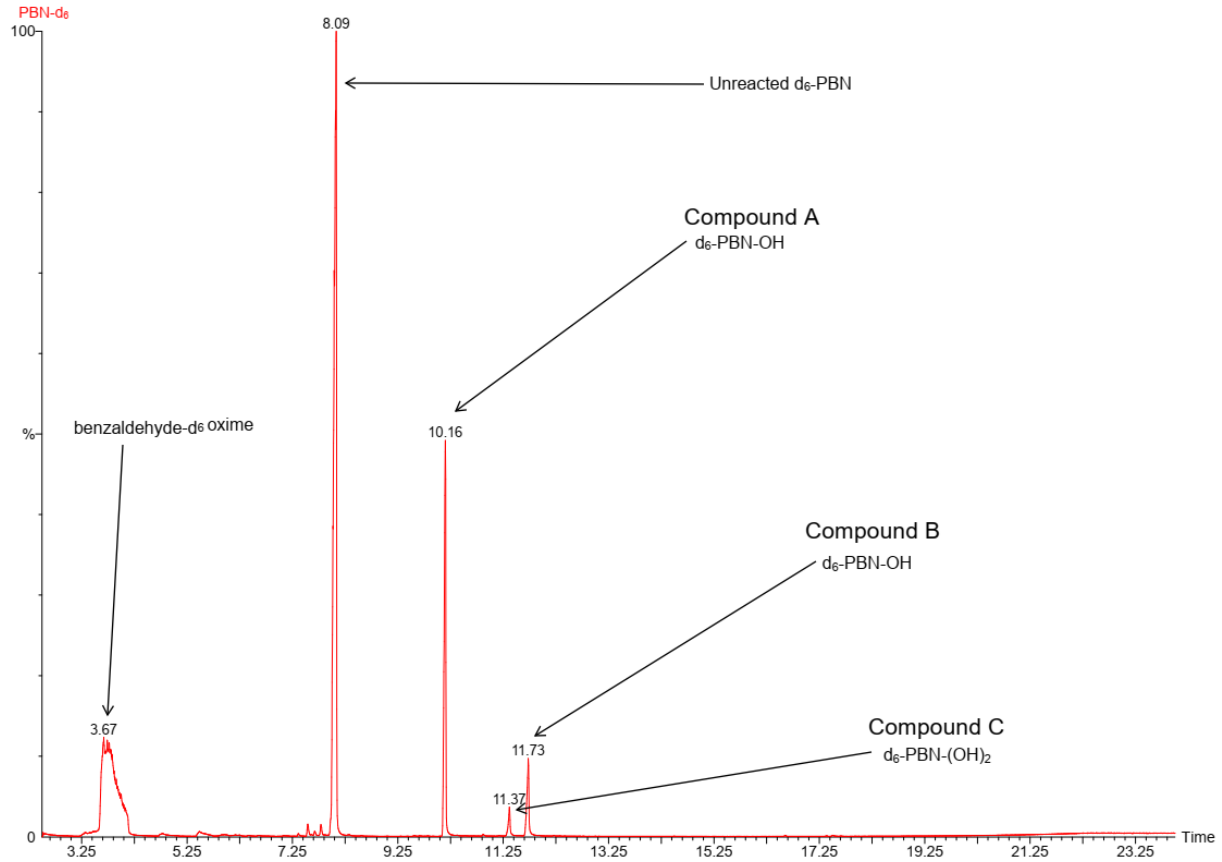

Figure 3.1.3 The total ion chromatogram obtained from the GC-MS analysis of the Fenton system with PBN-d_6 in the absence of a secondary radical source

The chromatogram in Figure 3.1.3 shows 5 peaks identified of which three may be assigned as PBN-d_6 hydroxyl adducts, a mono hydroxyl adduct to the phenyl ring (ortho/meta) of the spin trap {PBN-d_6-OH; 10.16 minutes; Compound **A,** (Figure 3.1.4)}; a second mono-hydroxyl adduct to the phenyl ring (para) of the spin trap; {PBN-d_6-OH; 11.73 minutes; Compound **B,** (Figure 3.1.4)}; and a dihydroxyl adduct to the phenyl ring of the spin trap; {PBN-$(OH)_2$; 11.37 minutes; Compound **C,** (Figure 3.1.4)}. Two of the peaks can be assigned to unreacted PBN-d_6 (8.09 minutes) and the PBN- d_6-Benzaldehyde oxime /PBN-d_6 Hydroxylamine (rt 3.67 minutes).

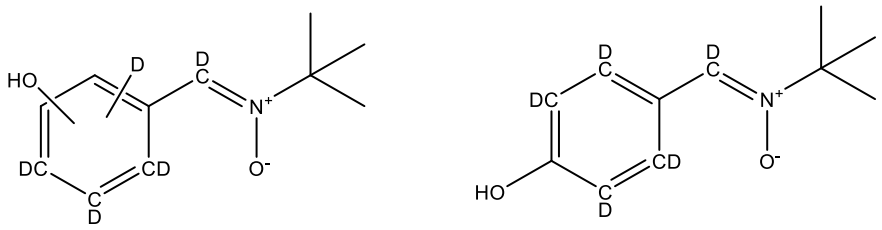

Compound A

Compound B

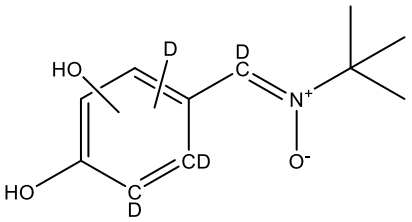

Compound C

Figure 3.1.4 The structures of compounds identified by GC-MS analysis of a Fenton-based reaction mixture containing PBN-d_6

3.1.3 F-PBN

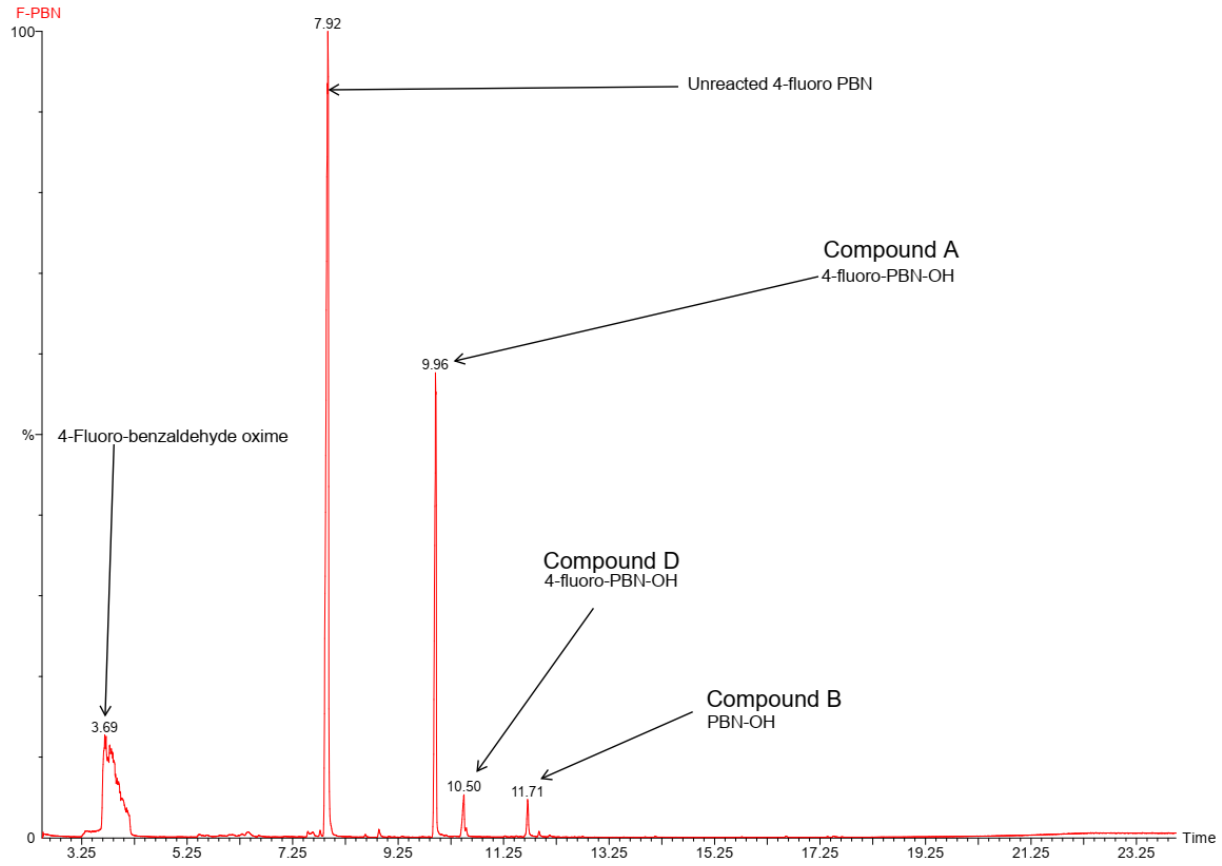

Figure 3.1.5 The total ion chromatogram obtained from the GC-MS analysis of the Fenton system with F-PBN in the absence of a secondary radical source

The chromatogram in Figure 3.1.5 shows 5 peaks identified of which three may be assigned as F-PBN hydroxyl adducts, a mono hydroxyl adduct to the phenyl ring (ortho/meta) of the spin trap {F-PBN-OH; 9.96 minutes; Compound **A** (Figure 3.1.5)}; a second mono-hydroxyl adduct to the phenyl ring (para) of the spin trap; {PBN-OH; 11.71 minutes; Compound **B** (Figure 3.1.5)}; and another monohydroxyl adduct to the phenyl ring of the spin trap; {FPBN-(OH); 10.5 minutes; Compound **D** (Figure 3.1.5)}. One of the peaks can be assigned to unreacted F-PBN (7.92 minutes) and the other is associated with the fluorobenzaldehyde oxime and F-PBN hydroxylamine (3.69 minutes). It cannot be elucidated for certain as to the position of the hydroxyl on the phenyl and whether it has added to the ortho or meta positions for compounds B and D.

3.2 Electron ionization-mass spectra (EI-MS) of PBN products

3.2.1 PEAK at 3.69 minutes- Hydroxylamine PBN

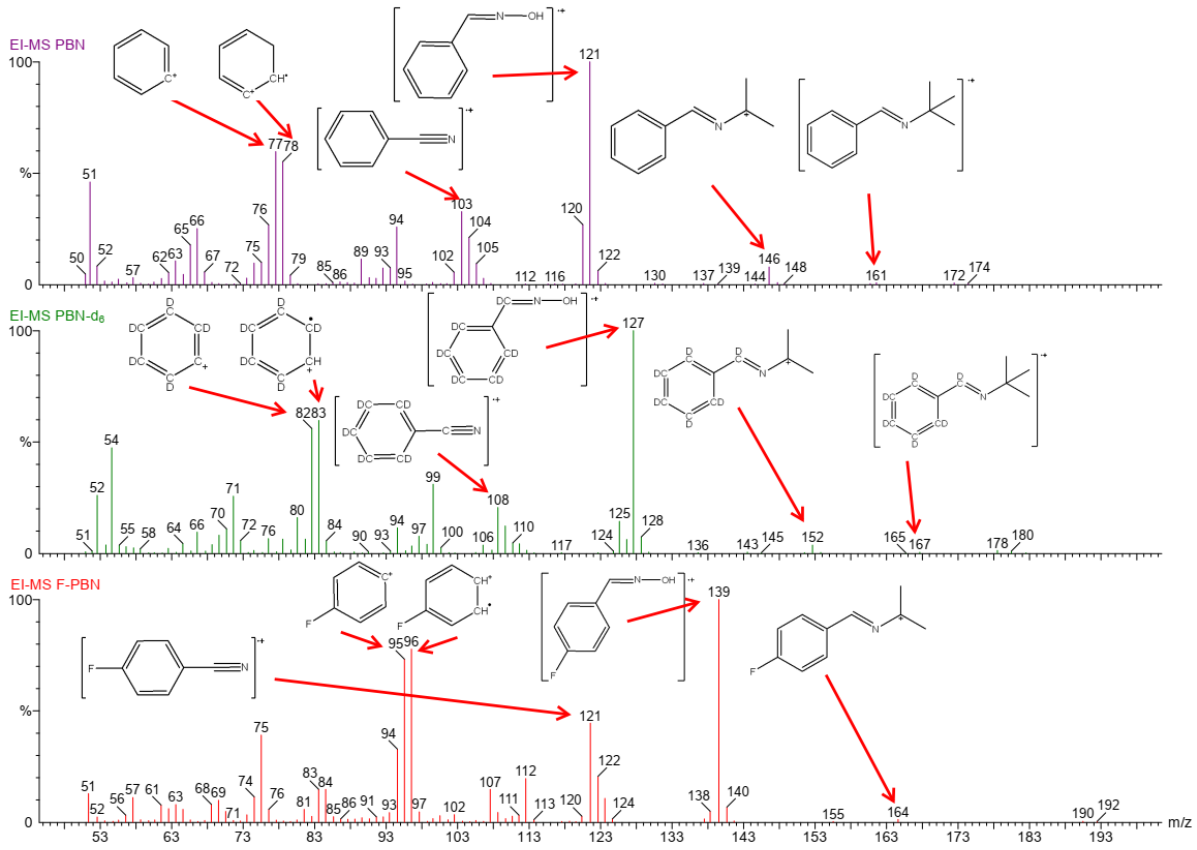

Figure 3.2.1 Electron Ionisation mass spectra corresponding to benzaldehyde oxime (EI-MS) obtained from the analysis of the Fenton reaction mixture containing PBN, PBN-d_6 and F-PBN at rt 3.69 minutes

The EI-MS in Figure 3.2.1 for the peak retained at rt 3.69 minutes corresponds to the hydroxylamine of PBN with a molecular ion at *m/z* 178 (EI-MS PBN); *m/z* 184 (EI-MS PBN-d_6); *m/z* 196 (EI-MS F-PBN). As the molecular ions are too weak, they do not appear on the spectra.

When PBN was used as the spin trap, the peak retained at 3.69 minutes is the combined benzaldehyde oxime and hydroxylamine of PBN. The expected peak at 178 *m/z* units would correspond to the molecular ion of PBN-OH (hydrogen adding to the oxygen) however is too weak to be visible. The fragment at *m/z* 161 is due to the loss of oxygen. The fragment at *m/z* 146 is due to the loss of a methyl group from the former fragment and is lost from the tertiary butyl (tBu) group). The loss of the tBu group from the molecular ion results in the base peak *m/z* 121, and the loss of oxygen from this fragment results in the

benzonitrile radical cation at *m/z* 103. The dissociation of the alpha carbon bond and the nitrogen gives the phenyl radical cation peak at *m/z* 78 and phenyl cation peak *m/z* 77. The peak at m/z 121 is also the molecular ion of the benzaldehyde oxime.

When PBN-d_6 was used as the spin trap, the peak retained at 3.69 minutes was the hydroxylamine of PBN-d_6. The expected peak at 184 *m/z* units would correspond to the molecular ion of PBN-d_6-OH (hydrogen adding to the oxygen) however is too weak to be visible. The fragment at *m/z* 167 is due to the loss of oxygen. The fragment at *m/z* 152 is due to the loss of a methyl group from the former fragment and is lost from the tertiary butyl (tBu) group). The loss of the tBu group from the molecular ion results in the base peak *m/z* 127 and the loss of oxygen from this fragment results in the benzonitrile-d_5 radical cation at *m/z* 108. The dissociation of the alpha carbon bond and the nitrogen gives the phenyl-d_5 radical cation peak at *m/z* 83 and phenyl-d_5 cation peak *m/z* 82

When 4F-PBN was used as the spin trap, the peak retained at 3.69 minutes was the hydroxylamine of F-PBN. The expected peak at 196 *m/z* units would correspond to the molecular ion of PBN-d_6-OH (hydrogen adding to the oxygen) however is too weak to be visible. The expected fragment at *m/z* 179 (also too weak to be detected) is due to the loss of oxygen. The fragment at *m/z* 164 is due to the loss of a methyl group from the former fragment and is lost from the tertiary butyl (tBu) group). The loss of the tBu group from the molecular ion results in the base peak *m/z* 139 and the loss of oxygen from this fragment results in the 4-fluorobenzonitrile radical cation at *m/z* 121. The dissociation of the alpha carbon bond and the nitrogen gives the 4-fluorophenyl radical cation peak at *m/z* 83 and phenyl-d_5 cation peak *m/z* 82

3.2.2 PEAK at 8.12 minutes - PBN and its derivatives

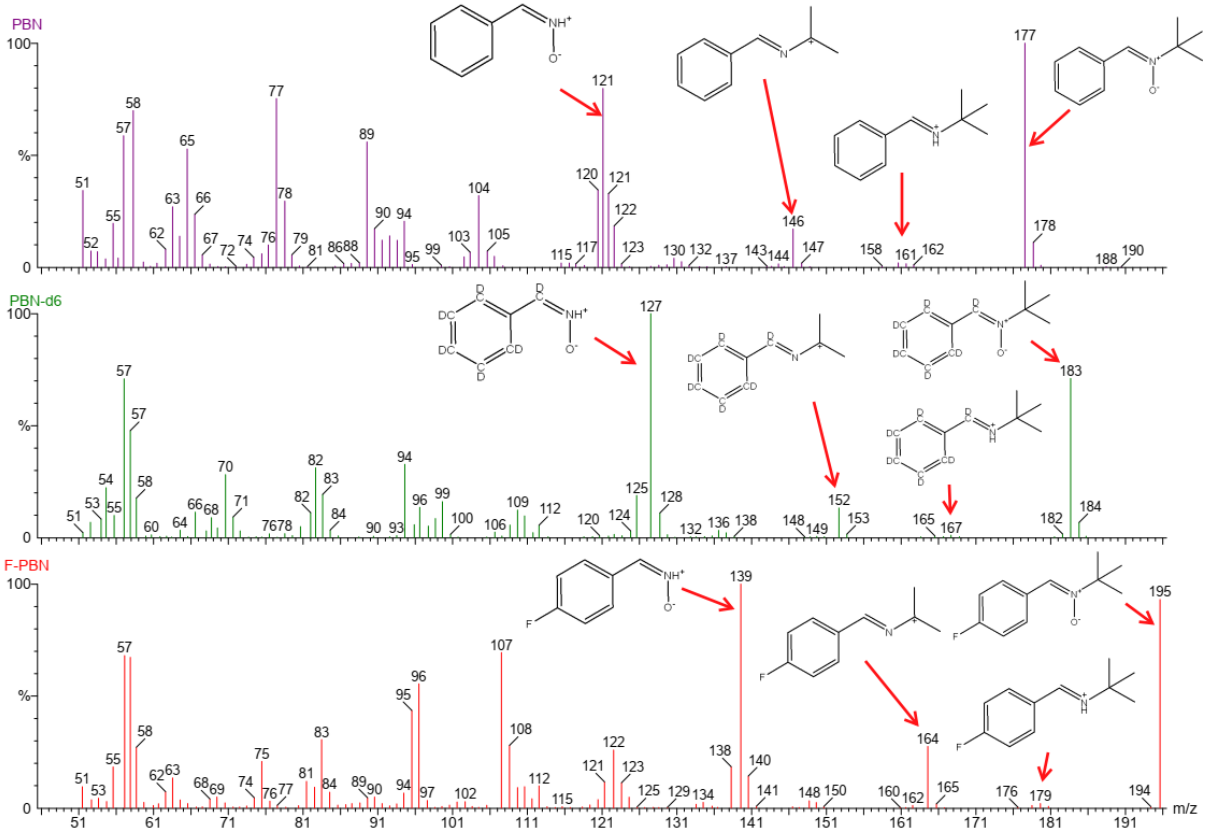

Figure 3.2.2 Electron Ionization mass spectra corresponding to PBN and its derivatives (EI-MS) obtained from the analysis of the Fenton reaction mixture containing PBN (top), d_6PBN (middle) and F-PBN (bottom) at rt 8.11 minutes

The EI mass spectra in Figure 3.2.2 correspond to a) PBN unreacted, (top spectrum), b) the PBN-d_6 unreacted (middle spectrum) and c) F-PBN unreacted(bottom spectrum).

Many chromatograms in this thesis contain the peak corresponding to PBN and its derivatives. The mass spectra for this peak are shown in Figure 3.2.2. The EI-mass spectrum for PBN (top spectrum) shows the molecular ion at *m/z* 177. Other key fragments include; *m/z* 161, *m/z* 146, *m/z* 121 benzaldehyde oxime (loss of the tertiary butyl (tBu) group from the nitrogen), *m/z* 104 phenyl methanimine cation, *m/z* 77 phenyl cation and *m/z* 57 tertiary butyl cation.

The EI mass spectrum for PBN-d_6 (middle spectrum) shows the molecular ion for PBN-d_6 at *m/z* 183 and for F-PBN at *m/z* 195. Other key ions include *m/z* 161 for PBN becoming *m/z* 152 for PBN-d6 and *m/z*

164 for F-PBN (loss of a methyl from the tBu group); base peak *m/z* 121 for PBN becoming *m/z* 127 for PBN-d6 and *m/z* 139 for F-PBN (loss of the tBu group from the nitrogen); *m/z* 77 for PBN becoming *m/z* 82 for PBN-d6 and *m/z* 95 for F-PBN (the phenyl cation with +5*m/z* for deuterons and +18 *m/z* for fluorine).

Table 3.1 Identity of PBN and derivatives

	identity	Rt	*m/z*
PBN	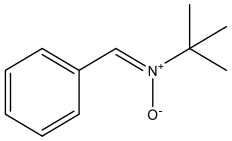	8.116	177
D6-PBN	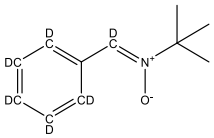	8.066	183
F-PBN	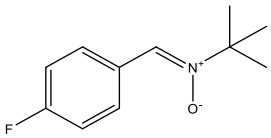	7.916	195

3.2.3 EI-MS of product of hydroxyl radical attack on phenyl ring of PBN-X @r.t. 10.20 Compound A

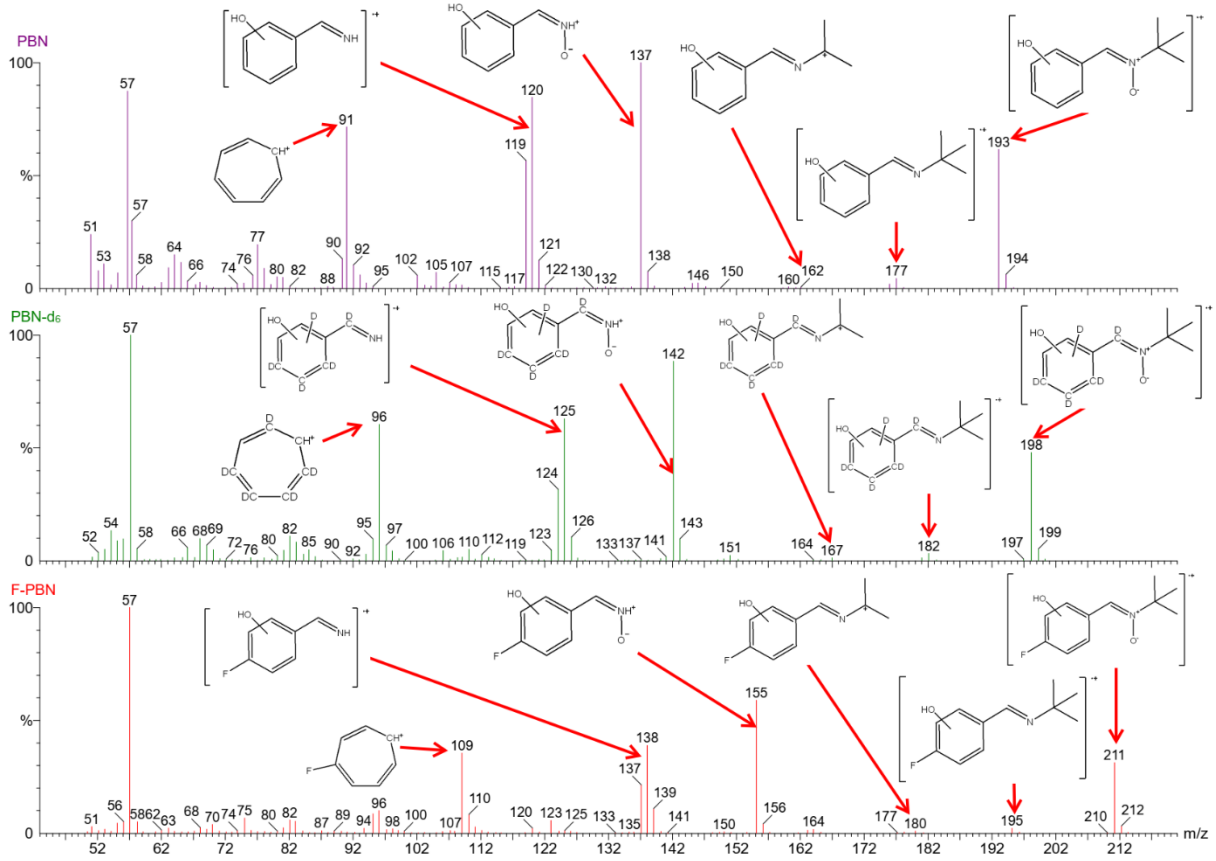

Figure 3.2.3 Electron Ionization mass spectra corresponding to PBN and its derivatives (EI-MS) obtained from the analysis of the Fenton reaction mixture containing PBN (top), d_6PBN (middle) and F-PBN (bottom) at rt 10.20 minutes

The Fenton reaction was carried out without any secondary source of radicals. This allowed the formation of a PBH-OH adduct. Hydroxyl radicals generated in the Fenton reaction were trapped by PBN to form PBN-OH. The EI-MS in Figure 3.2.3 for the peak retained at rt 10.20 minutes corresponds to the PBN-OH with a molecular ion $M^{+\bullet}$ at 193 (EI-MS PBN); $M^{+\bullet}$ 198 (EI-MS PBN-d_6); $M^{+\bullet}$ 211 (EI-MS F-PBN). The identities of the adduct are shown in

Table 3.2When the Fenton reaction was carried out in the presence of hydrogen peroxide as a primary source of radicals, and PBN as the spin trap, the hydroxyl radicals generated are trapped by PBN (top spectrum). The peak at 193 *m/z* units corresponds to the molecular ion of PBN-OH (one hydroxyl radical substituting a hydrogen atom on the phenyl ring. The fragment at *m/z* 177 is due to the loss of an oxygen from the molecular ion. The further loss of a methyl from the tBu. The loss of CH_2=CMe_2 from the molecular ion results in the base peak *m/z* 137 and further dissociation of oxygen from the nitrogen gives the radical cation peak at *m/z* 120. Further breakdown of this fragment results in a tropylium cation at *m/z* 91. The peak at *m/z* 57 is the tertiary butyl cation and is a characteristic fragmentation peak of PBN (Hinton and Janzen, 1992)

The addition of 16 *m/z* to the PBN indicates that a hydroxyl has replaced a hydrogen on the phenyl ring and this is further supported by the addition of 15 *m/z* units to PBN-d_6 (addition of 17 *m/z* and the loss of 2 *m/z*) indicating the substitution of a deuterium atom.
Analysis of the spectrum and those of the PBN derivatives show that the hydroxyl radical has added to either the meta or ortho position on the benzene ring. It cannot have added to the para position as this hypothesis is eliminated by the presence of the fluorinated adduct confirming that the hydroxyl did not substitute fluorine at the para position of the phenyl ring.

There is no peak in the chromatogram for the hydroxyl radical adduct to the alpha carbon at the C=N bond as previous studies by Hinton and Janzen, (1992) have shown the decay kinetics of the hydroxyl adduct of PBN at this site in aqueous phosphate buffer has been found to be 1st order with half-life of approximately 1 minute and thus cannot be detected directly. This is also supported by the absence of the addition of 17 *m/z* which would have indicated that a hydroxyl radical had added to the alpha carbon.

Table 3.2 Identity of PBN hydroxyl adducts formed at rt 10.20 minutes

	identity	Rt	*m/z*
PBN	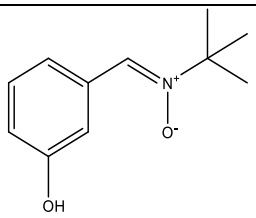	10.20	193
D6-PBN	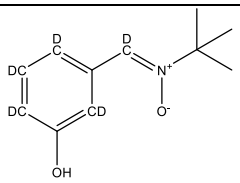	10.15	198
F-PBN	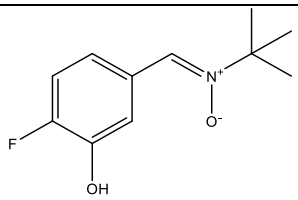	9.96	211

3.2.4 EI-MS of product of hydroxyl radical attack on phenyl ring of PBN-X @r.t. 11.71 Compound B

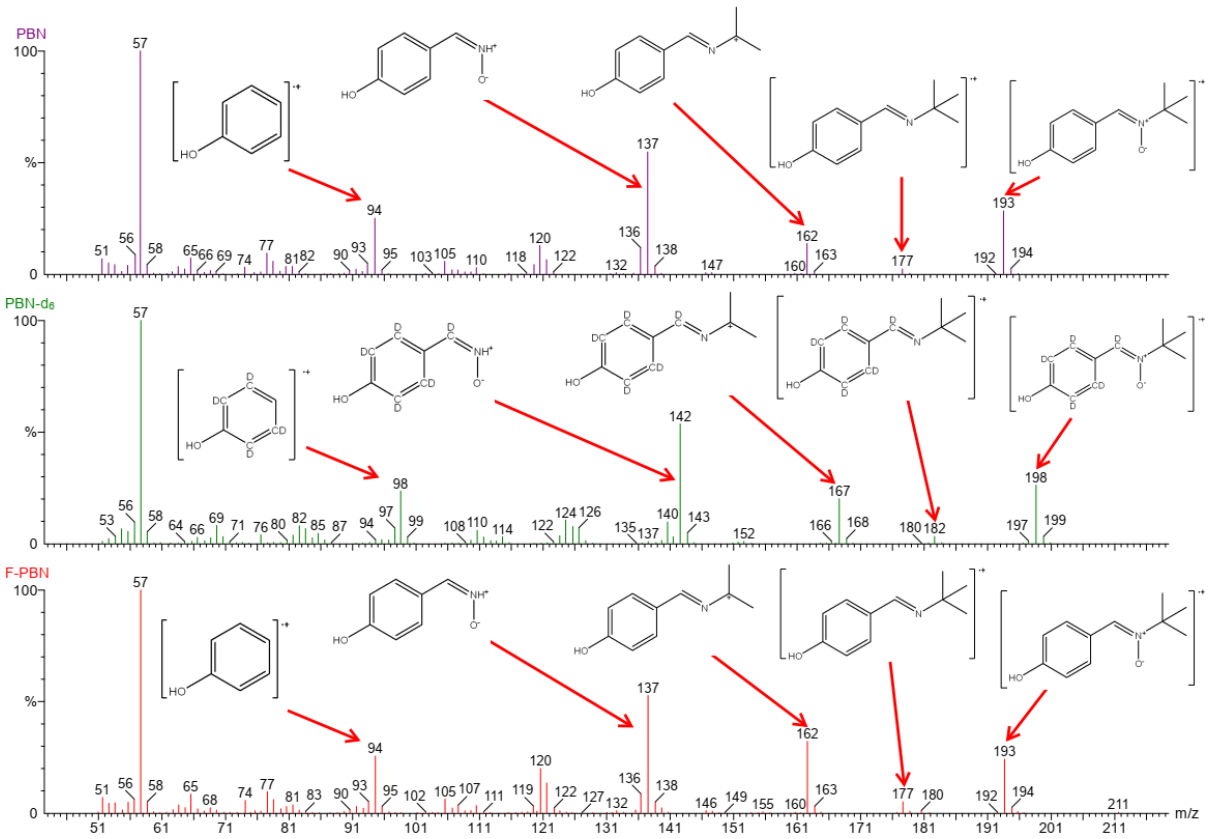

Figure 3.2.4 Electron Ionization mass spectra corresponding to PBN and its derivatives (EI-MS) obtained from the analysis of the Fenton reaction mixture containing PBN, d6PBN and F-PBN at rt 11.71 minutes

The EI-mass spectra in Figure 3.2.4 for the peak retained at rt 11.71 minutes corresponds to the PBN-OH (EI-MS-top); PBN-d_6-OH (EI-MS -middle); F-PBN (EI-MS -bottom). Identities and structures of the adducts are shown in Table 3.3

When the Fenton reaction was carried out in the presence of hydrogen peroxide as a primary source of radicals, and PBN as the spin trap, the hydroxyl radicals generated are trapped by PBN (top spectrum). The peak at 193 *m/z* units corresponds to the molecular ion of PBN-OH (one hydroxyl radical substituting a hydrogen atom on the phenyl ring. The fragment at *m/z* 177 is due to the loss of an oxygen from the molecular ion. The further loss of a methyl from the tBu. The loss of CH_2=CMe_2 from the molecular ion results in the base peak *m/z* 137 and further dissociation of oxygen from the nitrogen gives the radical cation peak at *m/z* 120. The peak at *m/z* 57 is the tertiary butyl cation

This is another monohydroxy PBN product where the hydroxyl radical has attacked the phenyl ring of PBN and due to structural differences has eluted later than the product at peak detected at rt 10.20 minutes (compound A). Hydroxyl radical attack on the phenyl ring is confirmed as the spectrum is identical to that of the spectrum of compound A, regarding the fragmentation pattern. It is likely the hydroxyl has added to the para position of the ring, whereas the product at peak detected at rt 10.20 minutes is mono hydroxyl on the phenyl at meta/ortho positions. This is supported by the substitution of the fluorine where 4-Fluoro-PBN is used as the spin trap however the molecular ion is *m/z* 193, indicating the absence of fluorine. There is an ion detected at *m/z* 211 however this is more likely an artifact, as the fragmentation pattern does not support the hypothesis that the fluorine is retained on the phenyl ring.

Table 3.3 Identity of PBN hydroxyl adducts formed at rt 11.78 minutes

Spin trap used	identity	Rt	*m/z*
PBN	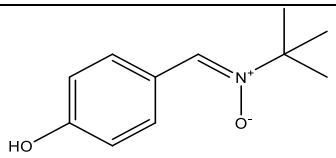	11.78	193
D6-PBN	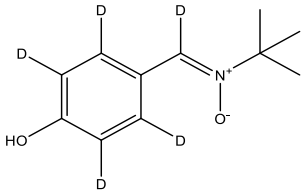	11.72	198
F-PBN	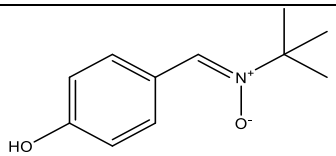	11.70	193

3.2.5 EI-MS of product of (di)hydroxyl radical attack on phenyl ring of PBN-X @r.t 11.41 Compound C

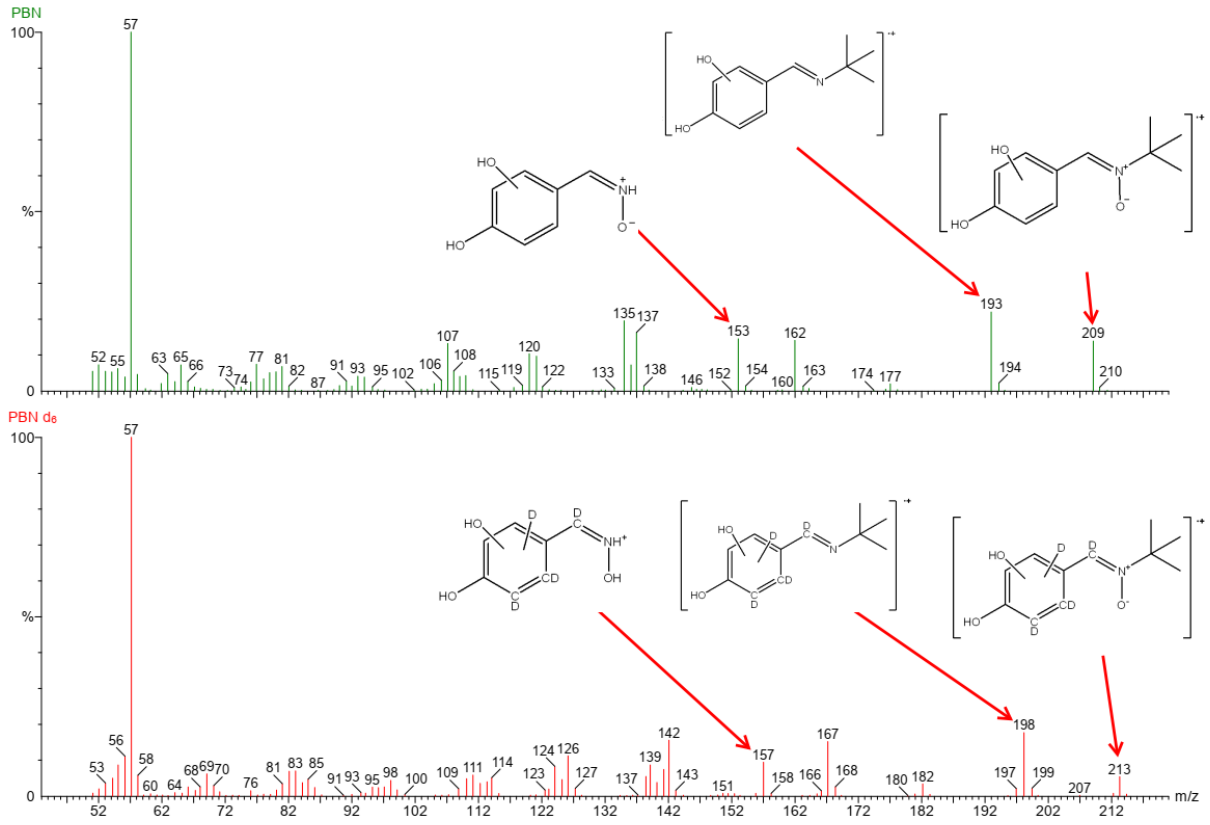

Figure 3.2.5 Electron Ionization mass spectra corresponding to PBN and its derivatives (EI-MS) obtained from the analysis of the Fenton reaction mixture containing PBN, d6PBN at rt 11.41 minutes

The EI-mass spectra in Figure 3.2.5 for the peak retained at rt 11.41 minutes corresponds to the PBN-$(OH)_2$ (EI-MS top); PBN-d_6-$(OH)_2$ (EI-MS PBN-d_6 bottom)

The addition of 32 Da to the PBN indicates that two hydroxyl radicals have replaced two hydrogens on the benzene ring and this is further supported by the addition of 30 *m/z* units to PBN-d_6 (addition of 34 *m/z* and the loss of 4 *m/z*) indicating the substitution of two deuterium atoms.

No equivalent peak is observed for a dihydroxyphenyl adduct of F-PBN. It is reasonable to postulate that this is due to the presence of a fluorine atom in the para position of the phenyl ring, although it is possible that the dihydroxy product was formed, but in a quantity too low to be detected, or was not soluble in the extraction buffer.

Table 3.4 Identity of PBN dihydroxyl adducts formed at rt 1140 minutes

	identity	Rt	*m/z*
PBN	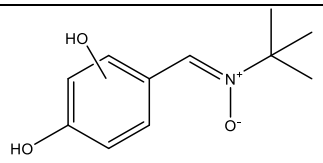	11.407	209
D6-PBN	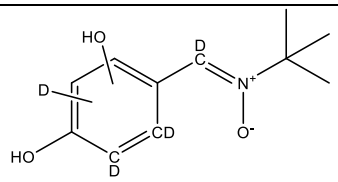	11.367	213

3.2.6 EI-MS of product of hydroxyl radical attack on phenyl ring of PBN-X @r.t. 10.50 Compound D

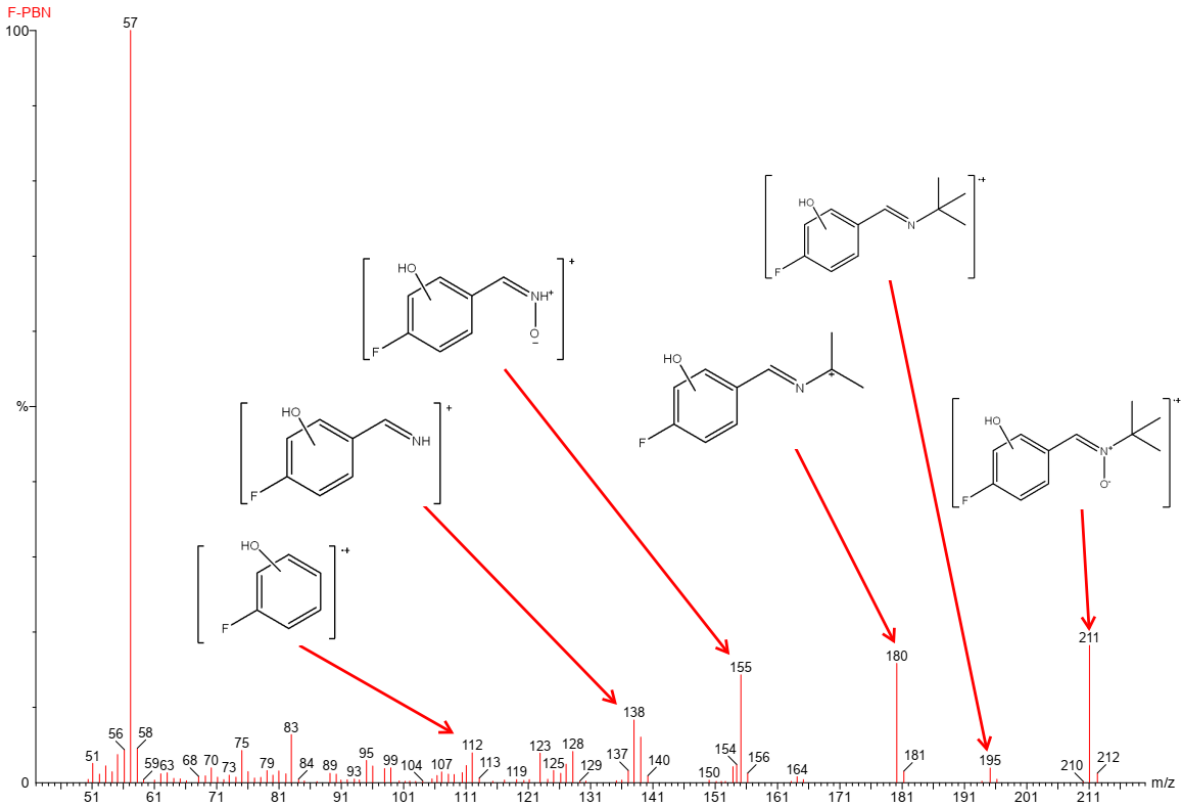

Figure 3.2.6 Electron Ionization mass spectra corresponding to F-PBN obtained from the analysis of the Fenton reaction mixture containing F-PBN at rt 10.50 minutes

The EI-mass spectrum in Figure 3.2.6 corresponds to the peak at rt 10.50 minutes. The mass spectrum shows a very strong molecular ion at 211. The fragmentation pattern shows a fragment at 195 due to the loss of oxygen from the molecular ion. The fragment at 180 *m/z* is due to the loss of a methyl group from *m/z* 195 The fragment at 155 is due to the loss of 2-methyl-1-propene from the $M^{+\bullet}$.

It should be noted the distinction between compound D and the fluorinated analogue of compound A. They are both mono-hydroxyl attack on the phenyl ring at either the ortho or meta position however it is impossible to distinguish the identity of either in regards to the location of the hydroxyl radical attack.

3.3 Discussion

The main aim of this chapter was to trap and identify the radicals that are generated from the reaction of the hydroxyl radical with PBN and its derivatives. In the Fenton reaction chelated Fe^{2+} reduces hydrogen peroxide generating hydroxyl radicals which react with PBN and its derivatives forming aromatic mono-hydroxy and di-hydroxy PBN derivatives. These adducts can then be extracted using chloroform and analysed via gas chromatography mass spectrometry (Krygsman *et al*., 1989; Janzen *et al*., 1990). It has been observed that phenolic products of PBN are produced in the presence of hydroxyl radicals and that hydroxy aromatic PBN adducts are formed (Reinke *et al*., 2000). The current studies demonstrate that mono-hydroxylated PBN (ortho/meta) is a major product, where a hydroxyl radical adds to either the ortho or meta position on the aromatic ring of PBN..

The TICs of the reaction containing PBN 3.1.1 shows various peaks that were eluted compared to the controls (see section 2.7). The resultant peaks (rt 3.69 minutes, rt 10.20 minutes, rt 11.41 minutes and rt 11.78 minutes) are products generated from the Fenton reaction with PBN.

The broad peak (Peak 1 retained at 3.69 minutes) is a combination of a benzaldehyde oxime and hydroxylamine PBN and is seen in control experiments in the absence of Fe^{2+} or hydrogen peroxide with a base peak of 77 *m/z* and characteristic fragment peaks at *m/z* 161,146 and 121 with the molecular ion not being present. It appears to be two overlapping peaks with one of the compounds having an EI-MS spectral pattern consistent with both benzaldehyde oxime and hydroxylamine PBN and the other with trimethylsilyl ether (Castro *et al*., 1998). Evidence by Podmore *et al*., (unpublished) supports the findings of a hydroxylamine/benzaldehyde oxime overlap.

The peak at rt 8.12 minutes (and 7.81 minutes) is the unreacted PBN, the peak at rt 10.20 minutes (Compound A) is monohydroxy PBN (meta/ortho), the peak at rt 11.41 minutes (compound C) is the dihydroxyl at the para and either meta or ortho position of the phenyl, , the *m/z* 211 in the F-PBN spectrum is an artifact and cannot be conclusively assigned. The peak at rt 11.78 minutes (compound B) is monohydroxy PBN at the para position of the phenyl ring which is indicated by the fact that the EI-MS for the PBN and F-PBN have significant similarity in the spectral patterns and the fluorinated tropylium ion which would be expected at *m/z* of 109 is absent.

When hydroxyl radicals add to the alpha carbon of PBN, the resulting spin adduct has a half-life of less than 1 minute at pH 7.0 and decomposes to release benzaldehyde and tert-butyl hydroxylamine (Kotake and Janzen, 1991). Studies by Reinke *et al*., (2000) indicate that benzaldehyde is formed by hydroxyl

radical attack at the nitrone group of the PBN liberating the benzaldehyde however the studies also indicated that 4-hydroxyphenyl PBN was detected at much greater levels relative to other PBN-OH adducts however this result was not consistent with the findings of this thesis. Based on the area under the peaks, PBN-$OH_{(o/m)}$(compound A) is more likely to be a product of hydroxyl attack on PBN than 4-OH phenyl PBN (compound B), followed by dihydroxyphenyl PBN (compound C).

According to studies by Reinke *et al*., (2000), PBN and its mono-hydroxylated derivatives were synthesized and analysed via LCMS, and it was found that the retention time of 2-hydroxyPBN was 27.2 minutes compared to the retention times of 3-hydroxyPBN at 8.2 minutes, and 4-hydroxyPBN at 6.4 minutes. Furthermore, the Fenton reaction was carried out using conditions similar to this study and 2-hydroxyPBN was not detected This would lead to a conclusion that although it cannot be conclusively reported on the identity of the peak at 10.2 minutes is either 2-hydroxy-PBN or 3-hydroxy-PBN, based on findings by Reinke *et al*, the probable candidate isolated is 2-hydroxyPBN.

The peak retained at 10.5 minutes (Figure 3.1.5)

In summary the primary product of the hydroxyl radical attack of PBN is compound A followed by compound B and C. It is impossible to detect the product of hydroxyl attack on the α-carbon of PBN due to its relatively short half-life.

The half-lives of free radicals in biological systems are typically exceedingly transient. *In vivo* detection techniques must therefore be sensitive, produce stable products, target compartments of interest, not interfere with normal metabolism, and have high specificity. While trapping aromatic hydroxyl products results in stable, non-toxic, and reasonably detectable products, it does not however, answer the question of what other possible adducts could be formed. If a methodology was developed that could characterise other PBN metabolites it might be a useful indicator of hydroxyl radical production in-vivo. An alternative approach for detecting hydroxyl radicals generated by the Fenton reaction could be to react with other compounds as competitive secondary radicals as butanal and dimethyl sulphoxide to form stable adducts that can also be analysed.

Chapter 4

4 Detection and analysis of spin-adducts from butanal and N-tert-butyl-a-phenyl nitrone (PBN) derivates using liquid injection gas chromatography-mass spectrometry

In this study, hydroxyl radicals generated from the Fenton chemistry have been used to generate alkyl radicals and alkoxy radicals from butanal and DMSO to produce ($^{\bullet}CH_2CH_2CH_3$), ($CH_3{}^{\bullet}CHCH_2CHO$), ($^{\bullet}CH_2CH_2CH_2CHO$) and ($^{\bullet}CH_3$) radicals. These radicals were then trapped by PBN and its derivatives to form stable adducts and sampled using liquid-liquid extraction with chloroform as a solvent. The extracted samples were subjected to GC/MS for detection and analysis. Numerous PBN radical adducts were identified and characterised and will be discussed in the following chapter.

4.1 Chromatograms of PBN derivatives and butanal

4.1.1 Fenton with butanal and PBN

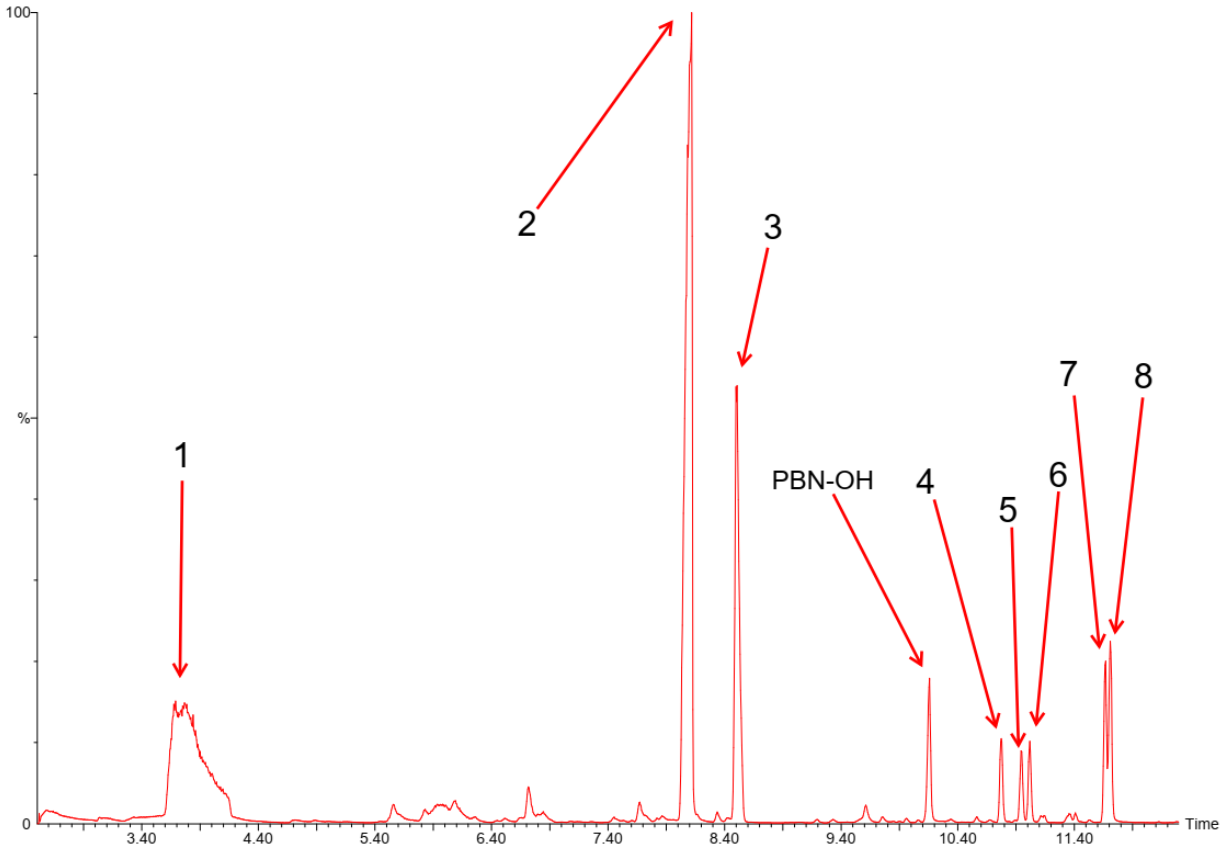

Figure 4.1.1 The total ion chromatogram obtained from the GC-MS analysis of the Fenton system with PBN in the presence of butanal.

The TIC shown in Figure 4.1.1 was obtained from the Fenton-based reaction containing PBN as the spin trap and butanal as the secondary source of free radicals. The 8 peaks that are labelled have been assigned, as follows (see Figure 4.1.2 for structures): Peak 1 (rt 3.69) is a mixture of two compounds, one of which appears to be benzaldehyde oxime; Peak 2 (rt 8.12) is unreacted PBN; Peak 3 (rt 8.51) corresponds to a di-propyl adduct of the spin trap {PBN-$(CH_2CH_2CH3)_2$; Peak 4 (rt 10.77) give the impression of a monopropyl PBN adduct {PBN-(CH_2CH_2CH3)}; Peak 5 (rt 10.85) appears to be a PBN butanal radical and propyl radical adduct {PBN-$(CH_2CH_2CH_2CHO)(CH_2CH_2CH_3)$}; Peak 6 (rt 11.02) appears to be an additional PBN butanal radical and propyl radical adduct {PBN-$(CH_2CH_2CH_2CHO)(CH_2CH_2CH_3)$}; Peak 7 (rt 11.61) appears to be an diastereomer of a butanal radical and propyl radical adduct of PBN {PBN-$(CH_3CHCH_2CHO)(CH_2CH_2CH_3)$; Peak 8 (rt 11.71) is an enantiomer of PBN where the propyl radical and

butanal radical have adducted to the alpha carbon and oxygen respectively {PBN($CH_2CH_2CH_3$)($CH_2CH_2CH_2CHO$)}.

Peaks not labelled in the chromatogram produced EI-mass spectra which were too weak to allow interpretation or were not resulting from the Fenton reaction with butanal.

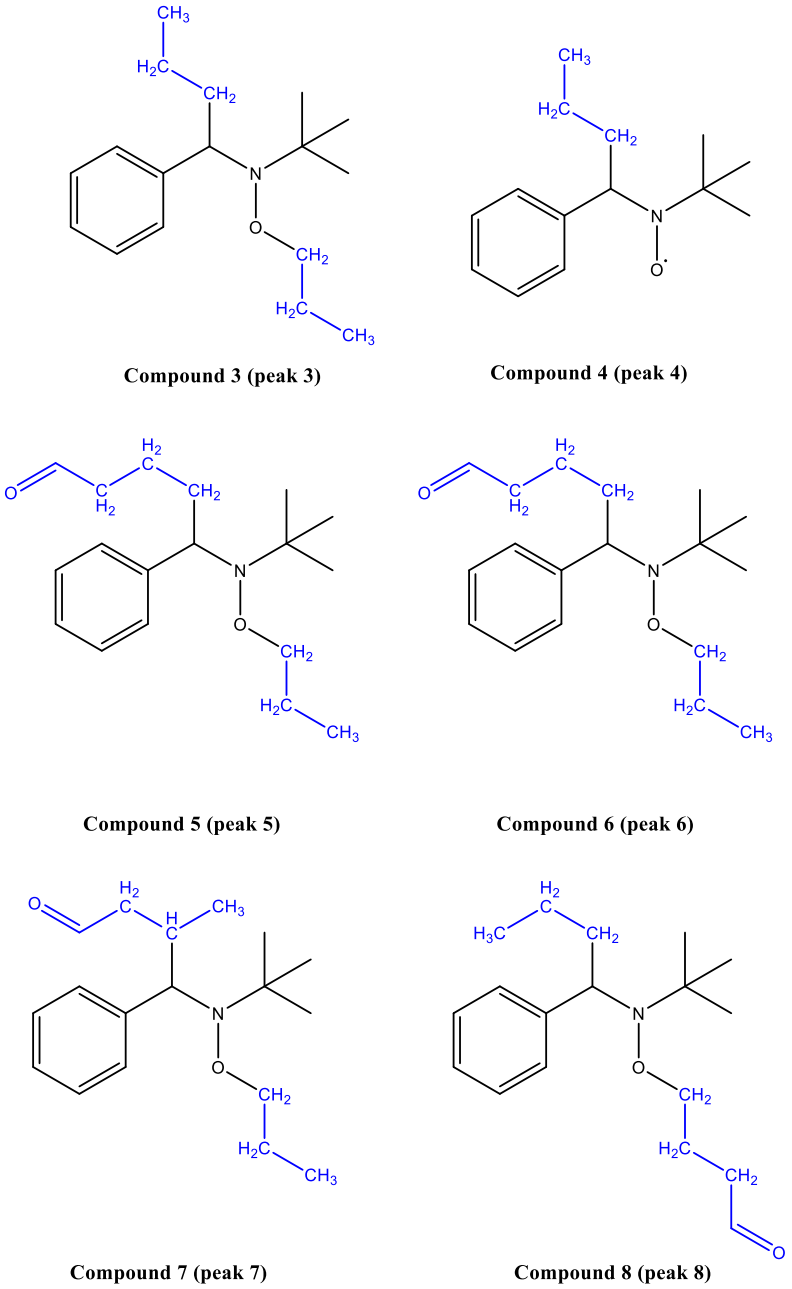

Figure 4.1.2 The structures of compounds identified by GC-MS analysis of a Fenton-based reaction mixture containing PBN and butanal. The atoms in blue are believed to be derived from butanal

Table 4.1 Peak number, molecular ion , base peak and identity for peaks obtained in Figure 4.1.1

Peak Number	Molecular ion	Base peak	Identity
1	178	121	Benzaldehyde oxime
2	177	121	PBN
3	263	133	Dipropyl adduct
4	220	164	Monopropyl adduct
5	291	164	Mono-oxobutyl monopropyl adduct a
6	291	164	Mono-oxobutyl monopropyl adduct
7	291	117	Mono-oxobutyl monopropyl adduct
8	291	97	Monopropyl mono-oxobutyl adduct

4.1.2 Fenton with butanal and PBN-d_6

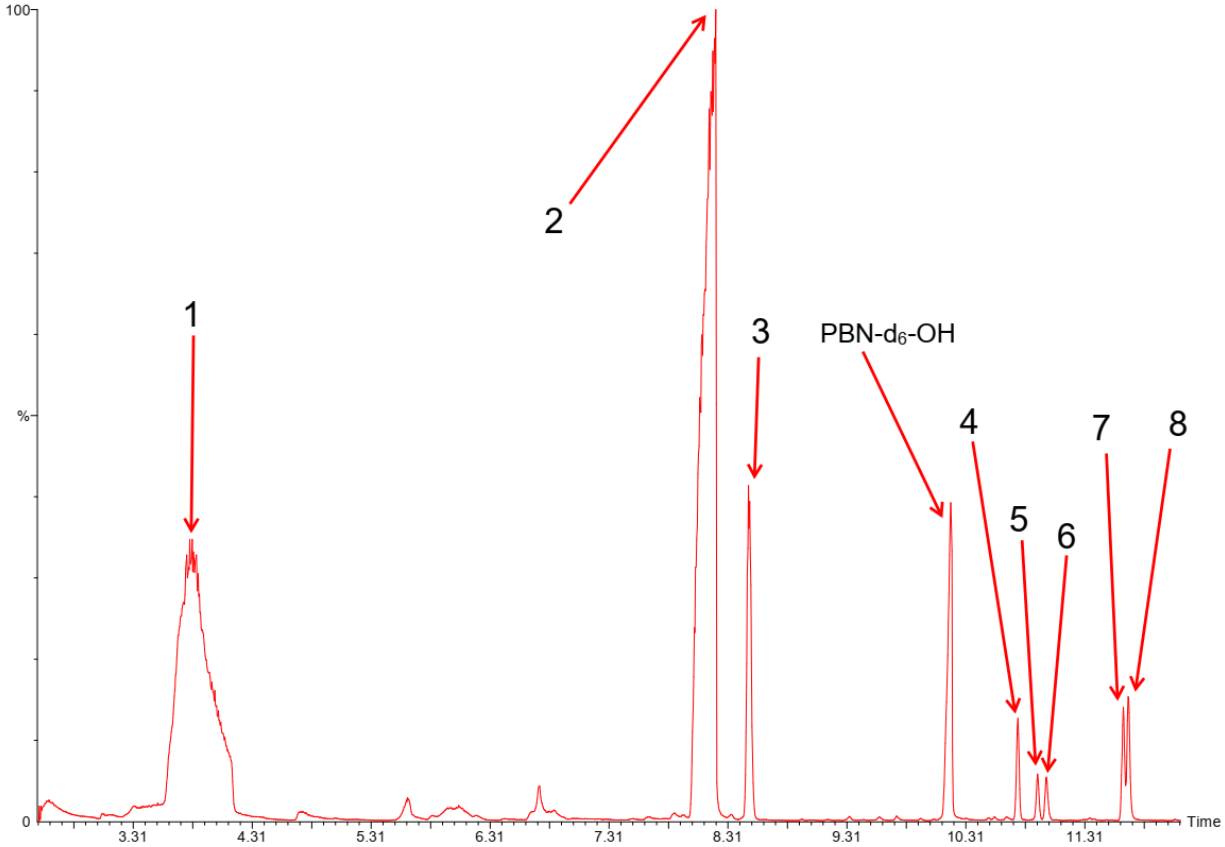

Figure 4.1.3 The total ion chromatogram obtained from the GC-MS analysis of the Fenton system with PBN-d_6 in the presence of butanal

The TIC shown in Figure 4.1.3 obtained from the Fenton reaction of PBN and butanal extracted into chloroform shows 8 peaks. Identified peaks are shown in Table 4.2

Table 4.1 Peak number, molecular ion , base peak and identity for peaks obtained in Figure 4.1.1

Peak Number	Molecular ion	Base peak	Identity
1	178	121	Benzaldehyde oxime
2	177	121	PBN
3	263	133	Dipropyl adduct
4	220	164	Monopropyl adduct
5	291	164	Mono-oxobutyl monopropyl adduct a
6	291	164	Mono-oxobutyl monopropyl adduct
7	291	117	Mono-oxobutyl monopropyl adduct
8	291	97	Monopropyl mono-oxobutyl adduct

The 8 peaks that are labelled have been assigned, as follows (see Figure 4.1.4 for structures): Peak 1 (rt 3.64) is a mixture of two compounds, one of which appears to be benzaldehyde-d_6 oxime; Peak 2 (rt 8.03) is unreacted PBN-d_6; Peak 3 (rt 8.47) corresponds to a di-propyl adduct of the spin trap {PBN-d_6-$(CH_2CH_2CH3)_2$; Peak 4 (rt 10.74) give the impression of a monopropyl PBN-d_6 adduct {PBN-d_6-(CH_2CH_2CH3)}; Peak 5 (rt 10.80) appears to be a PBN-d_6 butanal radical and propyl radical adduct {PBN-d_6-$(CH_2CH_2CH_2CHO)(CH_2CH_2CH_3)$}; Peak 6 (rt 10.98) appears to be an additional PBN-d_6 butanal radical and propyl radical adduct {PBN-d_6-$(CH_2CH_2CH_2CHO)(CH_2CH_2CH_3)$}; Peak 7 (rt 11.63) appears to be a diastereomer of a butanal radical and propyl radical adduct of PBN-d_6 {PBN-d_6-$(CH_3CHCH_2CHO)(CH_2CH_2CH_3)$; Peak 8 (rt 11.67) is an enantiomer of PBN where the propyl radical and butanal radical have adducted to the alpha carbon and oxygen respectively {PBN-d_6-$(CH_2CH_2CH_3)(CH_2CH_2CH_2CHO)$}. The PBN-$d_6$ products have a slightly shorter retention time than PBN products

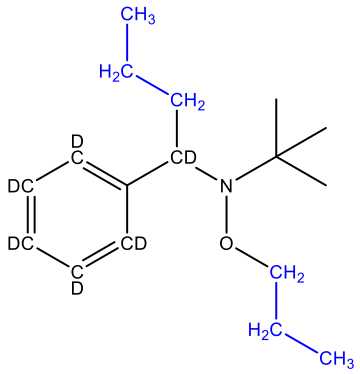

Compound 3 (peak 3)

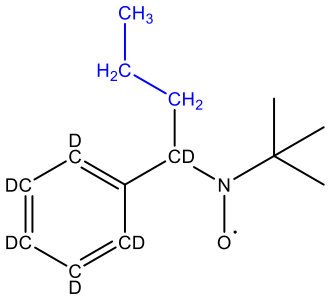

Compound 4 (peak 4)

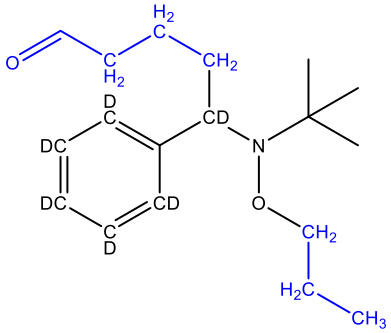

Compound 5 (peak 5)

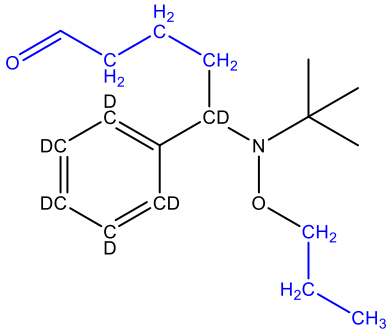

Compound 6 (peak 6)

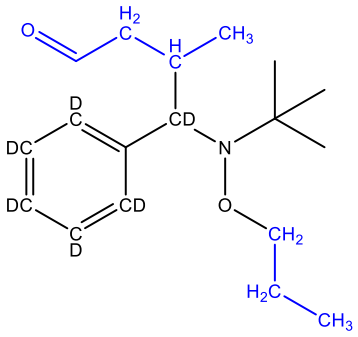

Compound 7 (peak 7)

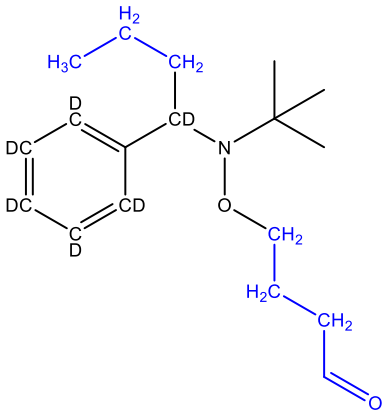

Compound 8 (peak 8)

Figure 4.1.4 The structures of compounds identified by GC-MS analysis of a Fenton-based reaction mixture containing PBN-d_6 and butanal. The atoms in blue are believed to be derived from butanal

Table 4.2 Peak number, molecular ion ,base peak and identity for peaks obtained in Figure 4.1.3

Peak Number	Molecular ion	Base peak	Identity
1	184	127	Benzaldehyde-d_6 oxime
2	183	127	PBN-d_6
3	269	97	Dipropyl adduct
4	226	170	Monopropyl adduct
5	297	170	Mono-oxobutyl monopropyl adduct
6	297	170	Mono-oxobutyl monopropyl adduct
7	297	123	Mono-oxobutyl monopropyl adduct
8	254	97	Monopropyl mono-oxobutyl adduct

4.1.3 Fenton with butanal and F-PBN

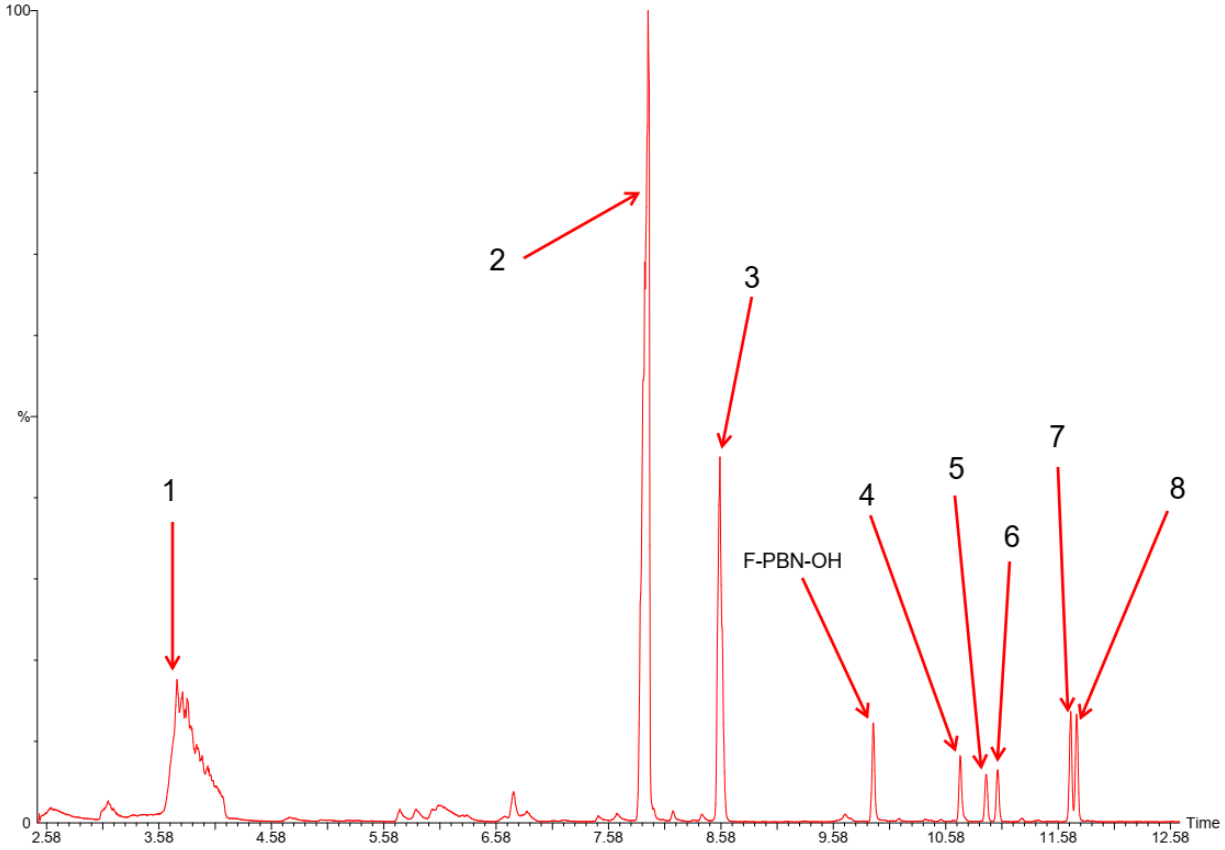

Figure 4.1.5 The total ion chromatogram obtained from the GC-MS analysis of the Fenton system with F-PBN in the presence of butanal

The TIC shown in Figure 4.1.5 obtained from the Fenton-based reaction containing F-PBN as the spin trap and butanal as the secondary source of free radicals. The 8 peaks that are labelled have been assigned, as follows (see Figure 4.1.6 for structures): Peak 1 (rt 3.74) is a mixture of two compounds, one of which appears to be 4-fluorobenzaldehyde oxime; Peak 2 (rt 7.94) is unreacted F-PBN; Peak 3 (rt 8.58) corresponds to a di-propyl adduct of the spin trap {F-PBN-$(CH_2CH_2CH3)_2$; Peak 4 (rt 10.71) gives the impression of a monopropyl F-PBN adduct trap {F-PBN-(CH_2CH_2CH3)}; Peak 5 (rt 10.85) appears to be a F-PBN butanal radical and propyl radical adduct {F-PBN-$(CH_2CH_2CH_2CHO)(CH_2CH_2CH_3)$}; Peak 6 (rt 11.05) appears to be an additional F-PBN butanal radical (oxobutyl) and propyl radical adduct {F-PBN-$(CH_2CH_2CH_2CHO)(CH_2CH_2CH_3)$}; Peak 7 (rt 11.61) appears to be an diastereomer of a butanal radical and propyl radical adduct of F-PBN {F-PBN-$(CH_3CHCH_2CHO)(CH_2CH_2CH_3)$; Peak 8 (rt 11.70) is an enantiomer of F-PBN where the propyl radical and butanal radical have adducted to the alpha carbon and oxygen respectively {F-PBN$(CH_2CH_2CH_3)(CH_2CH_2CH_2CHO)$}. Identified peaks are shown in Table 4.3

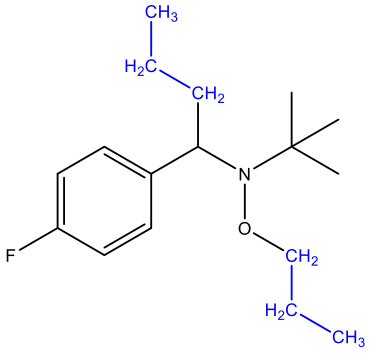

Compound 3 (peak 3)

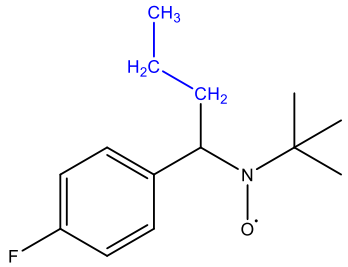

Compound 4 (peak 4)

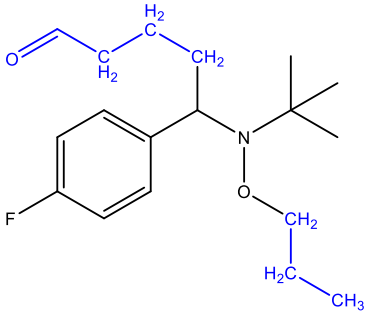

Compound 5 (peak 5)

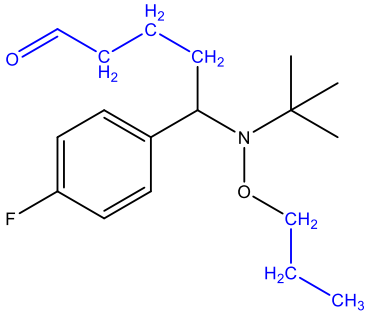

Compound 6 (peak 6)

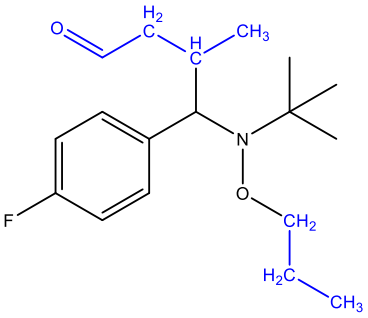

Compound 7 (peak 7)

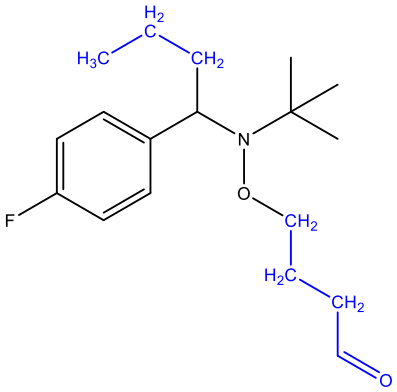

Compound 8 (peak 8)

Figure 4.1.6 The structures of compounds identified by GC-MS analysis of a Fenton-based reaction mixture containing 4-fluoro-PBN and butanal. The atoms in blue are believed to be derived from butanal

Table 4.3 Peak number, molecular ion , base peak and identity for peaks obtained in Figure 4.1.5

Peak Number	Molecular ion	Base peak	Identity
1	196	139	F-benzaldehyde oxime/hydroxylamine F-PBN
2	195	139	F-PBN
3	281	151	Dipropyl adduct
4	238	182	Monopropyl adduct
5	309	182	Mono-oxobutyl monopropyl adduct
6	309	182	Mono-oxobutyl monopropyl adduct
7	309	135	Mono-oxobutyl monopropyl adduct
8	309	109	Monopropyl mono-oxobutyl adduct

4.2 Electron ionization-mass spectra (EI-MS) of the di-propyl adduct of PBN (Compound 3)

4.2.1 Dipropyl adduct of PBN {PBN-$(CH_2CH_2CH_3)_2$} (Compound 3)

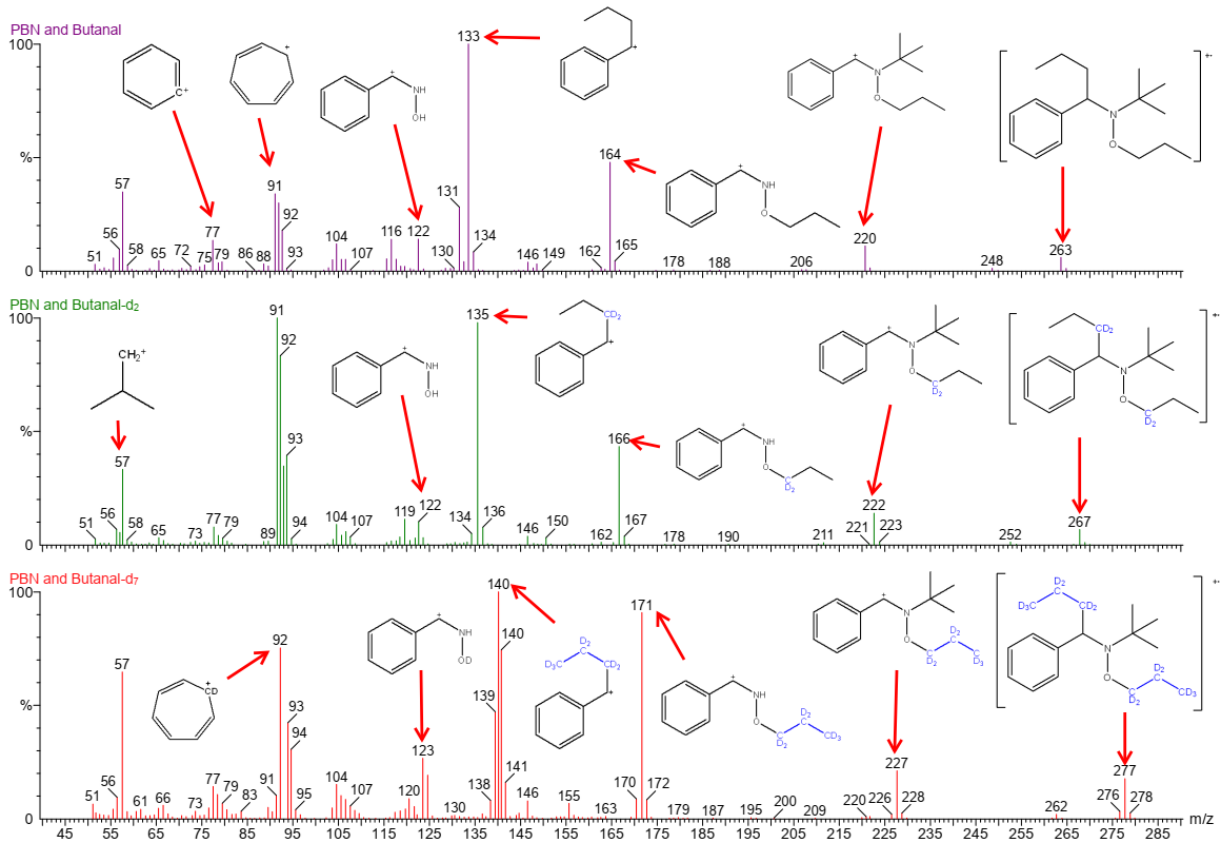

Figure 4.2.1 Electron Ionization mass spectra (EI-MS) corresponding to PBN adducts obtained from the analysis of the Fenton reaction mixture containing PBN, butanal and deuterated analogues at rt 8.51 minutes

The EI mass spectra in Figure 4.2.1 correspond to a) the PBN di-propyl adduct {PBN-$(CH_2CH_2CH_3)_2$} with a molecular ion at 263 *m/z* (EI-MS PBN and butanal, top spectrum); b) the PBN dideuterated di-propyl adduct {PBN-$(C\mathbf{D}_2CH_2CH_3)_2$} with a molecular ion at 267 *m/z* (EI-MS PBN and butanal-d_2, middle spectrum); the PBN perdeuterated di-propyl adduct and c) {PBN-$(CH_2CH_2CH_3)_2$} with a molecular ion at 277 *m/z* (EI-MS PBN and butanal-d_7, bottom spectrum).

When the Fenton reaction was carried out in the presence of butanal as a secondary source of radicals, propyl radicals ($^{\bullet}CH_2CH_2CH_3$) are generated by the reaction of $^{\bullet}OH$ with butanal and then trapped by PBN. The peak at 263 *m/z* units corresponds to the molecular ion of PBN-$Prop_2$ (one propyl adding to the carbon

atom of the C=N and the other adding to the oxygen). The fragment at *m/z* 248 is due to the loss of a methyl group from the molecular ion (from the tBu group). The loss of M-15 is not changed by the variation in the adduct formed due to a deuterated version of butanal being used showing that the methyl categorically originated from the tBu. The loss of CH_2=CMe_2 and the loss of a propyl group from the molecular ion results in *m/z* 164. The dissociation of the alpha carbon bond and the nitrogen gives the butyl benzene cation base peak at *m/z* 133 (loss of a tert-butyl propoxy azane group from the molecular ion). and further breakdown of this fragment results in a tropylium cation at *m/z* 91. The fragment *m/z* 122 is N-benzyl hydroxylamine and the peak at *m/z* 57 is the tertiary butyl cation

Replacing butanal with its deuterated analogues in the Fenton-based reaction demonstrates the production of deuterated propyl radicals and subsequent incorporation by the spin trap. As shown by an increase on the molecular ion of 4 *m/z* when butanal-d_2 was used and 14 *m/z* units when butanal-d_7 was used.

When the Fenton reaction was carried out in the presence of butanal-d_2 as a secondary source of radicals, deuterated propyl radicals ($^{\bullet}C\mathbf{D}_2CH_2CH_3$) are generated by the reaction of $^{\bullet}OH$ with butanal and then trapped by PBN. The peak at 267 *m/z* units corresponds to the molecular ion of PBN-(Prop-d_2)$_2$. The fragment at *m/z* 252 is due to the loss of a methyl group from the molecular ion (from the tBu group). The loss of CH_2=CMe_2 gives *m/z* 211 and the loss of a dideuterated propyl group from this fragment results in *m/z* 166. The dissociation of the alpha carbon bond and the nitrogen gives *m/z* 135 and further breakdown of this fragment results in a tropylium cation base peak at *m/z* 91. The fragment *m/z* 122 is N-benzyl hydroxylamine and the peak at *m/z* 57 is the tertiary butyl cation

When the Fenton reaction was carried out in the presence of butanal-d_7 as a secondary source of radicals, deuterated propyl radicals ($^{\bullet}C\mathbf{D}_2C\mathbf{D}_2C\mathbf{D}_3$) are generated by the reaction of $^{\bullet}OH$ with butanal and then trapped by PBN. The peak at 277 *m/z* units corresponds to the molecular ion of PBN-(Prop-d_7)$_2$. The fragment at *m/z* 262 is due to the loss of a methyl group from the molecular ion (from the tBu group). The loss of CH_2=CMe_2 and the loss of a deuterated propyl group from the molecular ion results in *m/z* 171. The dissociation of the alpha carbon bond and the nitrogen gives the base peak *m/z* 140 and further breakdown of this fragment results in a tropylium cation at *m/z* 91. The fragment *m/z* 123 is N-benzyl hydroxylamine-O-d, where a deuterated hydrogen has rearranged from the deuterated propyl group and added to the oxygen position of PBN. The peak at *m/z* 57 is the tertiary butyl cation

The tropylium ion is shown at *m/z* 91 with the fragment at *m/z* 65 characteristic of the rearrangement of tropylium, the tropylium cation is a seven-membered ring, $C_7H_7^+$, often formed from compounds containing a benzyl group. The bond between the methylene carbon of the benzyl group and the remainder of the molecule is cleaved and the benzyl ion rearranges into a more stable cyclic form with the charge delocalized around the ring (Mallet and Down, 2009).

The tBu cation can be seen at *m/z* 57 and is a distinguishable peak characteristic of the fragmentation pattern of PBN and its derivatives.

4.2.3 Dipropyl adducts of PBN-d_6 { PBN-d_6-$(CH_2CH_2CH_3)_2$} (Compound 3)

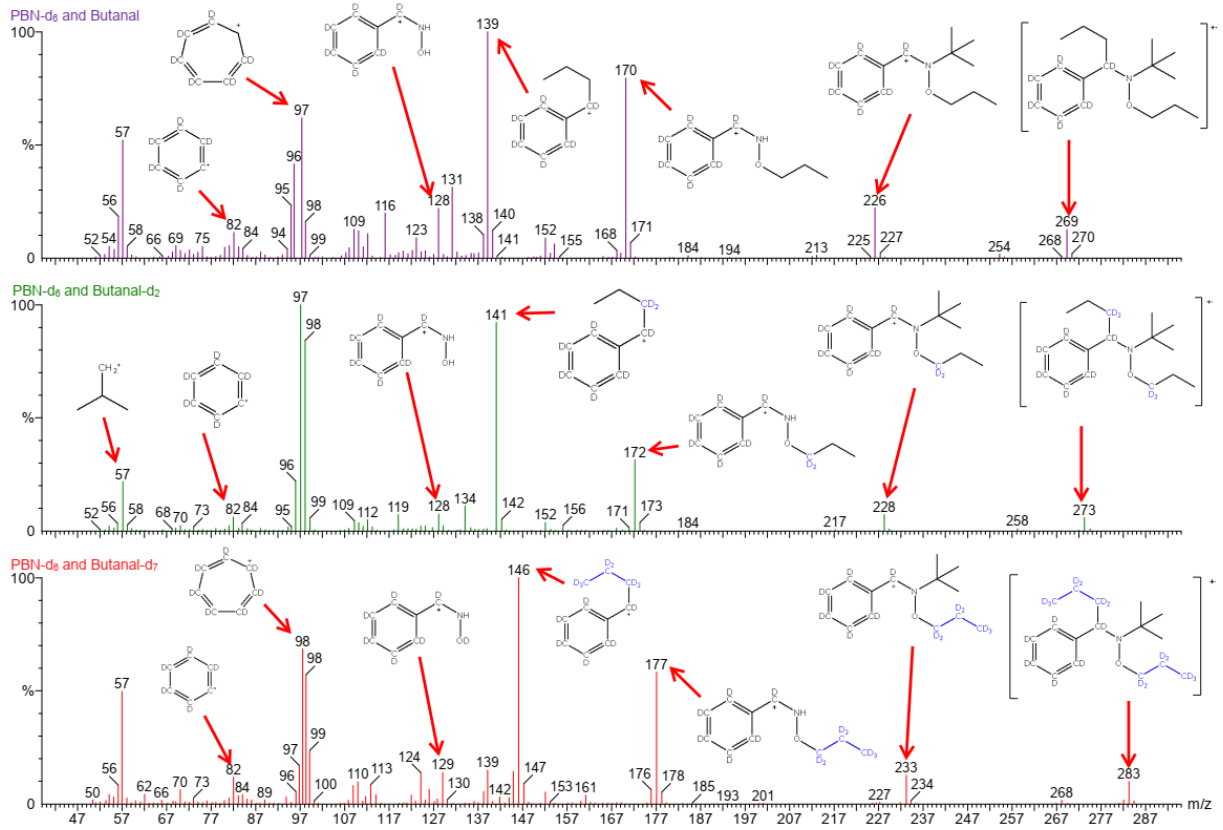

Figure 4.2.2 Electron Ionization mass spectra (EI-MS) corresponding to PBN adducts obtained from the analysis of the Fenton reaction mixture containing PBN-d_6, butanal and deuterated analogues at rt 8.51 minutes

The EI mass spectra in Figure 4.2.2 are for the peak retained at rt 8.51 minutes corresponding to the PBN-d_6 dipropyl adduct with a molecular ion $M^{+\bullet}$ at 269 (EI-MS PBN-d_6 and butanal); $M^{+\bullet}$ 273 (EI-MS PBN-d_6 and butanal-d_2); $M^{+\bullet}$ 277 (EI-MS PBN-d_6 and butanal-d_7). PBN-d_6 is 6 *m/z* units heavier than PBN and this reflects that all PBN-d_6 peaks have shifted right

When the Fenton reaction was carried out in the presence of butanal as a secondary source of radicals, propyl radicals ($^{\bullet}CH_2CH_2CH_3$) are generated by the reaction of $^{\bullet}OH$ with butanal and then trapped by PBNd_6. By the nature of PBN-d_6 all spin adducts gain 6 *m/z* units over using non-deuterated PBN. The peak at 269 *m/z* units corresponds to the molecular ion of PBN-d_6-Prop$_2$ (one propyl adding to the carbon atom of the C=N and the other adding to the oxygen). The fragment at *m/z* 254 is due to the loss of a methyl group from the molecular ion (from the tBu group). The loss of CH_2=CMe_2 and the loss of a propyl group

from the molecular ion results in *m/z* 170. The dissociation of the alpha carbon bond and the nitrogen gives the base peak *m/z* 139 (loss of a tert-butyl propoxy azane group from the molecular ion). and further breakdown of this fragment results in a perdeuterated tropylium cation at *m/z* 97. The fragment *m/z* 128 is N-benzyl hydroxylamine and the peak at *m/z* 57 is the tertiary butyl cation

Replacing butanal with its deuterated analogues in the Fenton-based reaction demonstrates the production deuterated propyl radicals and subsequent incorporation by the spin trap. As shown by an increase on the molecular ion of 4 *m/z* when butanal-d_2 was used and 14 *m/z* units when butanal-d_7 was used.

When the Fenton reaction was carried out in the presence of butanal-d_2 as a secondary source of radicals, deuterated propyl radicals ($^{\bullet}C\mathbf{D}_2CH_2CH_3$) are generated by the reaction of $^{\bullet}OH$ with butanal and then trapped by d_6PBN. The peak at 273 *m/z* units corresponds to the molecular ion of PBN-d_6(Prop-d_2)$_2$. The fragment at *m/z* 258 is due to the loss of a methyl group from the molecular ion (from the tBu group). The loss of CH_2=CMe_2 gives *m/z* 217 and the loss of a dideuterated propyl group from this fragment results in *m/z* 172. The dissociation of the alpha carbon bond and the nitrogen gives *m/z* 141 and further breakdown of this fragment results in a perdeuterated tropylium cation base peak at *m/z* 97. The fragment *m/z* 128 is N-benzyl hydroxylamine and the peak at *m/z* 57 is the tertiary butyl cation

When the Fenton reaction was carried out in the presence of butanal-d_7 as a secondary source of radicals, deuterated propyl radicals ($^{\bullet}C\mathbf{D}_2C\mathbf{D}_2C\mathbf{D}_3$) are generated by the reaction of $^{\bullet}OH$ with butanal and then trapped by d_6PBN. The peak at 283 *m/z* units corresponds to the molecular ion of PBN-d_6-(Prop-d_7)$_2$. The fragment at *m/z* 268 is due to the loss of a methyl group from the molecular ion (from the tBu group). The loss of CH_2=CMe_2 and the loss of a deuterated propyl group from the molecular ion results in *m/z* 177. The dissociation of the alpha carbon bond and the nitrogen gives the base peak *m/z* 146 and further breakdown of this fragment results in a perdeuterated tropylium cation at *m/z* 98. The fragment *m/z* 129 is N-benzyl hydroxylamine-O-d, where a deuterated hydrogen has rearranged from the deuterated propyl group and added to the oxygen position of PBN. The peak at *m/z* 57 is the tertiary butyl cation

4.2.4 Dipropyl adduct of F-PBN {F-PBN-$(CH_2CH_2CH_3)_2$} (Compound 3)

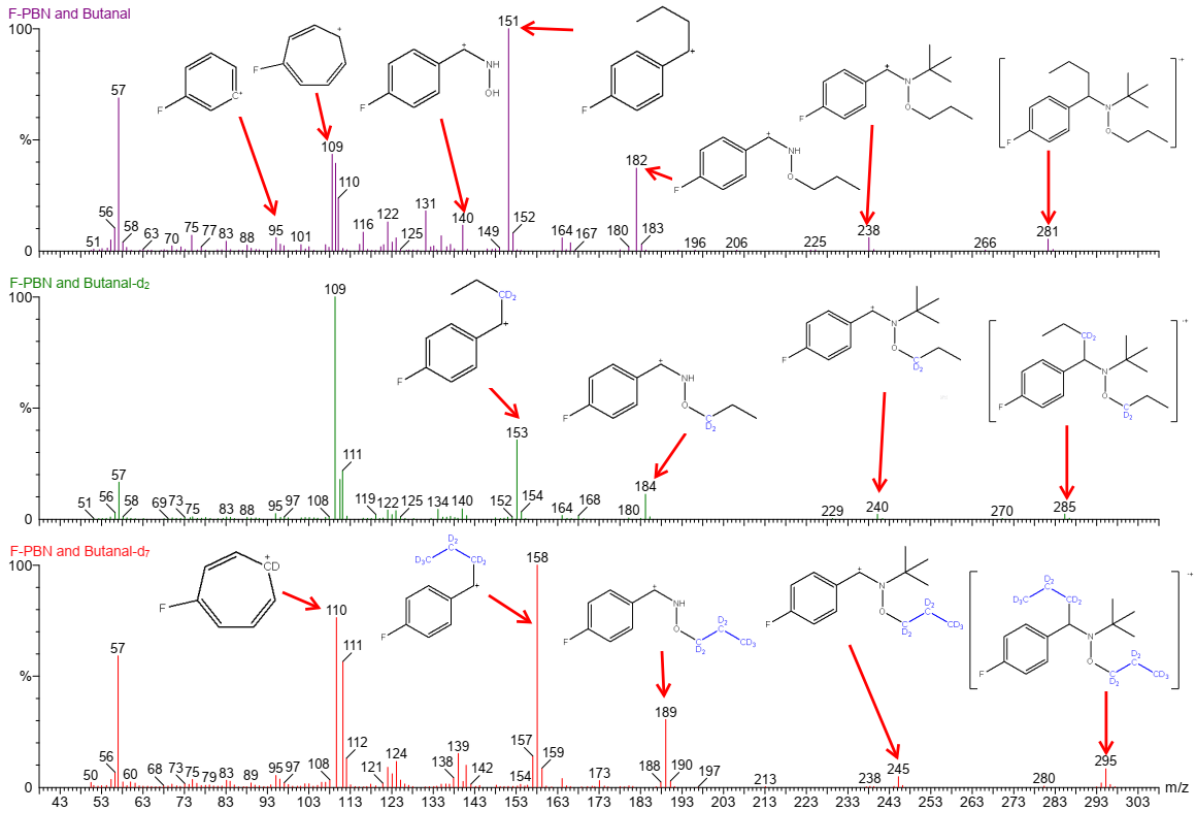

Figure 4.2.3 Electron Ionization mass spectra (EI-MS) corresponding to F-PBN adducts obtained from the analysis of the Fenton reaction mixture containing F-PBN, butanal and deuterated analogues at rt 8.51 minutes

The EI mass spectra in Figure 4.2.3 are for the peak retained at rt 8.51 minutes corresponding to the F-PBN dipropyl adduct with a molecular ion $M^{+\bullet}$ at 281 (EI-MS F-PBN and butanal); $M^{+\bullet}$ 285 (EI-MS F-PBN and butanal-d_2); $M^{+\bullet}$ 295 (EI-MS F-PBN and butanal-d_7).

When the Fenton reaction was carried out in the presence of butanal as a secondary source of radicals, propyl radicals ($^{\bullet}CH_2CH_2CH_3$) are generated by the reaction of $^{\bullet}OH$ with butanal and then trapped by 4-fluorinated PBN (F-PBN). By the nature of F-PBN all spin adducts gain 18 *m/z* units compared when using non-fluorinated PBN. The peak at 281 *m/z* units corresponds to the molecular ion of F-PBN-$Prop_2$ (one propyl adding to the carbon atom of the C=N and the other adding to the oxygen). The fragment at *m/z* 266 is due to the loss of a methyl group from the molecular ion (from the tBu group). The loss of M-15 is not changed by the variation in the adduct formed due to a deuterated version of butanal being used showing that the methyl categorically originated from the tBu. The loss of CH_2=CMe_2 and the loss of a

propyl group from the molecular ion results in *m/z* 182. The dissociation of the alpha carbon bond and the nitrogen gives the base peak *m/z* 151 (loss of a tert-butyl propoxy azane group from the molecular ion). and further breakdown of this fragment results in a fluoro-tropylium cation at *m/z* 109. The fragment *m/z* 140 is 4-fluorobenzyl hydroxylamine and the peak at *m/z* 57 is the tertiary butyl cation

Replacing butanal with its deuterated analogues in the Fenton-based reaction demonstrates the production deuterated propyl radicals and subsequent incorporation by the spin trap. As shown by an increase on the molecular ion of 4 *m/z* when butanal-d_2 was used and 14 *m/z* units when butanal-d_7 was used.

When the Fenton reaction was carried out in the presence of butanal-d_2 as a secondary source of radicals, deuterated propyl radicals ($^{\bullet}C\mathbf{D}_2CH_2CH_3$) are generated by the reaction of $^{\bullet}OH$ with butanal and then trapped by F-PBN. The peak at 285 *m/z* units corresponds to the molecular ion of F-PBN-(Prop-d_2)$_2$. The fragment at *m/z* 270 is due to the loss of a methyl group from the molecular ion (from the tBu group). The loss of CH_2=CMe_2 gives *m/z* 229 and the loss of a dideuterated propyl group from this fragment results in *m/z* 184. The dissociation of the alpha carbon bond and the nitrogen gives the *m/z* 153 and further breakdown of this fragment results in the fluorotropylium cation base peak at *m/z* 109. The fragment *m/z* 140 is N-benzyl hydroxylamine and the peak at *m/z* 57 is the tertiary butyl cation

When the Fenton reaction was carried out in the presence of butanal-d_7 as a secondary source of radicals, deuterated propyl radicals ($^{\bullet}C\mathbf{D}_2C\mathbf{D}_2C\mathbf{D}_3$) are generated by the reaction of $^{\bullet}OH$ with butanal and then trapped by F-PBN. The peak at 295 *m/z* units corresponds to the molecular ion of F-PBN-(Prop-d_7)$_2$. The fragment at *m/z* 280 is due to the loss of a methyl group from the molecular ion (from the tBu group). The loss of CH_2=CMe_2 and the loss of a deuterated propyl group from the molecular ion results in *m/z* 189. The dissociation of the alpha carbon bond and the nitrogen gives the base peak *m/z* 158 and further breakdown of this fragment results in a fluoro-tropylium-4-d cation at *m/z* 110. The peak at *m/z* 57 is the tertiary butyl cation

Table 4.4 Molecular ion($M^{+\bullet}$) m/z values for PBN di-propyl adducts detected by GC-MS analysis of the Fenton mixture containing PBN and butanal

Fenton system	Compound name or formula	$M^{+\bullet}$ (m/z)	other significant ions (*m/z*)
PBN + Butanal	PBN-$(CH_2CH_2CH_3)_2$	**263**	248, 220, 164, 133 (bp), 91, 77, 57
PBN + Butanal-d_2	PBN-$(CD_2CH_2CH_3)_2$	**267**	252, 222, 166, 135 (bp), 91, 77, 57
PBN + Butanal-d_7	PBN-$(CD_2CD_2CD_3)_2$	**277**	262, 227, 171, 140 (bp), 92, 77, 57
PBN-d_6+ Butanal	PBN-d_6-$(CH_2CH_2CH_3)_2$	**269**	254, 226, 170, 139 (bp), 97, 82, 57
PBN-d_6+ Butanal-d_2	PBN-d6-$(CD_2CH_2CH_3)_2$	**273**	258, 228, 172, 141 , 97(bp), 82, 57
PBN-d_6+ Butanal-d_7	PBN-d6-$(CD_2CD_2CD_3)_2$	**283**	268, 233,177, 146 (bp), 98, 82, 57
F-PBN + Butanal	F-PBN-$(CH_2CH_2CH_3)_2$	**281**	266, 238, 182, 151 (bp), 109, 95, 57
F-PBN + Butanal-d_2	F-PBN-$(CD_2CH_2CH_3)_2$	**285**	270, 240, 184, 153 (bp), 109, 95, 57
F-PBN + Butanal-d_7	F-PBN-$(CD_2CD_2CD_3)_2$	**295**	280, 245, 189, 158 (bp),109 ,95,57

4.3 Electron ionization-mass spectra (EI-MS) of the mono-propyl adduct of PBN compound 4

4.3.1 Monopropyl adduct of PBN {PBN-($CH_2CH_2CH_3$)} (compound 4)

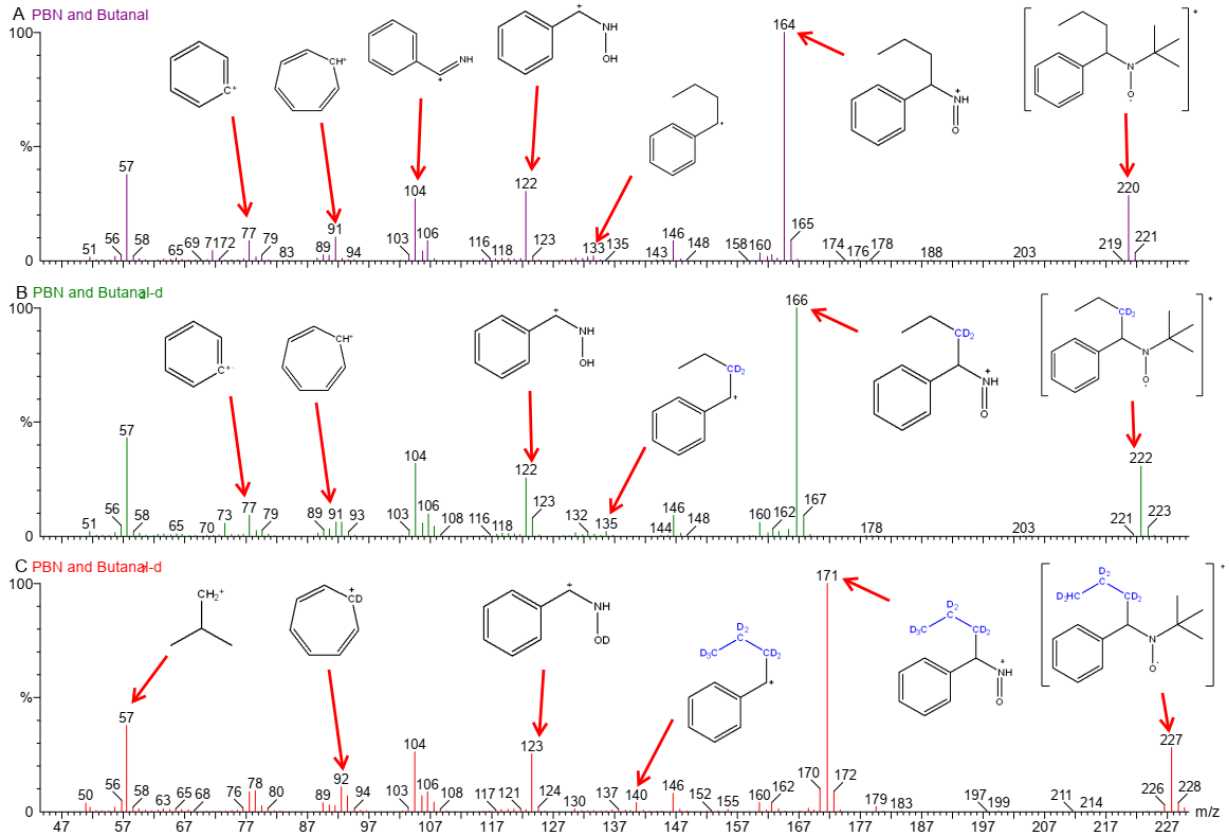

Figure 4.3.1 Electron Ionization mass spectra (EI-MS) corresponding to PBN adducts obtained from the analysis of the Fenton reaction mixture containing PBN, butanal and deuterated analogues at rt 10.78 minutes

The EI mass spectra in Figure 4.3.1 correspond to the a) the PBN mono-propyl adduct (top spectrum); b) the PBN dideuterated mono-propyl adduct (middle spectrum); c) the PBN perdeuterated mono-propyl adduct (bottom spectrum).

When the Fenton reaction was carried out in the presence of butanal as a secondary source of radicals, propyl radicals ($^{\bullet}CH_2CH_2CH_3$) are generated by the reaction of $^{\bullet}OH$ with butanal and then trapped by PBN. The peak at 220 *m/z* units corresponds to the molecular ion of PBN-Prop (one propyl adding to the carbon atom of the C=N). The loss of CH_2=CMe_2 results in base peak *m/z* 164 and the further loss of a propyl group

from the molecular ion results in *m/z* 122 N-benzyl hydroxylamine. The dissociation of the alpha carbon bond and the nitrogen gives the butyl benzene cation peak *m/z* 133, and further breakdown of this fragment results in a tropylium cation at *m/z* 91. The peak at *m/z* 104 is the phenylmethanimine cation and the peak at *m/z* 57 is the tertiary butyl cation

Replacing butanal with its deuterated analogues in the Fenton-based reaction demonstrates the production of deuterated propyl radicals and subsequent incorporation by the spin trap. As shown by an increase on the molecular ion of 2 *m/z* when butanal-d_2 was used and 7 *m/z* units when butanal-d_7 was used.

When the Fenton reaction was carried out in the presence of butanal-d_2 as a secondary source of radicals, deuterated propyl radicals ($^{\bullet}C\mathbf{D}_2CH_2CH_3$) are generated by the reaction of $^{\bullet}OH$ with butanal and then trapped by PBN. The peak at 222 *m/z* units corresponds to the molecular ion of PBN-Prop-d_2. The loss of $CH_2{=}CMe_2$ gives base peak *m/z* 166 and the loss of a dideuterated propyl group from this fragment results in *m/z* 122 N-benzyl hydroxylamine. The dissociation of the alpha carbon bond and the nitrogen gives *m/z* 135 and further breakdown of this fragment results in a tropylium cation peak at *m/z* 91. The peak at *m/z* 104 is the phenylmethanimine cation and the peak at *m/z* 57 is the tertiary butyl cation

When the Fenton reaction was carried out in the presence of butanal-d_7 as a secondary source of radicals, deuterated propyl radicals ($^{\bullet}C\mathbf{D}_2C\mathbf{D}_2C\mathbf{D}_3$) are generated by the reaction of $^{\bullet}OH$ with butanal and then trapped by PBN. The peak at 227 *m/z* units corresponds to the molecular ion of PBN-Prop-d_7. The loss of $CH_2{=}CMe_2$ gives *m/z* the base peak *m/z* 171 and the further loss of a deuterated propyl group from the molecular ion results in *m/z* 123 N-benzyl hydroxylamine-O-d, where a deuterated hydrogen has rearranged from the deuterated propyl group and added to the oxygen position of PBN. The dissociation of the alpha carbon bond and the nitrogen gives the peak *m/z* 140 and further breakdown of this fragment results in a tropylium cation at *m/z* 91. The peak at *m/z* 104 is the phenylmethanimine cation and the peak at *m/z* 57 is the tertiary butyl cation.

4.3.2 Monopropyl adduct of PBN-d_6 {PBN-d_6-($CH_2CH_2CH_3$)} (compound 4)

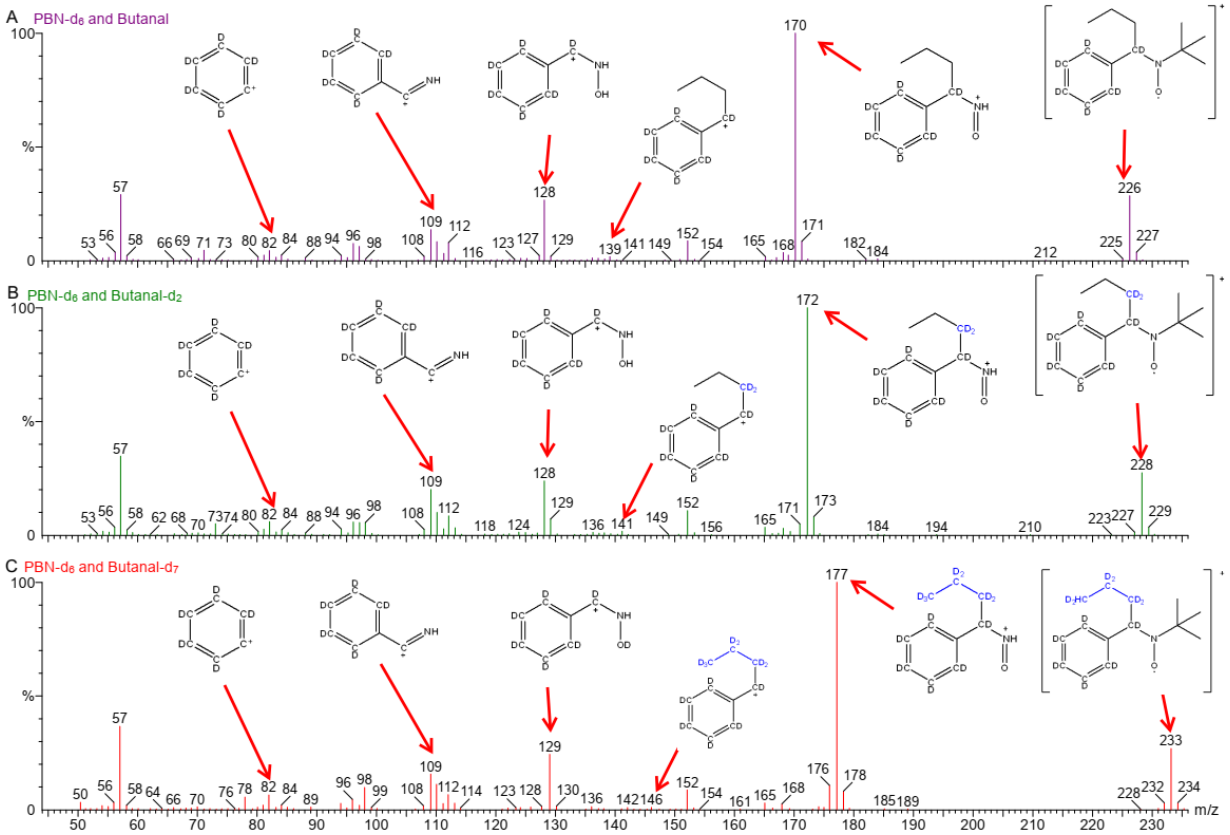

Figure 4.3.2 Electron Ionization mass spectra (EI-MS) corresponding to PBN adducts obtained from the analysis of the Fenton reaction mixture containing PBN-d_6, butanal and deuterated analogues at rt 10.78 minutes

The EI mass spectra in Figure 4.3.2 correspond to the a) the d_6PBN mono-propyl adduct with a molecular ion $M^{+\bullet}$ at 226 (EI-MS d_6PBN and butanal, top spectrum); b) the d_6PBN dideuterated mono-propyl adduct $M^{+\bullet}$ 228 (EI-MS d_6PBN and butanal-d_2, middle spectrum); c) the d_6PBN perdeuterated mono-propyl adduct $M^{+\bullet}$ 233 (EI-MS d_6PBN and butanal-d_7, bottom spectrum).

When the Fenton reaction was carried out in the presence of butanal as a secondary source of radicals, propyl radicals ($^{\bullet}CH_2CH_2CH_3$) are generated by the reaction of $^{\bullet}$OH with butanal and then trapped by d_6PBN. The peak at 226 *m/z* units corresponds to the molecular ion of PBN-d_6-Prop (one propyl adding to the carbon atom of the C=N). The loss of CH_2=CMe_2 results in base peak *m/z* 170 and the further loss of a propyl group from the molecular ion results in *m/z* 128 N-benzyl-d_5 hydroxylamine. The dissociation of the alpha carbon bond and the nitrogen gives the peak *m/z* 139 (loss of a N-tert-butyl hydroxylamine

group from the molecular ion). and further breakdown of this fragment results in a perdeuterated tropylium cation at *m/z* 97. The peak at *m/z* 57 is the tertiary butyl cation

Replacing butanal with its deuterated analogues in the Fenton-based reaction demonstrates the production of deuterated propyl radicals and subsequent incorporation by the spin trap. As shown by an increase on the molecular ion of 2 *m/z* when butanal-d_2 was used and 7 *m/z* units when butanal-d_7 was used.

When the Fenton reaction was carried out in the presence of butanal-d_2 as a secondary source of radicals, deuterated propyl radicals ($^{\bullet}C\mathbf{D}_2CH_2CH_3$) are generated by the reaction of $^{\bullet}OH$ with butanal and then trapped by PBN. The peak at 228 *m/z* units corresponds to the molecular ion of PBN-d_6-Prop-d_2. The loss of CH_2=CMe_2 gives base peak *m/z* 172 and the loss of a dideuterated propyl group from this fragment results in *m/z* 128 N-benzyl-d_5 hydroxylamine. The dissociation of the alpha carbon bond and the nitrogen gives *m/z* 141 and further breakdown of this fragment results in a perdeuterated tropylium cation peak at *m/z* 97. The peak at *m/z* 57 is the tertiary butyl cation

When the Fenton reaction was carried out in the presence of butanal-d_7 as a secondary source of radicals, deuterated propyl radicals ($^{\bullet}C\mathbf{D}_2C\mathbf{D}_2C\mathbf{D}_3$) are generated by the reaction of $^{\bullet}OH$ with butanal and then trapped by PBN. The peak at 227 *m/z* units corresponds to the molecular ion of PBN-d_6-Prop-d_7. The loss of CH_2=CMe_2 gives *m/z* the base peak *m/z* 177 and the further loss of a deuterated propyl group from the molecular ion results in *m/z* 129 N-benzyl-d_5 hydroxylamine-O-d, where a deuterated hydrogen has rearranged from the deuterated propyl group and added to the oxygen position of PBN-d_6. The dissociation of the alpha carbon bond and the nitrogen gives the peak *m/z* 146 and further breakdown of this fragment results in a perdeuterated tropylium cation at *m/z* 98. The peak at *m/z* 57 is the tertiary butyl cation

4.3.3 Monopropyl adduct of F-PBN {F-PBN-($CH_2CH_2CH_3$)}, (compound 4)

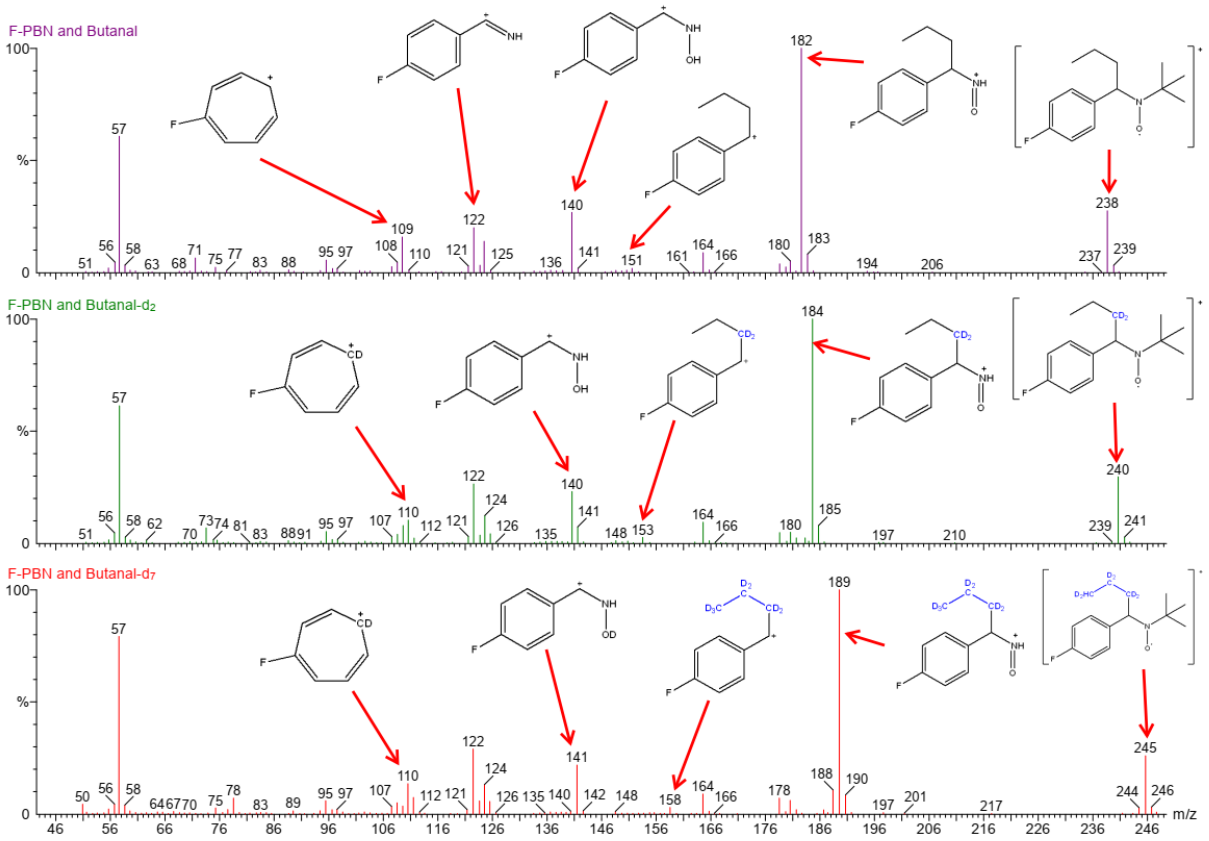

Figure 4.3.3 Electron Ionization mass spectra (EI-MS) corresponding to F-PBN adducts obtained from the analysis of the Fenton reaction mixture containing F-PBN, butanal and deuterated analogues at rt 10.78 minutes

The EI mass spectra in Figure 4.3.3 correspond to the a) the F-PBN mono-propyl adduct with a molecular ion $M^{+\bullet}$ at 238 (EI-MS F-PBN and butanal, top spectrum); b) the F-PBN dideuterated mono-propyl adduct $M^{+\bullet}$ 240 (EI-MS F-PBN and butanal-d_2, middle spectrum); c) the F-PBN perdeuterated mono-propyl adduct $M^{+\bullet}$ 245 (EI-MS F-PBN and butanal-d_7, bottom spectrum).

When the Fenton reaction was carried out in the presence of butanal as a secondary source of radicals, propyl radicals ($^{\bullet}CH_2CH_2CH_3$) are generated by the reaction of $^{\bullet}OH$ with butanal and then trapped by F-PBN. The peak at 238*m/z* units corresponds to the molecular ion of F-PBN-Prop (one propyl adding to the carbon atom of the C=N). The loss of CH_2=CMe_2 results in base peak *m/z* 182 and the further loss of a propyl group from the molecular ion results in *m/z* 140 N-(4-fluorobenzyl) hydroxylamine. The dissociation of the alpha carbon bond and the nitrogen gives the peak *m/z* 151 (loss of a tert-butyl propoxy azane group from the molecular ion) and further breakdown of this fragment results in a fluorotropylium cation

at *m/z* 109. The peak at *m/z* 122 is the fluorophenylmethanimine cation and the peak at *m/z* 57 is the tertiary butyl cation

Replacing butanal with its deuterated analogues in the Fenton-based reaction demonstrates the production of deuterated propyl radicals and subsequent incorporation by the spin trap. As shown by an increase on the molecular ion of 2 *m/z* when butanal-d_2 was used and 7 *m/z* units when butanal-d_7 was used.

When the Fenton reaction was carried out in the presence of butanal-d_2 as a secondary source of radicals, deuterated propyl radicals ($^{\bullet}C\mathbf{D}_2CH_2CH_3$) are generated by the reaction of $^{\bullet}OH$ with butanal and then trapped by F-PBN. The peak at 240 *m/z* units corresponds to the molecular ion of F-PBN-Prop-d_2. The loss of CH_2=CMe_2 gives base peak *m/z* 184 and the loss of a dideuterated propyl group from this fragment results in *m/z* 140 N-benzyl hydroxylamine. The dissociation of the alpha carbon bond and the nitrogen gives *m/z* 153 and further breakdown of this fragment results in a fluorotropylium-1-d cation peak at *m/z* 110. The peak at *m/z* 122 is the fluorophenylmethanimine cation and the peak at *m/z* 57 is the tertiary butyl cation

When the Fenton reaction was carried out in the presence of butanal-d_7 as a secondary source of radicals, deuterated propyl radicals ($^{\bullet}C\mathbf{D}_2C\mathbf{D}_2C\mathbf{D}_3$) are generated by the reaction of $^{\bullet}OH$ with butanal and then trapped by PBN. The peak at 227 *m/z* units corresponds to the molecular ion of F-PBN-Prop-d_7. The loss of CH_2=CMe_2 gives *m/z* the base peak *m/z* 171 and the further loss of a deuterated propyl group from the molecular ion results in *m/z* 123 N-benzyl hydroxylamine-O-d, where a deuterated hydrogen has rearranged from the deuterated propyl group and added to the oxygen position of PBN. The dissociation of the alpha carbon bond and the nitrogen gives the peak *m/z* 140 and further breakdown of this fragment results in a fluorotropylium-1-d cation at *m/z* 110. The peak at *m/z* 122 is the fluorophenylmethanimine cation and the peak at *m/z* 57 is the tertiary butyl cation.

4.4 Detection of butanal radical and propyl radical adduct of PBN derivatives (compound 5)

4.4.1 PBN-($CH_2CH_2CH_2CHO$)($CH_2CH_2CH_3$) (compound 5)

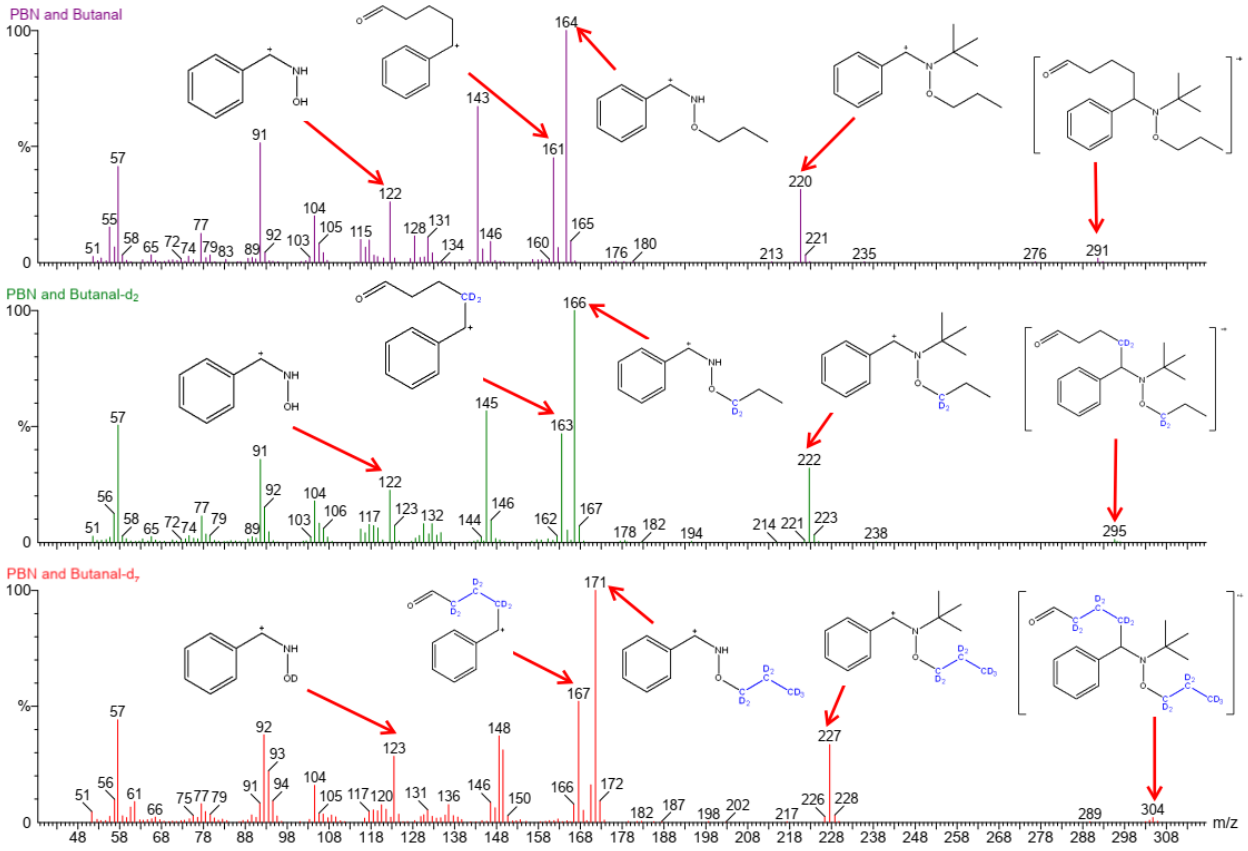

Figure 4.4.1 Electron Ionization mass spectra (EI-MS) corresponding to PBN adducts obtained from the analysis of the Fenton reaction mixture containing PBN, butanal and deuterated analogues at rt 10.94 minutes

The EI mass spectra in Figure 4.4.1 correspond to a) the PBN mono-butanal mono-propyl adduct, PBN ($CH_2CH_2CH_2CHO$)($CH_2CH_2CH_3$) (top spectrum), and b) the PBN dideutero mono-butanal mono-propyl adduct of PBN, PBN($CH_2CH_2C\mathbf{D}_2CHO$)($C\mathbf{D}_2CH_2CH_3$) (middle spectrum) and c) the PBN perdeutero mono-butanal mono-propyl adduct of PBN, PBN-($C\mathbf{D}_2C\mathbf{D}_2C\mathbf{D}_2CHO$)($C\mathbf{D}_2C\mathbf{D}_2C\mathbf{D}_3$) (bottom spectrum).

When the Fenton reaction was carried out in the presence of butanal as a secondary source of radicals (top spectrum), butanal radicals ($^{\bullet}CH_2CH_2CH_2CHO$) and propyl radicals ($^{\bullet}CH_2CH_2CH_3$) were generated by the reaction of $^{\bullet}OH$ with butanal and were then trapped by PBN. The peak at *m/z* 291 corresponds to the molecular ion of PBN-($CH_2CH_2CH_2CHO$)($CH_2CH_2CH_3$). The loss of a methyl group gives 276 *m/z* units. The

loss of the butanal group from the alpha carbon gives us *m/z* 220 and further fragmentation of this fragment results in *m/z* 164. The dissociation of the alpha carbon and nitrogen results in *m/z* 161. *m/z* 91 units is the tropylium ion.

When the Fenton reaction was carried out in the presence of butanal-2,2-d_2 as a secondary source of radicals (middle spectrum), butanal-d_2 radicals ($^{\bullet}CH_2CH_2C\mathbf{D}_2CHO$) and propyl-$d_2$ radicals ($^{\bullet}C\mathbf{D}_2CH_2CH_3$) were formed and trapped by PBN. The peak at *m/z* 295 units corresponds to the molecular ion of PBN-($CH_2CH_2C\mathbf{D}_2CHO$) ($C\mathbf{D}_2CH_2CH_3$), 4 *m/z* units higher with the inclusion of butanal-d_2 than without. The loss of the butanal group from the alpha carbon gives us *m/z* 222 and further fragmentation of this fragment results in *m/z* 166 (2 *m/z* units higher showing one of adducts is included). The dissociation of the alpha carbon and nitrogen results in *m/z* 163. *m/z* 91 units is the tropylium ion.

When the Fenton reaction was carried out in the presence of butanal-2,2,3,3,4,4,4-d_7 as a secondary source of radicals (bottom spectrum), butanal-d_6 radicals ($^{\bullet}C\mathbf{D}_2C\mathbf{D}_2C\mathbf{D}_2CHO$) and propyl-$d_7$ radicals ($^{\bullet}C\mathbf{D}_2C\mathbf{D}_2C\mathbf{D}_3$) were formed and trapped by PBN. The peak at *m/z* 304 units corresponds to the molecular ion of PBN-($C\mathbf{D}_2C\mathbf{D}_2C\mathbf{D}_2CHO$), ($C\mathbf{D}_2C\mathbf{D}_2C\mathbf{D}_3$) 13 *m/z* units higher with the inclusion of butanal-d_7 and propyl-d_7 than without. The loss of the butanal group from the alpha carbon gives us *m/z* 227 and further fragmentation of this fragment results in *m/z* 171 (7 *m/z* units higher showing the deuterated propyl adduct is included). The dissociation of the alpha carbon and nitrogen results in *m/z* 167. *m/z* 91 units is the tropylium ion.

4.4.2 PBN-d_6-($CH_2CH_2CH_2CHO$)($CH_2CH_2CH_3$) (compound 5)

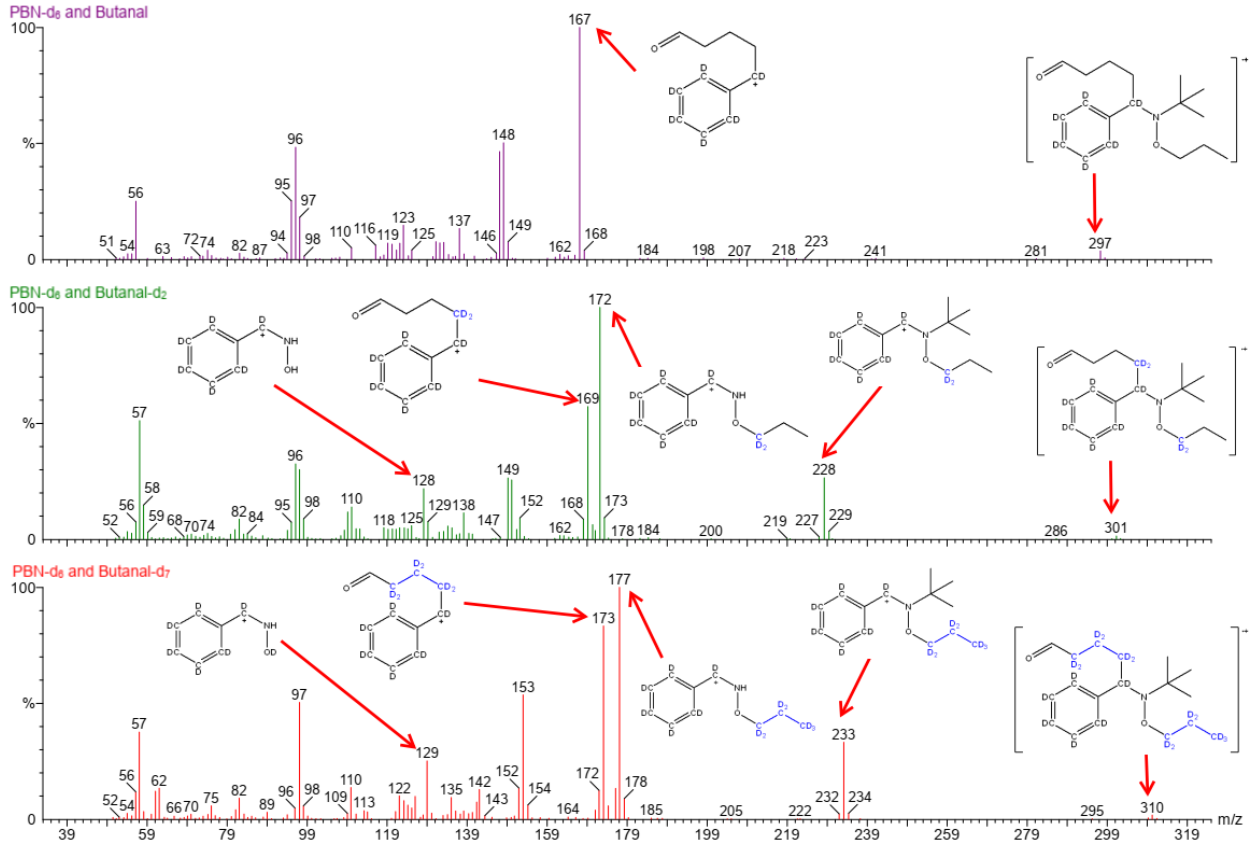

Figure 4.4.2 Electron Ionization mass spectra (EI-MS) corresponding to PBN-d_6 adducts obtained from the analysis of the Fenton reaction mixture containing PBN-d_6, butanal and deuterated analogues at rt 10.94 minutes

The EI mass spectra in Figure 4.4.2 correspond to a) the PBN-d_6 mono-butanal mono-propyl adduct, PBN-d_6($CH_2CH_2CH_2CHO$)($CH_2CH_2CH_3$) (top spectrum), and b) the PBN-d_6 dideutero mono-butanal mono-propyl adduct of PBN-d_6, PBN-d_6($CH_2CH_2C\mathbf{D}_2CHO$)($C\mathbf{D}_2CH_2CH_3$) (middle spectrum) and c) the PBN-d_6 perdeutero mono-butanal mono-propyl adduct of PBN-d_6, PBN-d_6-($C\mathbf{D}_2C\mathbf{D}_2C\mathbf{D}_2CHO$)($C\mathbf{D}_2C\mathbf{D}_2C\mathbf{D}_3$) (bottom spectrum).

When the Fenton reaction was carried out in the presence of butanal as a secondary source of radicals (top spectrum), butanal radicals ($^{\bullet}CH_2CH_2CH_2CHO$)and propyl radicals ($^{\bullet}CH_2CH_2CH_3$) were generated by the reaction of $^{\bullet}OH$ with butanal and were then trapped by PBN-d_6. The peak at *m/z* 297 corresponds to the molecular ion of PBN-d_6-($CH_2CH_2CH_2CHO$)($CH_2CH_2CH_3$). The loss of the butanal group from the alpha carbon should theoretically give us *m/z* 226 however this is not present and further fragmentation of this

fragment should have resulted in *m/z* 170. The dissociation of the alpha carbon and nitrogen results in the base peak *m/z* 167 units. *m/z* 96 units is the perdeuterated tropylium ion.

When the Fenton reaction was carried out in the presence of butanal-2,2-d_2 as a secondary source of radicals (middle spectrum), butanal-d_2 radicals ($^{\bullet}CH_2CH_2C\mathbf{D}_2CHO$) and propyl-$d_2$ radicals ($^{\bullet}C\mathbf{D}_2CH_2CH_3$) were formed and trapped by d_6PBN. The peak at *m/z* 301 units corresponds to the molecular ion of PBN-d_6-($CH_2CH_2C\mathbf{D}_2CHO$) ($C\mathbf{D}_2CH_2CH_3$), 4 *m/z* units higher with the inclusion of butanal-d_2 than without. The loss of the butanal group from the alpha carbon results in *m/z* 226 and further fragmentation of this fragment results in the base peak of *m/z* 172 (2 *m/z* units higher when butanal-d_2 is used than without, showing one of adducts is included). The dissociation of the alpha carbon and nitrogen results in *m/z* 169. *m/z* 96 units is the perdeuterated tropylium ion.

When the Fenton reaction was carried out in the presence of butanal-2,2,3,3,4,4,4-d_7 as a secondary source of radicals (bottom spectrum), butanal-d_6 radicals ($^{\bullet}C\mathbf{D}_2C\mathbf{D}_2C\mathbf{D}_2CHO$) and propyl-$d_7$ radicals ($^{\bullet}C\mathbf{D}_2C\mathbf{D}_2C\mathbf{D}_3$) were formed and trapped by PBN-d_6. The peak at *m/z* 310 units corresponds to the molecular ion of PBN-d_6-($C\mathbf{D}_2C\mathbf{D}_2C\mathbf{D}_2CHO$),($C\mathbf{D}_2C\mathbf{D}_2C\mathbf{D}_3$), 13 *m/z* units higher with the inclusion of butanal-d_7 and propyl-d_7 than without. The loss of the butanal group from the alpha carbon gives us *m/z* 233 and further fragmentation of this fragment results in *m/z* 177 (7 *m/z* units higher showing the propyl-d_7 adducts is included). The dissociation of the alpha carbon and nitrogen results in *m/z* 173. *m/z* 97 units is the perdeuterated tropylium ion.

4.4.3 (F-PBN-($CH_2CH_2CH_2CHO$)($CH_2CH_2CH_3$) (compound 5)

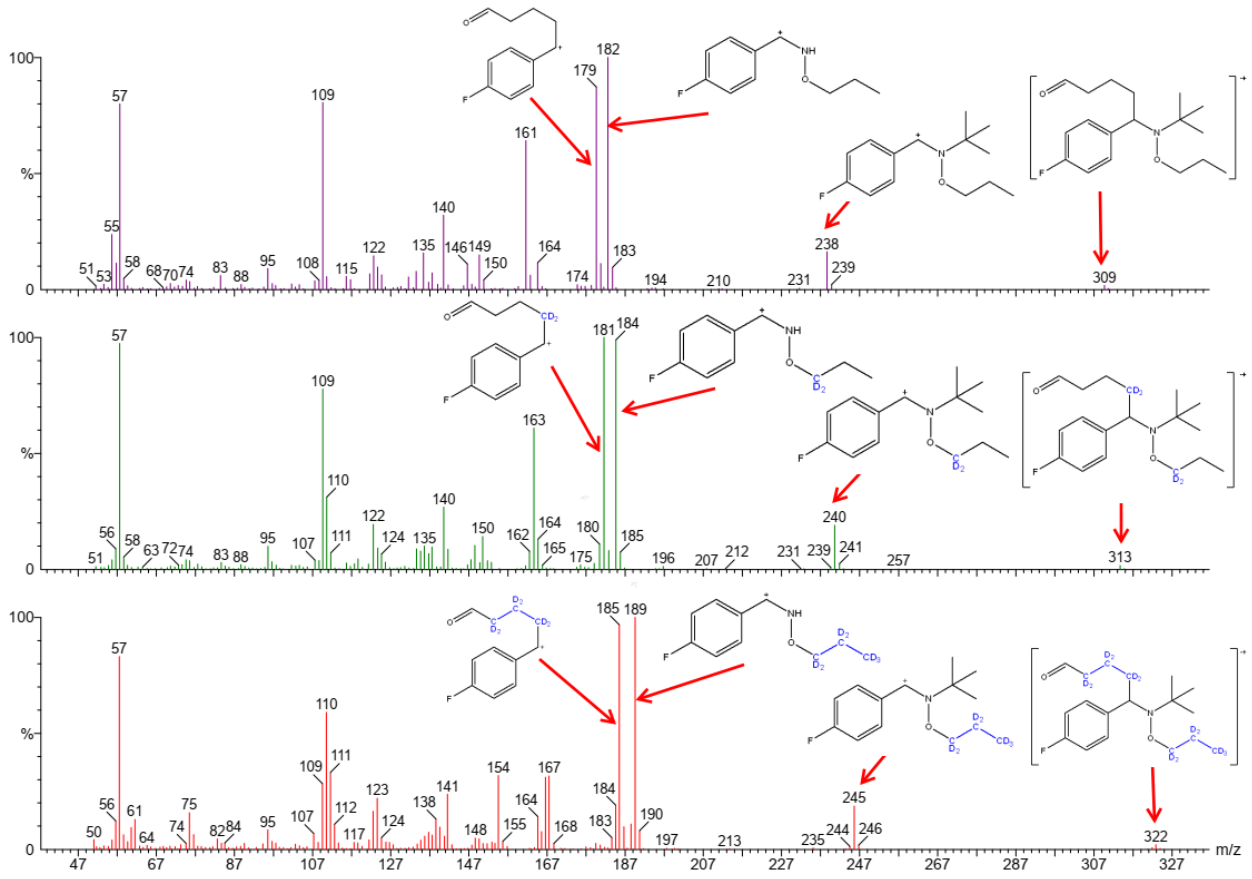

Figure 4.4.3 Electron Ionization mass spectra (EI-MS) corresponding to F-PBN adducts obtained from the analysis of the Fenton reaction mixture containing F-PBN, butanal and deuterated analogues at rt 10.94 minutes

The EI mass spectra Figure 4.4.3 correspond to a) the F-PBN mono-butanal mono-propyl adduct, PBN ($CH_2CH_2CH_2CHO$)($CH_2CH_2CH_3$) (top spectrum), and b) the F-PBN dideutero mono-butanal mono-propyl adduct of F-PBN, F-PBN($CH_2CH_2C\mathbf{D}_2CHO$)($C\mathbf{D}_2CH_2CH_3$) (middle spectrum) and c) the F-PBN perdeutero mono-butanal mono-propyl adduct of F-PBN, F-PBN-($C\mathbf{D}_2C\mathbf{D}_2C\mathbf{D}_2CHO$)($C\mathbf{D}_2C\mathbf{D}_2C\mathbf{D}_3$) (bottom spectrum).

When the Fenton reaction was carried out in the presence of butanal as a secondary source of radicals (top spectrum), butanal radicals ($^{\bullet}CH_2CH_2CH_2CHO$) and propyl radicals ($^{\bullet}CH_2CH_2CH_3$) were generated by the reaction of $^{\bullet}OH$ with butanal and were then trapped by F-PBN. The peak at *m/z* 309 corresponds to the molecular ion of F-PBN-($CH_2CH_2CH_2CHO$)($CH_2CH_2CH_3$). The loss of the butanal group from the alpha carbon gives us *m/z* 238 and further fragmentation of this fragment results in *m/z* 182. The dissociation of the alpha carbon and nitrogen results in *m/z* 179. *m/z* 109 units is the fluorotropylium cation.

When the Fenton reaction was carried out in the presence of butanal-2,2-d_2 as a secondary source of radicals (middle spectrum), butanal-d_2 radicals ($^{\bullet}C\mathbf{D}_2CH_2CH_2CHO$) and propyl-$d_2$ radicals ($^{\bullet}C\mathbf{D}_2CH_2CH_3$) were formed and trapped by F-PBN. The peak at *m/z* 313 units corresponds to the molecular ion of F-PBN-($C\mathbf{D}_2CH_2CH_2CHO$) ($C\mathbf{D}_2CH_2CH_3$), 4 *m/z* units higher with the inclusion of butanal-d_2 than without. The loss of the butanal group from the alpha carbon gives us *m/z* 240 and further fragmentation of this fragment results in *m/z* 184 (2 *m/z* units higher showing one of adducts is included). The dissociation of the alpha carbon and nitrogen results in *m/z* 181. *m/z* 109 units is the fluorotropylium cation.

When the Fenton reaction was carried out in the presence of butanal-2,2,3,3,4,4,4-d_7 as a secondary source of radicals (bottom spectrum), butanal-d_6 radicals ($^{\bullet}C\mathbf{D}_2C\mathbf{D}_2C\mathbf{D}_2CHO$) and propyl-$d_7$ radicals ($^{\bullet}C\mathbf{D}_2C\mathbf{D}_2C\mathbf{D}_3$) were formed and trapped by F-PBN. The peak at *m/z* 322 units corresponds to the molecular ion of F-PBN-($C\mathbf{D}_2C\mathbf{D}_2C\mathbf{D}_2CHO$), ($C\mathbf{D}_2C\mathbf{D}_2C\mathbf{D}_3$) 13 *m/z* units higher with the inclusion of butanal-d_7 and propyl-d_7 than without. The loss of the butanal group from the alpha carbon gives us *m/z* 245 and further fragmentation of this fragment results in *m/z* 189 (7 *m/z* units higher showing the deuterated propyl adduct is included). The dissociation of the alpha carbon and nitrogen results in *m/z* 185. *m/z* 110 units is the fluorotropylium-4-d cation.

4.5 Detection of a second butanal radical and propyl radical adduct of PBN (compound 6)

4.5.1 Electron ionization-mass spectra (EI-MS) of PBN($CH_2CH_2CH_2CHO$)($CH_2CH_2CH_3$) (compound 6)

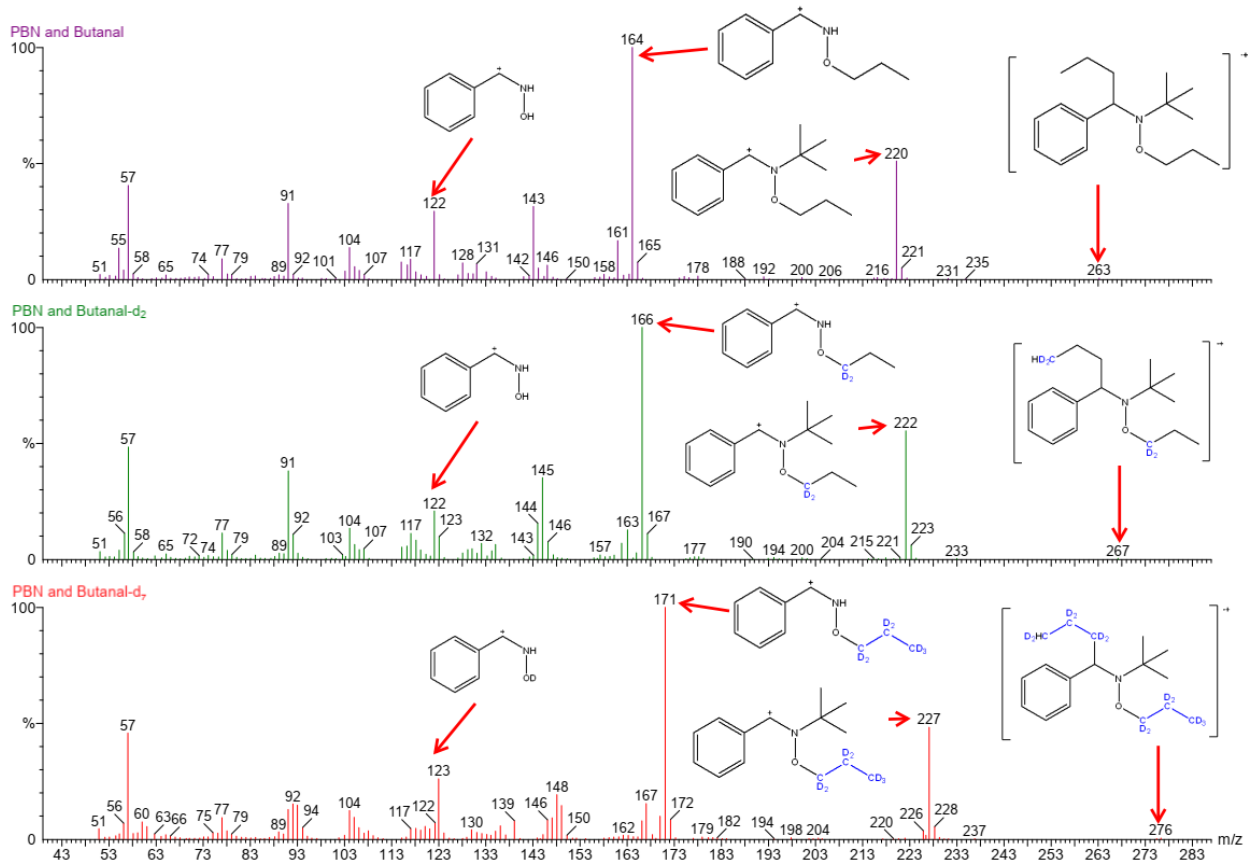

Figure 4.5.1 Electron Ionization mass spectra (EI-MS) corresponding to PBN adducts obtained from the analysis of the Fenton reaction mixture containing PBN, butanal and deuterated analogues at rt 11.02 minutes

The EI mass spectra in Figure 4.5.1 correspond to a) the PBN mono-butanal mono-propyl adduct, PBN($CH_2CH_2CH_2CHO$)($CH_2CH_2CH_3$) (top spectrum), and b) the PBN dideutero mono-butanal mono-propyl adduct of PBN, PBN-($CH_2CH_2C\mathbf{D}_2CHO$)($C\mathbf{D}_2CH_2CH_3$) (middle spectrum) and c) the PBN perdeutero mono-butanal mono-propyl adduct, PBN-($C\mathbf{D}_2C\mathbf{D}_2C\mathbf{D}_2CHO$)($C\mathbf{D}_2C\mathbf{D}_2C\mathbf{D}_3$) (bottom spectrum).

Compound 6 is a diastereomer of compound 5 and 7 (Figure 4.1.2)

When the Fenton reaction was carried out in the presence of butanal as a secondary source of radicals (top spectrum), butanal radicals ($^{\bullet}CH_2CH_2CH_2CHO$) and propyl radicals ($^{\bullet}CH_2CH_2CH_3$) were generated by the reaction of $^{\bullet}OH$ with butanal and were then trapped by PBN. The molecular ion of PBN $(CH_2CH_2CH_2CHO)(CH_2CH_2CH_3)$ expected at *m/z* 291 is too weak to be seen in the EI mass spectra (see Figure 4.5.2, A). The loss of a C=O from the butanal adduct gives 263 *m/z* units. The loss of the butanal group from the alpha carbon gives us *m/z* 220 the loss of $CH_2{=}CMe_2$ results in base peak *m/z* 164 and the further loss of a propyl group from the molecular ion results in *m/z* 122 N-benzyl hydroxylamine. The dissociation of the alpha carbon and nitrogen results in *m/z* 161 (loss of a tert-butyl propoxy azane group from the molecular ion). *m/z* 91 units is the tropylium ion.

When the Fenton reaction was carried out in the presence of butanal-2,2-d_2 as a secondary source of radicals (middle spectrum), butanal-d_2 radicals ($^{\bullet}CH_2CH_2C\mathbf{D}_2CHO$) and propyl-$d_2$ radicals ($^{\bullet}C\mathbf{D}_2CH_2CH_3$) were formed and trapped by PBN. The molecular ion of PBN-($CH_2CH_2C\mathbf{D}_2CHO$) ($C\mathbf{D}_2CH_2CH_3$) expected at *m/z* 295 is too weak and not detected (see Figure 4.5.2, B) in the EI mass spectra (expected 4 *m/z* units higher with the inclusion of butanal-d_2 than without). The loss of a C=O from the butanal adduct gives 267 *m/z* units is visible. The loss of the butanal group from the alpha carbon gives us *m/z* 222 and further fragmentation results in *m/z* 166 (2 *m/z* units higher showing one of adducts is included). The dissociation of the alpha carbon and nitrogen results in *m/z* 163. *m/z* 91 units is the tropylium ion.

When the Fenton reaction was carried out in the presence of butanal-2,2,3,3,4,4,4-d_7 as a secondary source of radicals (bottom spectrum), butanal-d_6 radicals ($^{\bullet}C\mathbf{D}_2C\mathbf{D}_2C\mathbf{D}_2CHO$) and propyl-$d_7$ radicals ($^{\bullet}C\mathbf{D}_2C\mathbf{D}_2C\mathbf{D}_3$) were formed and trapped by PBN. The molecular ion of PBN-($C\mathbf{D}_2C\mathbf{D}_2C\mathbf{D}_2CHO$), ($C\mathbf{D}_2C\mathbf{D}_2C\mathbf{D}_3$) expected at *m/z* 304 is too weak and is not detected (see Figure 4.5.2, C) in the EI mass spectra (expected 13 *m/z* units higher with the inclusion of butanal-d_7 and propyl-d_7 than without). The loss of a C=O from the butanal adduct gives 276 *m/z* units is visible. The loss of the butanal group from the alpha carbon gives us *m/z* 227 and further fragmentation of this fragment results in *m/z* 171 (7 *m/z* units higher showing the deuterated propyl adduct is included). The dissociation of the alpha carbon and nitrogen results in *m/z* 167. *m/z* 91 units is the tropylium ion.

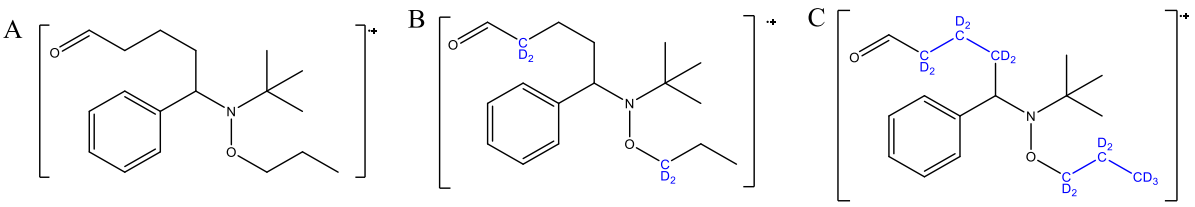

Figure 4.5.2 the molecular ions of compound 6 for A) butanal, B) butanal-d_2 and C) butanal-d_7

4.5.2 Electron ionization-mass spectra (EI-MS) of {{PBN-d_6-($CH_3CH_2CH_2)_2$} (compound 6)

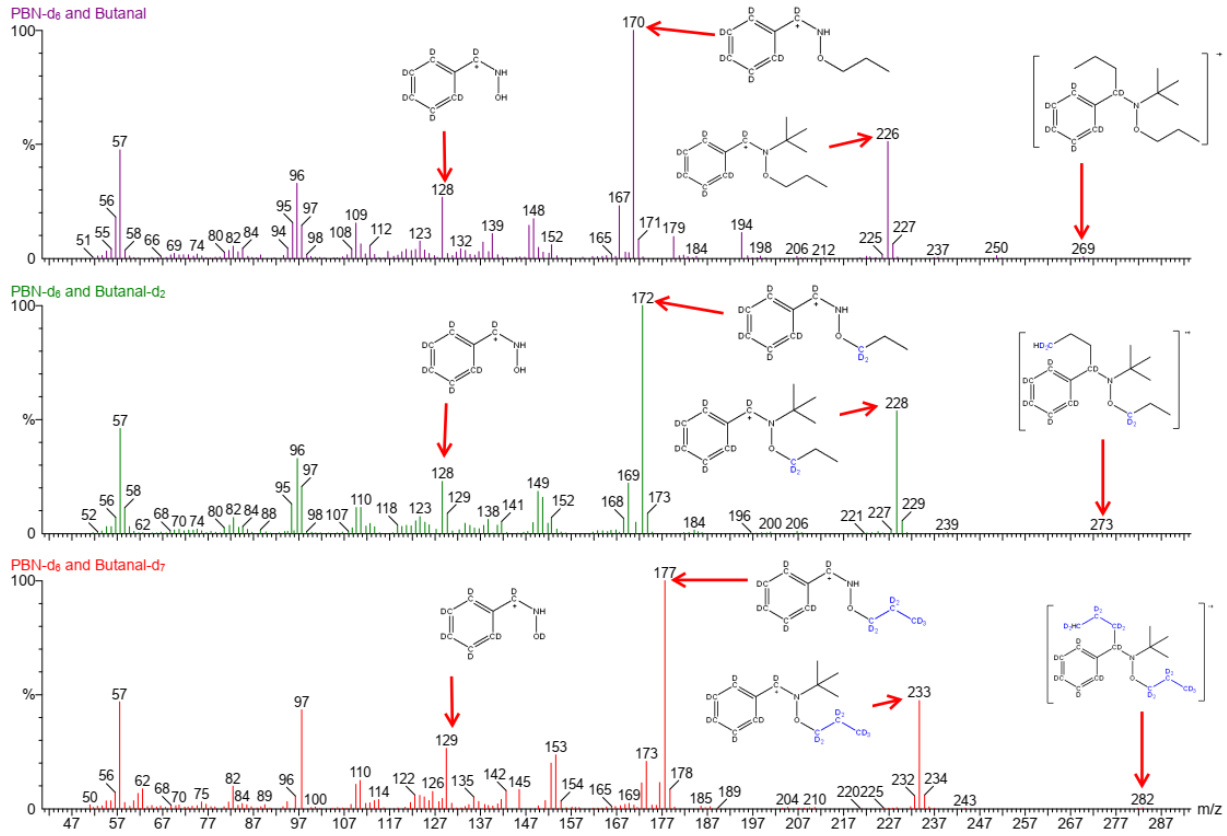

Figure 4.5.3 Electron Ionization mass spectra (EI-MS) corresponding to PBN adducts obtained from the analysis of the Fenton reaction mixture containing PBN-d_6, butanal and deuterated analogues at rt 11.02 minutes

The EI mass spectra in Figure 4.5.3 correspond to a) the PBN-d_6 mono-butanal mono-propyl adduct, PBN-d_6-($CH_2CH_2CH_2CHO$)($CH_2CH_2CH_3$) (top spectrum), and b) the PBN-d_6 dideutero mono-butanal mono-propyl adduct, PBN-d_6-($CH_2CH_2C\mathbf{D}_2CHO$)($C\mathbf{D}_2CH_2CH_3$) (middle spectrum) and c) the PBN-d_6 perdeutero mono-butanal mono-propyl adduct, PBN-d_6 ($C\mathbf{D}_2C\mathbf{D}_2C\mathbf{D}_2CHO$)($C\mathbf{D}_2C\mathbf{D}_2C\mathbf{D}_3$) (bottom spectrum).

This compound has a similar identity to compound 5 and 7 (see Figure 4.1.2) in that the structures are diastereomers of each other.

When the Fenton reaction was carried out in the presence of butanal as a secondary source of radicals (top spectrum), butanal radicals ($^{\bullet}CH_2CH_2CH_2CHO$) and propyl radicals ($^{\bullet}CH_2CH_2CH_3$) were generated by the reaction of $^{\bullet}OH$ with butanal and were then trapped by PBN-d_6. The molecular ion of PBN-d_6-($CH_2CH_2CH_2CHO$)($CH_2CH_2CH_3$) expected at *m/z* 297 is too weak to be seen in the EI mass spectra. The loss

of a C=O from the butanal adduct gives 269 *m/z* units. The loss of the butanal group from the alpha carbon gives us *m/z* 226 the loss of CH_2=CMe_2 results in base peak *m/z* 170 and the further loss of a propyl group from the molecular ion results in *m/z* 128 N-benzyl hydroxylamine. The dissociation of the alpha carbon and nitrogen results in *m/z* 161. *m/z* 91 units is the tropylium ion.

When the Fenton reaction was carried out in the presence of butanal-2,2-d_2 as a secondary source of radicals (middle spectrum), butanal-d_2 radicals ($^{\bullet}CH_2CH_2C\mathbf{D}_2CHO$) and propyl-$d_2$ radicals ($^{\bullet}C\mathbf{D}_2CH_2CH_3$) were formed and trapped by PBN-d_6. The molecular ion of PBN-d_6-($CH_2CH_2C\mathbf{D}_2CHO$) ($C\mathbf{D}_2CH_2CH_3$) expected at *m/z* 301 is too weak and not detected or displayed in the EI mass spectra (expected 4 *m/z* units higher with the inclusion of butanal-d_2 than without). The loss of a C=O from the butanal adduct gives 273 *m/z* units is visible. The loss of the butanal group from the alpha carbon gives us *m/z* 228 and further fragmentation results in *m/z* 172 (2 *m/z* units higher showing one of adducts is included). The dissociation of the alpha carbon and nitrogen results in *m/z* 172. *m/z* 91 units is the tropylium ion.

When the Fenton reaction was carried out in the presence of butanal-2,2,3,3,4,4,4-d_7 as a secondary source of radicals (bottom spectrum), butanal-d_6 radicals ($^{\bullet}C\mathbf{D}_2C\mathbf{D}_2C\mathbf{D}_2CHO$) and propyl-$d_7$ radicals ($^{\bullet}C\mathbf{D}_2C\mathbf{D}_2C\mathbf{D}_3$) were formed and trapped by PBN-d_6. The molecular ion of PBN-d_6-($C\mathbf{D}_2C\mathbf{D}_2C\mathbf{D}_2CHO$), ($C\mathbf{D}_2C\mathbf{D}_2C\mathbf{D}_3$) expected at *m/z* 304 is too weak and is not detected or displayed in the EI mass spectra (expected 13 *m/z* units higher with the inclusion of butanal-d_7 and propyl-d_7 than without). The loss of a C=O from the butanal adduct gives 276 *m/z* units is visible. The loss of the butanal group from the alpha carbon gives us *m/z* 227 and further fragmentation of this fragment results in *m/z* 171 (7 *m/z* units higher showing the deuterated propyl adduct is included). The dissociation of the alpha carbon and nitrogen results in *m/z* 167. *m/z* 91 units is the tropylium ion.

4.5.3 Electron ionization-mass spectra (EI-MS) of {{F-PBN-$(CH_3CH_2CH_2)_2$} (compound 6)

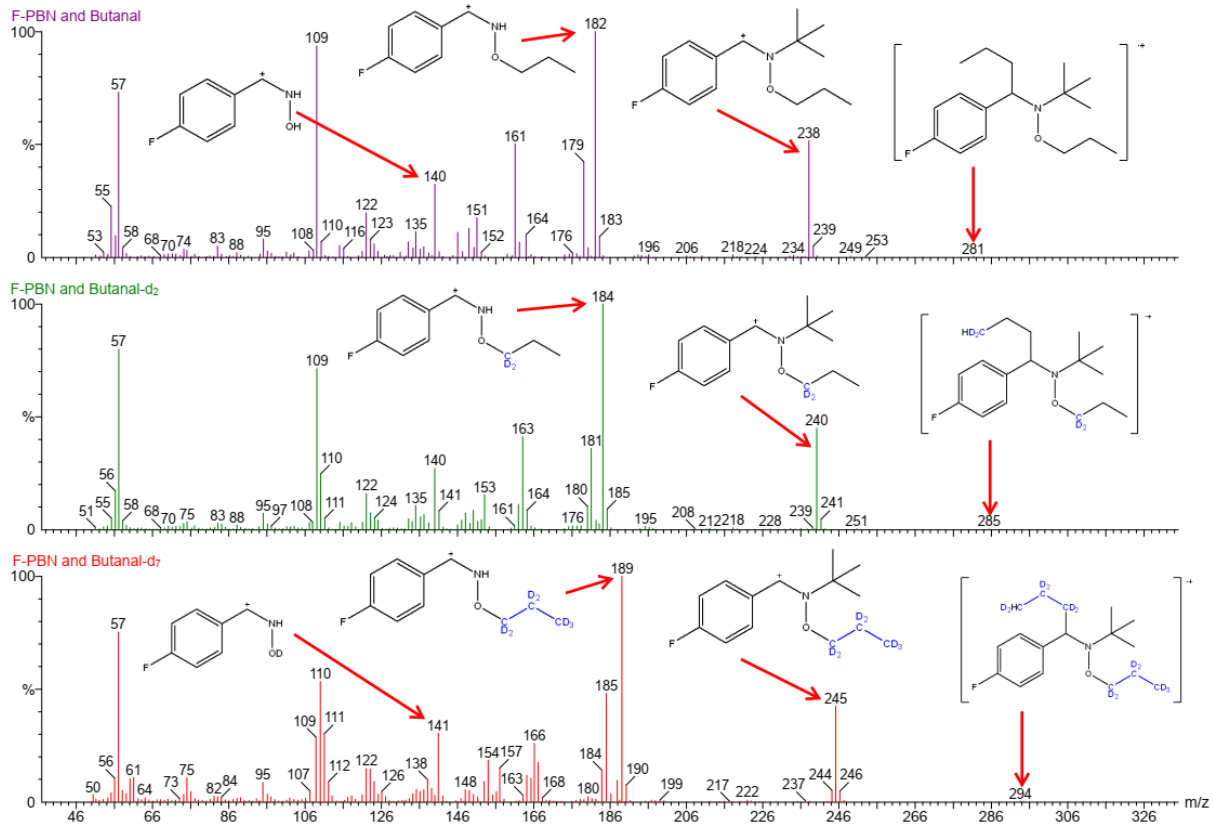

Figure 4.5.4 Electron Ionization mass spectra (EI-MS) corresponding to PBN adducts obtained from the analysis of the Fenton reaction mixture containing F-PBN, butanal and deuterated analogues at rt 11.02 minutes

The EI mass spectra in Figure 4.5.4 correspond to a) the F-PBN mono-butanal mono-propyl adduct, PBN($CH_2CH_2CH_2CHO$)($CH_2CH_2CH_3$) (top spectrum), and b) the F-PBN dideutero mono-butanal mono-propyl adduct, F-PBN-($CH_2CH_2C\mathbf{D}_2CHO$)($C\mathbf{D}_2CH_2CH_3$) (middle spectrum) and c) the F-PBN perdeutero mono-butanal mono-propyl adduct, F-PBN-($C\mathbf{D}_2C\mathbf{D}_2C\mathbf{D}_2CHO$)($C\mathbf{D}_2C\mathbf{D}_2C\mathbf{D}_3$) (bottom spectrum).

This compound has a similar identity to compound 5 and 7 (Figure 4.1.2) in that the structures are diastereomers of each other.

When the Fenton reaction was carried out in the presence of butanal as a secondary source of radicals (top spectrum), butanal radicals ($^{\bullet}CH_2CH_2CH_2CHO$) and propyl radicals ($^{\bullet}CH_2CH_2CH_3$) were generated by the reaction of $^{\bullet}OH$ with butanal and were then trapped by F-PBN. The molecular ion of F-PBN ($CH_2CH_2CH_2CHO$)($CH_2CH_2CH_3$) expected at *m/z* 309 is too weak to be seen in the EI mass spectra. The loss

of a C=O from the butanal adduct gives 281 *m/z* units. The loss of the butanal group from the alpha carbon gives us *m/z* 238 the loss of CH_2=CMe_2 results in base peak *m/z* 182 and the further loss of a propyl group from the molecular ion results in *m/z* 140 N-(4-fluorobenzyl) hydroxylamine. The dissociation of the alpha carbon and nitrogen results in *m/z* 179, the peak at *m/z* 122 is the (4-fluorophenyl)methanimine cation and *m/z* 109 units is the fluorotropylium cation.

When the Fenton reaction was carried out in the presence of butanal-2,2-d_2 as a secondary source of radicals (middle spectrum), butanal-d_2 radicals ($^{\bullet}CH_2CH_2C\mathbf{D}_2CHO$) and propyl-$d_2$ radicals ($^{\bullet}C\mathbf{D}_2CH_2CH_3$) were formed and trapped by F-PBN. The molecular ion of F-PBN-($CH_2CH_2C\mathbf{D}_2CHO$)($C\mathbf{D}_2CH_2CH_3$) expected at *m/z* 313 is too weak and not detected or displayed in the EI mass spectra (expected 4 *m/z* units higher with the inclusion of butanal-d_2 than without). The loss of a C=O from the butanal adduct gives 285 *m/z* units is visible. The loss of the butanal group from the alpha carbon gives us *m/z* 240 and further fragmentation results in *m/z* 184 (2 *m/z* units higher showing one of adducts is included). The dissociation of the alpha carbon and nitrogen results in base peak *m/z* 182. *m/z* 109 units is the fluorotropylium cation.

When the Fenton reaction was carried out in the presence of butanal-2,2,3,3,4,4,4-d_7 as a secondary source of radicals (bottom spectrum), butanal-d_6 radicals ($^{\bullet}C\mathbf{D}_2C\mathbf{D}_2C\mathbf{D}_2CHO$) and propyl-$d_7$ radicals ($^{\bullet}C\mathbf{D}_2C\mathbf{D}_2C\mathbf{D}_3$) were formed and trapped by F-PBN. The molecular ion of F-PBN-($C\mathbf{D}_2C\mathbf{D}_2C\mathbf{D}_2CHO$), ($C\mathbf{D}_2C\mathbf{D}_2C\mathbf{D}_3$) expected at *m/z* 322 is too weak and is not detected or displayed in the EI mass spectra (expected 13 *m/z* units higher with the inclusion of butanal-d_7 and propyl-d_7 than without). The loss of a C=O from the butanal adduct gives 294 *m/z* units is visible. The loss of the butanal group from the alpha carbon gives us *m/z* 245 and further fragmentation of this fragment results in *m/z* 189 (7 *m/z* units higher showing the deuterated propyl adduct is included). The dissociation of the alpha carbon and nitrogen results in base peak *m/z* 189. *m/z* 110 units is the fluorotropylium-4-d ion.

4.6 Detection of a third butanal radical and propyl radical adduct of PBN derivatives (compound 7)

4.6.1 Electron ionization-mass spectra of mono-oxybutyl mono-propyl adduct PBN(CH_3CHCH_2CHO)($CH_2CH_2CH_3$) (compound 7)

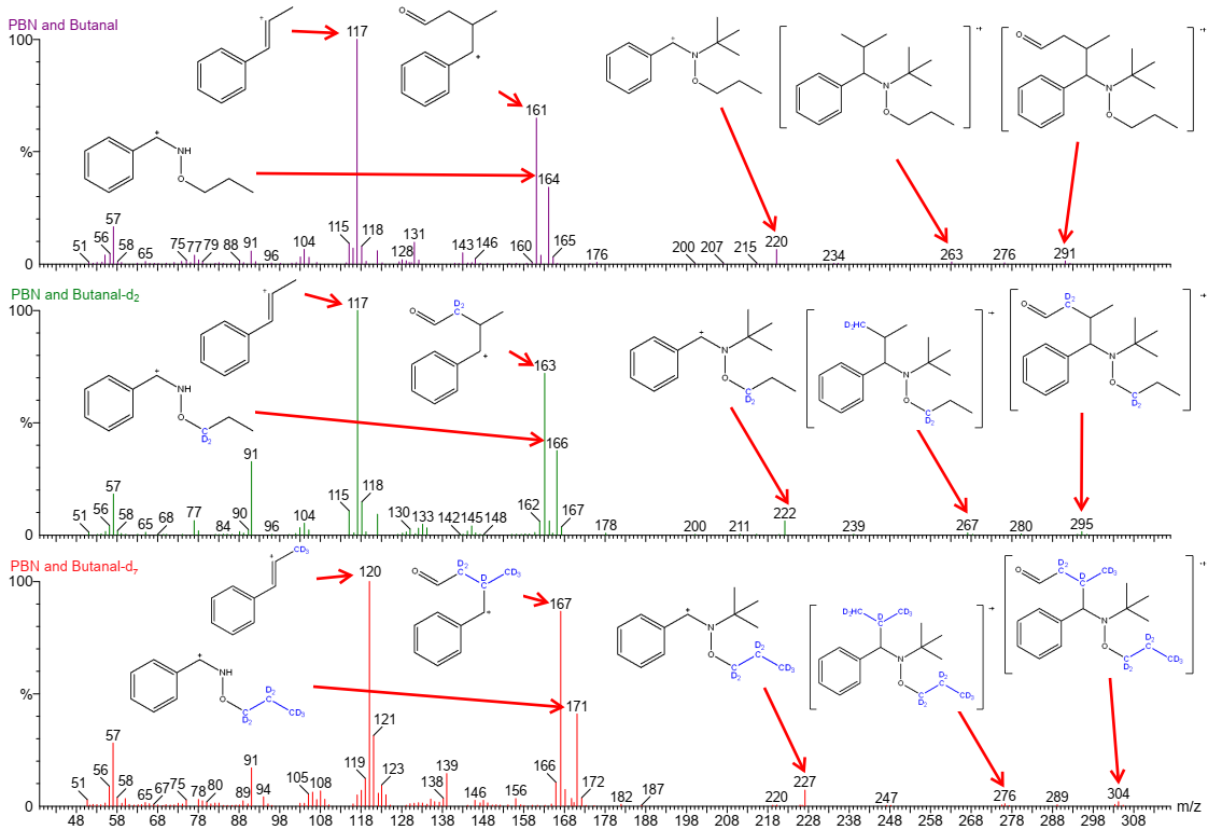

Figure 4.6.1 Electron Ionization mass spectra (EI-MS) corresponding to PBN adducts obtained from the analysis of the Fenton reaction mixture containing PBN, butanal and deuterated analogues at rt 11.67 minutes

The EI mass spectra in Figure 4.6.1 correspond to a) the PBN mono-butanal mono-propyl adduct, PBN(CH_3CHCH_2CHO)($CH_2CH_2CH_3$) (top spectrum), and b) the PBN dideutero mono-butanal mono-propyl adduct, PBN-($CH_3CHC\mathbf{D}_2CHO$)($C\mathbf{D}_2CH_2CH_3$) (middle spectrum) and c) the PBN perdeutero mono-butanal mono-propyl adduct, PBN-($C\mathbf{D}_3C\mathbf{D}C\mathbf{D}_2CHO$)($C\mathbf{D}_2C\mathbf{D}_2C\mathbf{D}_3$) (bottom spectrum).

This compound has a similar identity to compound 5 and 6 (Figure 4.1.2) in that the structures are diastereomers of one another.

When the Fenton reaction was carried out in the presence of butanal as a secondary source of radicals (top spectrum), butanal radicals ($CH_3^{\bullet}CHCH_2CHO$) and propyl radicals ($^{\bullet}CH_2CH_2CH_3$) were generated by the reaction of $^{\bullet}OH$ with butanal and were then trapped by PBN. The molecular ion of PBN ($(CH_3CHCH_2CHO)(CH_2CH_2CH_3)$) is at *m/z* 291. The loss of a C=O from the butanal adduct gives 263 *m/z* units. The loss of the butanal group from the alpha carbon gives us *m/z* 220 and further loss of $CH_2{=}CMe_2$ results in base peak *m/z* 164. The dissociation of the alpha carbon and nitrogen results in *m/z* 161 (loss of a tBu propoxy azane group from the molecular ion) and further fragmentation (CH_3CHO group is lost) leads to *m/z* 117 with the identity 1-phenylprop-1-en-2-ylium. *m/z* 91 units is the tropylium ion.

When the Fenton reaction was carried out in the presence of butanal-2,2-d_2 as a secondary source of radicals (middle spectrum), butanal-d_2 radicals ($CH_3^{\bullet}CHC\mathbf{D}_2CHO$) and propyl-$d_2$ radicals ($^{\bullet}C\mathbf{D}_2CH_2CH_3$) were formed and trapped by PBN. The molecular ion of PBN-($CH_3CHC\mathbf{D}_2CHO$) ($C\mathbf{D}_2CH_2CH_3$) is at *m/z* 295 (expected 4 *m/z* units higher with the inclusion of butanal-d_2 than without). The loss of a C=O from the butanal adduct gives 267 *m/z* units. The loss of the butanal group from the alpha carbon gives us *m/z* 222 and further fragmentation results in *m/z* 166 (2 *m/z* units higher showing one of adducts is included). The dissociation of the alpha carbon and nitrogen results in *m/z* 163) and further fragmentation (CD_2HCHO group is lost) leads to *m/z* 117 with the identity 1-phenylprop-1-en-2-ylium. *m/z* 91 units is the tropylium ion.

When the Fenton reaction was carried out in the presence of butanal-2,2,3,3,4,4,4-d_7 as a secondary source of radicals (bottom spectrum), butanal-d_6 radicals ($C\mathbf{D}_3^{\bullet}C\mathbf{D}C\mathbf{D}_2CHO$) and propyl-$d_7$ radicals ($^{\bullet}C\mathbf{D}_2C\mathbf{D}_2C\mathbf{D}_3$) were formed and trapped by PBN. The molecular ion of PBN-($C\mathbf{D}_3C\mathbf{D}C\mathbf{D}_2CHO$), ($C\mathbf{D}_2C\mathbf{D}_2C\mathbf{D}_3$) expected at *m/z* 304 (expected 13 *m/z* units higher with the inclusion of butanal-d_7 and propyl-d_7 than without). The loss of a C=O from the butanal adduct gives 276 *m/z* units. The loss of the butanal group from the alpha carbon gives us *m/z* 227 and further fragmentation of this fragment results in *m/z* 171 (7 *m/z* units higher showing the deuterated propyl adduct is included). The dissociation of the alpha carbon and nitrogen results in *m/z* 167and further fragmentation (CD_2HCHO group is lost) leads to *m/z* 120 units with the identity 1-phenylprop-1-en-2-ylium-3,3,3,-d_3. *m/z* 91 units is the tropylium ion.

4.6.2 Electron ionization-mass spectra of mono-oxybutyl mono-propyl adduct of PBN-d_6{PBN-d_6-($CH_2CH_2CH_3$)($CH_2CH_2CH_2CHO$)} (compound 7)

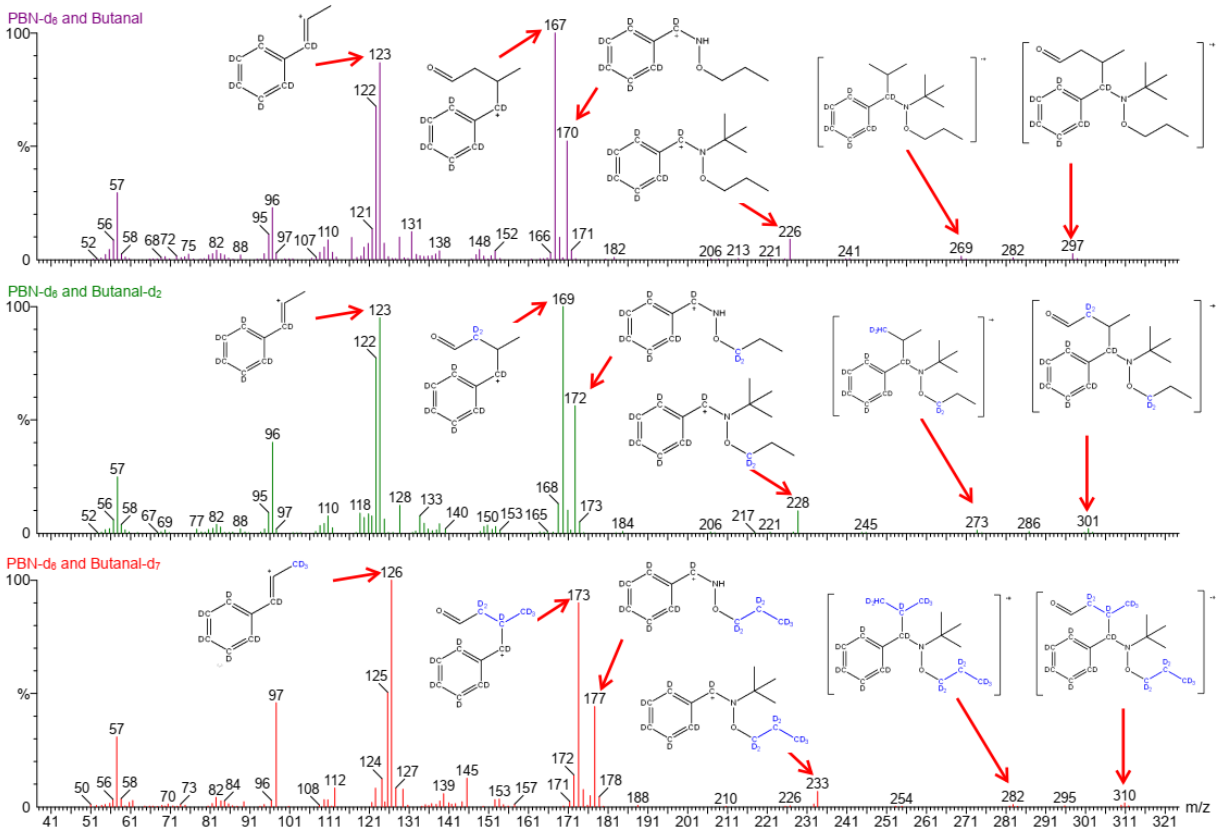

Figure 4.6.2 Electron Ionization mass spectra (EI-MS) corresponding to PBN adducts obtained from the analysis of the Fenton reaction mixture containing PBN-d_6, butanal and deuterated analogues at rt 11.67 minutes

The EI mass spectra in Figure 4.6.2 correspond to a) the PBN-d_6 mono-butanal mono-propyl adduct, PBN(CH_3CHCH_2CHO)($CH_2CH_2CH_3$) (top spectrum), and b) the PBN-d_6 dideutero mono-butanal mono-propyl adduct, PBN-d_6-($CH_3CHC\mathbf{D}_2CHO$)($C\mathbf{D}_2CH_2CH_3$) (middle spectrum) and c) the PBN-d_6 perdeutero mono-butanal mono-propyl adduct, PBN-d_6-($C\mathbf{D}_3C\mathbf{D}C\mathbf{D}_2CHO$)($C\mathbf{D}_2C\mathbf{D}_2C\mathbf{D}_3$) (bottom spectrum).

This compound has a similar identity to compound 5 and 6 (Figure 4.1.2) in that the structures are diastereomers of each other.

When the Fenton reaction was carried out in the presence of butanal as a secondary source of radicals (top spectrum), butanal radicals ($CH_3^{\bullet}CHCH_2CHO$) and propyl radicals ($^{\bullet}CH_2CH_2CH_3$) were generated by the

reaction of $^{\bullet}OH$ with butanal and were then trapped by PBN-d_6. The molecular ion of PBN-d_6-(CH_3CHCH_2CHO)($CH_2CH_2CH_3$) is at *m/z* 297. The loss of a C=O from the butanal adduct gives 269 *m/z* units. The loss of the butanal group from the alpha carbon gives us *m/z* 226 and further loss of $CH_2{=}CMe_2$ results in base peak *m/z* 170. The dissociation of the alpha carbon and nitrogen results in *m/z* 167 and further fragmentation (CH_3CHO group is lost) leads to *m/z* 117 with the identity 1-(phenyl-d_5)prop-1-en-2-ylium. *m/z* 96 units is the tropylium-d_5 ion.

When the Fenton reaction was carried out in the presence of butanal-2,2-d_2 as a secondary source of radicals (middle spectrum), butanal-d_2 radicals ($CH_3{}^{\bullet}CHC\mathbf{D}_2CHO$) and propyl-$d_2$ radicals ($^{\bullet}C\mathbf{D}_2CH_2CH_3$) were formed and trapped by PBN-d_6. The molecular ion of PBN-d_6-($CH_3CHC\mathbf{D}_2CHO$) ($C\mathbf{D}_2CH_2CH_3$) is at *m/z* 301 (expected 4 *m/z* units higher with the inclusion of butanal-d_2 than without). The loss of a C=O from the butanal adduct gives 273 *m/z* units. The loss of the butanal group from the alpha carbon gives us *m/z* 228 and further fragmentation results in *m/z* 172 (2 *m/z* units higher showing one of adducts is included). The dissociation of the alpha carbon and nitrogen results in *m/z* 169 and further fragmentation (CD_2HCHO group is lost) leads to *m/z* 117 with the identity 1-phenylprop-1-en-2-ylium. *m/z* 96 units is the tropylium-d_5 ion.

When the Fenton reaction was carried out in the presence of butanal-2,2,3,3,4,4,4-d_7 as a secondary source of radicals (bottom spectrum), butanal-d_6 radicals ($C\mathbf{D}_3{}^{\bullet}C\mathbf{D}C\mathbf{D}_2CHO$) and propyl-$d_7$ radicals ($^{\bullet}C\mathbf{D}_2C\mathbf{D}_2C\mathbf{D}_3$) were formed and trapped by PBN-d_6. The molecular ion of PBN-($C\mathbf{D}_3C\mathbf{D}C\mathbf{D}_2CHO$), ($C\mathbf{D}_2C\mathbf{D}_2C\mathbf{D}_3$) expected at *m/z* 310 (expected 13 *m/z* units higher with the inclusion of butanal-d_7 and propyl-d_7 than without). The loss of a C=O from the butanal adduct gives 282 *m/z* units. The loss of the butanal group from the alpha carbon gives us *m/z* 233 and further fragmentation of this fragment results in *m/z* 177 (7 *m/z* units higher showing the deuterated propyl adduct is included). The dissociation of the alpha carbon and nitrogen results in *m/z* 173and further fragmentation (CD_2HCHO group is lost) leads to *m/z* 120 units with the identity 1-phenylprop-1-en-2-ylium-3,3,3,-d_3. *m/z* 97 units is the tropylium-d_6 ion.

4.6.3 Electron ionization-mass spectra (EI-MS) of mono-oxybutyl mono-propyl adduct of F-PBN {F-PBN-($CH_2CH_2CH_3$)($CH_2CH_2CH_2CHO$)} (compound 7)

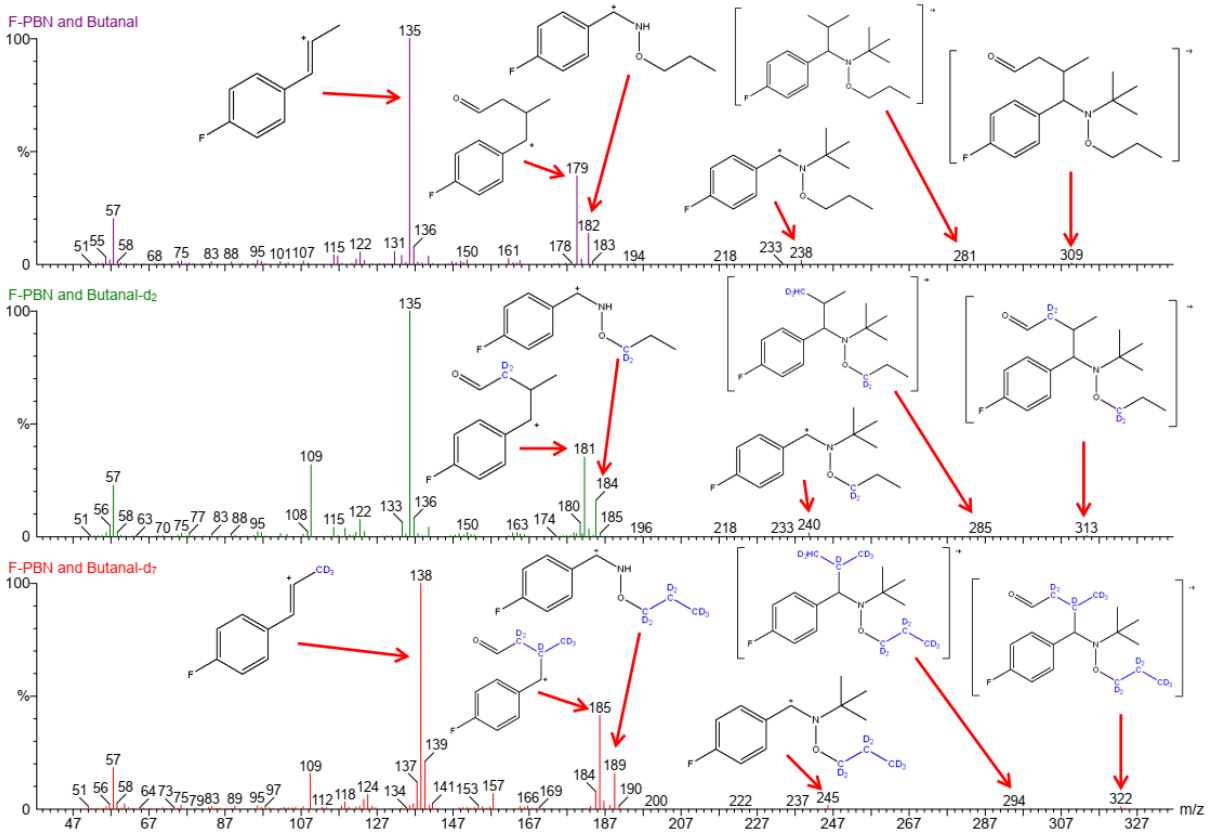

Figure 4.6.3 Electron Ionization mass spectra (EI-MS) corresponding to PBN adducts obtained from the analysis of the Fenton reaction mixture containing F-PBN, butanal and deuterated analogues at rt 11.67 minutes

The EI mass spectra in Figure 4.6.3 correspond to a) the F-PBN mono-butanal mono-propyl adduct, F-PBN(CH_3CHCH_2CHO)($CH_2CH_2CH_3$) (top spectrum), and b) the F-PBN dideutero mono-butanal mono-propyl adduct, F-PBN-($CH_3CHC\mathbf{D}_2CHO$)($C\mathbf{D}_2CH_2CH_3$) (middle spectrum) and c) the F-PBN perdeutero mono-butanal mono-propyl adduct, F-PBN-($C\mathbf{D}_3C\mathbf{D}C\mathbf{D}_2CHO$)($C\mathbf{D}_2C\mathbf{D}_2C\mathbf{D}_3$) (bottom spectrum).

This compound has a similar identity to compound 5 and 6 (Figure 4.1.2) in that the structures are diastereomers of each other.

When the Fenton reaction was carried out in the presence of butanal as a secondary source of radicals (top spectrum), butanal radicals ($CH_3{}^{\bullet}CHCH_2CHO$) and propyl radicals ($^{\bullet}CH_2CH_2CH_3$) were generated by the

reaction of $^{\bullet}OH$ with butanal and were then trapped by F-PBN. The molecular ion of F-PBN (CH_3CHCH_2CHO)($CH_2CH_2CH_3$) is at *m/z* 309. The loss of a C=O from the butanal adduct gives 281 *m/z* units. The loss of the butanal group from the alpha carbon gives us *m/z* 238 and further loss of $CH_2{=}CMe_2$ results in base peak *m/z* 182. The dissociation of the alpha carbon and nitrogen results in *m/z* 179 and further fragmentation (CH_3CHO group is lost) leads to *m/z* 135 with the identity 1-(4-fluorophenyl)prop-1-en-2-ylium.

When the Fenton reaction was carried out in the presence of butanal-2,2-d_2 as a secondary source of radicals (middle spectrum), butanal-d_2 radicals ($CH_3{}^{\bullet}CHC\mathbf{D}_2CHO$) and propyl-$d_2$ radicals ($^{\bullet}C\mathbf{D}_2CH_2CH_3$) were formed and trapped by F-PBN. The molecular ion of F-PBN-($CH_3CHC\mathbf{D}_2CHO$) ($C\mathbf{D}_2CH_2CH_3$) is at *m/z* 313 (expected 4 *m/z* units higher with the inclusion of butanal-d_2 than without). The loss of a C=O from the butanal adduct gives 285 *m/z* units. The loss of the butanal group from the alpha carbon gives us *m/z* 240 and further fragmentation results in *m/z* 184 (2 *m/z* units higher showing one of adducts is included). The dissociation of the alpha carbon and nitrogen results in *m/z* 181) and further fragmentation (CD_2HCHO group is lost) leads to *m/z* 135 with the identity 1-(4-fluorophenyl)prop-1-en-2-ylium. *m/z* 109 units is the fluorotropylium ion.

When the Fenton reaction was carried out in the presence of butanal-2,2,3,3,4,4,4-d_7 as a secondary source of radicals (bottom spectrum), butanal-d_6 radicals ($C\mathbf{D}_3{}^{\bullet}C\mathbf{D}C\mathbf{D}_2CHO$) and propyl-$d_7$ radicals ($^{\bullet}C\mathbf{D}_2C\mathbf{D}_2C\mathbf{D}_3$) were formed and trapped by F-PBN. The molecular ion of F-PBN-($C\mathbf{D}_3C\mathbf{D}C\mathbf{D}_2CHO$), ($C\mathbf{D}_2C\mathbf{D}_2C\mathbf{D}_3$) expected at *m/z* 322 (expected 13 *m/z* units higher with the inclusion of butanal-d_7 and propyl-d_7 than without). The loss of a C=O from the butanal adduct gives 294 *m/z* units. The loss of the butanal group from the alpha carbon gives us *m/z* 245 and further fragmentation of this fragment results in *m/z* 189 (7 *m/z* units higher showing the deuterated propyl adduct is included). The dissociation of the alpha carbon and nitrogen results in *m/z* 185and further fragmentation (CD_2HCHO group is lost) leads to *m/z* 120 units with the identity 1-(4-fluorophenyl)prop-1-en-2-ylium-3,3,3,-d_3. *m/z* 109 units is the fluorotropylium ion

4.7 Detection of PBN($CH_2CH_2CH_3$)(CH_3CHCH_2CHO) (compound 8)

4.7.1 Electron ionization-mass spectra of mono-propyl mono-oxybutyl adduct PBN($CH_2CH_2CH_3$)(CH_3CHCH_2CHO) Compound 8)

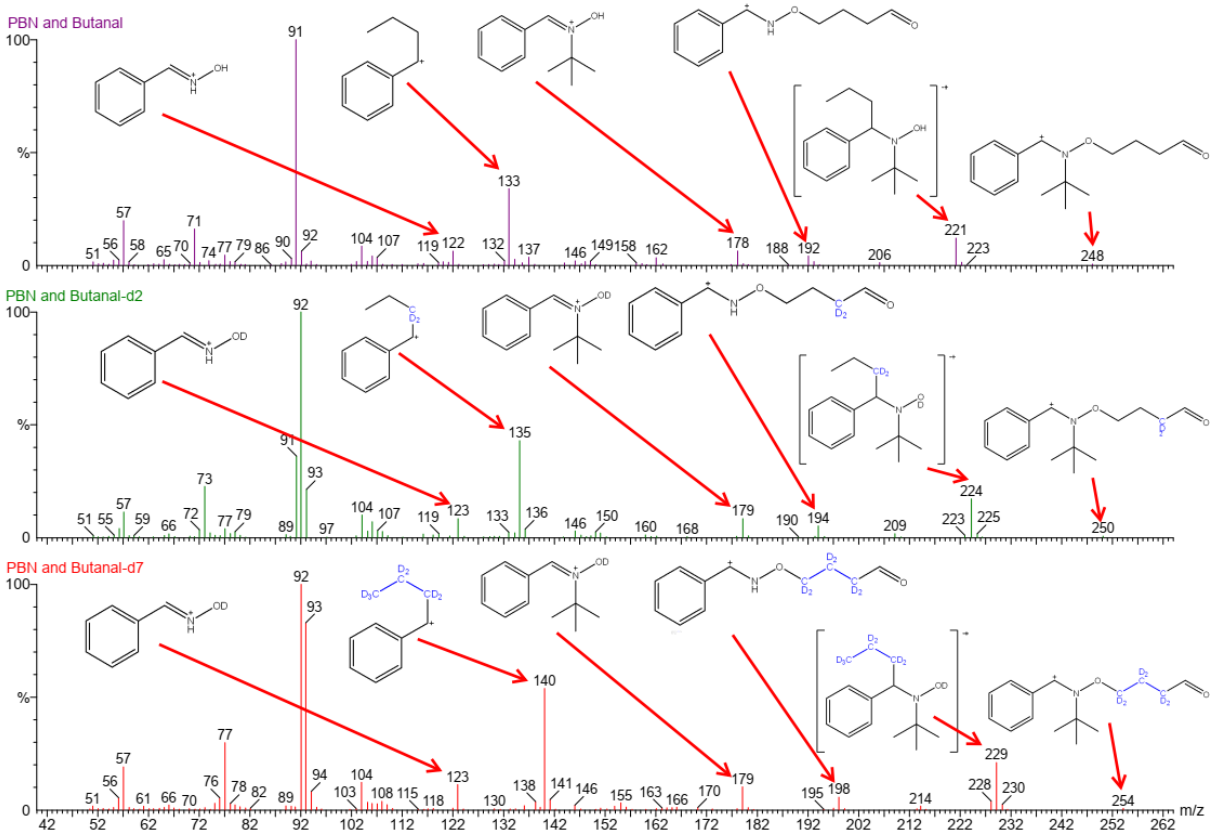

Figure 4.7.1 Electron Ionization mass spectra (EI-MS) corresponding to PBN adducts obtained from the analysis of the Fenton reaction mixture containing PBN, butanal and deuterated analogues at rt 11.72 minutes

The EI mass spectra in Figure 4.7.1 correspond to a) the PBN mono-propyl mono-butanal adduct, PBN($CH_2CH_2CH_3$)(CH_3CHCH_2CHO) (top spectrum), and b) the PBN dideutero mono-propyl mono-butanal adduct, PBN-($CH_3CHC\mathbf{D}_2CHO$)($C\mathbf{D}_2CH_2CH_3$) (middle spectrum) and c) the PBN perdeutero mono-propyl mono-butanal adduct, PBN-($C\mathbf{D}_3C\mathbf{D}C\mathbf{D}_2CHO$)($C\mathbf{D}_2C\mathbf{D}_2C\mathbf{D}_3$) (bottom spectrum).

This compound has a similar identity to compounds 5, 6 and 7 (Figure 4.1.2) in that the structure of compound 8 are diastereomers of each of them. Instead of the butanal radical adducting to the alpha carbon and propyl radical adducting on the oxygen of PBN like compounds 5, 6 and 7 the propyl radical has adducted to the alpha carbon and the butanal radical to the oxygen of PBN

When the Fenton reaction was carried out in the presence of butanal as a secondary source of radicals (top spectrum), butanal radicals ($^{\bullet}CH_2CH_2CH_2CHO$) and propyl radicals ($^{\bullet}CH_2CH_2CH_3$) were generated by the reaction of $^{\bullet}OH$ with butanal and were then trapped by PBN. The molecular ion of PBN ($CH_2CH_2CH_3$)($CH_2CH_2CH_2CHO$) expected at *m/z* 291 is too weak to be seen in the EI mass spectra. The loss of the propyl group from the molecular ion gives *m/z* 248 units and further fragmentation leads to the loss of CH_2=CMe_2 resulting in base peak *m/z* 192. The loss of the butanal group from the molecular ion gives us *m/z* 220 and further loss of a propyl group results in *m/z* 178 and further loss from this fragment of CH2=CMe2 results in *m/z* 122 N-benzyl hydroxylamine. The dissociation of the alpha carbon and nitrogen bond from the molecular ion results in the butyl benzene cation at *m/z* 133. *m/z* 91 units is the tropylium ion.

When the Fenton reaction was carried out in the presence of butanal-2,2-d_2 as a secondary source of radicals (middle spectrum), butanal-d_2 radicals ($^{\bullet}CH_2CH_2C\mathbf{D}_2CHO$) and propyl radicals ($^{\bullet}C\mathbf{D}_2CH_2CH_3$) were generated by the reaction of $^{\bullet}OH$ with butanal and were then trapped by PBN. The molecular ion of PBN ($C\mathbf{D}_2CH_2CH_3$)($CH_2CH_2C\mathbf{D}_2CHO$) expected at *m/z* 295 is too weak to be seen in the EI mass spectra. The loss of the propyl group from the molecular ion gives the peak at *m/z* 250 units and further fragmentation leads to the loss of CH_2=CMe_2 resulting in base peak *m/z* 194. The loss of the butanal group from the molecular ion gives us *m/z* 224 (where a deuterium atom has rearranged to add to the oxygen), and further loss of a propyl group results in *m/z* 179 and further loss from this fragment of CH2=CMe2 results in *m/z* 123 N-benzyl hydroxylamine-O-d. The dissociation of the alpha carbon and nitrogen bond from the molecular ion results in the butyl-d_2- benzene cation at *m/z* 135. *m/z* 92 units is the tropylium-1-d ion.

When the Fenton reaction was carried out in the presence of butanal-2,2,3,3,4,4,4-d_7 as a secondary source of radicals (bottom spectrum), propyl-d_7 radicals ($^{\bullet}C\mathbf{D}_2C\mathbf{D}_2C\mathbf{D}_3$) butanal-$d_6$ radicals ($^{\bullet}C\mathbf{D}_2C\mathbf{D}_2C\mathbf{D}_2CHO$) were generated by the reaction of $^{\bullet}OH$ with butanal and were then trapped by PBN. The molecular ion of PBN ($C\mathbf{D}_2CH_2CH_3$)($CH_2CH_2C\mathbf{D}_2CHO$) expected at *m/z* 304 is too weak to be seen in the EI mass spectra. The loss of the propyl group from the molecular ion gives the peak at *m/z* 254 units and further fragmentation leads to the loss of CH_2=CMe_2 resulting in base peak *m/z* 198. The loss of the butanal group from the molecular ion gives us *m/z* 229 (where a deuterium atom has rearranged to add to the oxygen) and further loss of a propyl group results in *m/z* 179 and further loss from this fragment of CH2=CMe2 results in *m/z* 123 N-benzyl hydroxylamine-O-d. The dissociation of the alpha carbon and nitrogen bond from the molecular ion results in the butyl-d_7- benzene cation at *m/z* 140. *m/z* 92 units is the tropylium-1-d ion.

4.7.2 Electron ionization-mass spectra of mono-oxybutyl mono-propyl adduct {$_{d6}$PBN ($CH_2CH_2CH_3$)($CH_2CH_2CH_2CHO$)} (Compound 8)

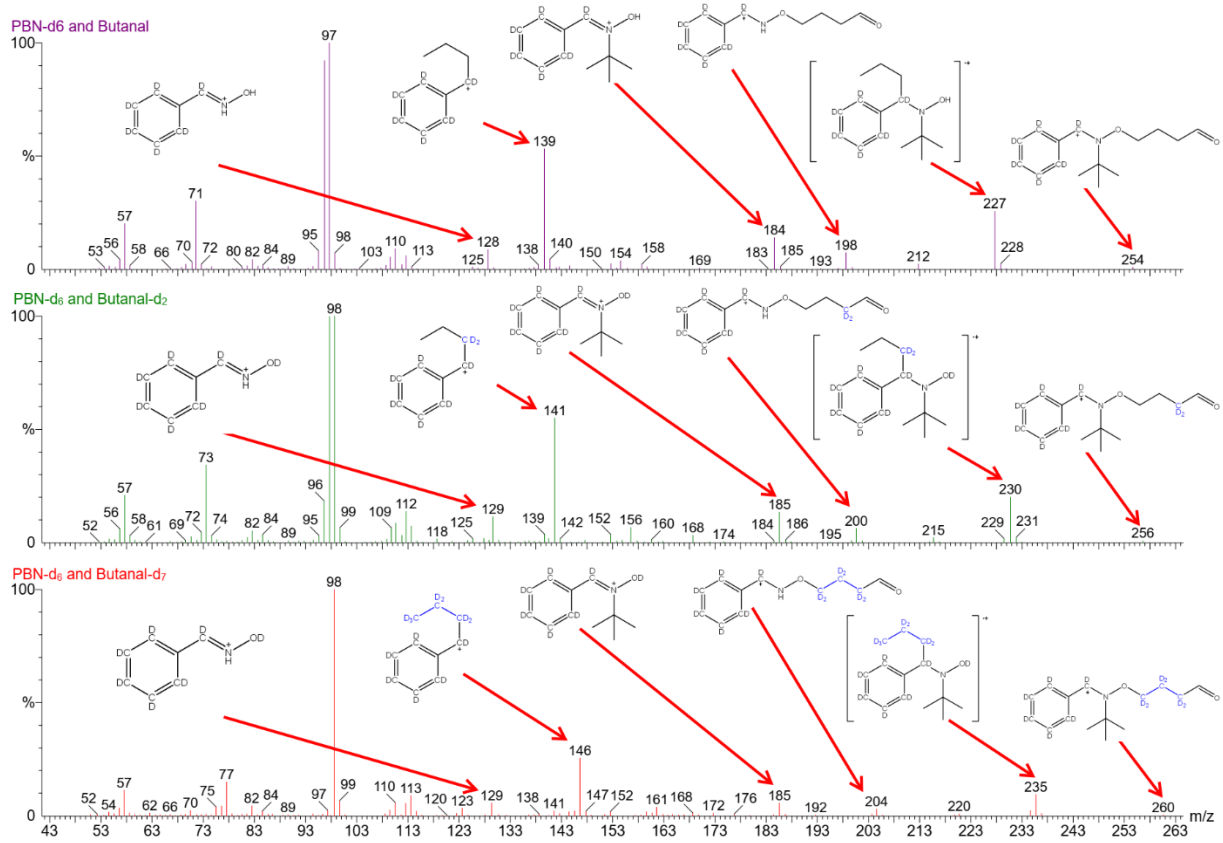

Figure 4.7.2 Electron Ionization mass spectra (EI-MS) corresponding to PBN adducts obtained from the analysis of the Fenton reaction mixture containing PBN-d_6, butanal and deuterated analogues at rt 11.72 minutes

The EI mass spectra in Figure 4.7.2 correspond to a) the PBN-d_6 mono-propyl mono-butanal adduct, PBN-d_6-($CH_2CH_2CH_3$)(CH_3CHCH_2CHO) (top spectrum), and b) the PBN-d_6 dideutero mono-propyl mono-butanal adduct, PBN-d_6-($CH_3CHC\mathbf{D}_2CHO$)($C\mathbf{D}_2CH_2CH_3$) (middle spectrum) and c) the PBN-d_6 perdeuterated mono-propyl mono-butanal adduct, PBN-($C\mathbf{D}_3C\mathbf{D}C\mathbf{D}_2CHO$)($C\mathbf{D}_2C\mathbf{D}_2C\mathbf{D}_3$) (bottom spectrum).

This compound has a similar identity to compounds 5, 6 and 7 (Figure 4.1.2) in that the structure of compound 8 are diastereomers of each of them. Instead of the butanal radical adducting to the alpha carbon and propyl radical adducting on the oxygen of PBN-d_6 like compounds 5, 6 and 7 the propyl radical has adducted to the alpha carbon and the butanal radical to the oxygen of PBN-d_6

When the Fenton reaction was carried out in the presence of butanal as a secondary source of radicals (top spectrum), butanal radicals ($^{\bullet}CH_2CH_2CH_2CHO$) and propyl radicals ($^{\bullet}CH_2CH_2CH_3$) were generated by the reaction of $^{\bullet}OH$ with butanal and were then trapped by PBN-d_6. The molecular ion of PBN-d_6-($CH_2CH_2CH_3$)($CH_2CH_2CH_2CHO$) expected at *m/z* 297 is too weak to be seen in the EI mass spectra. The loss of the propyl group from the molecular ion gives *m/z* 254 units and further fragmentation leads to the loss of CH_2=CMe_2 resulting in peak *m/z* 198. The loss of the butanal group from the molecular ion gives us *m/z* 227 (where a hydrogen atom has rearranged to add to the oxygen) and further loss of a propyl group results in *m/z* 184 and further loss from this fragment of CH_2=CMe_2 results in *m/z* 128 N-((phenyl-d_5)methylene-d)hydroxylammonium cation. The dissociation of the alpha carbon and nitrogen bond from the molecular ion results in the 1-(butyl-1-d)benzene-d_5 cation at *m/z* 139. *m/z* 97 units is the tropylium-d_6 ion.

When the Fenton reaction was carried out in the presence of butanal-2,2-d_2 as a secondary source of radicals (middle spectrum), butanal-d_2 radicals ($^{\bullet}CH_2CH_2C\mathbf{D}_2CHO$) and propyl radicals ($^{\bullet}C\mathbf{D}_2CH_2CH_3$) were generated by the reaction of $^{\bullet}OH$ with butanal and were then trapped by PBN-d_6. The molecular ion of PBN-d_6-($C\mathbf{D}_2CH_2CH_3$)($CH_2CH_2C\mathbf{D}_2CHO$) expected at *m/z* 301 is too weak to be seen in the EI mass spectra. The loss of the propyl group from the molecular ion gives the peak at *m/z* 256 units and further fragmentation leads to the loss of CH_2=CMe_2 resulting in peak *m/z* 200. The loss of the butanal group from the molecular ion gives us *m/z* 230 (where a deuterium atom has rearranged to add to the oxygen) and further loss of a propyl group results in *m/z* 185 and further loss from this fragment of CH2=CMe2 results in *m/z* 129 N-((phenyl-d_5)methylene-d)hydroxylammonium-O-d cation. The dissociation of the alpha carbon and nitrogen bond from the molecular ion results in the butyl-d_2-benzene cation at *m/z* 141. *m/z* 98 units is the tropylium-d_7 ion.

When the Fenton reaction was carried out in the presence of butanal-2,2,3,3,4,4,4-d_7 as a secondary source of radicals (bottom spectrum), propyl-d_7 radicals ($^{\bullet}C\mathbf{D}_2C\mathbf{D}_2C\mathbf{D}_3$) butanal-$d_6$ radicals ($^{\bullet}C\mathbf{D}_2C\mathbf{D}_2C\mathbf{D}_2CHO$) were generated by the reaction of $^{\bullet}OH$ with butanal and were then trapped by PBN-d_6. The molecular ion of PBN-d_6 ($C\mathbf{D}_2CH_2CH_3$)($CH_2CH_2C\mathbf{D}_2CHO$) expected at *m/z* 310 is too weak to be seen in the EI mass spectra. The loss of the propyl group from the molecular ion gives the peak at *m/z* 254 units and further fragmentation leads to the loss of CH_2=CMe_2 resulting in peak *m/z* 204. The loss of the butanal group from the molecular ion gives us *m/z* 235 (where a deuterium atom has rearranged to add to the oxygen) and further loss of a propyl group results in *m/z* 185 and further loss from this fragment of CH_2=CMe_2 results in *m/z* 129 N-((phenyl-d_5)methylene-d)hydroxylammonium-O-d cation. The dissociation

of the alpha carbon and nitrogen bond from the molecular ion results in the butyl-d_7-benzene cation at *m/z* 140. *m/z* 98 units is the tropylium-d_7 ion.

4.7.3 Electron ionization-mass spectra of mono-propyl mono-oxybutyl adduct {F-PBN-(CH_3•$CHCH_2CHO$)} (compound 8)

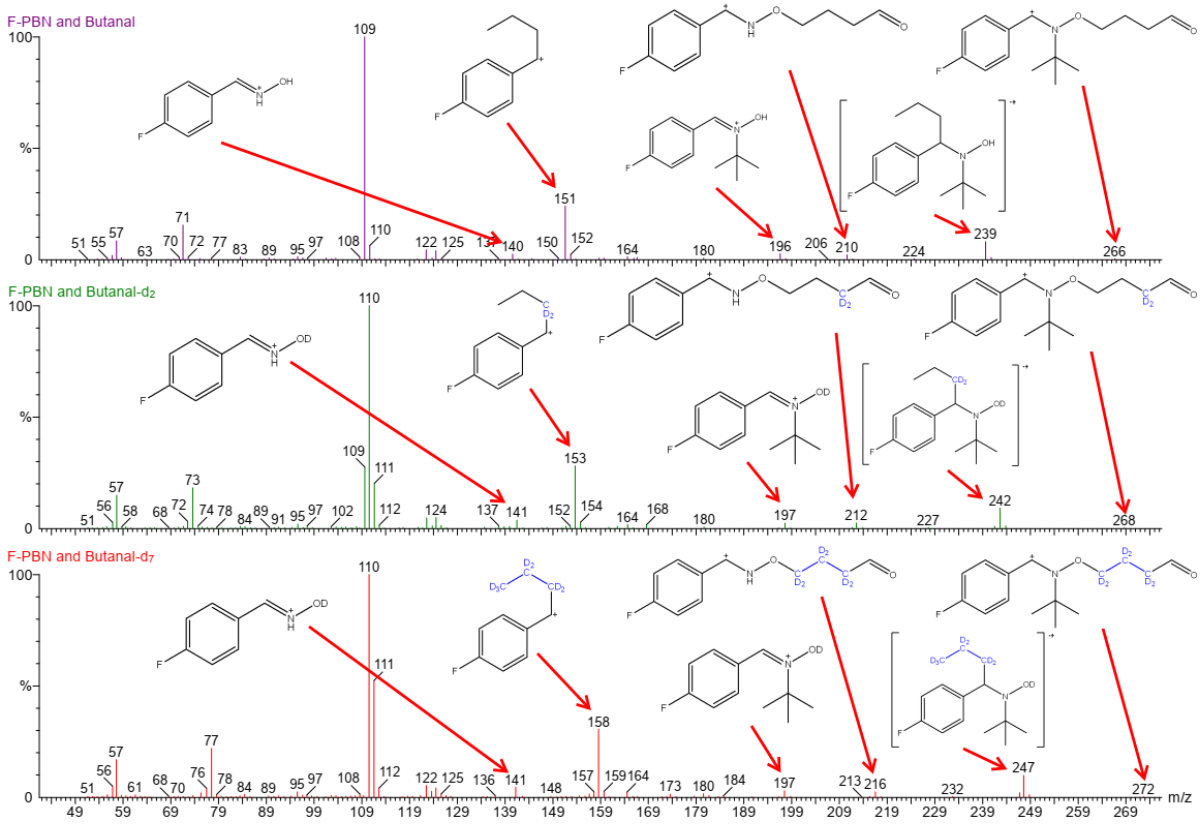

Figure 4.7.3 Electron Ionization mass spectra (EI-MS) corresponding to PBN adducts obtained from the analysis of the Fenton reaction mixture containing F-PBN, butanal and deuterated analogues at rt 11.72 minutes

The EI mass spectra in Figure 4.7.3 correspond to a) the F-PBN mono-propyl mono-butanal adduct, F-PBN ($CH_2CH_2CH_3$)(CH_3CHCH_2CHO) (top spectrum), and b) the F-PBN dideutero mono-propyl mono-butanal adduct, F-PBN-($CH_3CHC\mathbf{D}_2CHO$)($C\mathbf{D}_2CH_2CH_3$) (middle spectrum) and c) the PBN perdeutero mono-propyl mono-butanal adduct, F-PBN-($C\mathbf{D}_3C\mathbf{D}C\mathbf{D}_2CHO$)($C\mathbf{D}_2C\mathbf{D}_2C\mathbf{D}_3$) (bottom spectrum).

This compound has a similar identity to compounds 5, 6 and 7 (Figure 4.1.2) in that the structure of compound 8 are diastereomers of each of them. Instead of the butanal radical adducting to the alpha carbon and propyl radical adducting on the oxygen of F-PBN like compounds 5, 6 and 7 the propyl radical has adducted to the alpha carbon and the butanal radical to the oxygen of F-PBN

When the Fenton reaction was carried out in the presence of butanal as a secondary source of radicals (top spectrum), butanal radicals ($^{\bullet}CH_2CH_2CH_2CHO$) and propyl radicals ($^{\bullet}CH_2CH_2CH_3$) were generated by the reaction of $^{\bullet}OH$ with butanal and were then trapped by F-PBN. The molecular ion of F-PBN ($CH_2CH_2CH_3$)($CH_2CH_2CH_2CHO$) expected at *m/z* 309 is too weak to be seen in the EI mass spectra. The loss of the propyl group from the molecular ion gives *m/z* 266 units and further fragmentation leads to the loss of CH_2=CMe_2 resulting in peak *m/z* 210. The loss of the butanal group from the molecular ion gives us *m/z* 239 and further loss of a propyl group results in *m/z* 196 and further loss from this fragment of CH_2=CMe_2 results in *m/z* 140 N-benzyl hydroxylamine. The dissociation of the alpha carbon and nitrogen bond from the molecular ion results in the 1-butyl-4-fluorobenzene cation at *m/z* 151. *m/z* 91 units is the tropylium ion.

When the Fenton reaction was carried out in the presence of butanal-2,2-d_2 as a secondary source of radicals (middle spectrum), butanal-d_2 radicals ($^{\bullet}CH_2CH_2C\mathbf{D}_2CHO$) and propyl radicals ($^{\bullet}C\mathbf{D}_2CH_2CH_3$) were generated by the reaction of $^{\bullet}OH$ with butanal and were then trapped by F-PBN. The molecular ion of F-PBN ($C\mathbf{D}_2CH_2CH_3$)($CH_2CH_2C\mathbf{D}_2CHO$) expected at *m/z* 313 is too weak to be seen in the EI mass spectra. The loss of the propyl group from the molecular ion gives the peak at *m/z* 250 units and further fragmentation leads to the loss of CH_2=CMe_2 resulting in peak *m/z* 212. The loss of the butanal group from the molecular ion gives us *m/z* 242 (where a deuterium atom has rearranged to add to the oxygen) and further loss of a propyl group results in *m/z* 179 and further loss from this fragment of CH2=CMe2 results in *m/z* 141 N-(4-fluorobenzyl)hydroxylamine-O-d. The dissociation of the alpha carbon and nitrogen bond from the molecular ion results in the 1-butyl-d_2-4-fluorobenzene cation at *m/z* 153. *m/z* 110 units is the tropylium-4-d ion.

When the Fenton reaction was carried out in the presence of butanal-2,2,3,3,4,4,4-d_7 as a secondary source of radicals (bottom spectrum), propyl-d_7 radicals ($^{\bullet}C\mathbf{D}_2C\mathbf{D}_2C\mathbf{D}_3$) butanal-$d_6$ radicals ($^{\bullet}C\mathbf{D}_2C\mathbf{D}_2C\mathbf{D}_2CHO$) were generated by the reaction of $^{\bullet}OH$ with butanal and were then trapped by F-PBN. The molecular ion of F-PBN ($C\mathbf{D}_2CH_2CH_3$)($CH_2CH_2C\mathbf{D}_2CHO$) expected at *m/z* 322 is too weak to be seen in the EI mass spectra. The loss of the propyl group from the molecular ion gives the peak at *m/z* 254 units and further fragmentation leads to the loss of CH_2=CMe_2 resulting in peak *m/z* 216. The loss of the butanal group from the molecular ion gives us *m/z* 247 (where a deuterium atom has rearranged to add to the oxygen) and further loss of a propyl group results in *m/z* 197 and further loss from this fragment of CH2=CMe2 results in *m/z* 141 N-(4-fluorobenzyl)hydroxylamine-O-d. The dissociation of the alpha carbon

and nitrogen bond from the molecular ion results in the 1-butyl-d_7-4-fluorobenzene cation at *m/z* 158. *m/z* 110 units is the fluorotropylium-4-d ion.

4.8 Chromatograms of spin trapped PBN derivatives using butanal and DMSO as a competing source of secondary radicals forming methyl radicals

To understand the orientation of the adducts formed a secondary competing source of radicals was introduced in the form of methyl radicals derived from DMSO. It was hypothesised that alkyl/alkoxy and methyl hybrid adducts would form and show as new peaks on the TIC.

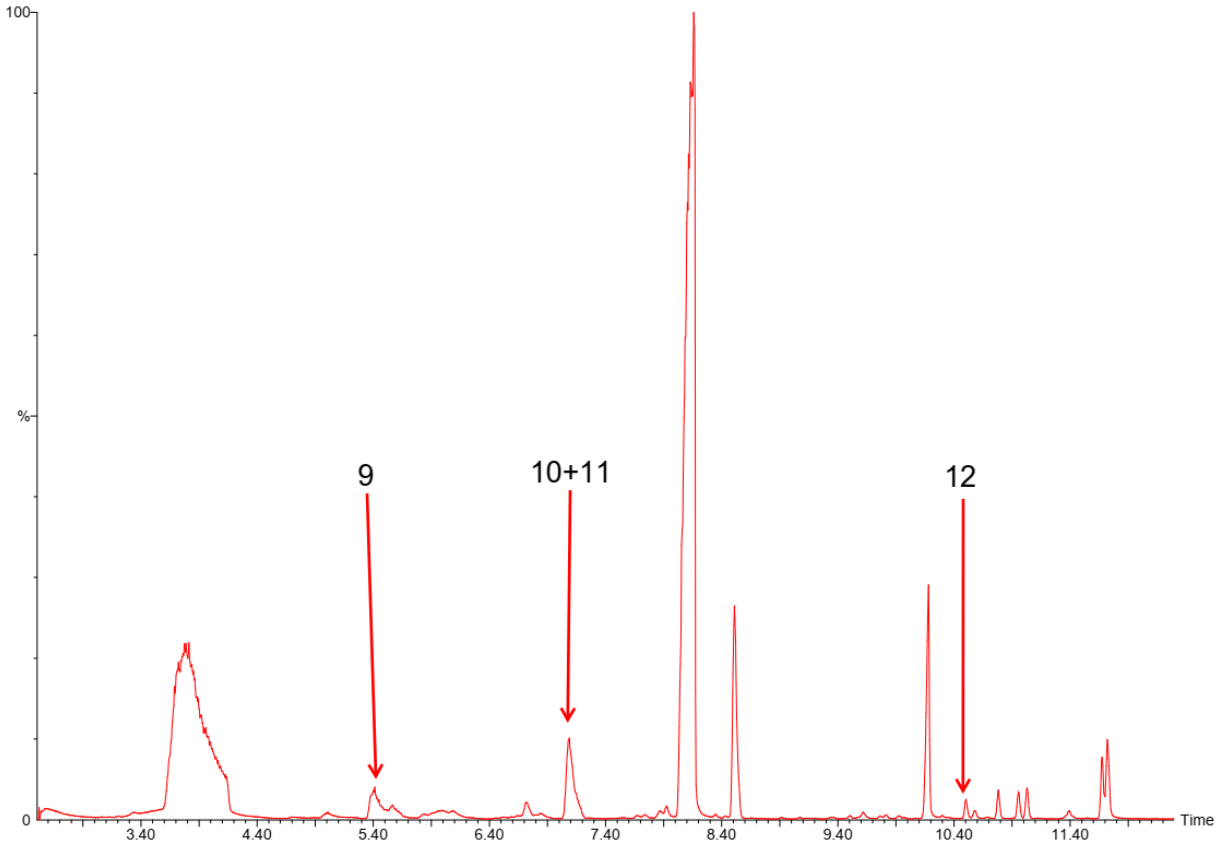

Figure 4.8.1 The total ion chromatogram obtained from the GC-MS analysis of the Fenton system with PBN in the presence of butanal and DMSO

The TIC shown in Figure 4.8.1 is similar to the chromatogram shown in Figure 4.1.1 however three more significant peaks at rt 5.41 minutes, rt 7.09 minutes and rt 10.49 minutes have appeared. The peak at 5.41 minutes (peak 9) corresponds to the PBN-$(CH_3)_2$ adduct, the peak at rt 7.09 minutes (peak 10+11) is a combination of two diastereomers corresponding to PBN(CH_3) -$(CH_2CH_2CH_3)$ (compound 10) and the PBN-$(CH_2CH_2CH_3)(CH_3)$(compound 11) and the peak at rt 10.49 minutes (peak 12) corresponds to the PBN-$(CH_2CH_2CH_2CHO)(CH_3)$. Peak 10+11 is a relatively broad peak compared to other peaks on the TIC alluding to it being a combination of two individual peaks.

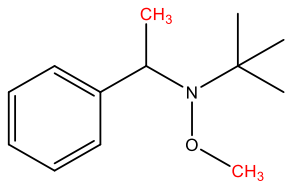

Compound 9 (peak 9)

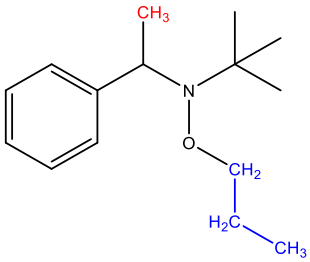

Compound 10 (peak 10+11)

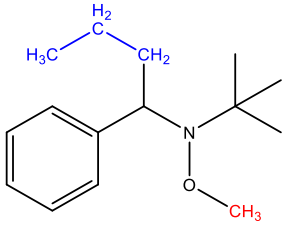

Compound 11 (peak 10+11)

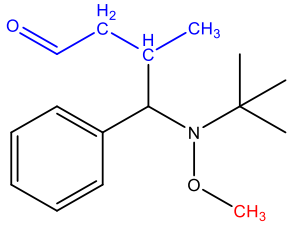

Compound 12 (peak 12)

Figure 4.8.2 The structures of additional compounds identified by GC-MS analysis of a Fenton based reaction mixture containing PBN, butanal and DMSO. The atoms in red are believed to be derived from DMSO and the blue from butanal

Table 4.5 Peak number, molecular ion , base peak and identity for peaks obtained in Figure 4.8.1

Peak Number	Molecular ion	Base peak	Identity
9	207	105	Dimethyl adduct
10	235	91	Monomethyl monopropyl adduct
11	235	91	Monopropyl monomethyl adduct
12	263	117	Mono-oxobutyl monomethyl adduct

4.9 Detection of Methyl (•CH_3) radical from DMSO (compound 9)

4.9.1 The dimethyl adduct of PBN (compound 9)

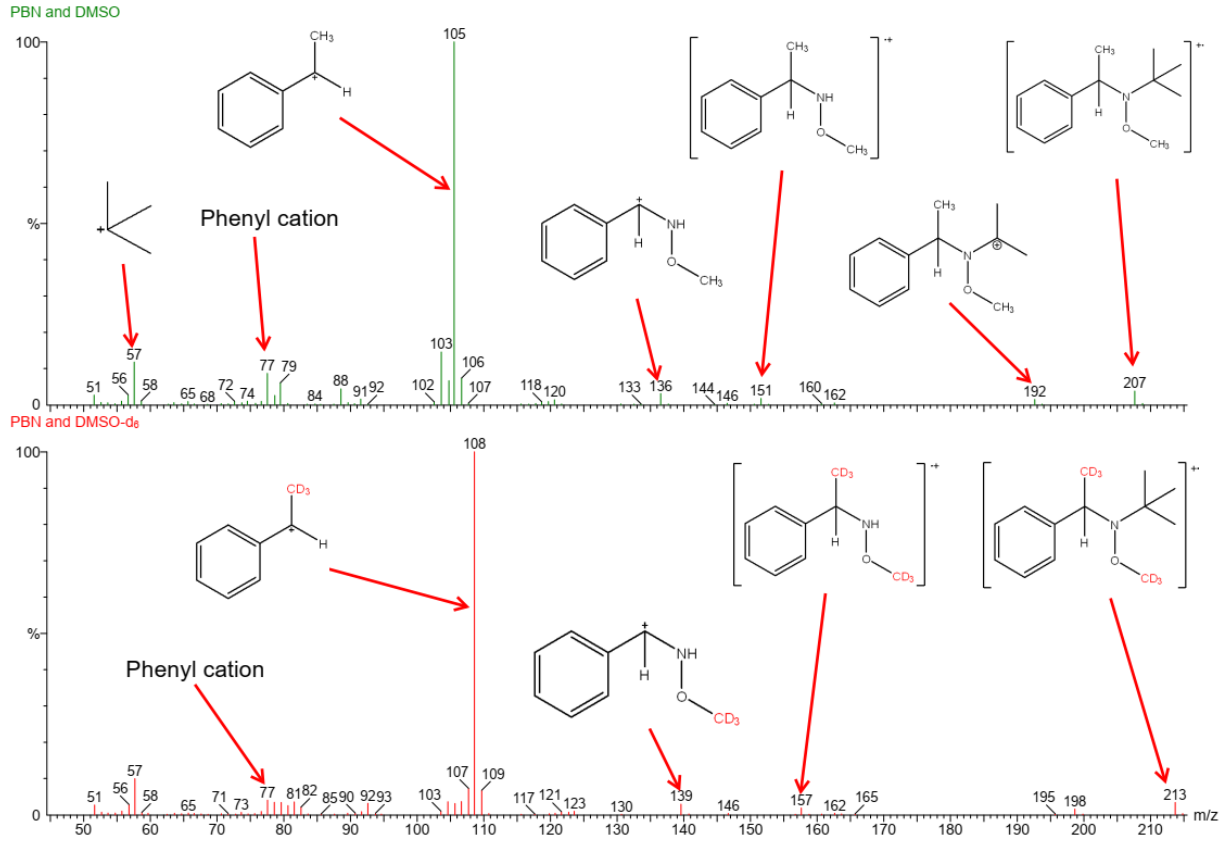

Figure 4.9.1 Electron Ionization mass spectra (EI-MS) corresponding to PBN obtained from the analysis of the Fenton reaction mixture containing PBN, butanal and DMSO or DMSO-d_6 at rt 5.41 minutes

The EI mass spectra shown in Figure 4.9.1 correspond to a) the dimethyl adduct, PBN-$(CH_3)_2$, (top spectrum), and b) the dideutero methyl adduct of PBN, PBN-$(CD_3)_2$, (bottom spectrum).

When the Fenton reaction was carried out in the presence of butanal and with DMSO as a competing secondary source of radicals (top spectrum), methyl radicals (•CH_3) were also generated by the reaction of •OH with DMSO and were then trapped by PBN. The peak at *m/z* 207 corresponds to the molecular ion of PBN-Me_2. The fragment at *m/z* 192 is the loss of a methyl group from the molecular ion (from the tBu group). The loss of CH_2=CMe_2 gives *m/z* 151 and the loss of a methyl group from this fragment results in *m/z* 136. The dissociation of the alpha carbon bond and the nitrogen gives the base peak *m/z* 105 and further breakdown of this fragment results in a phenyl cation at *m/z* 77. The peak at *m/z* 57 is the tertiary butyl cation.

When the Fenton reaction was carried out with butanal and with DMSO-d_6 as a source of competing secondary radicals (bottom spectrum), deuterated methyl radicals ($^{\bullet}CD_3$) were generated and trapped by PBN. Replacing DMSO with d_6-DMSO in the Fenton-based reaction mixture gives rise to an increase in the *m/z* value of the molecular ion of 6 *m/z* units. The peak at *m/z* 213 corresponds to the molecular ion of PBN-$(CD_3)_2$, a difference of 6 *m/z* units confirming the presence of two methyl groups in the structure of the compound. The fragment at *m/z* 198 is the loss of a methyl group from the molecular ion (again from the tBu group thus only losing 15 *m/z* units) in the ion source of the mass spectrometer. The loss of CH_2=CMe_2 gives *m/z* 157 and the loss of a CD_3 from this fragment results in *m/z* 139. The dissociation of the alpha carbon bond and the nitrogen gives the base peak *m/z* 108 (retaining one CD_3 group) and further breakdown of this fragment results in a phenyl cation at *m/z* 77.

It is important to note that the dimethyl adduct of PBN was first characterised by Janzen *et al*., (1985) and I have confirmed the identification here. It is also important to note that the methyl radicals have been trapped in other spin traps such as α-[4-pyridyl N-oxide]-N-tButyl nitrone (POBN) (Mistry *et al.*, 2008)

4.9.2 The dimethyl adduct of PBN-d_6 (compound 9)

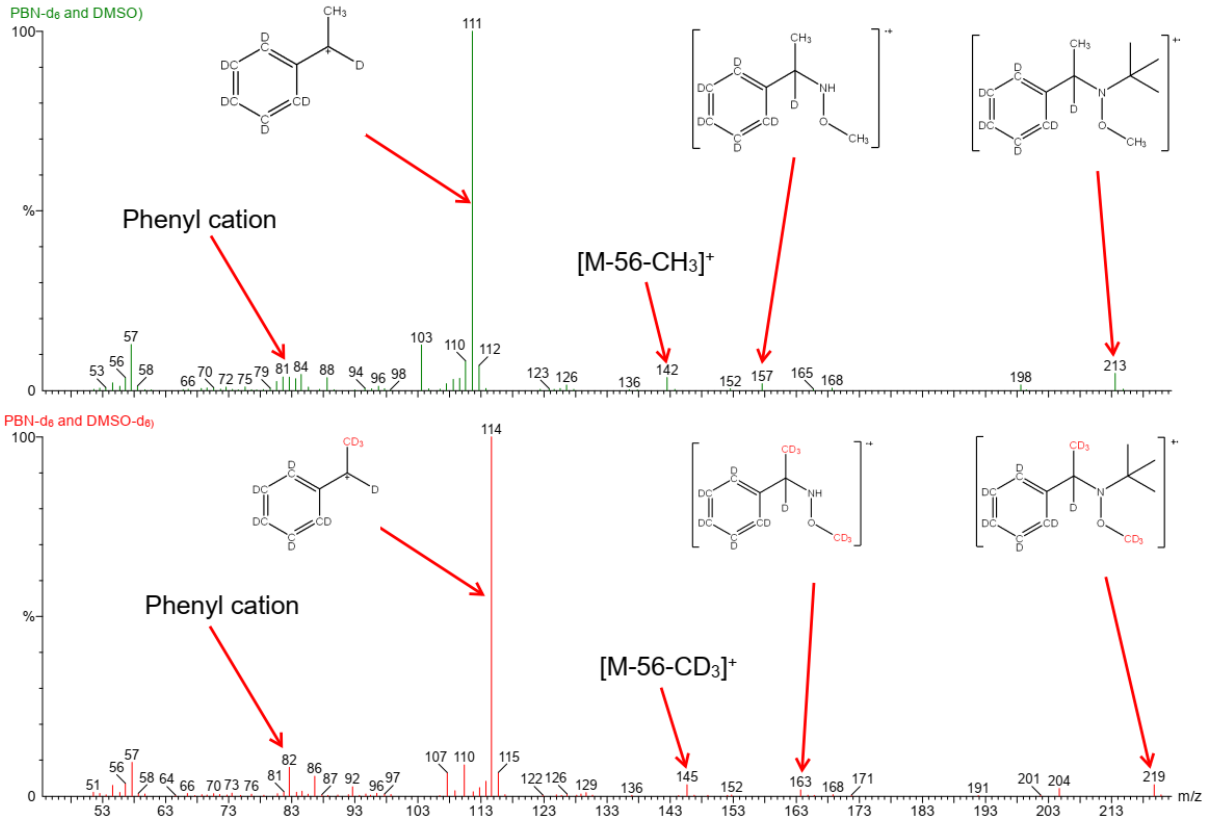

Figure 4.9.2 Electron Ionization mass spectra (EI-MS) corresponding to PBN-d_6 obtained from the analysis of the Fenton reaction mixture containing PBN, butanal and DMSO (top spectrum) or DMSO-d_6 (bottom spectrum

The EI-MS shown in Figure 4.9.2 correspond to the dimethyl adduct of PBN-d_6 {PBN-d_6-$(CH_3)_2$} (top spectrum), and the dideutero dimethyl adduct of PBN-d_6 {PBN-d_6-$(CD_3)_2$} (bottom spectrum). PBN was replaced by PBN-d_6, as the spin-trap, which leads to the spectra with *m/z* values 6 units higher for the molecular ion.

For the top spectrum, the molecular ion was *m/z* 213. The fragment at *m/z* 198 is due to the loss of a methyl radical from the molecular ion (from the tBu group) in the ion source. The loss of CH_2=CMe_2 results in *m/z* 157 and the loss of a methyl group from this fragment results in *m/z* 142. The dissociation of the alpha carbon bond and the nitrogen gives the base peak *m/z* 111, 6 *m/z* units higher than when non-deuterated PBN was used as the spin trap confirming the retention of the deuterated phenyl and deuterated alpha carbon, and further breakdown of this fragment results in a phenyl cation at *m/z* 82. The peak at *m/z* 57 corresponds to the tertiary butyl cation.

When the Fenton reaction was carried out with DMSO-d_6 as a competing source of secondary radicals, deutronated methyl radicals ($^{\bullet}CD_3$) were generated. These add to PBN as confirmed by the presence of the molecular ion peak at *m/z* 219, the *m/z* value of which is 6 *m/z* units higher than when DMSO is used a competing secondary source of free radicals. The fragment at *m/z* 204 is due to the loss of a methyl radical from the molecular ion (again from the tBu group thus only losing 15 *m/z*). The loss of CH_2=CMe_2 corresponds to *m/z* 163 and the loss of a $^{\bullet}CD_3$ from this fragment results in *m/z* 145, indicating the inclusion of the other CD_3. The dissociation of the alpha carbon bond and the nitrogen gives the base peak *m/z* 114 (retaining one CD_3 group) and further breakdown of this fragment results in a phenyl cation at *m/z* 82 (losing the CD_3 group).

4.9.3 The dimethyl adduct of F-PBN (compound 9)

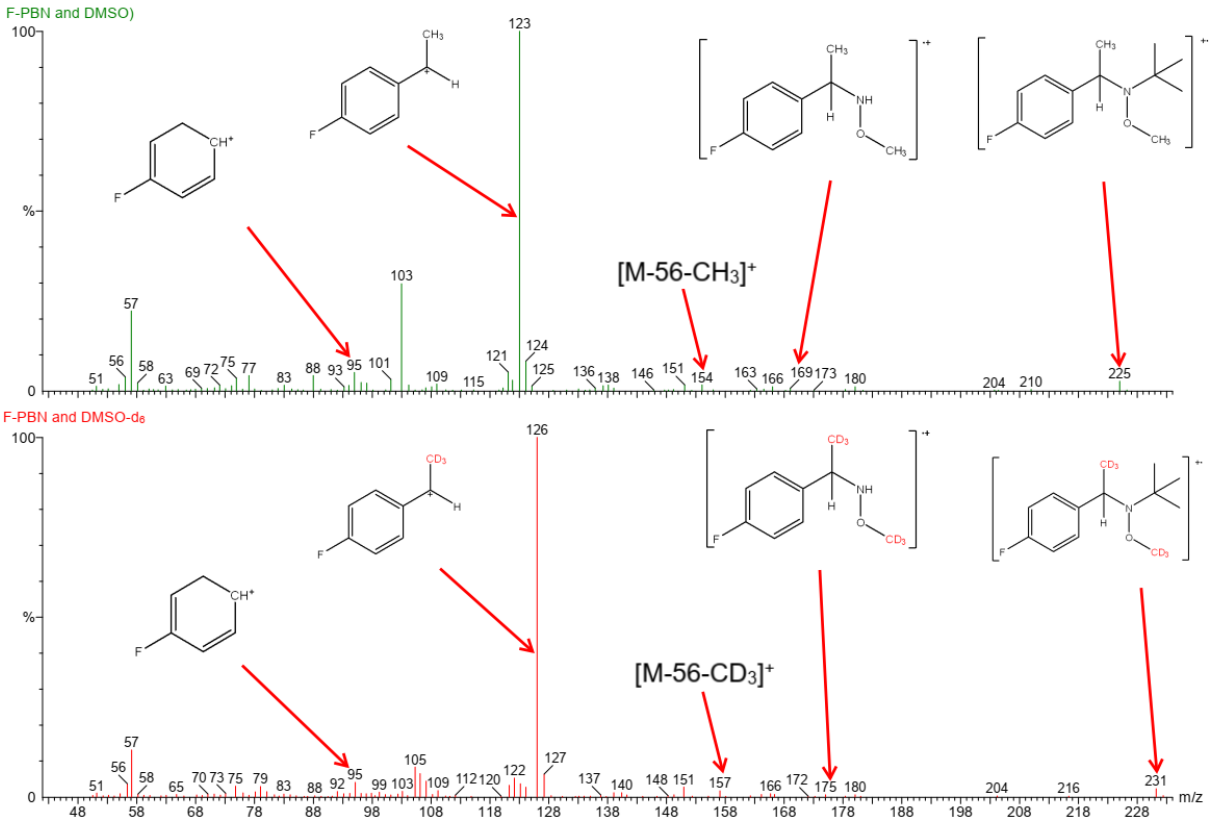

Figure 4.9.3 Electron Ionization mass spectra (EI-MS) corresponding to dimethyl adduct (top spectrum) or dideutro methyl adduct (bottom spectrum) of F-PBN obtained from the analysis of the Fenton reaction mixture containing F-PBN, butanal and DMSO (top spectrum) or DMSO-d_6 (bottom spectrum)

The EI mass spectra shown in Figure 4.9.3 correspond to the F-PBN dimethyl adduct F-PBN-$(CH_3)_2$ (top spectra), and the dideutero methyl adduct F-PBN dimethyl adduct FPBN-$(CD_3)_2$ (bottom spectra). When PBN was replaced by Fluorinated PBN (F-PBN), as the spin-trap, the molecular ion was 18 *m/z* units higher When the Fenton reaction was carried out in the presence of DMSO as a competing secondary source of radicals, methyl radicals ($^{\bullet}CH_3$).

The fragment peak at *m/z* 223 corresponds to the molecular ion of F-PBN-Me_2. The *m/z* value was 18 *m/z* higher than when non-fluorinated PBN was used clearly indicating that the 18 *m/z* were derived from the F-PBN, confirming the identity of the adduct. The fragment at *m/z* 210 units was due to the loss of a methyl radical from the molecular ion (from the tBu group). The loss of CH_2=CMe_2 was at *m/z* 169 and the loss of a methyl group from this fragment results in *m/z* 154. The dissociation of the alpha carbon bond and the

nitrogen gives the base peak *m/z* 123 and further breakdown of this fragment results in a 4-fluoro-phenyl cation at *m/z* 95. The peak at *m/z* 57 was the tertiary butyl cation.

The peak at *m/z* 231 corresponds to the molecular ion of F-PBN-$(CD_3)_2$. The fragment peak at *m/z* 216 was due the loss of a methyl group from the molecular ion (again from the tBu group thus only losing 15 *m/z* units). The loss of the CH_2=CMe_2 was *m/z* 175 and the loss of a methyl group from this fragment results in *m/z* 157, indicating the inclusion of the other CD_3. The dissociation of the alpha carbon bond and the nitrogen gives the base peak *m/z* 126 (retaining one CD_3 group) and further breakdown of this fragment results in a -4-fluoro-phenyl cation at *m/z* 95 (losing the CD_3 group).

Table 4.6 Summary of fragments for the dimethyl adduct of PBN and derivatives

Fenton system	Compound name or formula	$M^{+\bullet}$ (m/z)	other significant ions (*m/z*)
PBN + Butanal + DMSO	PBN-$(CH_3)_2$	**207**	192,151,136, 105 (bp),88,77,57
PBN + Butanal + DMSO-d_6	PBN-$(CD_3)_2$	**213**	198,157,139, 108 (bp),92,77,57
PBN-d_6+ Butanal +DMSO	PBN-d_6-$(CH_3)_2$	**213**	198,157,142,111 (bp),103,82,57
PBN-d_6+ Butanal +DMSO-d_6	PBN-d_6-$(CD_3)_2$	**219**	204,163,145, 114 (bp),107,82,57
F-PBN + Butanal + DMSO	F-PBN-$(CH_3)_2$	**225**	210,169,154, 123 (bp),103,95,57
F-PBN + Butanal + DMSO-d_6	F-PBN-$(CD_3)_2$	**231**	216,175,157, 126 (bp),105,95,57

4.10 Detection of Methyl ($^{\bullet}CH_3$) radical and propyl ($^{\bullet}CH_3CH_2CH_2$) radical from DMSO (Compound 10)

The peak at 7.09 minutes (peak 10+11) is believed to contain two peaks overlapping each other. It is believed they contain diastereomers with compound 10 (discussed in the following section) arranged with a methyl on the alpha carbon and a propyl on the oxygen and compound 11 (further discussed in section 4.11) with the propyl on the alpha carbon and methyl on the oxygen.

4.10.1 Monomethyl monopropyl adduct of PBN with butanal and DMSO (Compound 10)

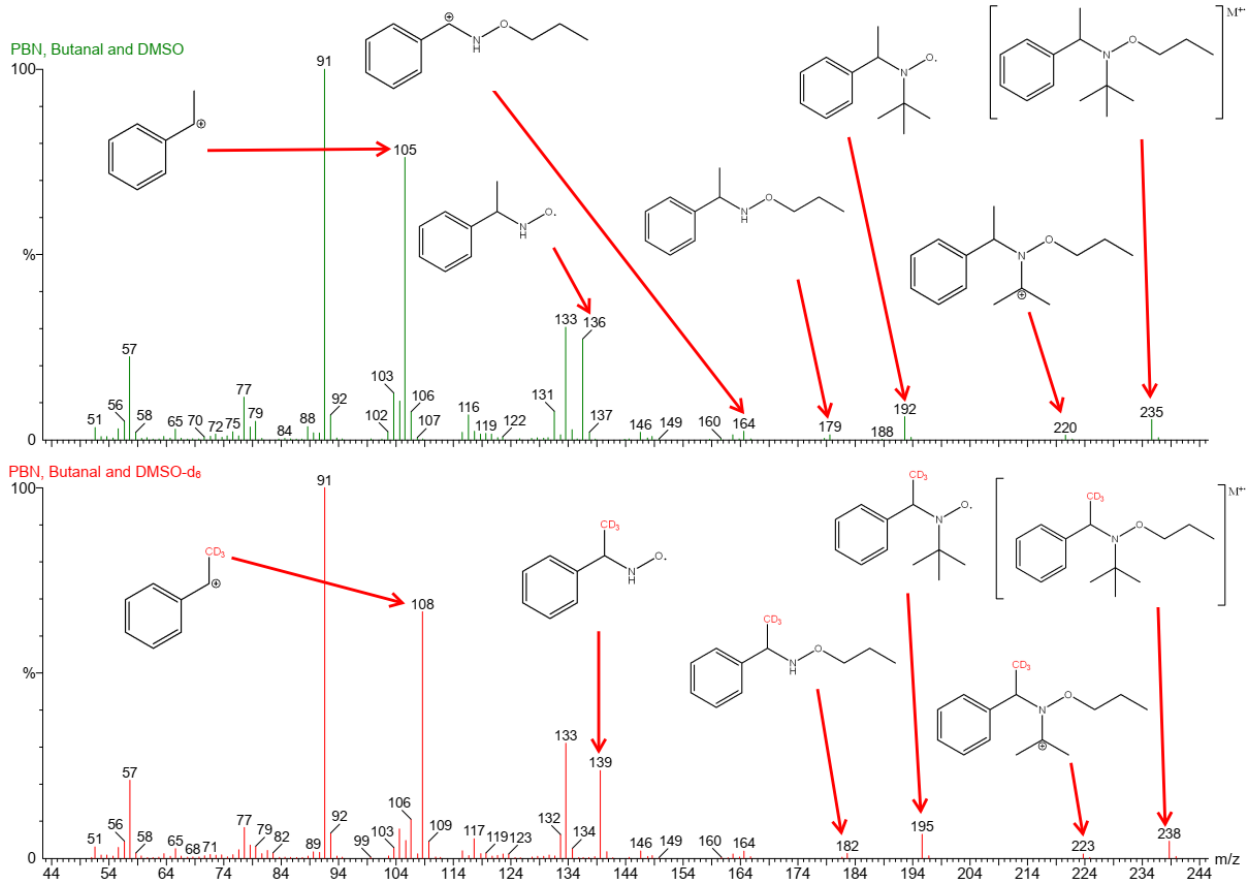

Figure 4.10.1 Electron Ionization mass spectra (EI-MS) corresponding to PBN adduct obtained from the analysis of the Fenton reaction mixture containing PBN, butanal and DMSO or DMSO-d_6 at rt 7.09 minutes

The EI mass spectra shown in Figure 4.10.1 correspond to the a)PBN C-(propyl)-O-(methyl) adduct PBN-($CH_2CH_2CH_3$)(CH_3) (top spectra), and b) the deuterated methyl group PBN C-(propyl)-O-(methyl) adduct PBN-($CH_2CH_2CH_3$)($C\mathbf{D}_3$) (bottom spectra).

When the Fenton reaction was carried out in the presence of butanal and with DMSO as a competing secondary source of radicals (top spectrum), methyl radicals ($^{\bullet}CH_3$) were also generated by the reaction of $^{\bullet}OH$ with DMSO and were then trapped by PBN. The peak at *m/z* 235 units corresponds to the molecular ion of PBN-Me-Prop with the orientation of the methyl on the alpha carbon and the propyl adducted on the oxygen. The fragment at *m/z* 220 is due to the loss of a methyl group from the molecular ion (from the tBu group). The loss of the propyl group from the oxygen results in *m/z* 192. The loss of CH_2=CMe_2 from the molecular ion gives *m/z* 179 and the loss of a methyl group from this fragment results in *m/z* 164. Further dissociation of the propyl from the oxygen gives *m/z* 136. The dissociation of the alpha carbon bond and the nitrogen gives the base peak *m/z* 105 and further breakdown of this fragment results in a phenyl cation at *m/z* 77. The peak at *m/z* 57 is the tertiary butyl cation. The peak at *m/z* 133 will be discussed in section 4.11

When the Fenton reaction was carried out in the presence of butanal and deuterated DMSO as a competing secondary source of radicals, deuterated methyl radicals ($^{\bullet}CD_3$) were also generated by the reaction of $^{\bullet}OH$ with DMSO and were then trapped by PBN. Replacing DMSO with d_6-DMSO in the Fenton-based reaction mixture gives rise to an increase in the *m/z* value of the molecular ion of 3 *m/z* units. The peak at *m/z* 238 units corresponds to the molecular ion of PBN-Me-Prop. The fragment at *m/z* 223 is the loss of a methyl group from the molecular ion (from the tBu group) thus proving that there is no loss of the (deuterated) methyl at the alpha carbon. The loss of the propyl group from the oxygen results in *m/z* 195. The loss of CH_2=CMe_2 gives *m/z* 182 and the loss of the deuterated methyl group from this fragment results in *m/z* 164. Further dissociation of the propyl from the oxygen gives *m/z* 139 showing the CD_3 group is retained on this fragment. The dissociation of the alpha carbon bond and the nitrogen gives the base peak *m/z* 108 thus showing that incorporation of the CD_3 in the ion and further breakdown of this fragment results in a phenyl cation at *m/z* 77. The peak at *m/z* 57 is the tertiary butyl cation.

4.10.2 Monomethyl monopropyl adduct of PBN with butanal d_2 and DMSO (Compound 10)

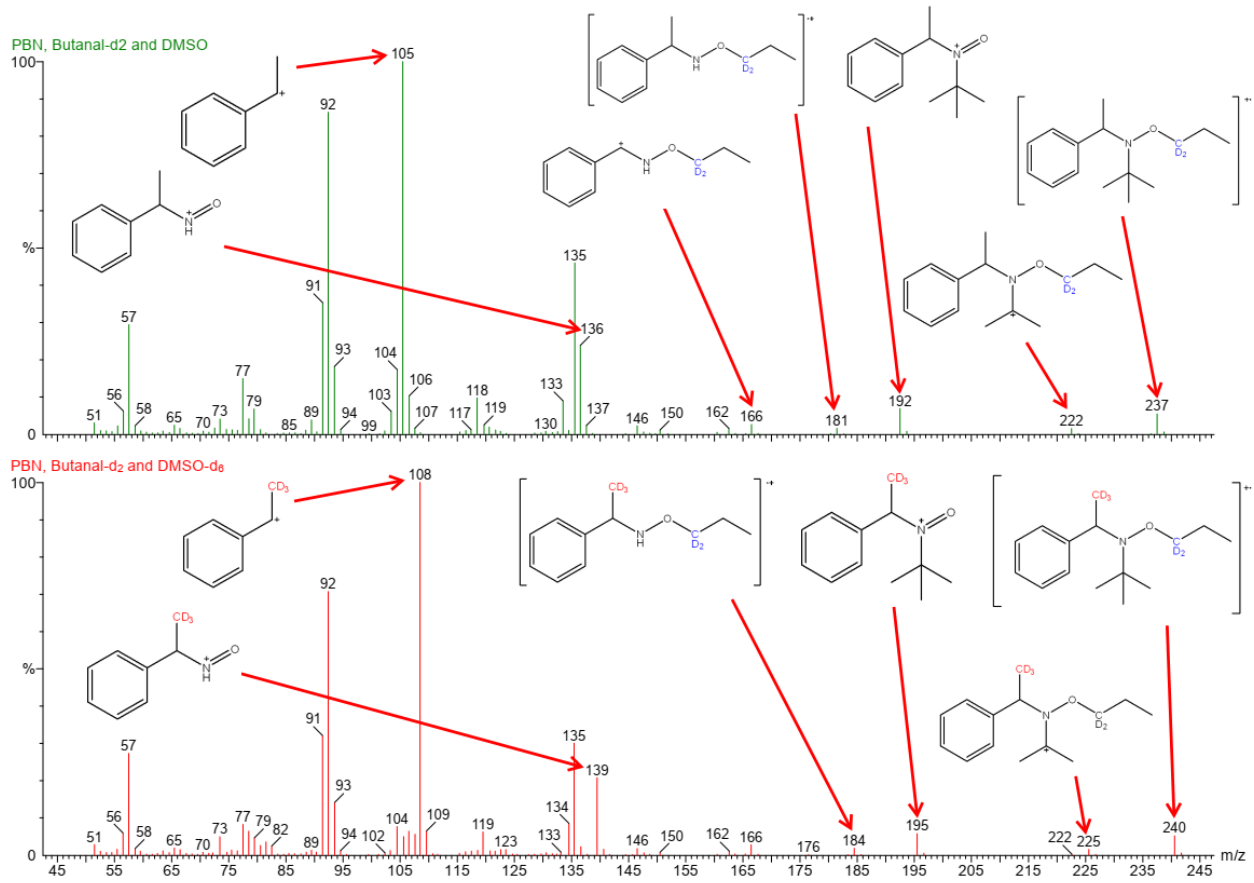

Figure 4.10.2 Electron Ionization mass spectra (EI-MS) corresponding to PBN adduct obtained from the analysis of the Fenton reaction mixture containing PBN, butanal-d_2 and DMSO or DMSO-d_6 at rt 7.09 minutes

The EI mass spectra shown in Figure 4.10.2 correspond to the a)PBN C-(propyl)-O-(methyl) adduct PBN-($CH_2CH_2CH_3$)(CH_3) (top spectra), and b) the dideuterated propyl deuterated methyl group PBN C-(propyl)-O-(methyl) adduct PBN-(C**D**$_2$$CH_2CH_3$)(C**D**$_3$) (bottom spectra).

When the Fenton reaction was carried out in the presence of butanal-d_2 and with DMSO as a competing secondary source of radicals (top spectrum), methyl radicals ($^{\bullet}CH_3$) were also generated by the reaction of $^{\bullet}OH$ with DMSO and were then trapped by PBN. The peak at *m/z* 237 units corresponds to the molecular ion of PBN-Me-Prop with the orientation of the methyl on the alpha carbon and the dideuterated propyl adducted on the oxygen. The increase of 2 *m/z* units demonstrates the incorporation of the dideuterated propyl adduct. The fragment at *m/z* 222 is the loss of a methyl group from the molecular ion (from the tBu group). The loss of the propyl group from the oxygen results in *m/z* 192 showing the incorporation of

the dideuterated propyl radical. The loss of CH_2=CMe_2 from the molecular ion gives *m/z* 181 and the loss of a methyl group from this fragment results in *m/z* 166. Further dissociation of the propyl from the oxygen gives *m/z* 136 demonstrating that the propyl adduct is dideuterated. The dissociation of the alpha carbon bond and the nitrogen gives the base peak *m/z* 105 and further breakdown of this fragment results in a phenyl cation at *m/z* 77. The peak at *m/z* 57 is the tertiary butyl cation. The peak at *m/z* 135 will be discussed in section 4.11

When the Fenton reaction was carried out in the presence of butanal-d_2 and deuterated DMSO as a competing secondary source of radicals deuterated methyl radicals ($^{\bullet}CD_3$) were also generated by the reaction of $^{\bullet}OH$ with DMSO and were then trapped by PBN. Replacing DMSO with d_6-DMSO in the Fenton-based reaction mixture gives rise to an increase in the *m/z* value of the molecular ion of 3 *m/z* units. The peak at *m/z* 240 units corresponds to the molecular ion of PBN-Me-Prop. The fragment at *m/z* 225 is the loss of a methyl group from the molecular ion (from the tBu group) thus proving that there is no loss of the methyl at the alpha carbon. The loss of the propyl group from the oxygen results in *m/z* 195 showing the incorporation of the dideuterated propyl radical. The loss of the tertiary butyl group gives *m/z* 184 and the loss of the deuterated methyl group from this fragment results in *m/z* 166. Further dissociation of the propyl from the oxygen gives *m/z* 139 showing the CD_3 group is retained on this fragment. The dissociation of the alpha carbon bond and the nitrogen gives the base peak *m/z* 108 thus showing that incorporation of the CD_3 in the ion and further breakdown of this fragment results in a phenyl cation at *m/z* 77. The peak at *m/z* 57 is the tertiary butyl cation.

4.10.3 Monomethyl monopropyl adduct of PBN with butanal d_7 and DMSO (Compound 10)

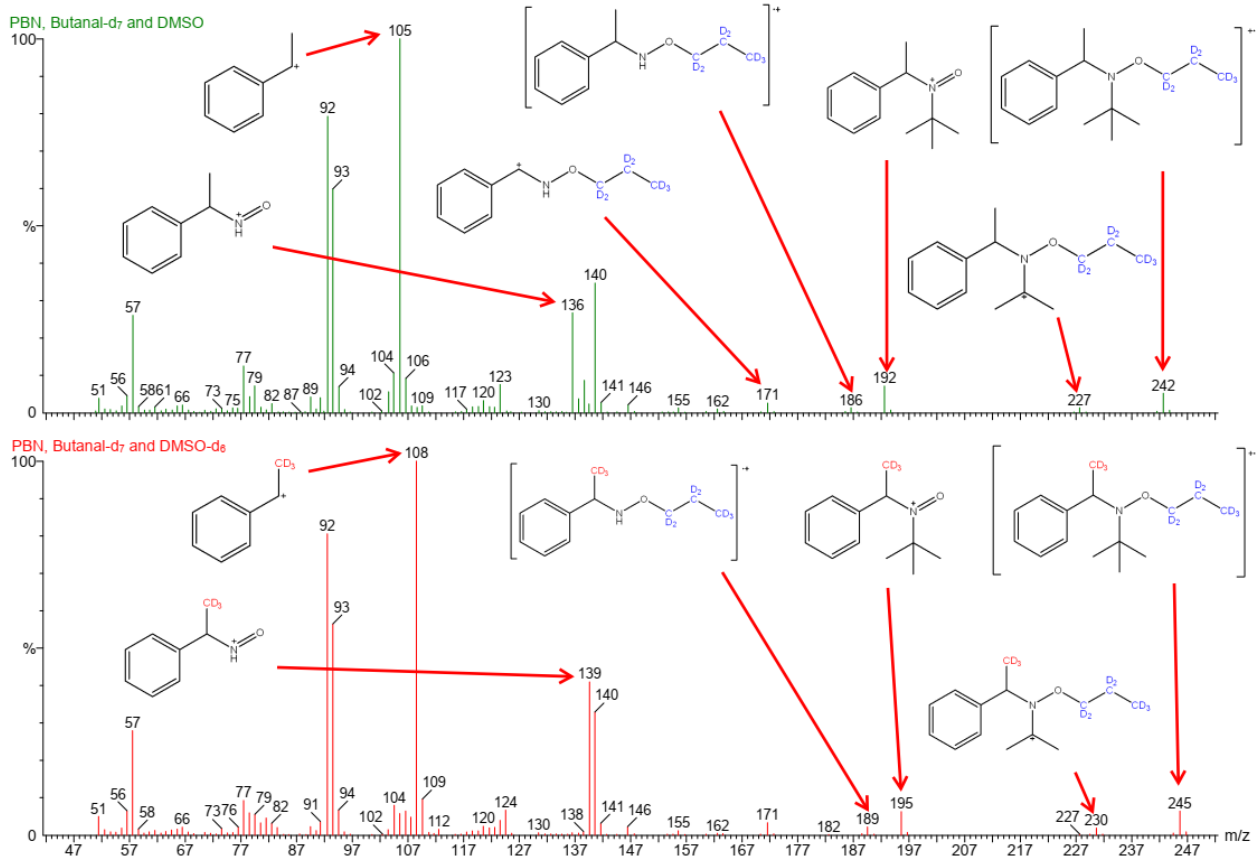

Figure 4.10.3 Electron Ionization mass spectra (EI-MS) corresponding to PBN adduct obtained from the analysis of the Fenton reaction mixture containing PBN, butanal-d_7 and DMSO or DMSO-d_6 at rt 7.09 minutes

The EI mass spectra shown in Figure 4.10.3 correspond to the a)PBN C-(propyl)-O-(methyl) adduct PBN-($CH_2CH_2CH_3$)(CH_3) (top spectra), and b) the deuterated propyl deuterated methyl group PBN C-(propyl)-O-(methyl) adduct PBN-($C\mathbf{D}_2C\mathbf{D}_2C\mathbf{D}_3$)($C\mathbf{D}_3$) (bottom spectra).

When the Fenton reaction was carried out in the presence of butanal-d_7 and DMSO as a competing secondary source of radicals methyl radicals ($^{\bullet}CH_3$) were also generated by the reaction of $^{\bullet}OH$ with DMSO and were then trapped by PBN. The peak at *m/z* 242 units corresponds to the molecular ion of PBN-Me-Prop with the orientation of the methyl on the alpha carbon and the perdeuterated propyl radical adducted on the oxygen. The fragment at *m/z* 227 is due to the loss of a methyl group from the molecular ion (from the tBu group). The loss of the propyl group from the oxygen results in *m/z* 192 showing the incorporation of the perdeuterated propyl radical. The loss of CH_2=CMe_2 from the molecular ion gives *m/z*

186 and the loss of a methyl group from this fragment results in *m/z* 171. Further dissociation of the propyl from the oxygen gives *m/z* 136. The dissociation of the alpha carbon bond and the nitrogen gives the base peak *m/z* 105 and further breakdown of this fragment results in a phenyl cation at *m/z* 77. The peak at *m/z* 57 is the tertiary butyl cation. The peak at *m/z* 140 will be discussed in section 4.11

When the Fenton reaction was carried out in the presence of buntal-d_7 and deuterated DMSO as a competing secondary source of radicals deuterated methyl radicals ($^{\bullet}CD_3$) were also generated by the reaction of $^{\bullet}OH$ with DMSO and were then trapped by PBN. Replacing DMSO with d_6-DMSO in the Fenton-based reaction mixture gives rise to an increase in the *m/z* value of the molecular ion of 3 *m/z* units. The peak at *m/z* 245 units corresponds to the molecular ion of PBN-Me-Prop. The fragment at *m/z* 230 is the loss of a methyl group from the molecular ion (from the tBu group) thus proving that there is no loss of the methyl at the alpha carbon. The loss of the propyl group from the oxygen results in *m/z* 195 showing the incorporation of the perdeuterated propyl radical. The loss of CH2=CMe2 gives *m/z* 189 and the loss of the deuterated methyl group from this fragment results in *m/z* 171. Further dissociation of the propyl from the oxygen gives *m/z* 139 showing the CD_3 group is retained on this fragment. The dissociation of the alpha carbon bond and the nitrogen gives the base peak *m/z* 108 thus showing that incorporation of the CD_3 in the ion and further breakdown of this fragment results in a phenyl cation at *m/z* 77. The peak at *m/z* 57 is the tertiary butyl cation

4.10.4 Monomethyl monopropyl adduct of PBN-d_6 with butanal and DMSO (Compound 10)

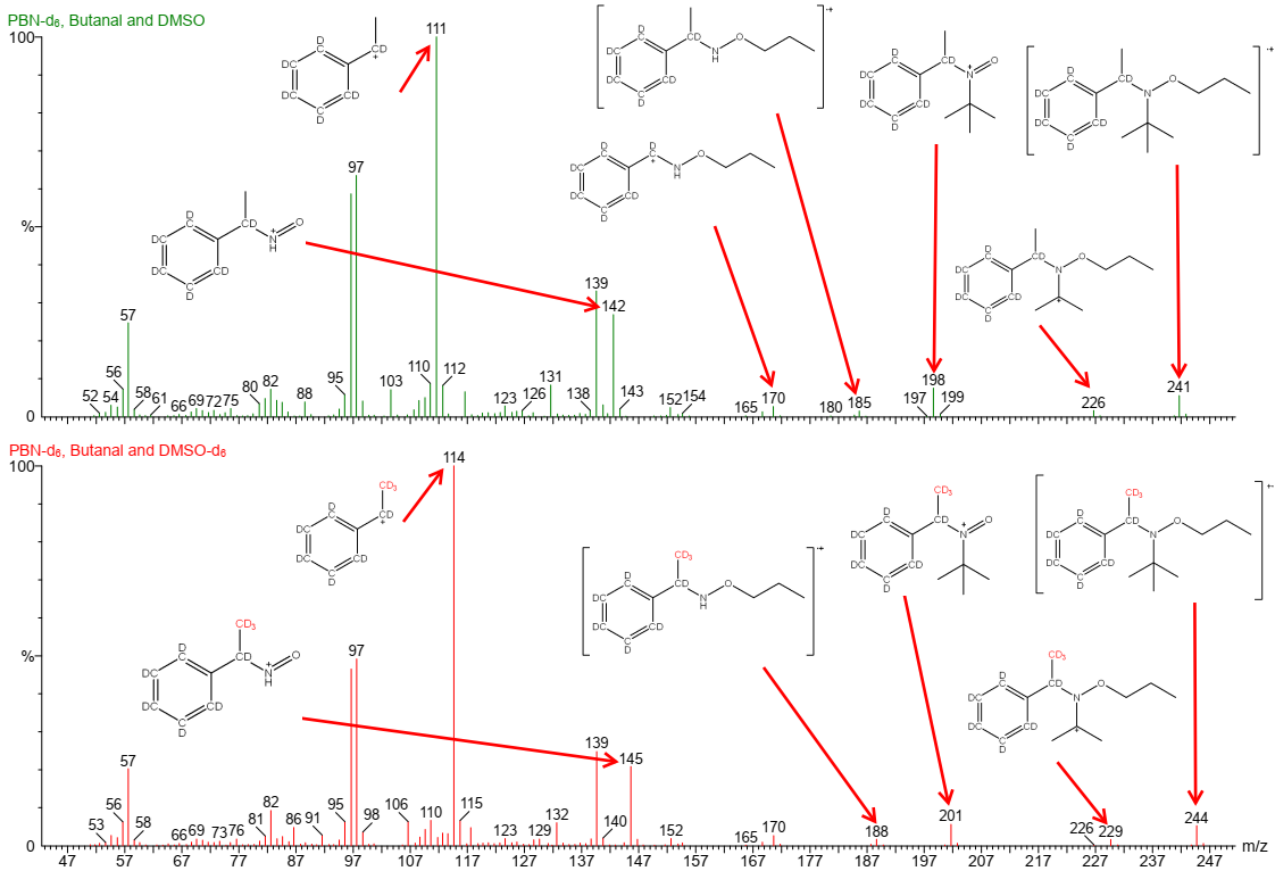

Figure 4.10.4 Electron Ionization mass spectra (EI-MS) corresponding to PBN adduct obtained from the analysis of the Fenton reaction mixture containing PBN-d_6, butanal and DMSO or DMSO-d_6 at rt 7.09 minutes

The EI mass spectra shown in Figure 4.10.4 correspond to the a)d_6PBN C-(propyl)-O-(methyl) adduct d_6PBN-($CH_2CH_2CH_3$)(CH_3) (top spectra), and b) the deuterated methyl group d_6PBN C-(propyl)-O-(methyl) adduct d_6PBN -($CH_2CH_2CH_3$)($C\mathbf{D}_3$) (bottom spectra).

When the Fenton reaction was carried out in the presence of butanal and DMSO as a competing secondary source of radicals methyl radicals ($^{\bullet}CH_3$) were also generated by the reaction of $^{\bullet}OH$ with DMSO and were then trapped by PBN. The peak at *m/z* 241 units corresponds to the molecular ion of d_6PBN-Me-Prop with the orientation of the methyl on the alpha carbon and the propyl adducted on the oxygen. The fragment at *m/z* 226 is due to the loss of a methyl group from the molecular ion (from the tBu group). The loss of the propyl group from the oxygen results in *m/z* 198. The loss of CH2=CMe2 from the molecular ion gives *m/z* 185 and the loss of a methyl group from this fragment results in *m/z* 170. Further dissociation of the

propyl from the oxygen gives *m/z* 142. The dissociation of the alpha carbon bond and the nitrogen gives the base peak *m/z* 111 and further breakdown of this fragment results in a phenyl cation at *m/z* 82. The peak at *m/z* 57 is the tertiary butyl cation. The peak at *m/z* 139 will be discussed in section 4.11

When the Fenton reaction was carried out in the presence of butanal and deuterated DMSO as a competing secondary source of radicals deuterated methyl radicals ($^{\bullet}CD_3$) were also generated by the reaction of $^{\bullet}OH$ with DMSO and were then trapped by d_6PBN. Replacing DMSO with d_6-DMSO in the Fenton-based reaction mixture gives rise to an increase in the *m/z* value of the molecular ion of 3 *m/z* units. The peak at *m/z* 244 units corresponds to the molecular ion of d_6PBN Me-Prop. The fragment at *m/z* 229 is the loss of a methyl group from the molecular ion (from the tBu group) thus proving that there is no loss of the methyl at the alpha carbon. The loss of the propyl group from the oxygen results in *m/z* 201. The loss of CH2=CMe2 gives *m/z* 188 and the loss of the deuterated methyl group from this fragment results in *m/z* 170. Further dissociation of the propyl from the oxygen gives *m/z* 145 showing the CD_3 group is retained on this fragment. The dissociation of the alpha carbon bond and the nitrogen gives the base peak *m/z* 114 thus showing that incorporation of the CD_3 in the ion and further breakdown of this fragment results in a phenyl cation at *m/z* 82. The peak at *m/z* 57 is the tertiary butyl cation.

4.10.5 Monomethyl monopropyl adduct of PBN-d_6 with butanal d_2 and DMSO (Compound 10)

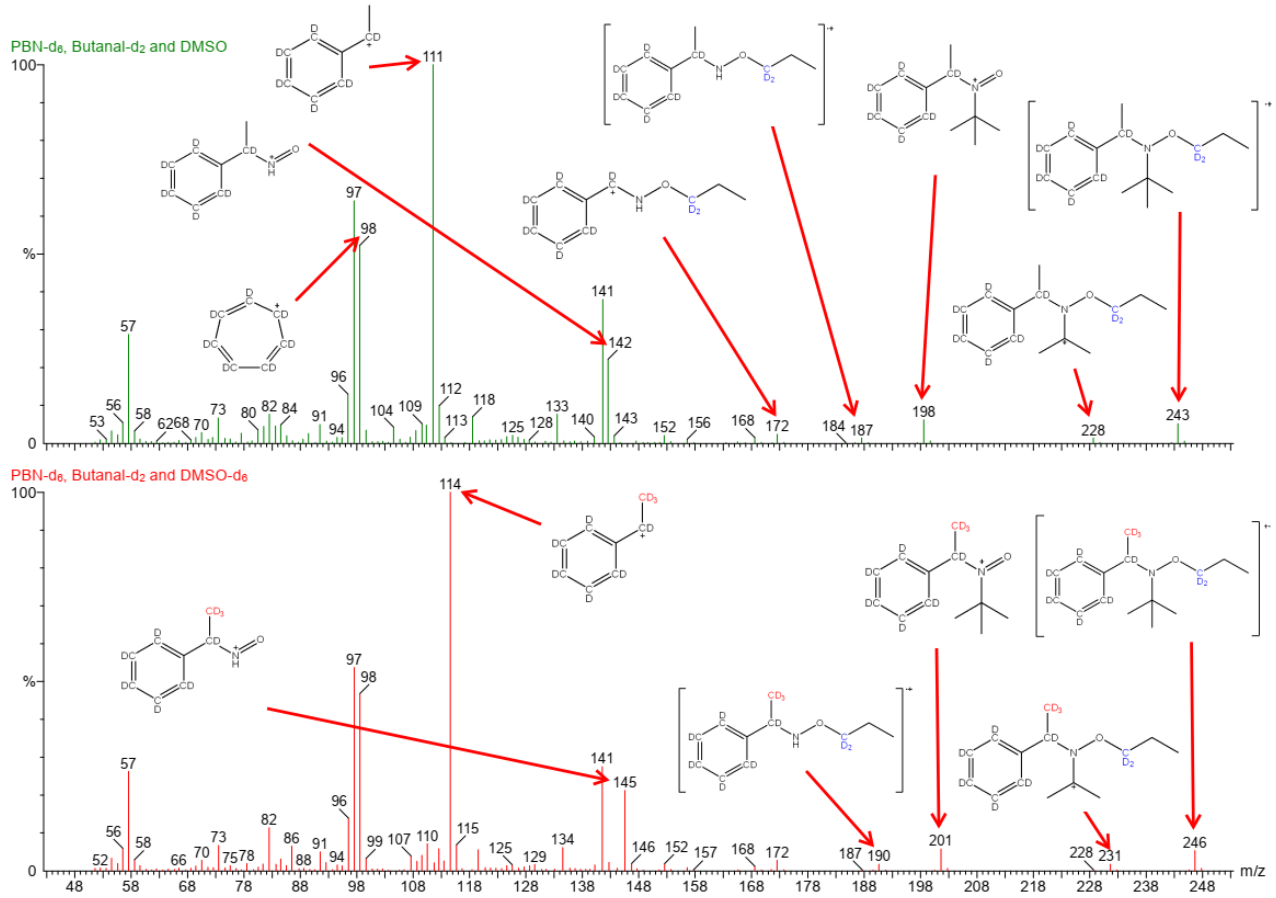

Figure 4.10.5 Electron Ionization mass spectra (EI-MS) corresponding to PBN adduct obtained from the analysis of the Fenton reaction mixture containing PBN-d_6, butanal-d_2 and DMSO or DMSO-d_6 at rt 7.09 minutes

The EI mass spectra shown in Figure 4.10.5Figure 4.10.1 correspond to the a)d_6PBN C-(propyl)-O-(methyl) adduct PBN-($CH_2CH_2CH_3$)(CH_3) (top spectra), and b) the dideuterated propyl deuterated methyl group d_6PBN C-(propyl)-O-(methyl) adduct d_6PBN -($CD_2CH_2CH_3$)(CD_3) (bottom spectra).

When the Fenton reaction was carried out in the presence of butanal-d_2 and DMSO as a competing secondary source of radicals methyl radicals ($^{\bullet}CH_3$) were also generated by the reaction of $^{\bullet}OH$ with DMSO and were then trapped by PBN. The peak at *m/z* 243 units corresponds to the molecular ion of PBN-Me-Prop with the orientation of the methyl on the alpha carbon and the dideuterated propyl adducted on the oxygen. The increase of 2 *m/z* units demonstrates the incorporation of the dideuterated propyl adduct. The fragment at *m/z* 228 is the loss of a methyl group from the molecular ion (from the tBu group). The loss of the propyl group from the oxygen results in *m/z* 198 showing the incorporation of the dideuterated

propyl radical. The loss of CH2=CMe2 from the molecular ion gives *m/z* 187 and the loss of a methyl group from this fragment results in *m/z* 172. Further dissociation of the propyl from the oxygen gives *m/z* 142 demonstrating that the propyl adduct is dideuterated. The dissociation of the alpha carbon bond and the nitrogen gives the base peak *m/z* 111 and further breakdown of this fragment results in a phenyl cation at *m/z* 82. The peak at *m/z* 57 is the tertiary butyl cation. The peak at *m/z* 141 will be discussed in section 4.11

When the Fenton reaction was carried out in the presence of butanal-d_2 and deuterated DMSO as a competing secondary source of radicals deuterated methyl radicals ($^{\bullet}CD_3$) were also generated by the reaction of $^{\bullet}OH$ with DMSO and were then trapped by PBN. Replacing DMSO with d_6-DMSO in the Fenton-based reaction mixture gives rise to an increase in the *m/z* value of the molecular ion of 3 *m/z* units. The peak at *m/z* 246 units corresponds to the molecular ion of PBN-Me-Prop. The fragment at *m/z* 231 is the loss of a methyl group from the molecular ion (from the tBu group) thus proving that there is no loss of the methyl at the alpha carbon. The loss of the propyl group from the oxygen results in *m/z* 201 showing the incorporation of the dideuterated propyl radical. The loss of CH2=CMe2 gives *m/z* 190 and the loss of the deuterated methyl group from this fragment results in *m/z* 172. Further dissociation of the propyl from the oxygen gives *m/z* 145 showing the CD_3 group is retained on this fragment. The dissociation of the alpha carbon bond and the nitrogen gives the base peak *m/z* 111 thus showing that incorporation of the CD_3 in the ion and further breakdown of this fragment results in a phenyl cation at *m/z* 82. The peak at *m/z* 57 is the tertiary butyl cation.

4.10.6 Monopropyl monomethyl adduct of PBN-d_6 with butanal d_7 and DMSO (Compound 10)

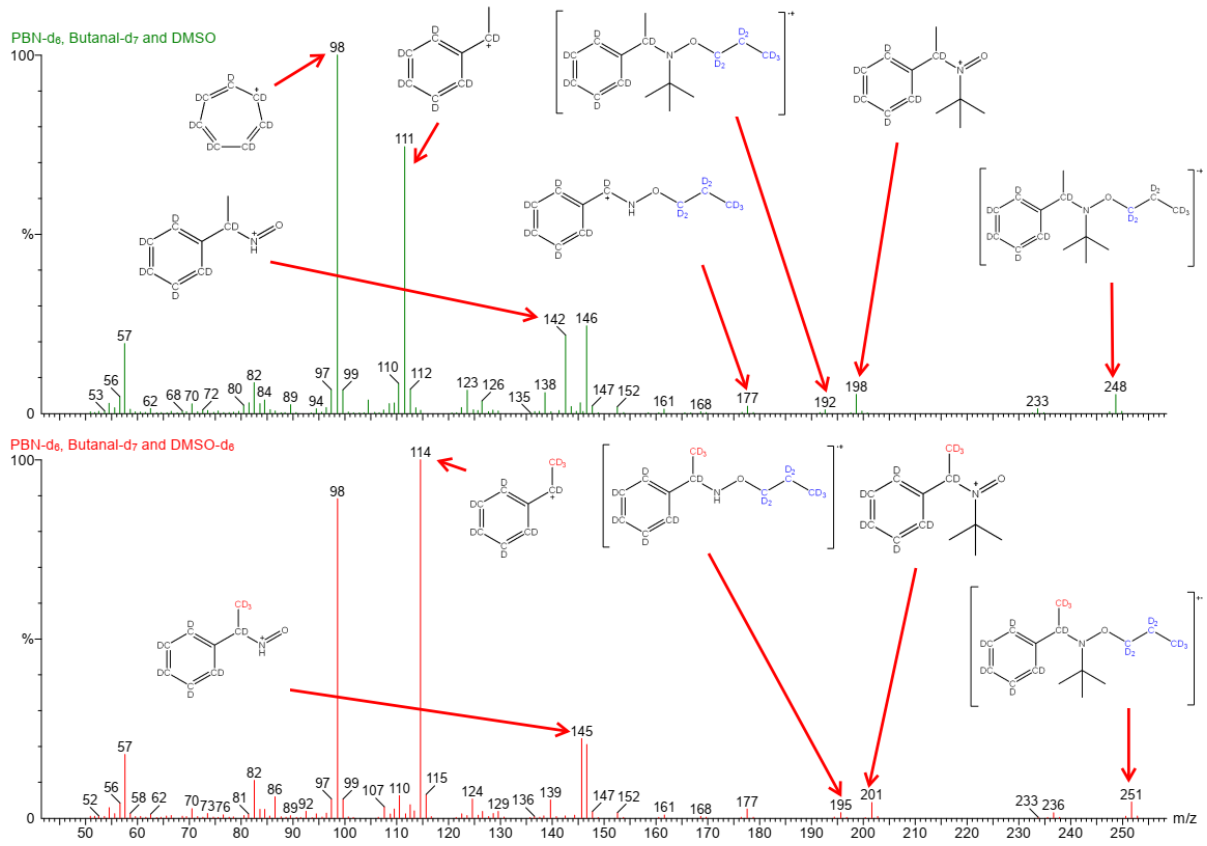

Figure 4.10.6 Electron Ionization mass spectra (EI-MS) corresponding to PBN adduct obtained from the analysis of the Fenton reaction mixture containing PBN-d_6, butanal-d_7 and DMSO or DMSO-d_6 at rt 7.09 minutes

The EI mass spectra shown in Figure 4.10.6 correspond to the a)d_6PBN C-(propyl)-O-(methyl) adduct PBN-($CH_2CH_2CH_3$)(CH_3) (top spectra), and b) the deuterated propyl deuterated methyl group d_6PBN C-(propyl)-O-(methyl) adduct d_6PBN -($C\mathbf{D}_2C\mathbf{D}_2C\mathbf{D}_3$)($C\mathbf{D}_3$) (bottom spectra).

When the Fenton reaction was carried out in the presence of butanal-d_7 and DMSO as a competing secondary source of radicals methyl radicals ($^{\bullet}CH_3$) were also generated by the reaction of $^{\bullet}$OH with DMSO and were then trapped by PBN. The peak at *m/z* 248 units corresponds to the molecular ion of d_6PBN-Me-Prop with the orientation of the methyl on the alpha carbon and the perdeuterated propyl radical adducted on the oxygen. The fragment at *m/z* 233 is due to the loss of a methyl group from the molecular ion (from the tBu group). The loss of the propyl group from the oxygen results in *m/z* 198 showing the incorporation of the perdeuterated propyl radical. The loss of CH2=CMe2 from the molecular ion gives *m/z* 192 and the loss of a methyl group from this fragment results in *m/z* 177. Further dissociation of the

propyl from the oxygen gives *m/z* 142. The dissociation of the alpha carbon bond and the nitrogen gives the base peak *m/z* 111 and further breakdown of this fragment results in a phenyl cation at *m/z* 82. The peak at *m/z* 57 is the tertiary butyl cation. The peak at *m/z* 146 will be discussed in section 4.11

When the Fenton reaction was carried out in the presence of deuterated DMSO as a competing secondary source of radicals deuterated methyl radicals ($^{\bullet}CD_3$) were generated by the reaction of $^{\bullet}OH$ with DMSO and were then trapped by d_6PBN. Replacing DMSO with d_6-DMSO in the Fenton-based reaction mixture gives rise to an increase in the *m/z* value of the molecular ion of 3 *m/z* units. The peak at *m/z* 251 units corresponds to the molecular ion of PBN-Me-Prop. The fragment at *m/z* 236 is the loss of a methyl group from the molecular ion (from the tBu group) thus proving that there is no loss of the methyl at the alpha carbon. The loss of the propyl group from the oxygen results in *m/z* 201 showing the incorporation of the perdeuterated propyl radical. The loss of CH2=CMe2 gives *m/z* 195 and the loss of the deuterated methyl group from this fragment results in *m/z* 177. Further dissociation of the propyl from the oxygen gives *m/z* 145 showing the CD_3 group is retained on this fragment. The dissociation of the alpha carbon bond and the nitrogen gives the base peak *m/z* 114 thus showing that incorporation of the CD_3 in the ion and further breakdown of this fragment results in a phenyl cation at *m/z* 82. The peak at *m/z* 57 is the tertiary butyl cation

4.11 Detection of propyl ($^{\bullet}CH_3CH_2CH_2$) radical and methyl ($^{\bullet}CH_3$) radical from DMSO (compound 11)

The peak at 7.09 minutes is believed to contain two peaks overlapping each other. It is believed they contain diastereomers with compound 11 (discussed in the following section) with the propyl adding on the alpha carbon and methyl on the oxygen. Compound 10 was previously discussed in section 4.10

4.11.1 Monopropyl monomethyl adduct of PBN with butanal and DMSO (compound 11)

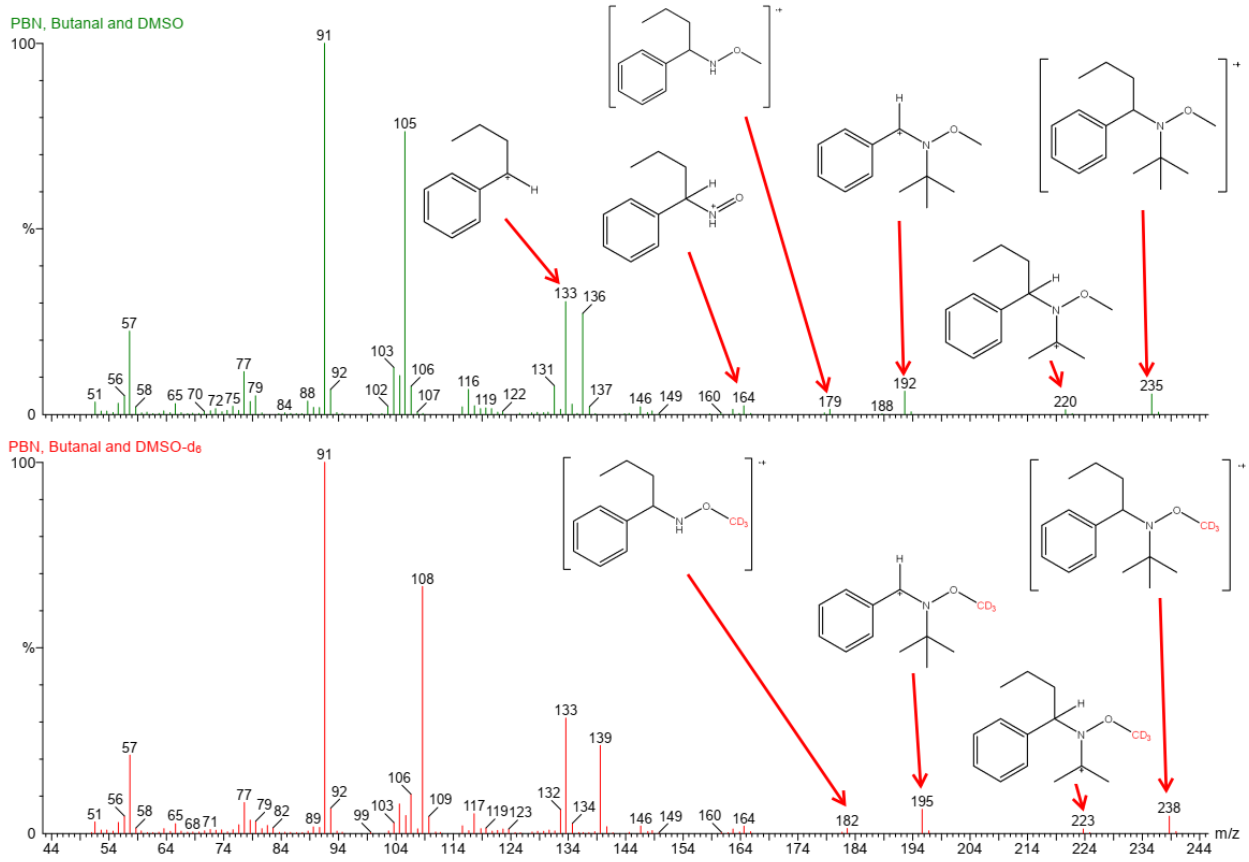

Figure 4.11.1 Electron Ionization mass spectra (EI-MS) corresponding to PBN adduct obtained from the analysis of the Fenton reaction mixture containing PBN, butanal and DMSO or DMSO-d_6 at rt 7.09 minutes

The EI mass spectra shown in Figure 4.11.1 correspond to the a)PBN C-(propyl)-O-(methyl) adduct PBN-($CH_2CH_2CH_3$)(CH_3) (top spectra), and b) the deuterated methyl group PBN C-(propyl)-O-(methyl) adduct PBN-($CH_2CH_2CH_3$)($C\mathbf{D}_3$) (bottom spectra).

When the Fenton reaction was carried out in the presence of butanal and DMSO as a competing secondary source of radicals, methyl radicals ($^{\bullet}CH_3$) were also generated by the reaction of $^{\bullet}OH$ with DMSO and were then trapped by PBN. The peak at *m/z* 235 units corresponds to the molecular ion of PBN-Prop-Me. The

fragment at *m/z* 220 is the loss of a methyl group from the molecular ion (from the tBu group). The loss from the molecular ion of the propyl group from the alpha carbon position results in *m/z* 192. The loss of CH2=CMe2 gives *m/z* 179 and the loss of a methyl group from this fragment results in *m/z* 164 .The dissociation of the alpha carbon bond and the nitrogen gives the butyl benzene cation at *m/z* 133. Further breakdown of this fragment results in the base peak *m/z* 91 tropylium cation and a phenyl cation at *m/z* 77. The peak at *m/z* 57 is the tertiary butyl cation

When the Fenton reaction was carried out in the presence of butanal and deuterated DMSO as a competing secondary source of radicals deuterated methyl radicals ($^{\bullet}CD_3$) were also generated by the reaction of $^{\bullet}OH$ with DMSO and were then trapped by PBN. Replacing DMSO with d_6-DMSO in the Fenton-based reaction mixture gives rise to an increase in the *m/z* value of the molecular ion of 3 *m/z* units. The peak at *m/z* 238 units corresponds to the molecular ion of PBN-Prop-Me. The fragment at *m/z* 223 is the loss of a methyl group from the molecular ion (from the tBu group) thus proving that there is no loss of the (deuterated) methyl from the oxygen. The loss of $CH_2=CMe_2$ gives *m/z* 182 and the loss of a methyl group from this fragment results in *m/z* 164. The dissociation of the alpha carbon bond and the nitrogen gives the butyl benzene cation at *m/z* 133. Further breakdown of this fragment results in the base peak *m/z* 91 tropylium cation and a phenyl cation at *m/z* 77. The peak at *m/z* 57 is the tertiary butyl cation

4.11.2 Monopropyl monomethyl adduct of PBN with butanal d_2 and DMSO (compound 11)

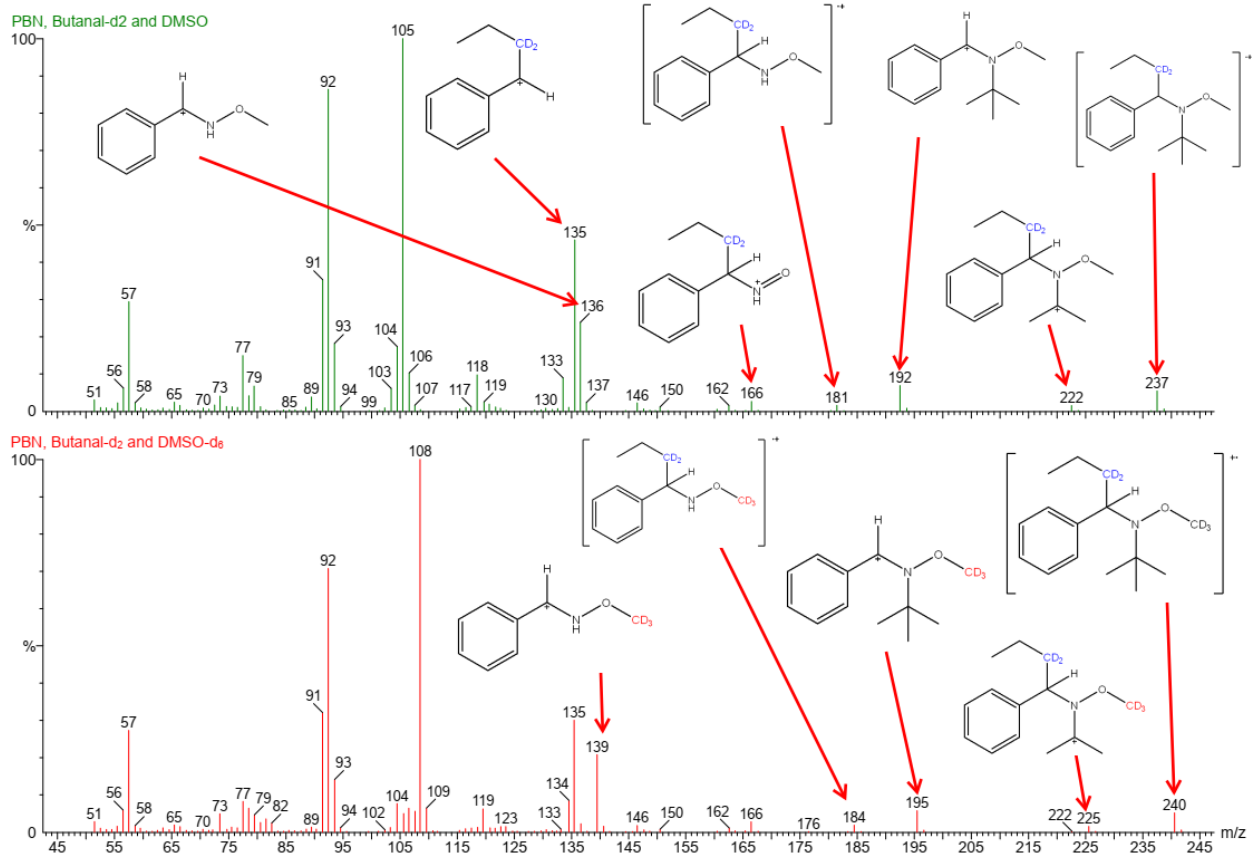

Figure 4.11.2 Electron Ionization mass spectra (EI-MS) corresponding to PBN adduct obtained from the analysis of the Fenton reaction mixture containing PBN, butanal-d_2 and DMSO or DMSO-d_6 at rt 7.09 minutes

The EI mass spectra shown in Figure 4.11.2 correspond to the a)PBN C-(propyl)-O-(methyl) adduct PBN-($CH_2CH_2CH_3$)(CH_3) (top spectra), and b) the dideuterated propyl deuterated methyl group PBN C-(propyl)-O-(methyl) adduct PBN-(C**D**$_2$$CH_2CH_3$)(C**D**$_3$) (bottom spectra).

When the Fenton reaction was carried out in the presence of butanal-d_2 and DMSO as a competing secondary source of radicals, methyl radicals ($^{\bullet}CH_3$) were also generated by the reaction of $^{\bullet}OH$ with DMSO and were then trapped by PBN. The peak at *m/z* 237 units corresponds to the molecular ion of PBN-Prop-Me. The fragment at *m/z* 222 is the loss of a methyl group from the molecular ion (from the tBu group). The loss from the molecular ion of the propyl group from the alpha carbon position results in *m/z* 192 (showing that the propyl adduct contained d_2). The loss of CH_2=CMe_2 gives *m/z* 181 and the loss of a methyl group from this fragment results in *m/z* 166 .The dissociation of the alpha carbon bond and the

nitrogen gives the butyl-d_2 benzene cation at *m/z* 135. Further breakdown of this fragment results in peak *m/z* 92 tropylium-1-d cation (a deuterium from the propyl has rearranged to add onto the tropylium) and a phenyl cation at *m/z* 77. The peak at *m/z* 57 is the tertiary butyl cation

When the Fenton reaction was carried out in the presence of butanal-d_2 deuterated DMSO as a competing secondary source of radicals deuterated methyl radicals ($^{\bullet}CD_3$) were also generated by the reaction of $^{\bullet}OH$ with DMSO and were then trapped by PBN. Replacing DMSO with d_6-DMSO in the Fenton-based reaction mixture gives rise to an increase in the *m/z* value of the molecular ion of 3 *m/z* units. The peak at *m/z* 240 units corresponds to the molecular ion of PBN-Prop-Me. The fragment at *m/z* 225 is the loss of a methyl group from the molecular ion (from the tBu group). The loss of CH_2=CMe_2 gives *m/z* 184 and the loss of a methyl group from this fragment results in *m/z* 166. The dissociation of the alpha carbon bond and the nitrogen gives the butyl-d_2 benzene cation at *m/z* 135. Further breakdown of this fragment results in peak *m/z* 92 tropylium-1-d cation (a deuterium from the propyl has rearranged to add onto the tropylium) and a phenyl cation at *m/z* 77. The peak at *m/z* 57 is the tertiary butyl cation

4.11.3 Monopropyl monomethyl adduct of PBN with butanal d_7 and DMSO (compound 11)

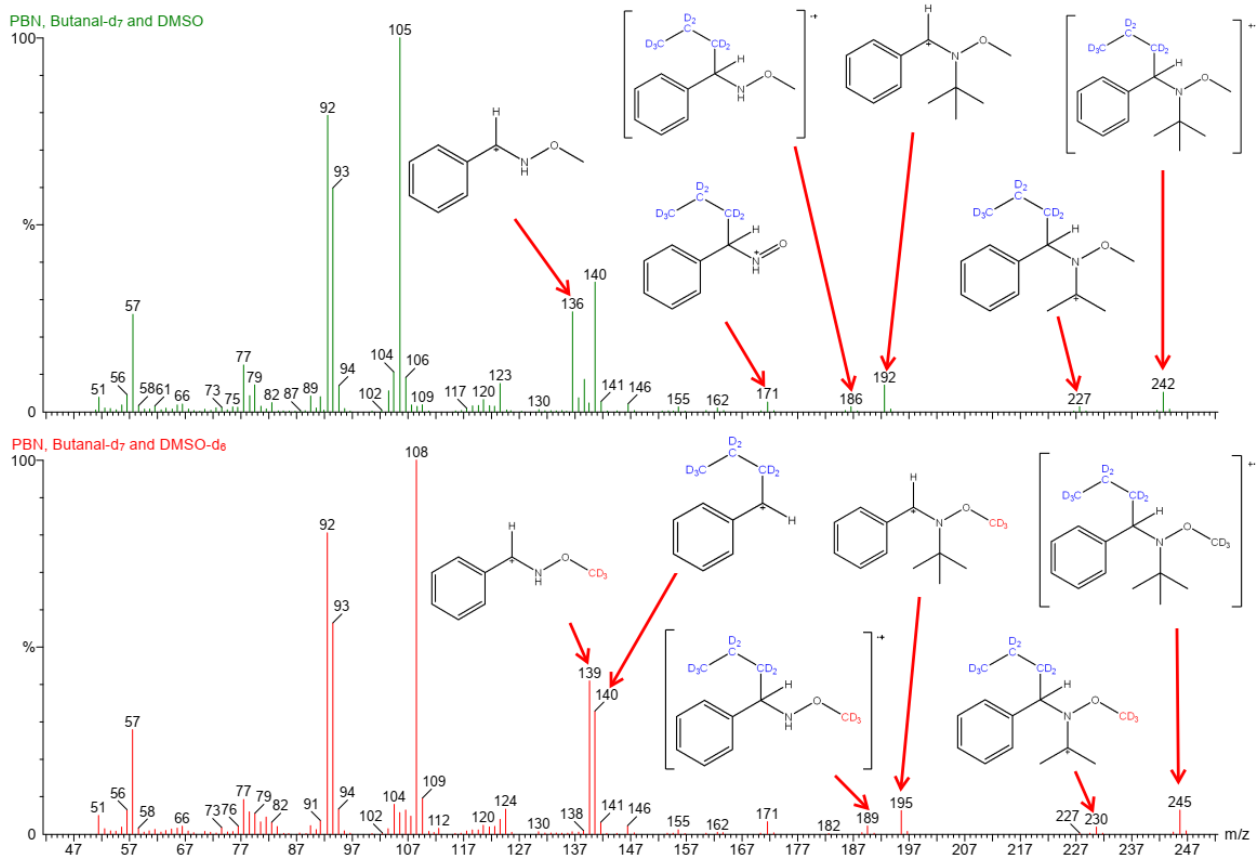

Figure 4.11.3 Electron Ionization mass spectra (EI-MS) corresponding to PBN adduct obtained from the analysis of the Fenton reaction mixture containing PBN, butanal-d_7 and DMSO or DMSO-d_6 at rt 7.09 minutes

The EI mass spectra shown in Figure 4.11.3 correspond to the a)PBN C-(propyl)-O-(methyl) adduct PBN-($CH_2CH_2CH_3$)(CH_3) (top spectra), and b) the dideuterated propyl deuterated methyl group PBN C-(propyl)-O-(methyl) adduct PBN-(C**D**$_2$$CH_2CH_3$)(C**D**$_3$) (bottom spectra).

When the Fenton reaction was carried out in the presence of butanal-d_7 and DMSO as a competing secondary source of radicals, methyl radicals ($^{\bullet}CH_3$) were also generated by the reaction of $^{\bullet}OH$ with DMSO and were then trapped by PBN. The peak at *m/z* 242 units corresponds to the molecular ion of PBN-Prop-Me. The fragment at *m/z* 227 is the loss of a methyl group from the molecular ion (from the tBu group). The loss from the molecular ion of the propyl group from the alpha carbon position results in *m/z* 192 (showing that the propyl adduct contained d_2). The loss of CH_2=CMe_2 gives *m/z* 186 and the loss of a methyl group from this fragment results in *m/z* 171. The dissociation of the alpha carbon bond and the

nitrogen gives the butyl-d_7 benzene cation at *m/z* 140. Further breakdown of this fragment results in peak *m/z* 92 tropylium-1-d cation (a deuterium from the propyl has rearranged to add onto the tropylium) and a phenyl cation at *m/z* 77. The peak at *m/z* 57 is the tertiary butyl cation

When the Fenton reaction was carried out in the presence of butanal-d_7 and deuterated DMSO as a competing secondary source of radicals deuterated methyl radicals ($^{\bullet}CD_3$) were also generated by the reaction of $^{\bullet}OH$ with DMSO and were then trapped by PBN. Replacing DMSO with d_6-DMSO in the Fenton-based reaction mixture gives rise to an increase in the *m/z* value of the molecular ion of 3 *m/z* units. The peak at *m/z* 245 units corresponds to the molecular ion of PBN-Prop-Me. The fragment at *m/z* 230 is the loss of a methyl group from the molecular ion (from the tBu group). The loss of $CH_2{=}CMe_2$ gives *m/z* 189 and the loss of a methyl group from this fragment results in *m/z* 171. The dissociation of the alpha carbon bond and the nitrogen gives the butyl-d_7 benzene cation at *m/z* 140. Further breakdown of this fragment results in peak *m/z* 92 tropylium-1-d cation (a deuterium from the propyl has rearranged to add onto the tropylium) and a phenyl cation at *m/z* 77. The peak at *m/z* 57 is the tertiary butyl cation

4.11.4 Monopropyl monomethyl adduct of PBN-d_6 with butanal and DMSO (compound 11)

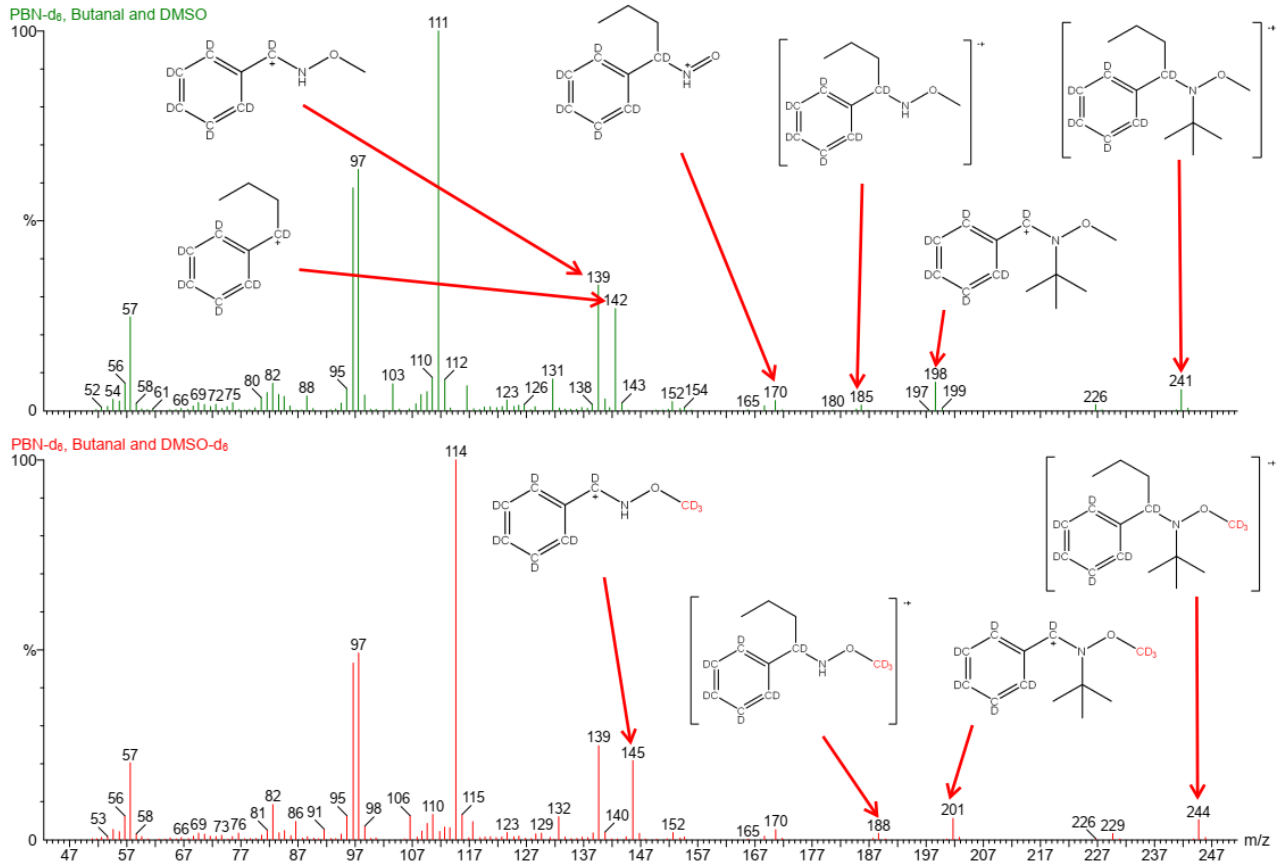

Figure 4.11.4 Electron Ionization mass spectra (EI-MS) corresponding to PBN adduct obtained from the analysis of the Fenton reaction mixture containing PBN-d_6, butanal and DMSO or DMSO-d_6 at rt 7.09 minutes

The EI mass spectra shown in Figure 4.11.4 correspond to the a)PBN-d_6 C-(propyl)-O-(methyl) adduct PBN-($CH_2CH_2CH_3$)(CH_3) (top spectra), and b) the deuterated methyl group PBN-d_6 C-(propyl)-O-(methyl) adduct PBN-($CH_2CH_2CH_3$)($C\mathbf{D}_3$) (bottom spectra).

When the Fenton reaction was carried out in the presence of butanal and DMSO as a competing secondary source of radicals, methyl radicals ($^{\bullet}CH_3$) were also generated by the reaction of $^{\bullet}OH$ with DMSO and were then trapped by PBN-d_6. The peak at *m/z* 241 units corresponds to the molecular ion of PBN-d_6 -Prop-Me. The fragment at *m/z* 226 is the loss of a methyl group from the molecular ion (from the tBu group). The loss from the molecular ion of the propyl group from the alpha carbon position results in *m/z* 198. The loss of CH_2=CMe_2 gives *m/z* 185 and the loss of a methyl group from this fragment results in *m/z* 170 .The dissociation of the alpha carbon bond and the nitrogen gives the butyl benzene cation at *m/z* 139. Further

breakdown of this fragment results in the base peak *m/z* 97 tropylium-d_6 cation and a phenyl-d_5 cation at *m/z* 82. The peak at *m/z* 57 is the tertiary butyl cation

When the Fenton reaction was carried out in the presence of butanal deuterated DMSO as a competing secondary source of radicals deuterated methyl radicals ($^{\bullet}CD_3$) were also generated by the reaction of $^{\bullet}OH$ with DMSO and were then trapped by PBN-d_6. Replacing DMSO with d_6-DMSO in the Fenton-based reaction mixture gives rise to an increase in the *m/z* value of the molecular ion of 3 *m/z* units. The peak at *m/z* 244 units corresponds to the molecular ion of PBN-d_6 -Prop-Me. The fragment at *m/z* 229 is the loss of a methyl group from the molecular ion (from the tBu group). The loss of CH_2=CMe_2 gives *m/z* 188 and the loss of a methyl group from this fragment results in *m/z* 170. The dissociation of the alpha carbon bond and the nitrogen gives the butyl benzene cation at *m/z* 139. Further breakdown of this fragment results in the base peak *m/z* 97 tropylium-d_6 cation and a phenyl-d_5 cation at *m/z* 82. The peak at *m/z* 57 is the tertiary butyl cation

4.11.5 Monopropyl monomethyl adduct of PBN-d_6 with butanal d_2 and DMSO (compound 11)

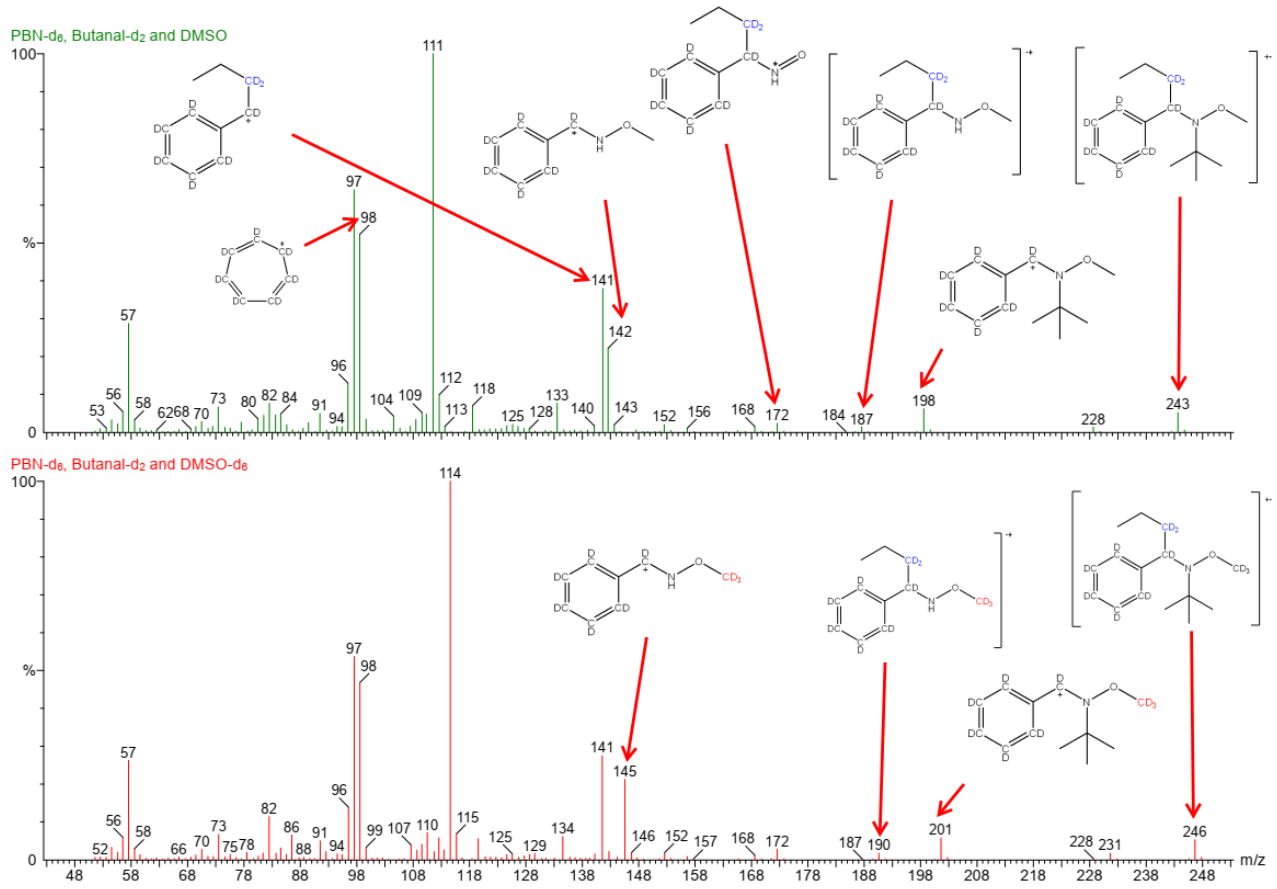

Figure 4.11.5 Electron Ionization mass spectra (EI-MS) corresponding to PBN adduct obtained from the analysis of the Fenton reaction mixture containing PBN-d_6, butanal-d_2 and DMSO or DMSO-d_6 at rt 7.09 minutes

The EI mass spectra shown in Figure 4.11.5 correspond to the a)PBN-d_6 C-(propyl)-O-(methyl) adduct PBN-(C**D**$_2$CH$_2$CH$_3$)(CH$_3$) (top spectra), and b) the deuterated methyl group PBN-d_6 C-(propyl)-O-(methyl) adduct PBN-(C**D**$_2$CH$_2$CH$_3$)(C**D**$_3$) (bottom spectra).

When the Fenton reaction was carried out in the presence of butanal-d_2 and DMSO as a competing secondary source of radicals, methyl radicals ($^{\bullet}$CH$_3$) were also generated by the reaction of $^{\bullet}$OH with DMSO and were then trapped by PBN-d_6. The peak at *m/z* 243 units corresponds to the molecular ion of PBN-Prop-Me. The fragment at *m/z* 228 is the loss of a methyl group from the molecular ion (from the tBu group). The loss from the molecular ion of the propyl group from the alpha carbon position results in *m/z* 198. The loss of CH$_2$=CMe$_2$ gives *m/z* 187 and the loss of a methyl group from this fragment results in *m/z* 172 .The dissociation of the alpha carbon bond and the nitrogen gives the butyl benzene cation at *m/z*

141. Further breakdown of this fragment results in the base peak *m/z* 97 tropylium-d_6 cation and a phenyl-d_5 cation at *m/z* 82. The peak at *m/z* 57 is the tertiary butyl cation

When the Fenton reaction was carried out in the presence of butanal-d_2 and deuterated DMSO as a competing secondary source of radicals deuterated methyl radicals ($^{\bullet}CD_3$) were also generated by the reaction of $^{\bullet}OH$ with DMSO and were then trapped by PBN-d_6. Replacing DMSO with d_6-DMSO in the Fenton-based reaction mixture gives rise to an increase in the *m/z* value of the molecular ion of 3 *m/z* units. The peak at *m/z* 244 units corresponds to the molecular ion of PBN-Prop-Me. The fragment at *m/z* 229 is the loss of a methyl group from the molecular ion (from the tBu group). The loss of CH_2=CMe_2 gives *m/z* 188 and the loss of a methyl group from this fragment results in *m/z* 170. The dissociation of the alpha carbon bond and the nitrogen gives the butyl benzene cation at *m/z* 139. Further breakdown of this fragment results in the base peak *m/z* 97 tropylium-d_6 cation and a phenyl-d_5 cation at *m/z* 82. The peak at *m/z* 57 is the tertiary butyl cation

4.11.6 Monopropyl monomethyl adduct of PBN-d_6 with butanal d_7 and DMSO (compound 11)

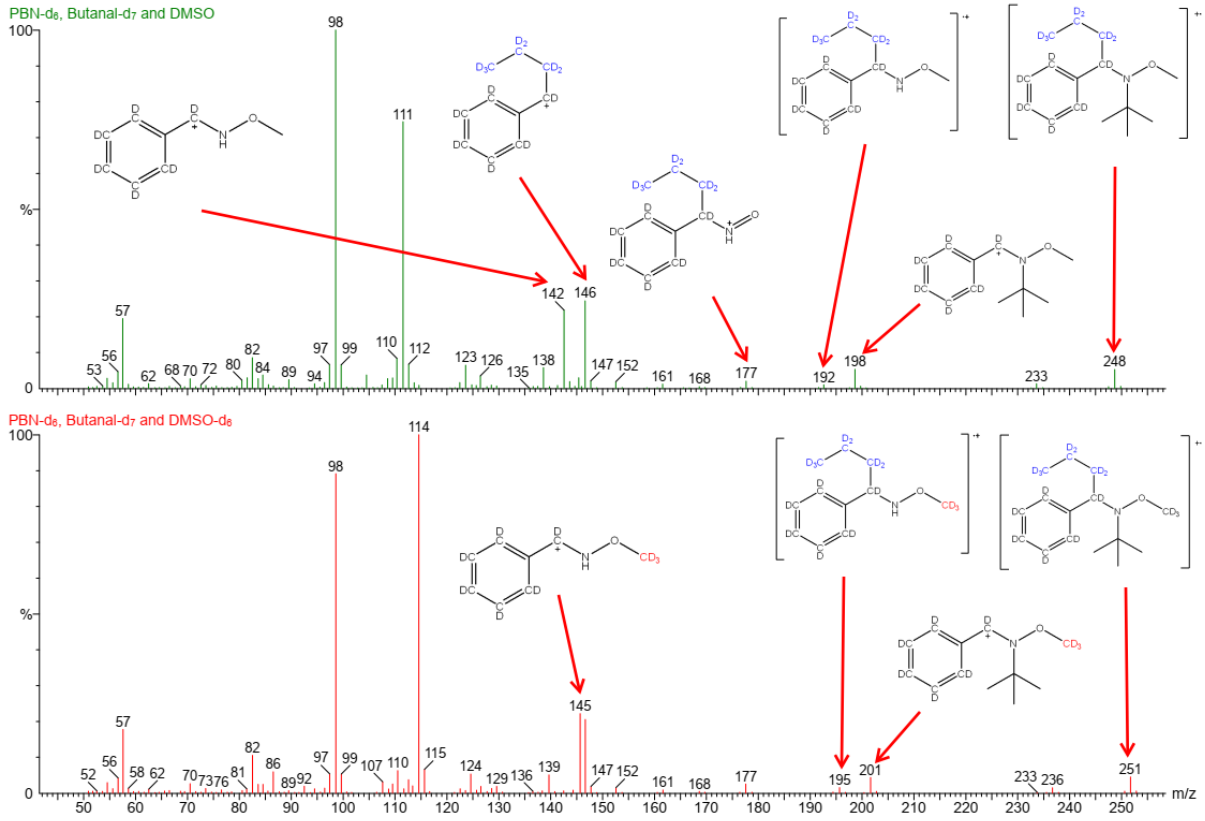

Figure 4.11.6 Electron Ionization mass spectra (EI-MS) corresponding to PBN adduct obtained from the analysis of the Fenton reaction mixture containing PBN-d_6, butanal-d_7 and DMSO or DMSO-d_6 at rt 7.09 minutes

The EI mass spectra shown in Figure 4.11.6 correspond to the a)PBN-d_6 C-(propyl)-O-(methyl) adduct PBN-(**C**D_2**C**D_2**C**D_3)(CH_3) (top spectra), and b) the deuterated methyl group PBN-d_6 C-(propyl)-O-(methyl) adduct PBN-d_6 -(**C**D_2**C**D_2**C**D_3)(**C**D_3) (bottom spectra).

When the Fenton reaction was carried out in the presence of butanal-d_7 and DMSO as a competing secondary source of radicals, methyl radicals ($^{\bullet}CH_3$) were also generated by the reaction of $^{\bullet}OH$ with DMSO and were then trapped by PBN-d_6. The peak at *m/z* 248 units corresponds to the molecular ion of PBN-d_6 -Prop-Me. The fragment at *m/z* 233 is the loss of a methyl group from the molecular ion (from the tBu group). The loss from the molecular ion of the propyl group from the alpha carbon position results in *m/z* 198. The loss of CH_2=CMe_2 gives *m/z* 192 and the loss of a methyl group from this fragment results in *m/z* 177 .The dissociation of the alpha carbon bond and the nitrogen gives the butyl benzene cation at *m/z*

146. Further breakdown of this fragment results in the base peak *m/z* 98 tropylium-d_7 cation and a phenyl-d_5 cation at *m/z* 82. The peak at *m/z* 57 is the tertiary butyl cation

When the Fenton reaction was carried out in the presence of butanal-d_7 and deuterated DMSO as a competing secondary source of radicals deuterated methyl radicals ($^{\bullet}CD_3$) were also generated by the reaction of $^{\bullet}OH$ with DMSO and were then trapped by PBN-d_6. Replacing DMSO with d_6-DMSO in the Fenton-based reaction mixture gives rise to an increase in the *m/z* value of the molecular ion of 3 *m/z* units. The peak at *m/z* 244 units corresponds to the molecular ion of PBN-d_6 -Prop-Me. The fragment at *m/z* 229 is the loss of a methyl group from the molecular ion (from the tBu group). The loss of CH_2=CMe_2 gives *m/z* 195 and the loss of a methyl group from this fragment results in *m/z* 177. The dissociation of the alpha carbon bond and the nitrogen gives the butyl benzene cation at *m/z* 146. Further breakdown of this fragment results in the base peak *m/z* 98 tropylium-d_7 cation and a phenyl-d_5 cation at *m/z* 82. The peak at *m/z* 57 is the tertiary butyl cation

4.12 Detection of Methyl ($^{\bullet}CH_3$) radical and oxybutyl ($^{\bullet}CH_3CH_2CH_2CHO$) radical DMSO (compound 12)

4.12.1 Mono-oxybutyl monomethyl adduct of PBN with butanal and DMSO (compound 12)

Figure 4.12.1 Electron Ionization mass spectra (EI-MS) corresponding to PBN adduct obtained from the analysis of the Fenton reaction mixture containing PBN, butanal and DMSO or DMSO-d_6 at rt 10.47 minutes

The EI mass spectra shown in Figure 4.12.1 correspond to a) the PBN mono-butanal mono-methyl adduct, PBN(CH_3CHCH_2CHO)-CH_3) (top spectrum), and b) the PBN mono-butanal mono-perdeuterated methyl-adduct, PBN-(CH_3CHCH_2CHO)($C\mathbf{D}_3$) (bottom spectrum)

When the Fenton reaction was carried out in the presence of butanal DMSO as a competing secondary source of radicals, methyl radicals ($^{\bullet}CH_3$) were also generated by the reaction of $^{\bullet}OH$ with DMSO and were then trapped by PBN. The peak at *m/z* 263 units corresponds to the molecular ion of PBN-Butanal-Me. The fragment at *m/z* 248 is the loss of a methyl group from the molecular ion (from the tBu group). The loss from the molecular ion of the butanal group from the alpha carbon position results in *m/z* 192 and

further loss from this fragment of CH_2=CMe_2 gives *m/z* 136. The dissociation of the alpha carbon and nitrogen results in *m/z* 161 (loss of a tBu methoxy azane group from the molecular ion) and further fragmentation (CH_3CHO group is lost) leads to *m/z* 117 with the identity 1-phenylprop-1-en-2-ylium. *m/z* 91 units is the tropylium ion and the peak at *m/z* 57 is the tertiary butyl cation

When the Fenton reaction was carried out in the presence of deuterated DMSO as a competing secondary source of radicals deuterated methyl radicals ($^{\bullet}CD_3$) were generated by the reaction of $^{\bullet}OH$ with DMSO and were then trapped by PBN. Replacing DMSO with d_6-DMSO in the Fenton-based reaction mixture gives rise to an increase in the *m/z* value of the molecular ion of 3 *m/z* units. The peak at *m/z* 266 units corresponds to the molecular ion of PBN-Butanal-Me. The fragment at *m/z* 251 is the loss of a methyl group from the molecular ion (from the tBu group). The loss from the molecular ion of the butanal group from the alpha carbon position results in *m/z* 195 and further loss from this fragment of CH_2=CMe_2 gives *m/z* 139. The dissociation of the alpha carbon and nitrogen results in *m/z* 161 (loss of a tBu methoxy azane group from the molecular ion) and further fragmentation (CH_3CHO group is lost) leads to *m/z* 117 with the identity 1-phenylprop-1-en-2-ylium. Further breakdown of this fragment results in the peak *m/z* 91 tropylium cation and a phenyl cation at *m/z* 77. The peak at *m/z* 57 is the tertiary butyl cation

4.12.2 Mono oxybutyl monomethyl adduct of PBN with butanal-d_2 and DMSO (compound 12)

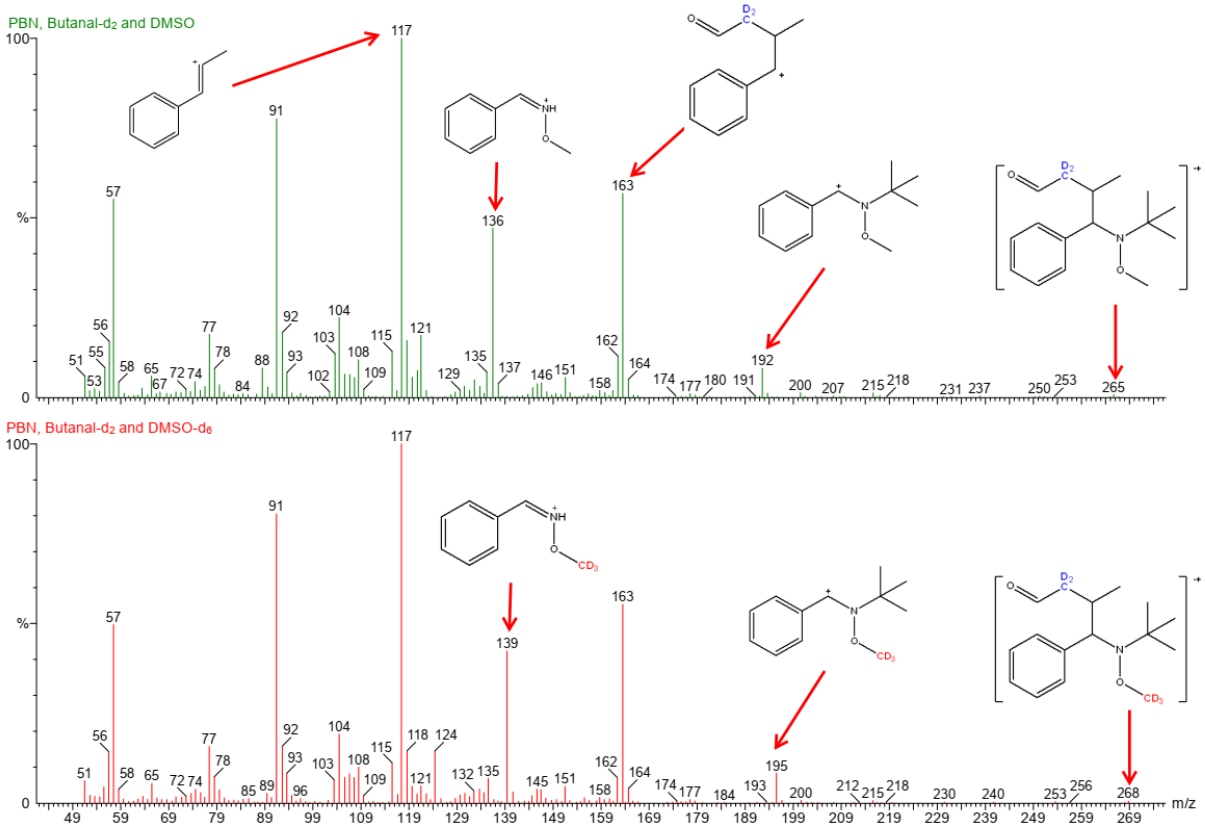

Figure 4.12.2 Electron Ionization mass spectra (EI-MS) corresponding to PBN adduct obtained from the analysis of the Fenton reaction mixture containing PBN, butanal-d_2 and DMSO or DMSO-d_6 at rt 10.47 minutes

The EI mass spectra shown in Figure 4.12.2 correspond to a) the PBN mono-butanal mono-methyl adduct, PBN($CH_3CHC\mathbf{D}_2CHO$)(CH_3) (top spectrum), and b) the PBN mono-butanal mono-perdeuterated methyl-adduct, PBN-($CH_3CHC\mathbf{D}_2CHO$)($C\mathbf{D}_3$) (bottom spectrum)

When the Fenton reaction was carried out in the presence of DMSO as a competing secondary source of radicals, methyl radicals ($^{\bullet}CH_3$) were generated by the reaction of $^{\bullet}OH$ with DMSO and were then trapped by PBN. The peak at *m/z* 265 units corresponds to the molecular ion of PBN-Butanal-Me. The fragment at *m/z* 250 is the loss of a methyl group from the molecular ion (from the tBu group). The loss from the molecular ion of the butanal group from the alpha carbon position results in *m/z* 192 and further loss from this fragment of CH_2=CMe_2 gives *m/z* 136. The dissociation of the alpha carbon and nitrogen results in *m/z* 163 (loss of a tBu methoxy azane group from the molecular ion) and further fragmentation (CH_3CHO group

is lost) leads to *m/z* 117 with the identity 1-phenylprop-1-en-2-ylium. *m/z* 104 is phenylmethanimine, *m/z* 91 units is the tropylium ion and the peak at *m/z* 57 is the tertiary butyl cation

When the Fenton reaction was carried out in the presence of deuterated DMSO as a competing secondary source of radicals deuterated methyl radicals ($^{\bullet}CD_3$) were generated by the reaction of $^{\bullet}OH$ with DMSO and were then trapped by PBN. Replacing DMSO with d_6-DMSO in the Fenton-based reaction mixture gives rise to an increase in the *m/z* value of the molecular ion of 3 *m/z* units. The peak at *m/z* 268 units corresponds to the molecular ion of PBN-Butanal-Me. The fragment at *m/z* 253 is the loss of a methyl group from the molecular ion (from the tBu group). The loss from the molecular ion of the butanal group from the alpha carbon position results in *m/z* 195 and further loss from this fragment of CH_2=CMe_2 gives *m/z* 139. The dissociation of the alpha carbon and nitrogen results in *m/z* 163 (loss of a tBu methoxy azane group from the molecular ion) and further fragmentation (CH_3CHO group is lost) leads to *m/z* 117 with the identity 1-phenylprop-1-en-2-ylium. Further breakdown of this fragment results in the peak *m/z* 91 tropylium cation and a phenyl cation at *m/z* 77. The peak at *m/z* 57 is the tertiary butyl cation

4.12.3 Mono oxybutyl monomethyl adduct of PBN with butanal-d_7 and DMSO (compound 12)

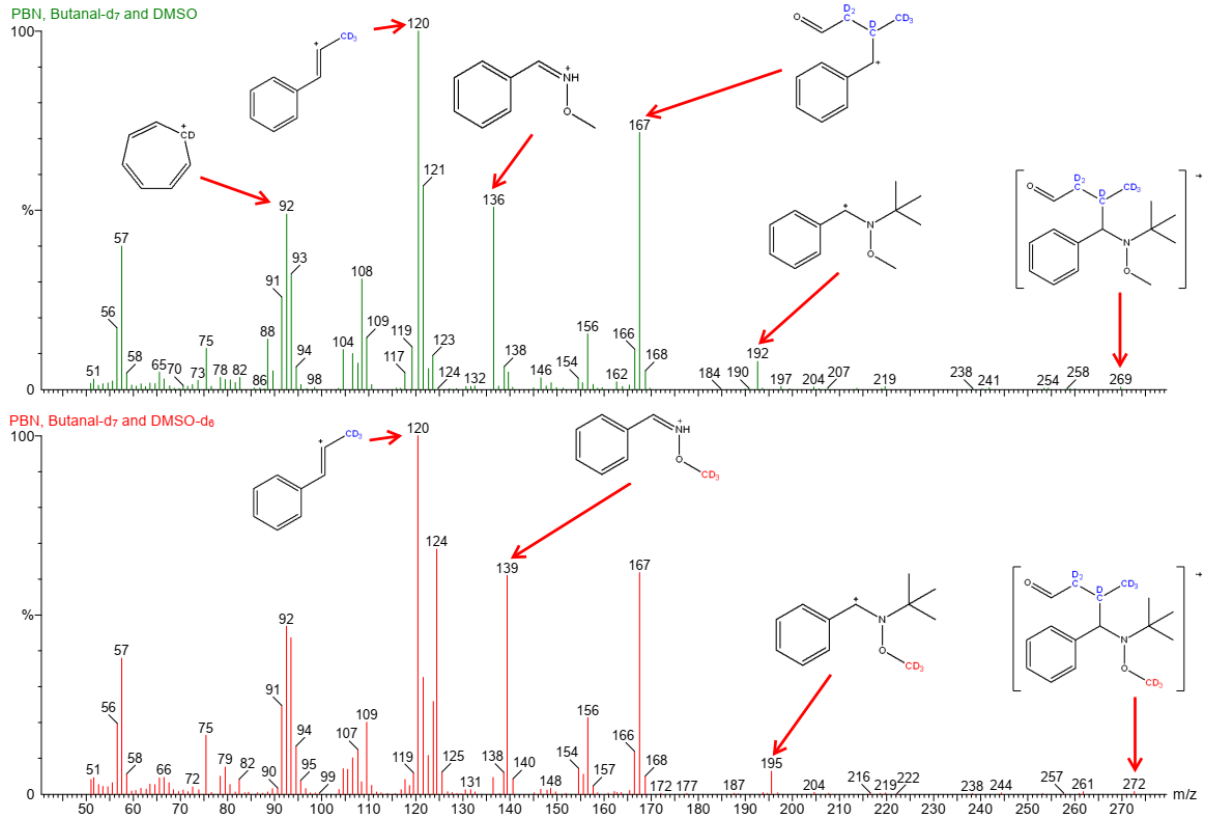

Figure 4.12.3 Electron Ionization mass spectra (EI-MS) corresponding to PBN adduct obtained from the analysis of the Fenton reaction mixture containing PBN, butanal-d_7 and DMSO or DMSO-d_6 at rt 10.47 minutes

The EI mass spectra shown in Figure 4.12.3 correspond to a) the PBN mono-butanal mono-methyl adduct, PBN(C**D**$_3$C**D**C**D**$_2$CHO)(CH$_3$) (top spectrum), and b) the PBN mono-butanal mono-perdeuterated methyl-adduct, PBN-(C**D**$_3$C**D**C**D**$_2$CHO)(C**D**$_3$) (bottom spectrum)

When the Fenton reaction was carried out in the presence of DMSO as a competing secondary source of radicals, methyl radicals ($^{\bullet}$CH$_3$) were generated by the reaction of $^{\bullet}$OH with DMSO and were then trapped by PBN. The peak at *m/z* 269 units corresponds to the molecular ion of PBN-Butanal-Me. The fragment at *m/z* 254 is the loss of a methyl group from the molecular ion (from the tBu group). The loss from the molecular ion of the butanal group from the alpha carbon position results in *m/z* 192 and further loss from this fragment of CH$_2$=CMe$_2$ gives *m/z* 136. The dissociation of the alpha carbon and nitrogen results in *m/z* 167 (loss of a tBu methoxy azane group from the molecular ion) and further fragmentation (CD$_2$HCHO

group is lost) leads to *m/z* 120 units with the identity 1-phenylprop-1-en-2-ylium-3,3,3,-d_3. *m/z* 91 units is the tropylium ion and the peak at *m/z* 57 is the tertiary butyl cation.

When the Fenton reaction was carried out in the presence of deuterated DMSO as a competing secondary source of radicals deuterated methyl radicals ($^{\bullet}CD_3$) were generated by the reaction of $^{\bullet}OH$ with DMSO and were then trapped by PBN. Replacing DMSO with d_6-DMSO in the Fenton-based reaction mixture gives rise to an increase in the *m/z* value of the molecular ion of 3 *m/z* units. The peak at *m/z* 272 units corresponds to the molecular ion of PBN-Butanal-Me. The fragment at *m/z* 257 is the loss of a methyl group from the molecular ion (from the tBu group). The loss from the molecular ion of the butanal group from the alpha carbon position results in *m/z* 195 and further loss from this fragment of CH_2=CMe_2 gives *m/z* 139. The dissociation of the alpha carbon and nitrogen results in *m/z* 167 (loss of a tBu methoxy azane group from the molecular ion) and further fragmentation (CD_2HCHO group is lost) leads to *m/z* 120 units with the identity 1-phenylprop-1-en-2-ylium-3,3,3,-d_3. *m/z* 91 units is the tropylium ion and the peak at *m/z* 57 is the tertiary butyl cation.

4.12.4 Mono oxybutyl monomethyl adduct of PBN-d_6 with butanal and DMSO (compound 12)

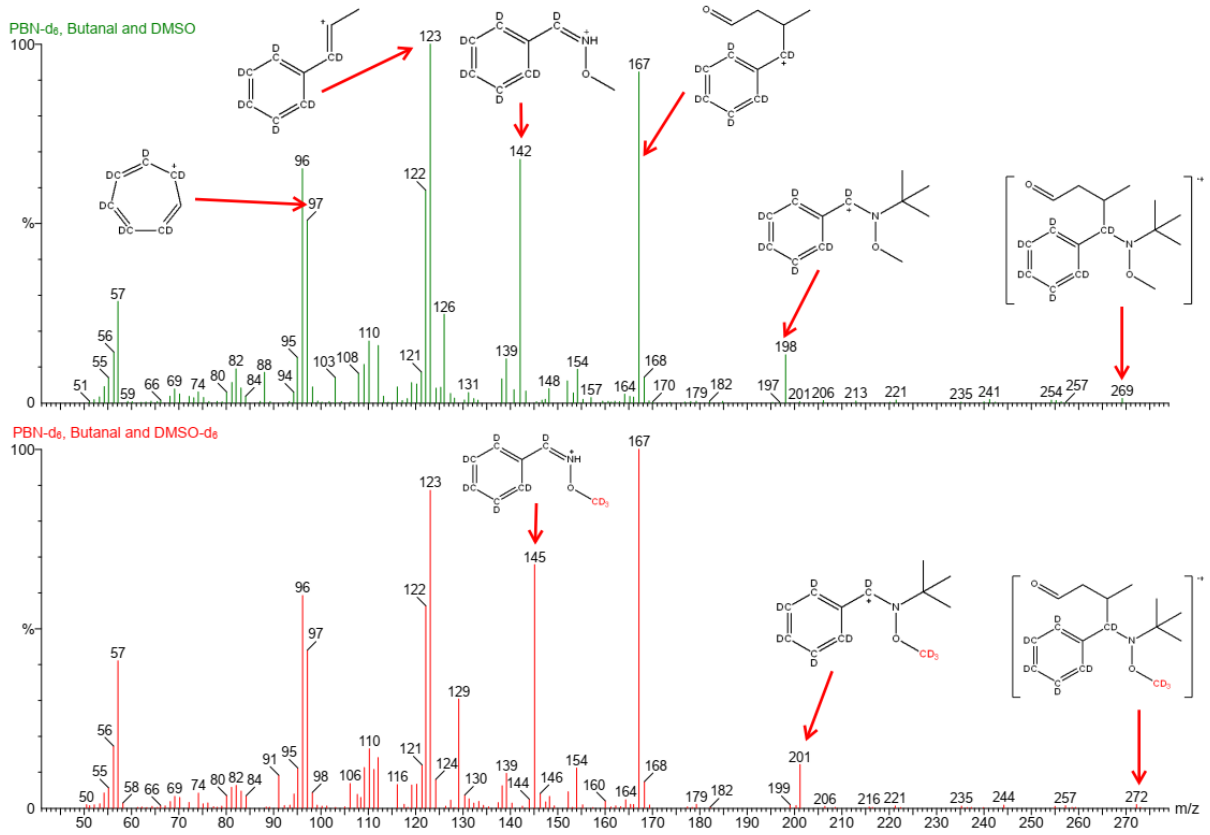

Figure 4.12.4 Electron Ionization mass spectra (EI-MS) corresponding to PBN adduct obtained from the analysis of the Fenton reaction mixture containing PBN-d_6, butanal and DMSO or DMSO-d_6 at rt 10.47 minutes

The EI mass spectra shown in Figure 4.12.4correspond to a) the PBN-d_6 mono-butanal mono-methyl adduct, PBN-d_6 (CH_3CHCH_2CHO)-CH_3) (top spectrum), and b) the PBN-d_6 mono-butanal mono-perdeuterated methyl-adduct, PBN-d_6-(CH_3CHCH_2CHO)($C\mathbf{D}_3$) (bottom spectrum)

When the Fenton reaction was carried out in the presence of DMSO as a competing secondary source of radicals, methyl radicals ($^{\bullet}CH_3$) were generated by the reaction of $^{\bullet}OH$ with DMSO and were then trapped by PBN-d_6. The peak at *m/z* 269 units corresponds to the molecular ion of PBN-d_6-Butanal-Me. The fragment at *m/z* 254 is the loss of a methyl group from the molecular ion (from the tBu group). The loss from the molecular ion of the butanal group from the alpha carbon position results in *m/z* 198 and further loss from this fragment of CH_2=CMe_2 gives *m/z* 142. The dissociation of the alpha carbon and nitrogen results in base peak *m/z* 167 (loss of a tBu methoxy azane group from the molecular ion) and further fragmentation (CH_3CHO group is lost) leads to *m/z* 123 with the identity 1-(phenyl-d_5)prop-1-en-2-ylium-

1-*d*. *m/z* 97 units is the tropylium ion, a phenyl-d_5 cation at *m/z* 82 and the peak at *m/z* 57 is the tertiary butyl cation

When the Fenton reaction was carried out in the presence of deuterated DMSO as a competing secondary source of radicals deuterated methyl radicals ($^{\bullet}CD_3$) were generated by the reaction of $^{\bullet}OH$ with DMSO and were then trapped by PBN-d_6. Replacing DMSO with d_6-DMSO in the Fenton-based reaction mixture gives rise to an increase in the *m/z* value of the molecular ion of 3 *m/z* units. The peak at *m/z* 272 units corresponds to the molecular ion of PBN-d_6-Butanal-Me. The fragment at *m/z* 257 is the loss of a methyl group from the molecular ion (from the tBu group). The loss from the molecular ion of the butanal group from the alpha carbon position results in *m/z* 201 and further loss from this fragment of CH_2=CMe_2 gives *m/z* 145. The dissociation of the alpha carbon and nitrogen results in *m/z* 167 (loss of a tBu methoxy azane group from the molecular ion) and further fragmentation (CH_3CHO group is lost) leads to *m/z* 123 with the identity 1-(phenyl-d_5)prop-1-en-2-ylium-1-*d*. Further breakdown of this fragment results in the peak *m/z* 97 tropylium cation. The peak at *m/z* 57 is the tertiary butyl cation

4.12.5 Mono oxybutyl monomethyl adduct of PBN-d_6 with butanal-d_2 and DMSO (compound 12)

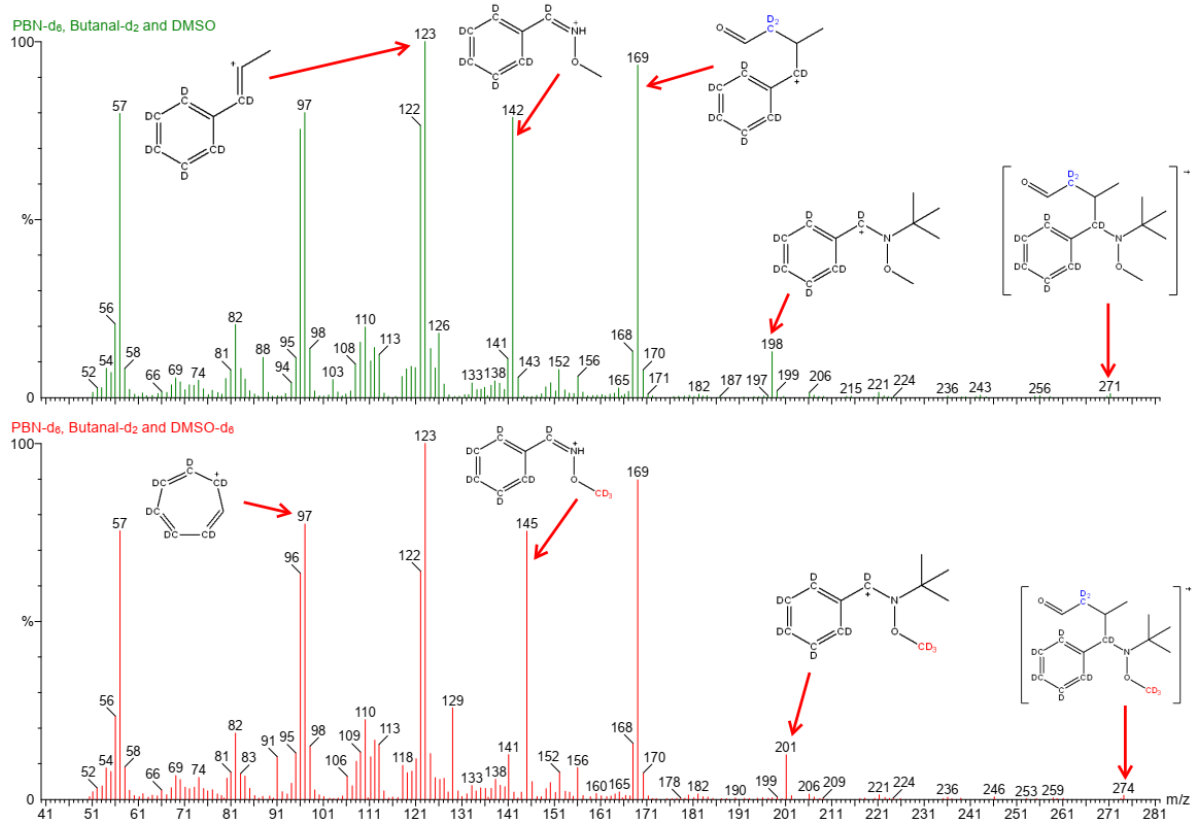

Figure 4.12.5 Electron Ionization mass spectra (EI-MS) corresponding to PBN adduct obtained from the analysis of the Fenton reaction mixture containing PBN-d_6, butanal-d_2 and DMSO or DMSO-d_6 at rt 10.47 minutes

The EI mass spectra shown in Figure 4.12.5 correspond to a) the PBN-d_6 mono-butanal mono-methyl adduct, PBN-d_6 ($CH_3CHC\mathbf{D}_2CHO$)-CH_3) (top spectrum), and b) the PBN-d_6 mono-butanal mono-perdeuterated methyl-adduct, PBN-d_6-($CH_3CHC\mathbf{D}_2CHO$)($C\mathbf{D}_3$) (bottom spectrum)

When the Fenton reaction was carried out in the presence of DMSO as a competing secondary source of radicals, methyl radicals ($^{\bullet}CH_3$) were generated by the reaction of $^{\bullet}OH$ with DMSO and were then trapped by PBN-d_6. The peak at *m/z* 271 units corresponds to the molecular ion of PBN-d_6-Butanal-Me. The fragment at *m/z* 256 is the loss of a methyl group from the molecular ion (from the tBu group). The loss from the molecular ion of the butanal group from the alpha carbon position results in *m/z* 198 and further loss from this fragment of CH_2=CMe_2 gives *m/z* 142. The dissociation of the alpha carbon and nitrogen results in peak *m/z* 169 (loss of a tBu methoxy azane group from the molecular ion) and further fragmentation (CH_3CHO group is lost) leads to *m/z* 123 with the identity 1-(phenyl-d_5)prop-1-en-2-ylium-

1-*d*. *m/z* 97 units is the tropylium ion, a phenyl-d_5 cation at *m/z* 82 and the peak at *m/z* 57 is the tertiary butyl cation

When the Fenton reaction was carried out in the presence of deuterated DMSO as a competing secondary source of radicals deuterated methyl radicals ($^{\bullet}CD_3$) were generated by the reaction of $^{\bullet}OH$ with DMSO and were then trapped by PBN-d_6. Replacing DMSO with d_6-DMSO in the Fenton-based reaction mixture gives rise to an increase in the *m/z* value of the molecular ion of 3 *m/z* units. The peak at *m/z* 272 units corresponds to the molecular ion of PBN-d_6-Butanal-Me. The fragment at *m/z* 257 is the loss of a methyl group from the molecular ion (from the tBu group). The loss from the molecular ion of the butanal group from the alpha carbon position results in *m/z* 201 and further loss from this fragment of CH_2=CMe_2 gives *m/z* 145. The dissociation of the alpha carbon and nitrogen results in *m/z* 167 (loss of a tBu methoxy azane group from the molecular ion) and further fragmentation (CH_3CHO group is lost) leads to *m/z* 123 with the identity 1-(phenyl-d_5)prop-1-en-2-ylium-1-*d*. Further breakdown of this fragment results in the peak *m/z* 97 tropylium cation. The peak at *m/z* 57 is the tertiary butyl cation

4.12.6 Mono oxybutyl monomethyl adduct of PBN-d_6 with butanal-$d_7$and DMSO (compound 12)

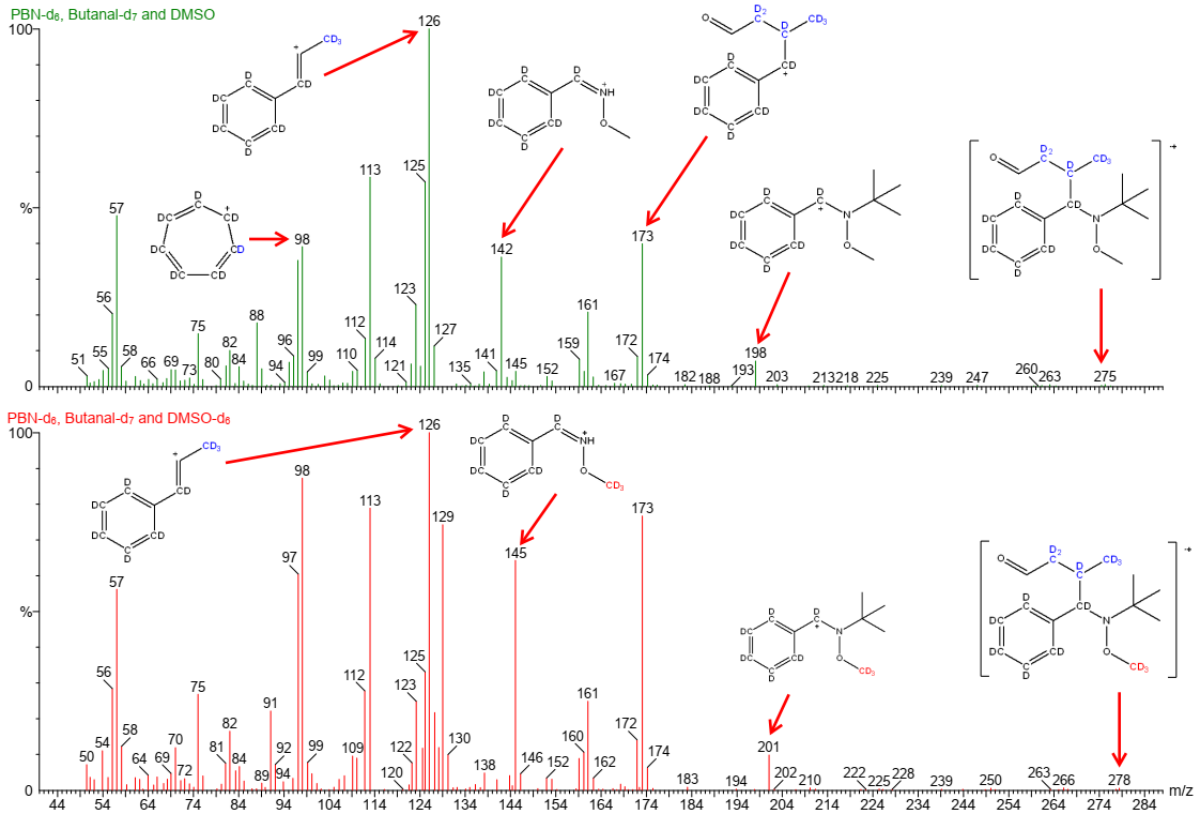

Figure 4.12.6 Electron Ionization mass spectra (EI-MS) corresponding to PBN adduct obtained from the analysis of the Fenton reaction mixture containing PBN-d_6, butanal-d_7 and DMSO or DMSO-d_6 at rt 10.47 minutes

The EI mass spectra shown in Figure 4.12.6 correspond to a) the PBN-d_6 mono-butanal mono-methyl adduct, PBN-d_6 (CH_3CHCD_2CHO)-CH_3) (top spectrum), and b) the PBN-d_6 mono-butanal mono-perdeuterated methyl-adduct, PBN-d_6-(CH_3CHCD_2CHO)(CD_3) (bottom spectrum)

When the Fenton reaction was carried out in the presence of DMSO as a competing secondary source of radicals, methyl radicals ($^{\bullet}CH_3$) were generated by the reaction of $^{\bullet}OH$ with DMSO and were then trapped by PBN-d_6. The peak at *m/z* 271 units corresponds to the molecular ion of PBN-d_6-Butanal-Me. The fragment at *m/z* 256 is the loss of a methyl group from the molecular ion (from the tBu group). The loss from the molecular ion of the butanal group from the alpha carbon position results in *m/z* 198 and further loss from this fragment of CH_2=CMe_2 gives *m/z* 142. The dissociation of the alpha carbon and nitrogen results in peak *m/z* 169 (loss of a tBu methoxy azane group from the molecular ion) and further fragmentation (CH_3CHO group is lost) leads to *m/z* 123 with the identity 1-(phenyl-d_5)prop-1-en-2-ylium-

1-*d*. *m/z* 97 units is the tropylium ion, a phenyl-d_5 cation at *m/z* 82 and the peak at *m/z* 57 is the tertiary butyl cation

When the Fenton reaction was carried out in the presence of deuterated DMSO as a competing secondary source of radicals deuterated methyl radicals ($^{\bullet}CD_3$) were generated by the reaction of $^{\bullet}OH$ with DMSO and were then trapped by PBN-d_6. Replacing DMSO with d_6-DMSO in the Fenton-based reaction mixture gives rise to an increase in the *m/z* value of the molecular ion of 3 *m/z* units. The peak at *m/z* 272 units corresponds to the molecular ion of PBN-d_6-Butanal-Me. The fragment at *m/z* 257 is the loss of a methyl group from the molecular ion (from the tBu group). The loss from the molecular ion of the butanal group from the alpha carbon position results in *m/z* 201 and further loss from this fragment of CH_2=CMe_2 gives *m/z* 145. The dissociation of the alpha carbon and nitrogen results in *m/z* 167 (loss of a tBu methoxy azane group from the molecular ion) and further fragmentation (CH_3CHO group is lost) leads to *m/z* 123 with the identity 1-(phenyl-d_5)prop-1-en-2-ylium-1-*d*. Further breakdown of this fragment results in the peak *m/z* 97 tropylium cation. The peak at *m/z* 57 is the tertiary butyl cation

4.13 Miscellaneous peaks

4.13.1 Chromatographic peak at 6.72 minutes

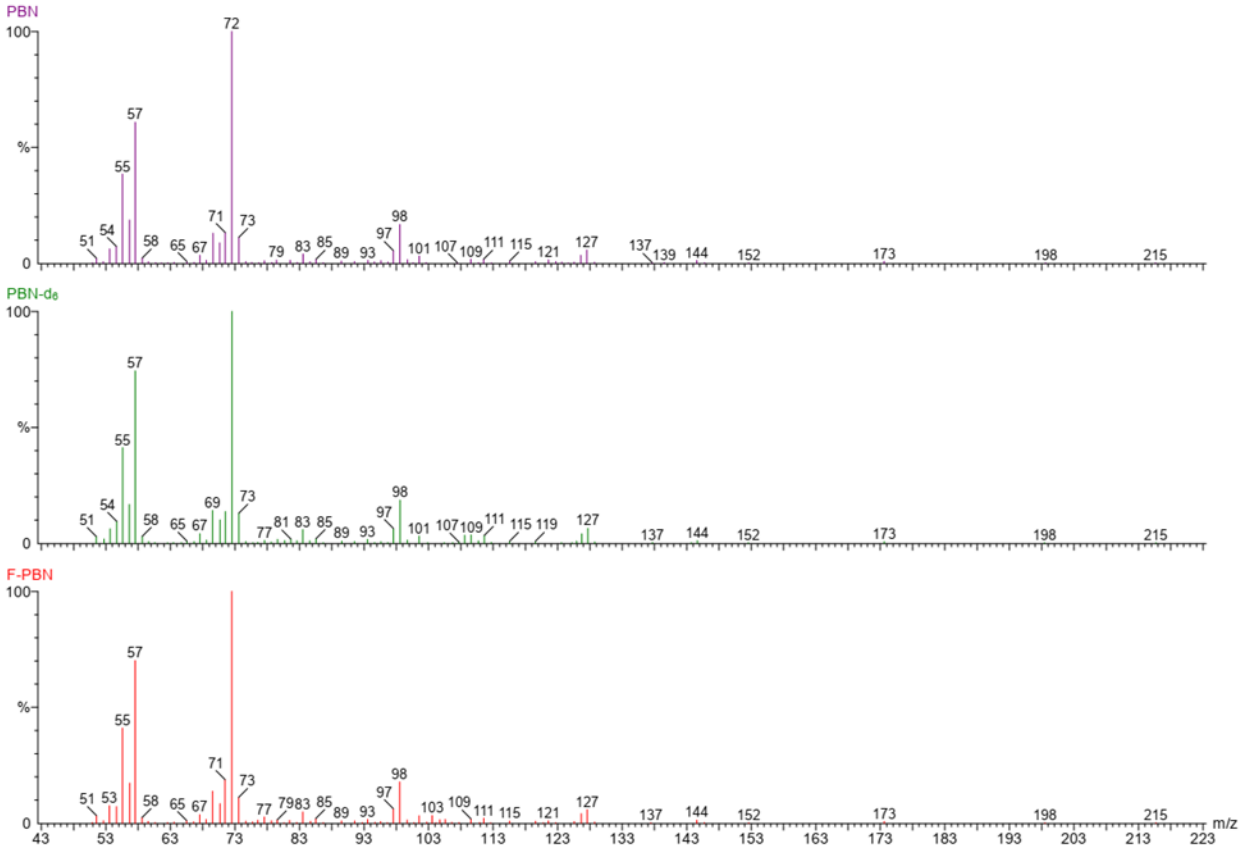

Figure 4.13.1 Electron Ionization mass spectra (EI-MS) corresponding to compound obtained from the analysis of the Fenton reaction mixture containing PBN and butanal (top spectrum), PBN-d_6 and butanal (middle spectrum) and F-PBN and butanal (bottom spectrum) at rt 6.72 minutes

The EI mass spectra in Figure 4.13.1 shows the identity of the compound obtained at rt 6.72 minutes. The interpretation of these spectra show that the molecular ion is at *m/z* 215 regardless of the spin trap used. Other key ions in common include *m/z* 173, *m/z* 127, *m/z* 98, *m/z* 72, *m/z* 57 and *m/z* 55. This demonstrates that the compound does not include any PBN derivative and therefore is not originating from the Fenton reaction This peak was also seen in the control experiments where no hydrogen peroxide and iron were added (see section 2.7).

4.14 Discussion

4.14.1 Discussion of compounds 3 and 5 (di propyl and mono propyl)

The aim of this series of experiments was to trap the free radicals generated from butanal by using Fenton chemistry as described in section 2.3.2. butanal was used as a secondary source of free radicals, derived from hydroxyl radicals produced in the Fenton system. PBN and its derivatives were used as trapping agents to form stable adducts that could be analysed via GCMS and identify free radicals generated when the hydroxyl radical reacts with butanal.

Six new peaks were observed when the Fenton reaction was run in the presence of butanal as a secondary source of radicals (Figure 4.1.1) compared to control reactions, and three additional peaks were observed when DMSO was added as a competitive secondary source of radicals (Figure 4.8.1). The resulting adducts have been identified in the previous sections. The chromatogram (Figure 3.1.1) shows the Fenton reaction in the absence of a secondary sources of radicals confirming that the peaks are derived from the inclusion of butanal

The TIC of the chloroform extracted from the Fenton mixture containing butanal (Figure 4.1.1) shows various peaks that are generated, that are not present when in the absence of butanal (Figure 3.1.1). On comparison it was found that compounds at peaks 3,5,6,7,8 and 9 were generated from the butanal containing reaction mixture as these peaks were not present in the reaction mixture where butanal was absent. The broad peak (Peak 1 retained at 3.69 minutes) is the benzaldehyde oxime and is seen in control experiments in the absence of Fe^{2+} or hydrogen peroxide (see chapter 3) with a characteristic peak of 77 *m/z* indicating the presence of the phenyl cation and molecular ion fragment peak at *m/z* 121 It appears to be two overlapping peaks with one of the compounds having an EI-MS spectral pattern consistent with benzaldehyde oxime and the other with trimethylsilyl ether (Castro *et al*., 1998). Trimethylsilyl ether has a molecular ion at *m/z* 161. The peak (2) retained at 8.12 minutes is for unreacted PBN as this peak is also present in the control experiment, with a strong molecular ion at *m/z* 177 and characteristic fragment peaks at *m/z* 161, 146, 77 and a strong base peak at *m/z* 121. *m/z* 57 is also a characteristic peak for PBN as mentioned by Janzen and DuBose (Janzen and DuBose, 1993). The deuterated unreacted PBN-d6 is retained at 8.09 minutes with the molecular ion at *m/z*183 and key ions include *m/z* 167, 152, 127, 82 and a strong base peak at *m/z* 127

4.14.2 Analysis of spin trapped propyl radical from butanal

The chromatogram in Figure 4.1.1 shows several peaks which are absent when no butanal was used as a secondary source of radicals (Figure 3.1.1) confirming them as products of the Fenton reaction in the presence of butanal as a secondary source of radicals. The intense peak (peak 3, Figure 4.1.1) at 8.51 minutes has been identified as a dipropyl adduct of PBN(PBN-$Prop_2$). The formation of the di-propyl adduct of PBN is a two-step process. The first step involves trapping the propyl radical at the alpha carbon turning the molecule into a nitroxide, then another propyl is trapped on the oxygen, generating a stable non radical adduct

4.14.3 Discussing the dipropyl adduct

To confirm whether butanal was the source of the radicals, deuterated isotope labelled analogues of butanal were used. dideutero-propyl radicals were generated from butanal-2,2-d_2 ($^{\bullet}CD_2CH_2CH_3$) and perdeutero-propyl radicals ($^{\bullet}CD_2CD_2CD_3$) from butanal-2,2,3,3,4,4,4-d_7 and these were trapped by PBN showing a shift in the mass spectrum of 4 *m/z* units and 14 *m/z* units respectively indicating that the radicals were formed of the deuterated radicals. The Table 4.7 shows the dipropyl adducts from different PBN derivatives and butanal isotopic isoforms with significant ions.

Table 4.7 dipropyl adducts from different PBN derivatives and butanal isotopic isoforms

Fenton system	Compound name or formula	$M^{+\bullet}$ (m/z)	other significant ions (*m/z*)
PBN + Butanal	PBN-$(CH_2CH_2CH_3)_2$	**263**	248, 220, 164, 133 (bp), 91, 77, 57
PBN + Butanal-d_2	PBN-$(CD_2CH_2CH_3)_2$	**267**	252, 222, 166, 135 (bp), 91, 77, 57
PBN + Butanal-d_7	PBN-$(CD_2CD_2CD_3)_2$	**277**	262, 227, 171, 140 (bp), 92, 77, 57
PBN-d_6+ Butanal	PBN-d_6-$(CH_2CH_2CH_3)_2$	**269**	254, 226, 170, 139 (bp), 97, 82, 57
PBN-d_6+ Butanal-d_2	PBN-d6-$(CD_2CH_2CH_3)_2$	**273**	258, 228, 172, 141 , 97(bp), 82, 57
PBN-d_6+ Butanal-d_7	PBN-d6-$(CD_2CD_2CD_3)_2$	**283**	268, 233,177, 146 (bp), 98, 82, 57
F-PBN + Butanal	F-PBN-$(CH_2CH_2CH_3)_2$	**281**	266, 238, 182, 151 (bp), 109, 95, 57
F-PBN + Butanal-d_2	F-PBN-$(CD_2CH_2CH_3)_2$	**285**	270, 240, 184, 153 (bp), 109, 95, 57
F-PBN + Butanal-d_7	F-PBN-$(CD_2CD_2CD_3)_2$	**295**	280, 245, 189, 158 (bp),109 ,95,57

The mass spectrum Figure 4.2.1 shows the molecular ion is *m/z* 263 where butanal is used, *m/z* 267 where butanal-d_2 is used (an increase of 4 *m/z* units) and *m/z* 277 where butanal-d_7 us used (an increase of 14 *m/z* units). The identity of the adduct is clearly demonstrated by use of the deuterated analogues to generate deuterated propyl radicals that have added to PBN. The fragment pattern of the molecular ion

also demonstrates where the adducts have added. The base peak at *m/z* 133 where butanal is used (Figure 4.2.1) identified as a butylbenzene cation, has retained one of the propyl adducts on the alpha carbon, thus *m/z* 133 becomes *m/z* 135 where butanal-d_2 is used (showing 2 deuterium are retained) and becomes *m/z* 140 where butanal-d_7 is used (showing 7 deuterium are retained).

Further evidence of the di-propyl adduct formation can be seen in Figure 4.2.2 where PBN is replaced by its deuterated analogue PBN-d_6 where the 5 hydrogens of the aromatic ring and the hydrogen on the alpha carbon have been replaced with deuterium atoms. The molecular ion is *m/z* 269 where butanal is used, *m/z* 273 where butanal-d_2 is used and *m/z* 283 where butanal-d_7 is used. The base peak (butyl-1-d benzene-2,3,4,5,6-d_5 cation) is replaced with *m/z* 139 (where butanal is used), *m/z* 141 (where butanal-d_2 is used) and *m/z* 146 (where butanal d_7 is used) indicating that the adducts have not attached to the aromatic ring and have done so on the alpha carbon. Any radical attack of the phenyl ring can be ruled out by the use of the PBN-d_6 as an increase of anything other than 6 *m/z* units would indicate the involvement of the phenyl ring.

The mass spectrum in Figure 4.2.1 (top spectrum) shows the molecular ion at *m/z* 263 which loses a methyl radical to become *m/z* 248. This is typical of the loss of the methyl from the tertiary butyl group (tBu) as this can also be seen where butanal was replaced with its deuterated analogues. In order to confirm the origins of the methyl (M-15) deuterated analogues replaced butanal. Where butanal-d_2 was used Figure 4.2.1 (middle spectrum) the *m/z* 248 becomes *m/z* 252 and where butanal-d_7 was used Figure 4.2.1 (bottom spectrum) *m/z* 248 becomes *m/z* 262, a loss of M-15 for all three conditions, clearly demonstrating that the M-15 fragment is not derived from the deuterated analogues and therefore originates in the tBu. This observation has been reported previously by Janzen *et al*., (1995)

PBN spin adducts usually produce an abundant fragment by EI, namely, *m/z* 57 ($C_4H_9^+$), the tertiary butyl group. This fragment can be lost as a tertiary butyl cation (M-57) or alternatively undergo an internal hydrogen transfers via a McLafferty-like rearrangement where one of the hydrogens is added to the oxygen and the resultant loss of an isobutylene (M-56) (Janzen *et al*., 1995).

A scheme is presented in Figure 4.14.1 showing the mechanism for the formation of the propyl radical, the formation of the nitroxide and the final 1,3-dipropyl adduct.

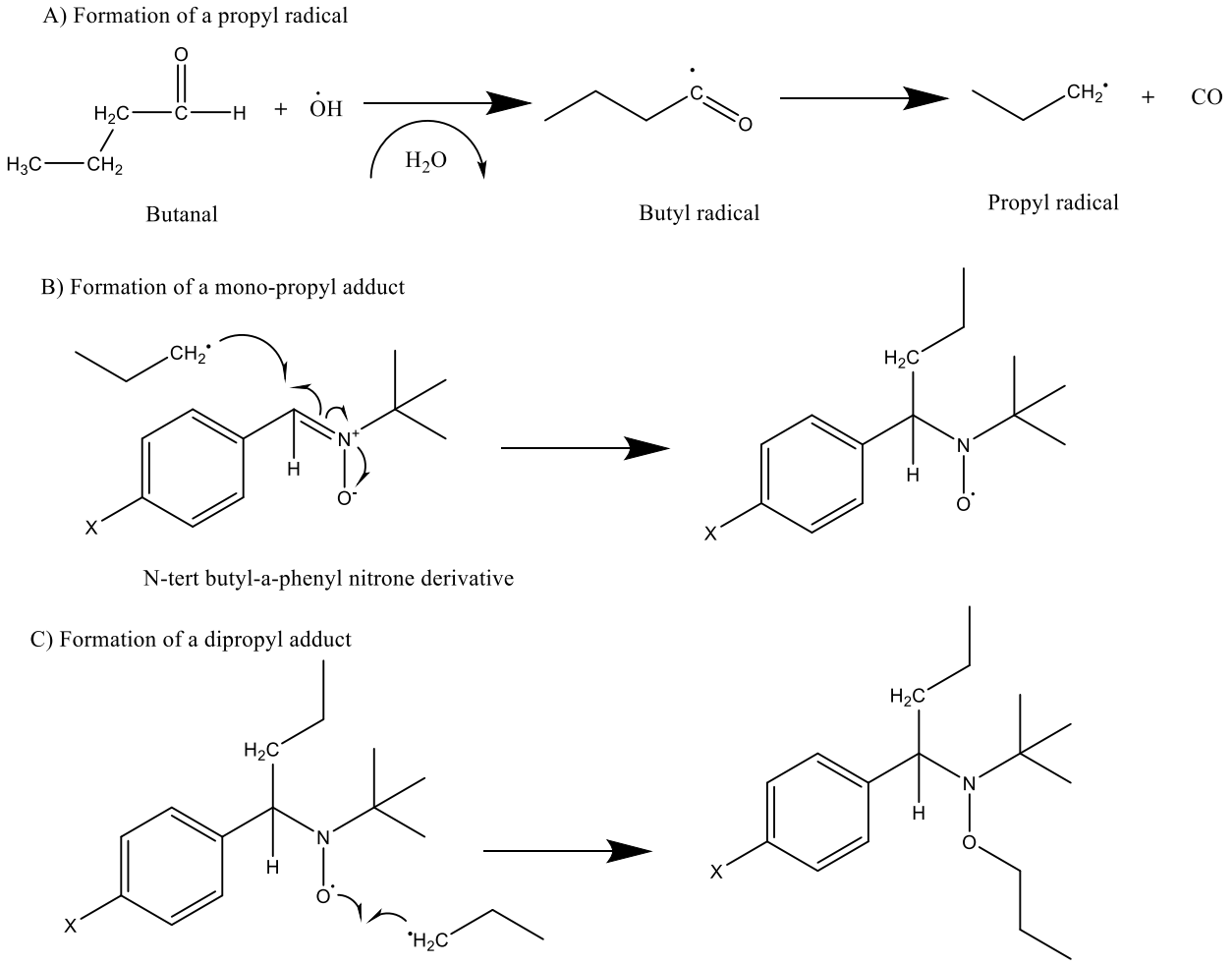

Figure 4.14.1 Schematic representation for (A) formation of the propyl radical from butanal through the Fenton mechanism, (B) the propyl radical is trapped by PBN at the α carbon site to form a monopropyl PBN derivative adduct, (C) the second propyl radical is added to the oxygen site of the monopropyl to form a dipropyl PBN derivative adduct (adapted from Janzen et al., 1985).

4.14.4 Discussing the butanal radical adducts

Compounds 6,7 8 and 12 are formed by a butanal radical (oxo-butyl) adding to the alpha carbon of the spin trap and compound 9 is formed by a butanal adding to the oxygen site of the spin trap. In a study by Gupta and Rajakumar, (2020) various reaction sites involved in the reaction of butanal were identified (see Figure 4.14.2) from where hydrogen could be abstracted by hydroxyl radicals to form a oxobutyl radical. It was reported that the most stable radical to least stable radical is in the order 1-oxo-1-butyl (butanoyl) > 1-oxo-2-butyl > 1-oxo-3-butyl > 1-oxo-4-butyl radical, suggesting that a radical is more likely to react in the inverse order to form an adduct with PBN.

Further support for this is provided in a study by Papajak *et al*., (2012) where thermodynamic properties of radicals formed by the abstraction of hydrogen were analysed and it was reported that 4 possible conformations of the butanal radical are possible. The relative stability of the butanal radicals was computed based on lowest free energy and it was found to decrease in the order butanoyl > 1-oxo-2-butyl > 1-oxo-3-butyl > 1-oxo-4-butyl radical.

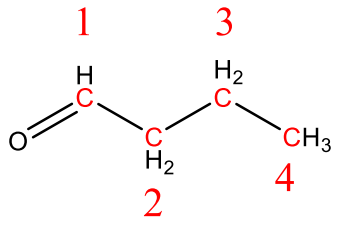

Figure 4.14.2 Potential sites where a radical can form on butanal (hydrogen abstraction sites highlighted in red)(adapted from Gupta and Rajakumar, 2020)

Of the four possible radicals that are postulated, two are likely candidates for forming radical adducts based on observed characteristics. The possible candidates are discussed below.

The existence of a 1-oxo-4-butyl radical is postulated. This radical adds to the alpha carbon of compound 5 and 6. When the C=N bond of compound 5 and 6 dissociates, the formation of the fragment 5-phenyl pentanal cation (5-oxo-1-phenylpentan-1-ylium) at *m/z* 161 is formed (also *m/z* 163 when butanal-d_2 is used and, *m/z* 167 when butanal-d_7 is used) confirming that the butanal radical has added there, and by the absence of the fragment at *m/z* 117 (*m/z* 120 when butanal-d_7 is used) indicating there is no formation of 1-phenylprop-1-en-2-ylium.

The existence of a 1-oxo-3-butyl radical is postulated. This radical adds to the alpha carbon of compounds 7 and 12. When the C=N bond of compound 7 and 12 dissociates, the formation of the fragment 3-methyl-4-phenyl butanal cation (2-methyl-4-oxo-1-phenylbutan-1-ylium) at *m/z* 161 is formed (see Figure 4.14.3) also *m/z* 163 when butanal-d_2 is used and, *m/z* 167 when butanal-d_7 is used), however further fragmentation generates a fragment at *m/z* 117 (*m/z* 120 when butanal-d_7 is used) which has the identity 1-phenylprop-1-en-2-ylium and the identity 1-phenylprop-1-en-2-ylium-3,3,3-d_3, when butanal-d_7 is used.

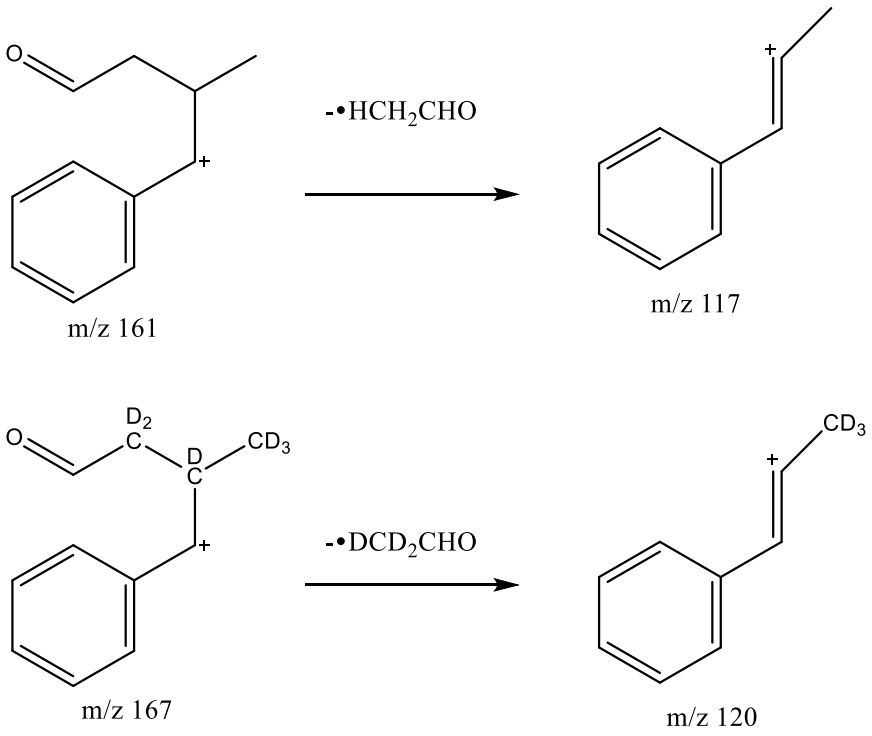

Figure 4.14.3 The fragmentation of 3-methyl-4-phenyl butanal to form 1-phenylprop-1-en-2-ylium (top scheme) and the deuterated aspect (below)

4.14.5 Discussing the monopropyl monomethyl adduct (compound 10 and 11)

Compounds 10 and 11 are diastereomers where the methyl is on the alpha carbon and the propyl is on the oxygen for 10, and for 11 the propyl is on the alpha carbon and the methyl radical on the oxygen site. The diastereomers have the exact same retention time coincidentally however on closer inspection a 'shoulder' is visible on the right side of the peak (peak 10+11, Figure 4.8.1), and it is not as sharp as other peaks on the chromatogram indicating that there are two peaks. As a result, the spectra for these compounds are overlayed and impossible to separate where fragmentation patterns for both compounds appear side by side. As the molecules are diastereomers the product ion is the same for both species. The formation of a PBN monopropyl-monomethyl adduct {PBN($CH_2CH_2CH_3$)(CH_3)} adduct is a two-step mechanism by which either the propyl/methyl radical is trapped at the α-carbon site initially and then adding to the oxygen site. This results in two different adducts with the same molecular weight yet differing fragmentation patterns.

To confirm whether there are two different spin adducts in peak 10+11, the alpha carbon site of the spin trap has been employed by analysing the fragments derived when breaking the C-N bond of the molecular ions. In particular, the dissociation of the C-N bond that results in an ethyl benzene fragment (*m/z* 105) where a methyl has added to the alpha carbon and alternatively a butyl benzene fragment (*m/z* 133) results where a propyl has added to the alpha carbon.

Additionally, to confirm the identity of the butyl benzene cation, the source of the propyl radicals (deuterated butanal-d_2 and butanal-d_7) was utilised to form isotopologues that were employed in the Fenton system to generate deuterated propyl radicals ($^{\bullet}CD_2CH_2CH_3$, $^{\bullet}CD_2CD_2CD_3$, respectively) increasing the *m/z* of the *m/z* 133 fragment by 2 units and 7 units respectively, conclusively demonstrating the origin of the radicals (Figure 4.11.1, Figure 4.11.2, Figure 4.11.3)

To confirm the source of the methyl radical, deuterated DMSO-d_6 was employed generating deuteron methyl radicals ($^{\bullet}CD_3$) increasing the *m/z* of the *m/z* 105 by 3 units conclusively showing where the methyl originated from (Figure 4.11.1).

The fragmentation pattern is given in Figure 4.14.4 and Figure 4.14.5

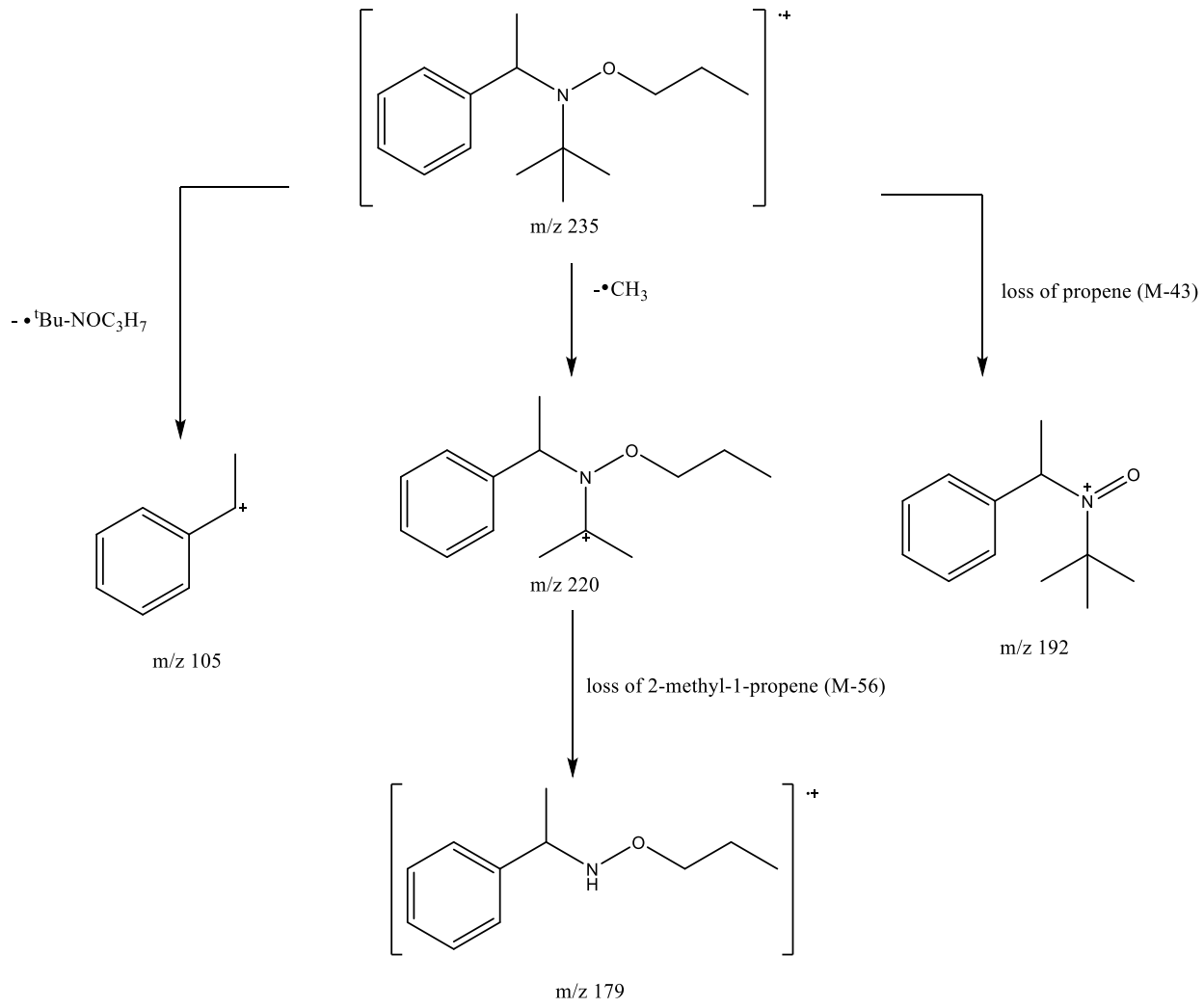

Figure 4.14.4 Fragmentation pattern of the PBN monomethyl monopropyl adduct (adduct 10)

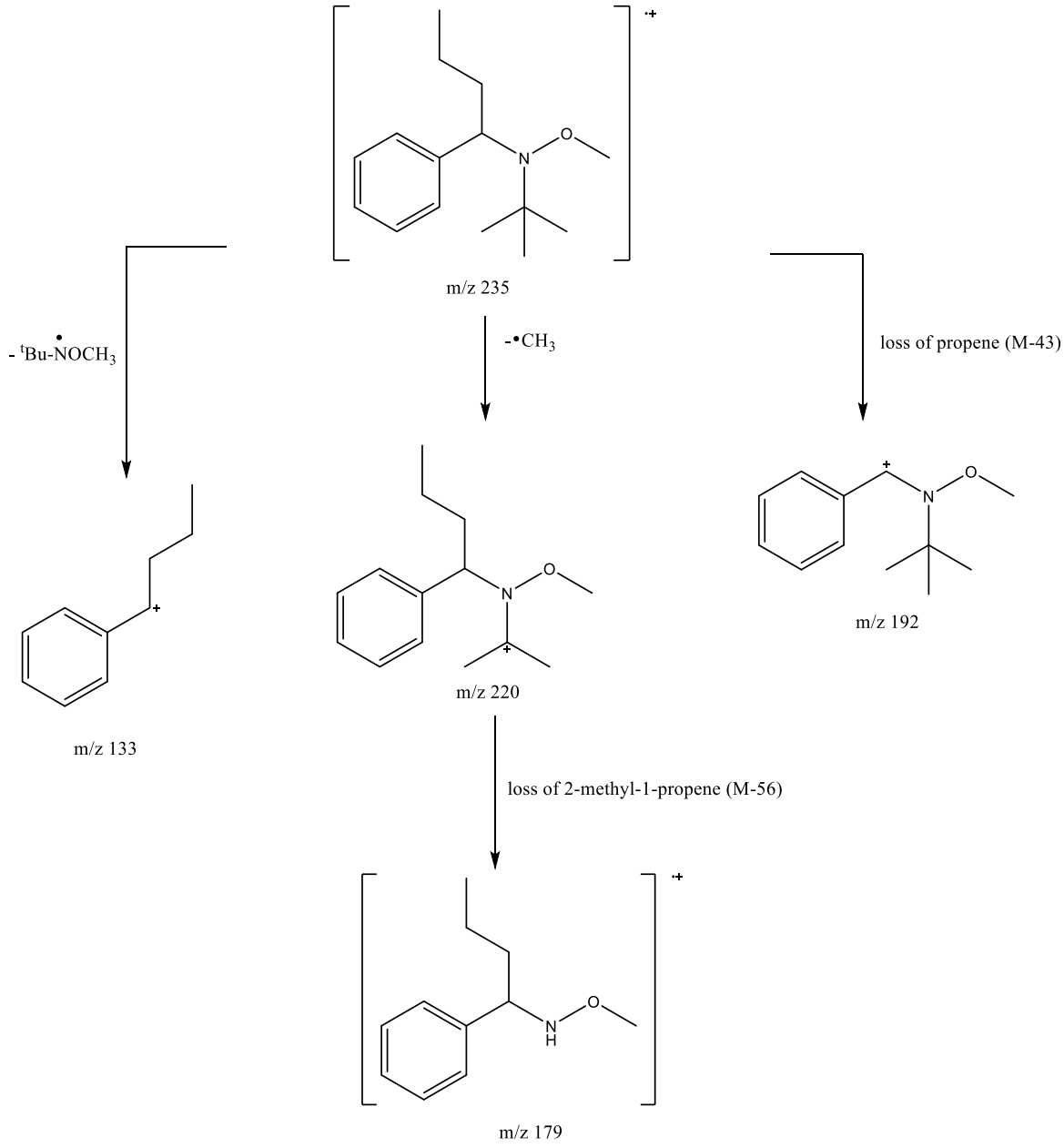

Figure 4.14.5 Fragmentation pattern of the PBN monopropyl monomethyl adduct (adduct 11)

4.14.6 Discussing the dimethyl adduct (compound 10)

Compound 9 corresponds to the dimethyl adduct, PBN-$(CH_3)_2$, and is a result of DMSO acting as a secondary source of radicals generated by the reaction of $^{\bullet}OH$ with DMSO and subsequent capture by PBN. Identification was confirmed when DMSO was replaced with the deuterated analogue (DMSO-d_6). The spectrum (Figure 4.9.1, top) shows the peak at *m/z* 207 corresponding to the molecular ion of PBN-Me_2. The fragment at *m/z* 192 is the loss of a methyl group from the molecular ion (from the tBu group). The loss of CH_2=CMe_2 gives *m/z* 151 and the loss of a methyl group from this fragment results in *m/z* 136. The dissociation of the alpha carbon bond and the nitrogen gives the base peak *m/z* 105 and further breakdown of this fragment results in a phenyl cation at *m/z* 77. This EI spectrum has been observed in a previous study by Janzen *et al*., (1985) Replacing PBN with either PBN-d_6 or F-PBN results in an increase in *m/z* value of the molecular ion by 6 and 18 units respectively. Using deuterated DMSO (DMSO-d_6) leads to an increase of 6 *m/z* units in the spectrum, clearly demonstrating the incorporation of two deuteron methyl groups into the structure.

It is assumed the formation of the dimethyl adduct initially starts with a methyl radical adding to the alpha carbon of PBN forming a nitroxide (Figure 4.14.6), then a subsequent methyl adds to the oxygen site forming the di-adduct (Boyd and Boyd, 1994). Interestingly this nitroxide which is detected in EPR spectroscopy studies (Janzen and Lopp, 1972; Berliner, 2012) is not detected by GCMS as it is assumed to lack volatility to be detected or completely consumed by the methyl radicals to form the di-methyl adduct (Manzoor *et al*., 2020).

A scheme is presented for the formation of the methyl radical and the eventual formation of the 1,3-dimethyl adduct in Figure 4.14.6

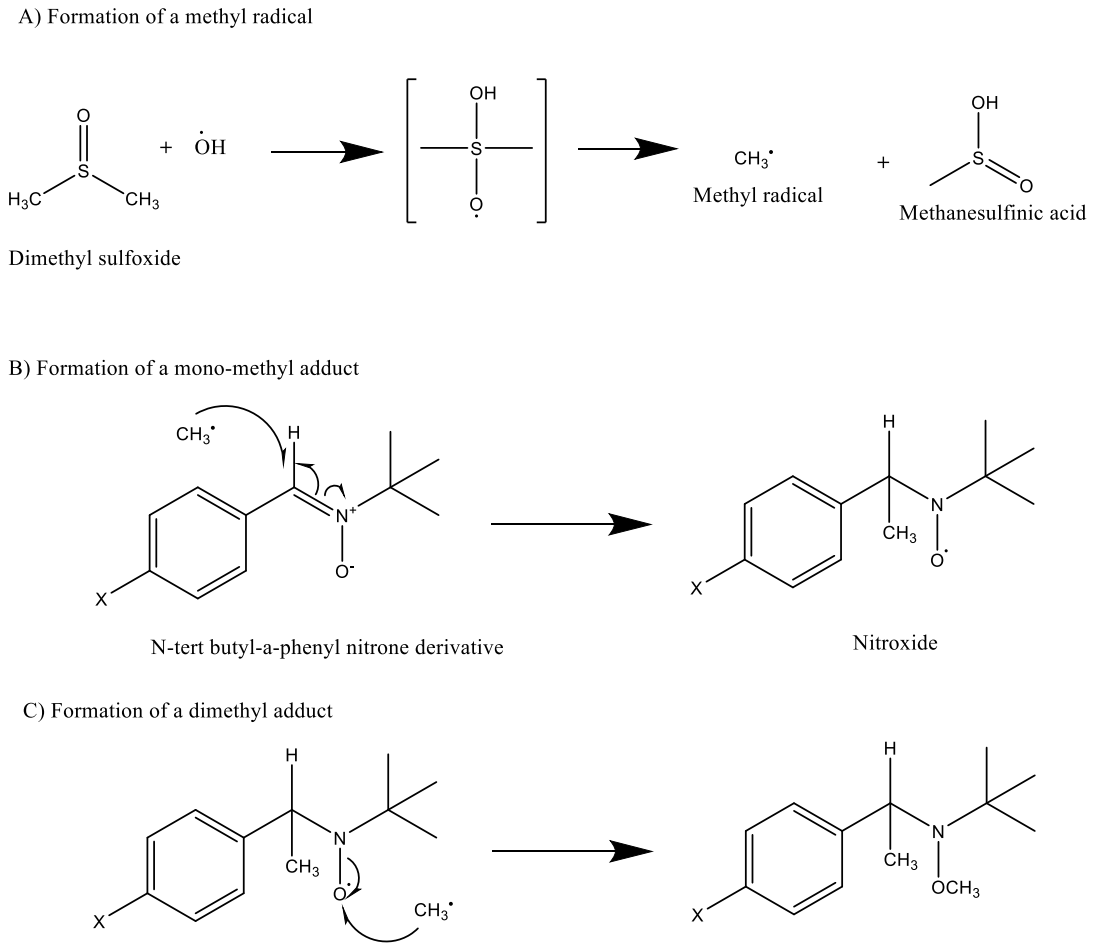

Figure 4.14.6 A) Formation of a methyl radical from DMSO; B)formation of a monomethyl nitroxide adduct; C) formation of the dimethyl adduct of PBN

4.14.8 Discussing the chirality of PBN diadducts

As mentioned previously PBN diadducts are chiral molecules with two stereochemical centres (see Figure 1.17.3). Unfortunately, little attention has been given to this subject in literature. To understand the adducts formed from PBN, one has to understand that PBN when in the nitroxide form or di-adduct form exhibits optical isomerism and is a chiral compound with multiple stereogenic sites as previously mentioned. The alpha carbon (see Figure 1.17.3,in red) when adducted to a species other than hydrogen is asymmetric due to 4 different species including hydrogen, the nitrogen, the phenyl group and the R group being investigated. The other chiral centre is the Nitrogen (see Figure 1.17.3,in blue) which exhibits optical isomerism due to the alpha carbon, the oxygen, the tertiary butyl group and a lone pair of electrons on the nitrogen. This allows PBN to have multiple stereometric configurations with the same molecular weight yet differing retention times. However, GC can separate diastereomers to an extent however more specialised methods such as CSP (none-racemic chiral stationary phase) are required to separate the enantiomers.

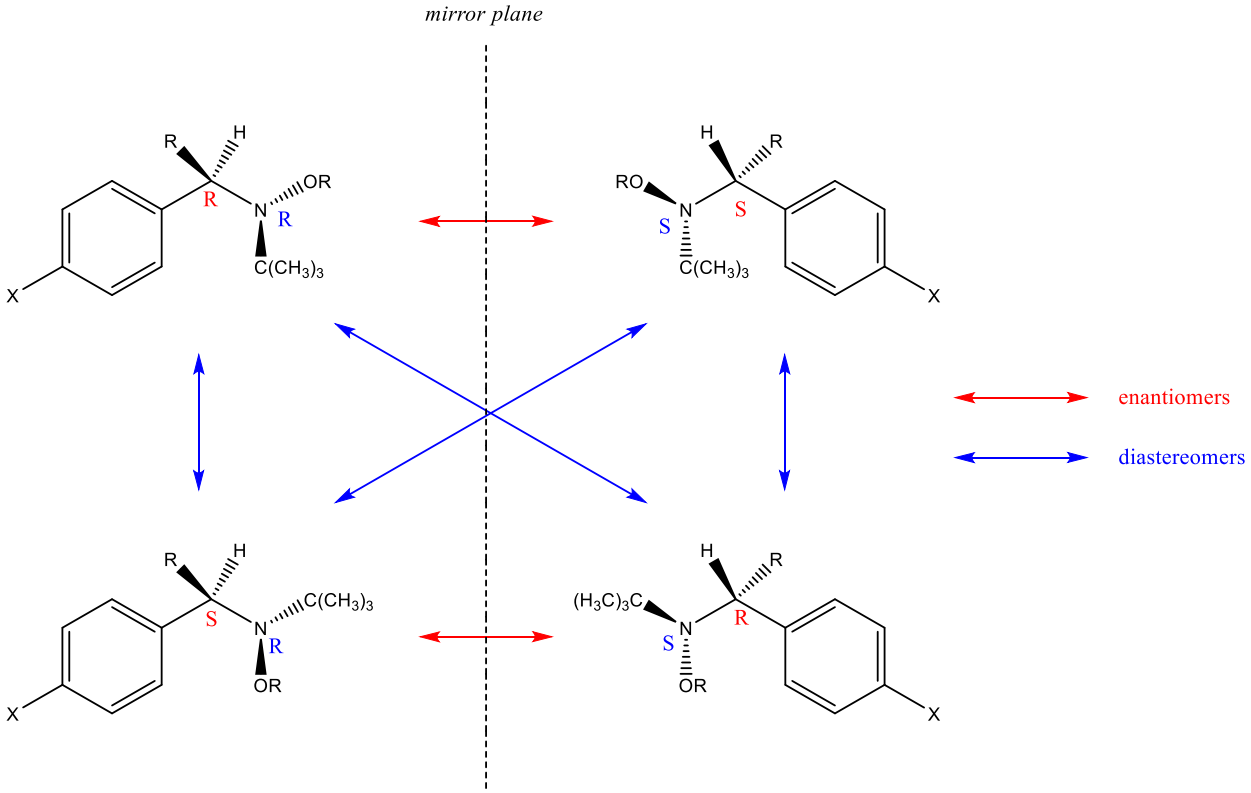

Figure 4.14.7 showing possible enantiomers and diastereomers adducts formed from PBN

4.14.9 Miscellaneous discussion

A crucial insight into the fragmentation patterns show the inadvertent hydrogen-deuterium exchange occurring in several spectra (see figure 4.4.1 and figure 4.5.1) where the deuterium is replacing hydrogen at the oxygen site. This is particularly relevant where the fragmentation leads to the benzaldehyde oxime formation where the deuterons present on the deuterated adduct replace hydrogen post fragmentation via an unknown rearrangement mechanism. Experiments where this is intentionally achieved usually supplement the solvent with D_2O (Englander *et al*., 1997) and is commonly applied in protein structure mass spectrometry to analyse the ligand binding capacity of proteins and dynamics (Konermann *et al*., 2011).

Chapter 5

5 Detection and analysis of spin-adducts from 3-methylbutanal and N-tert-butyl-a-phenyl nitrone (PBN) derivates using liquid injection gas chromatography-mass spectrometry

In this study, hydroxyl radicals generated from the Fenton chemistry have been used to generate alkyl radicals and alkoxy radicals from 3-methyl butanal and DMSO to produce 2-methyl propyl radicals ($^{\bullet}CH_2CH(CH_3)_2$), various acyl radicals (oxoallylic)($CH_3{}^{\bullet}C(CH_3)CH_2CHO$), and ($^{\bullet}CH_3$) radicals. These radicals were then trapped by PBN and its derivatives to form stable adducts and sampled using liquid-liquid extraction with chloroform as a solvent. The extracted samples were subjected to GC/MS for detection and analysis. Numerous PBN radical adducts were identified and characterised and will be discussed in the following chapter.

5.1 Chromatograms of spin trapping PBN derivatives and 3-methylbutanal

5.1.1 Fenton with PBN and 3-methylbutanal

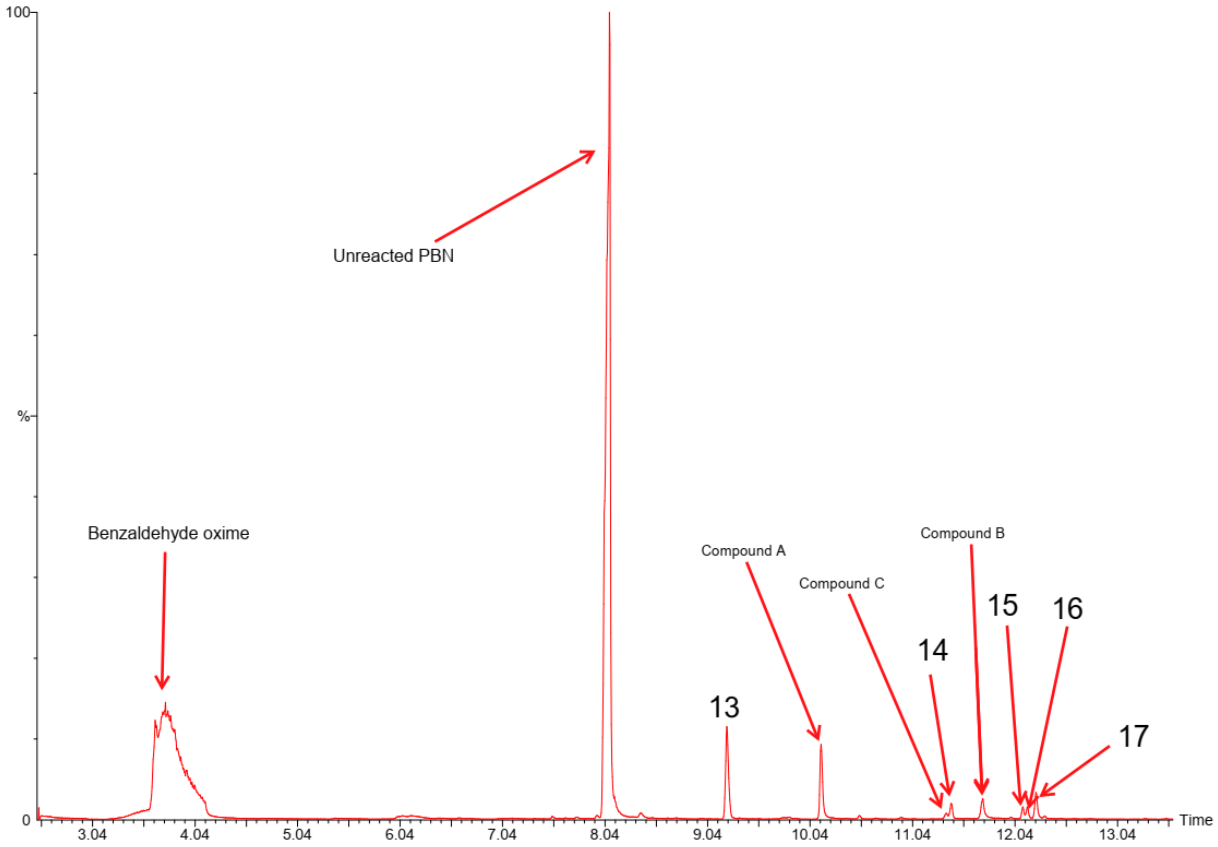

Figure 5.1.1 The total ion chromatogram obtained from the GC-MS analysis of the Fenton system with PBN in the presence of 3-methyl butanal

The TIC shown in Figure 5.1.1 obtained from the Fenton reaction of PBN and 3-methylbutanal extracted into chloroform shows 5 additional peaks. The peaks that are labelled have been assigned, as follows (see Figure 5.1.2): Peak 13 (rt 9.23) corresponds to a di-2-methyl propyl adduct of the spin trap { PBN-($CH_2CH(CH_3)_2)_2$}; Peak 14 (rt 11.41) give the impression of a mono(2-methyl)propyl PBN adduct trap { PBN-($CH_2CH(CH_3)_2$)}; Peak 15 (rt 12.10) PBN 3-methyl butanal radical and 2-methyl propyl radical adduct {PBN-($CH_3C(CH_3)CH_2CHO$)($CH_2CH(CH_3)_2$) }; Peak 16 (rt 12.15) appears to be an diastereomer of a 3-methyl butanal radical and 2-methyl propyl radical adduct of PBN { PBN-($CH_3C(CH_3)CH_2CHO$)($CH_2CH(CH_3)_2$)); Peak 17 (rt 12.23) is an enantiomer of PBN where the 2-methyl propyl radical and 3-methyl butanal radical have added to the alpha carbon and oxygen respectively { PBN-($CH_2CH(CH_3)_2$)($C(CH_3)_2CH_2CHO$)}.

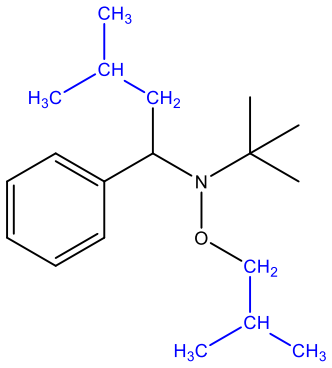

Compound 13 (peak 13)

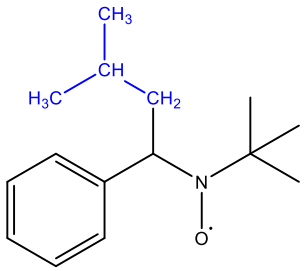

Compound 14 (peak 14)

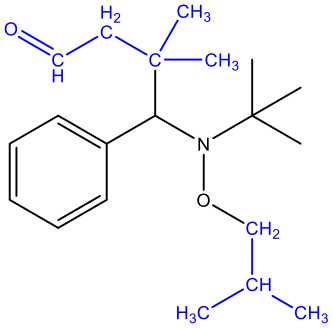

Compound 15 (peak 15)

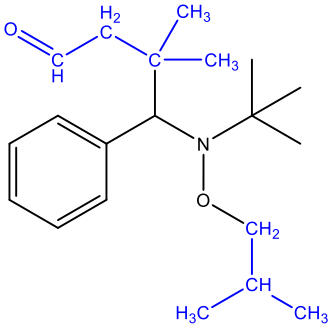

Compound 16 (peak 16)

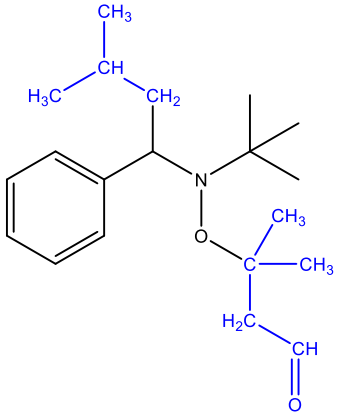

Compound 17 (peak 17)

Figure 5.1.2 The structures of compounds identified by GC-MS analysis of a Fenton-based reaction mixture containing PBN and 3-methyl butanal. The atoms in blue are believed to be derived from 3-methyl butanal

5.1.2 Fenton with PBN-d_6 and 3-methylbutanal

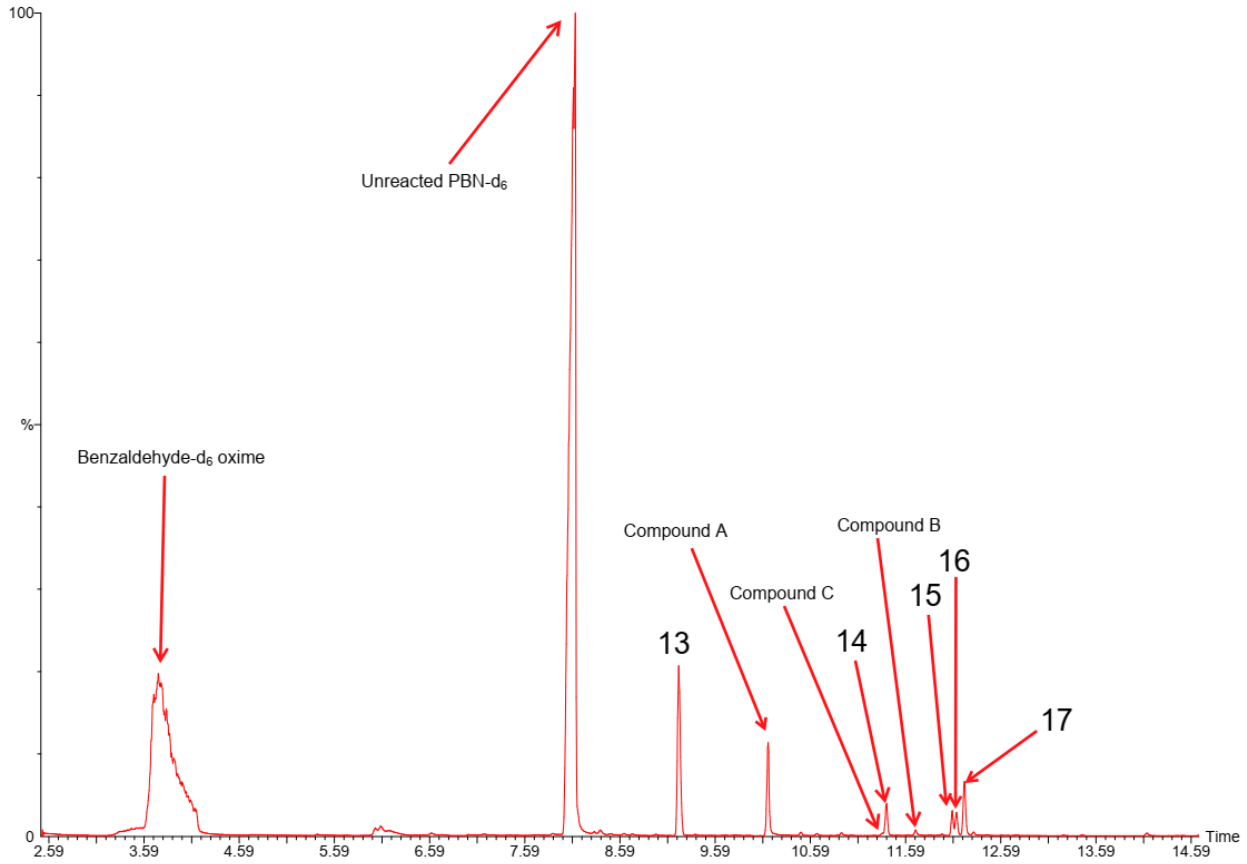

Figure 5.1.3 The total ion chromatogram obtained from the GC-MS analysis of the Fenton system with PBN-d_6 in the presence of 3-methyl butanal

The TIC shown in Figure 5.1.3 obtained from the Fenton reaction of PBN-d_6 and 3-methylbutanal extracted into chloroform shows 5 additional peaks. The peaks that are labelled have been assigned, as follows (Figure 5.1.4): Peak 13 (rt 9.23) corresponds to a di-2-methyl propyl adduct of the spin trap { PBN-d_6 -$(CH_2CH(CH_3)_2)_2$}; Peak 14 (rt 11.41) give the impression of a mono(2-methyl)propyl PBN-d_6 adduct trap { PBN-d_6 -$(CH_2CH(CH_3)_2)$}; Peak 15 (rt 12.10) PBN-d_6 3-methyl butanal radical and 2-methyl propyl radical adduct {PBN-d_6 -$(CH_3C(CH_3)CH_2CHO)(CH_2CH(CH_3)_2)$ }; Peak 16 (rt 12.15) appears to be an diastereomer of a 3-methyl butanal radical and 2-methyl propyl radical adduct of PBN-d_6 { PBN-d_6 -$(CH_3C(CH_3)CH_2CHO)(CH_2CH(CH_3)_2)$); Peak 17 (rt 12.23) is an enantiomer of PBN -d_6 where the 2-methyl propyl radical and 3-methyl butanal radical have added to the alpha carbon and oxygen respectively { PBN-d_6 -$(CH_2CH(CH_3)_2)(C(CH_3)_2CH_2CHO)$}.

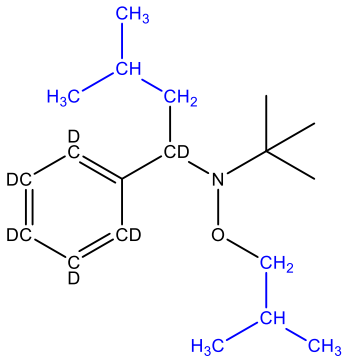

Compound 13 (peak 13)

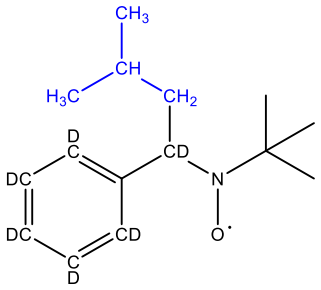

Compound 14 (peak 14)

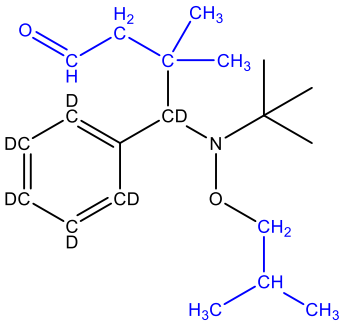

Compound 15 (peak 15)

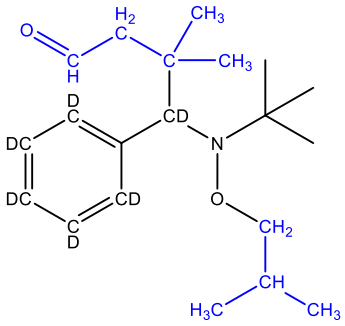

Compound 16 (peak 16)

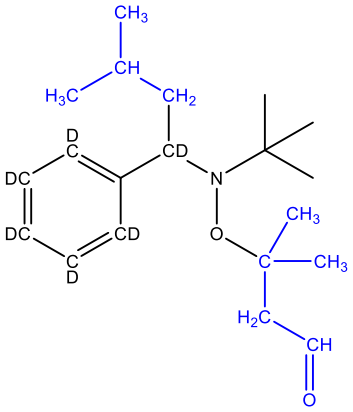

Compound 17 (peak 17)

Figure 5.1.4 The structures of compounds identified by GC-MS analysis of a Fenton-based reaction mixture containing PBN-d_6 and 3-methyl butanal. The atoms in blue are believed to be derived from 3-methyl butanal

5.1.3 Fenton with F-PBN and 3-methylbutanal

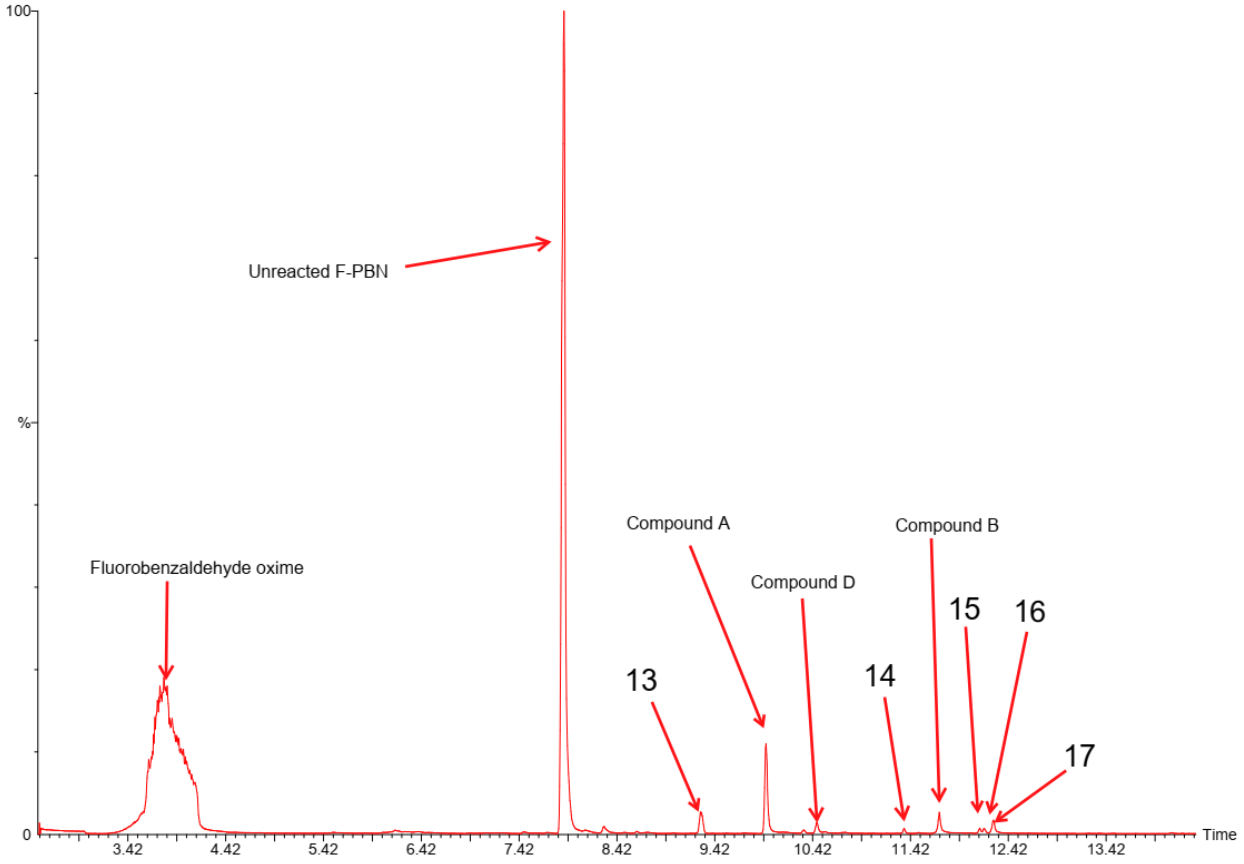

Figure 5.1.5 The total ion chromatogram obtained from the GC-MS analysis of the Fenton system with F-PBN in the presence of 3-methyl butanal

The TIC shown in Figure 5.1.5 obtained from the Fenton reaction of F-PBN and 3-methylbutanal extracted into chloroform shows 9 peaks. The 9 peaks that are labelled have been assigned, as follows: Peak 13 (rt 9.23) corresponds to a di-2-methyl propyl adduct of the spin trap { F-PBN-$(CH_2CH(CH_3)_2)_2$}; Peak 14 (rt 11.41) give the impression of a mono(2-methyl)propyl F-PBN adduct trap { F-PBN-$(CH_2CH(CH_3)_2)$}; Peak 15 (rt 12.10) F-PBN 3-methyl butanal radical and 2-methyl propyl radical adduct {F-PBN-$(CH_3C(CH_3)CH_2CHO)(CH_2CH(CH_3)_2)$ }; Peak 16 (rt 12.15) appears to be an diastereomer of a 3-methyl butanal radical and 2-methyl propyl radical adduct of PBN { F-PBN-$(CH_3C(CH_3)CH_2CHO)(CH_2CH(CH_3)_2)$); Peak 17 (rt 12.23) is an enantiomer of F-PBN where the 2-methyl propyl radical and 3-methyl butanal radical have added to the alpha carbon and oxygen respectively { F-PBN-$(CH_2CH(CH_3)_2)(C(CH_3)_2CH_2CHO)$}. See Figure 5.1.6 for structures

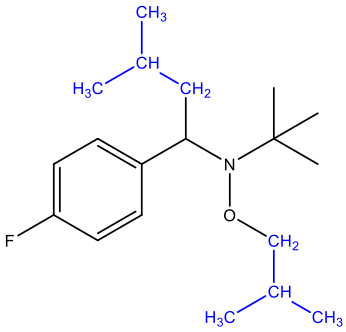

Compound 13 (peak 13)

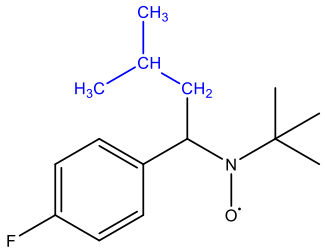

Compound 14 (peak 14)

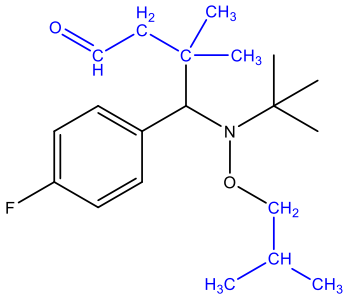

Compound 15 (peak 15)

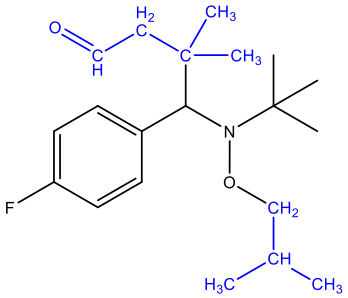

Compound 16 (peak 16)

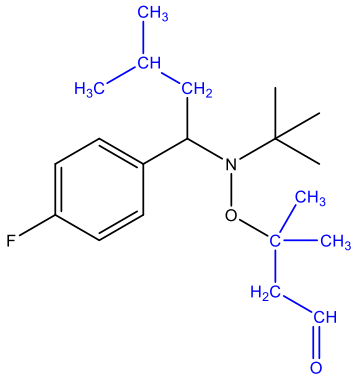

Compound 17 (peak 17)

Figure 5.1.6 The structures of compounds identified by GC-MS analysis of a Fenton-based reaction mixture containing F-PBN and 3-methyl butanal. The atoms in blue are believed to be derived from 3-methyl butanal

5.2 Detection of 2-methyl propyl $((CH_3)_2CH^{\bullet}CH_2)_2$ radical adduct (compound 13)

5.2.1 Di-(2-methyl) propyl adduct of PBN with 3-methyl butanal (compound 13)

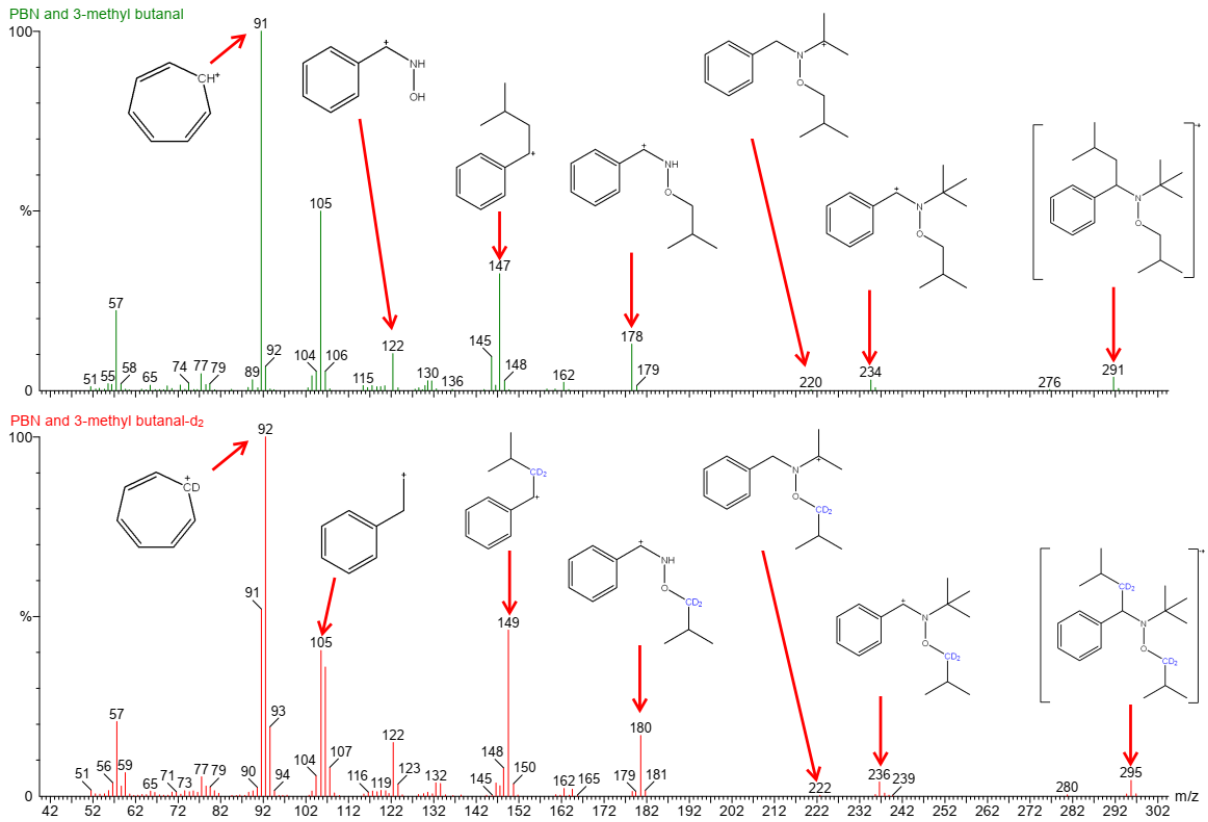

Figure 5.2.1 Electron Ionization mass spectra (EI-MS) corresponding to PBN adducts obtained from the analysis of the Fenton reaction mixture containing PBN, 3-methyl butanal (top) and deuterated 3-methyl butanal-d_2 (bottom) at rt 9.23 minutes

The EI mass spectra in Figure 5.2.1 correspond to a) the PBN di-(2-methyl) propyl adduct {PBN-$(CH_2CH(CH_3)_2)_2$}, top (spectrum); and b) the di-deuterated PBN di-isobutyl adduct {PBN-(C**D**$_2$CH$(CH_3)CH_3)_2$} (bottom spectrum).

When the Fenton reaction was carried out in the presence of 3-methyl butanal as a secondary source of radicals, 2-methyl propyl radicals ($^{\bullet}CH_2CH(CH_3)_2$) are generated by the reaction of $^{\bullet}OH$ with 3-methyl butanal and then trapped by PBN. The peak at 291 *m/z* units corresponds to the molecular ion of PBN-isobut$_2$ di-adduct (one 2-methyl propyl radical adding to the alpha carbon atom of the C=N and the other adding to the oxygen). The fragment at *m/z* 276 is due to the loss of a methyl group from the molecular

ion (from the tBu group). The loss of the 2-methyl propene from the alpha carbon (on the C=N bond) of the molecular ion results in *m/z* 234 and subsequent loss from this fragment of a methyl from the tBu group gives the ion 220 *m/z*. The further loss of propyl from this subsequent fragment (from the nitrogen) leads to 178 *m/z*. The dissociation of the alpha carbon bond and the nitrogen gives *m/z* 147 and further breakdown of this fragment results in *m/z* 122 N-benzyl hydroxylamine. *m/z* 105 is the ethyl benzene cation, the base peak at *m/z* 91 is the tropylium cation and *m/z* 57 is the tertiary butyl cation

Replacing 3-methyl butanal with its deuterated analogue in the Fenton-based reaction demonstrates the production of deuterated 2-methyl propyl radicals and subsequent incorporation by the spin trap. As shown by an increase on the molecular ion of 2 *m/z* when 3-methyl butanal-d_2 is used

When the Fenton reaction was carried out in the presence of 3-methyl butanal-2,2-d_2 as a secondary source of radicals (bottom spectrum), 2-methyl propyl radicals ($^{\bullet}C\mathbf{D}_2CH(CH_3)_2$) are generated by the reaction of $^{\bullet}OH$ with 3-methyl butanal and then trapped by PBN. Replacing 3-methyl butanal with 3-methyl butanal-2,2-d_2 in the Fenton-based reaction mixture increases the molecular ion by 4 *m/z* units. The peak at 295 *m/z* is the molecular ion. The fragment at *m/z* 280 is due to the loss of a methyl group from the molecular ion (from the tBu group) The loss of M-15 shows that the methyl categorically originated from the tBu. The loss of the 2-methyl propene from the alpha carbon (on the C=N bond) of the molecular ion results in *m/z* 236 and subsequent loss from this fragment of a methyl from the tBu group gives the ion 222 *m/z*. The further loss of the 2-methyl propyl group from this subsequent fragment (from the nitrogen) leads to 180 *m/z*. The ion at *m/z* 149 is due to the C=N bond dissociation. This fragment provides clear evidence as to the position of the ($C\mathbf{D}_2CH(CH_3)_2$) group. *m/z* 122 is the N-benzyl hydroxylamine and the base peak at *m/z* 91 is the tropylium ion. *m/z* 57 is the tertiary butyl cation

5.2.2 Di-(2-methyl) propyl adduct of PBN-d_6 with 3-methyl butanal (compound 13)

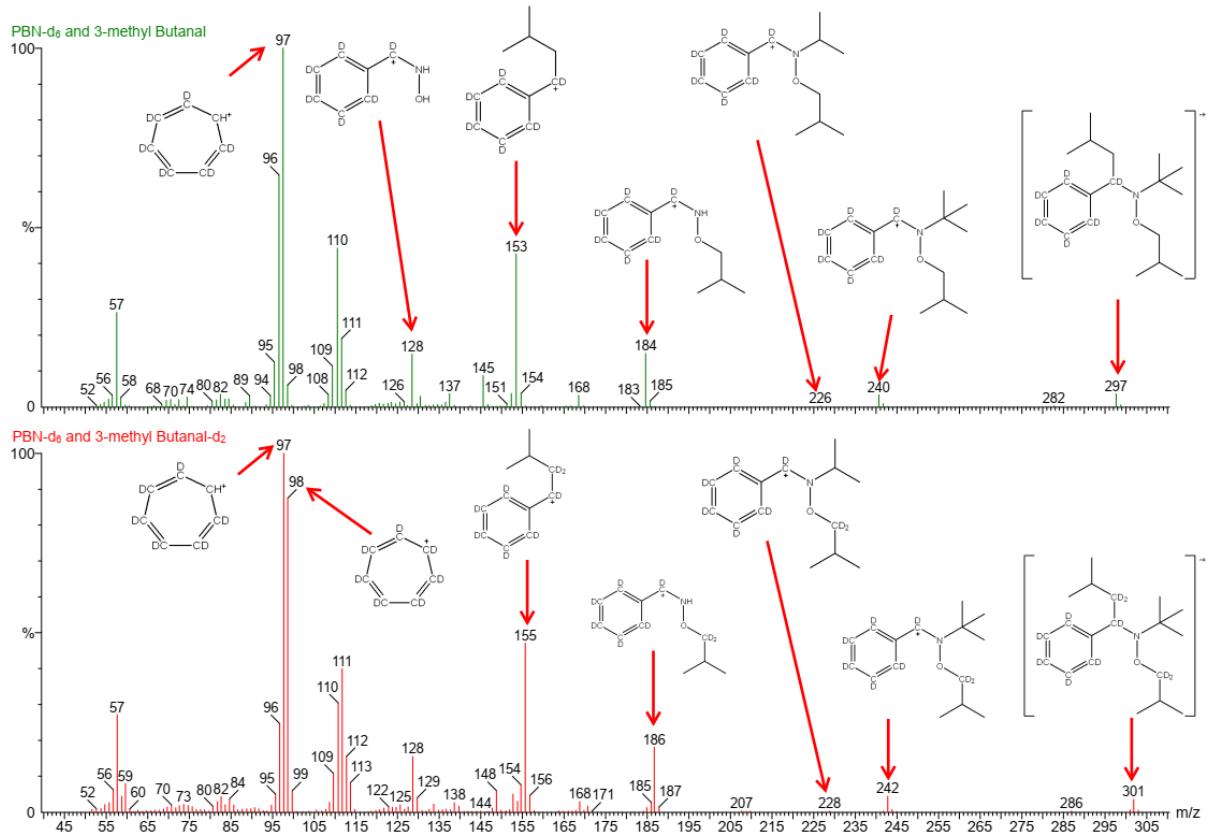

Figure 5.2.2 Electron Ionization mass spectra (EI-MS) corresponding to PBN adducts obtained from the analysis of the Fenton reaction mixture containing PBN-d_6, 3-methyl butanal (top) and deuterated 3-methyl butanal-d_2 (bottom) at rt 9.23 minutes

The EI mass spectra in Figure 5.2.2 correspond to a) the PBN-d_6 di-isobutyl adduct {PBN-d_6-$(CH_2CH(CH_3)_2)_2$} (top spectrum); and b) the di-deuterated PBN di-isobutyl adduct {PBN-d_6-$(C\mathbf{D}_2CH(CH_3)_2)_2$} (bottom spectrum).

When the Fenton reaction was carried out in the presence of 3-methyl butanal as a secondary source of radicals, 2-methyl propyl radicals ($^{\bullet}CH_2CH(CH_3)_2$) are generated by the reaction of $^{\bullet}OH$ with 3-methyl butanal and then trapped by PBN-d_6. The peak at 297 *m/z* units corresponds to the molecular ion of PBN-d_6-isobut$_2$ diadduct (one 2-methyl propyl radical adding to the alpha carbon atom of the C=N and the other adding to the oxygen). The fragment at *m/z* 282 is due to the loss of a methyl group from the molecular ion (from the tBu group). The loss of the 2-methyl propene from the alpha carbon (on the C=N bond) of the molecular ion results in *m/z* 240 and subsequent loss from this fragment of a methyl from the tBu group gives the ion 226 *m/z*. The further loss of propyl from this subsequent fragment (from the

nitrogen) leads to 184 *m/z*. The dissociation of the alpha carbon bond and the nitrogen gives *m/z* 153 and further breakdown of this fragment results in *m/z* 128 N-benzyl-d_5 hydroxylamine-1-*d* and the base peak at *m/z* 97 is the tropylium-d_6 ion. *m/z* 57 is the tertiary butyl cation

Replacing 3-methyl butanal with its deuterated analogue in the Fenton-based reaction demonstrates the production of deuterated 2-methyl propyl radicals and subsequent incorporation by the spin trap. As shown by an increase on the molecular ion of 2 *m/z* when 3-methyl butanal-d_2 is used

When the Fenton reaction was carried out in the presence of 3-methyl butanal-2,2-d_2 as a secondary source of radicals (bottom spectrum), 2-methyl propyl radicals ($^{\bullet}C\mathbf{D}_2CH(CH_3)_2$) are generated by the reaction of $^{\bullet}OH$ with 3-methyl butanal and then trapped by PBN. Replacing 3-methyl butanal with 3-methyl butanal-2,2-d_2 in the Fenton-based reaction mixture increases the molecular ion by 4 *m/z* units. The peak at 301 *m/z* is the molecular ion. The fragment at *m/z* 286 is due to the loss of a methyl group from the molecular ion (from the tBu group) The loss of M-15 shows that the methyl categorically originated from the tBu. The loss of the 2-methyl propene from the alpha carbon (on the C=N bond) of the molecular ion results in *m/z* 242 and subsequent loss from this fragment of a methyl from the tBu group gives the ion 228 *m/z*. The further loss of the 2-methyl propyl group from this subsequent fragment (from the nitrogen) leads to 186 *m/z*. The ion at *m/z* 155 is due to the C=N bond dissociation. This fragment provides clear evidence as to the position of the ($C\mathbf{D}_2CH(CH_3)_2$) group. *m/z* 128 is the N-benzyl hydroxylamine and the base peak at *m/z* 97 is the tropylium-d_6 ion. *m/z* 57 is the tertiary butyl cation

5.2.3 Di-(2-methyl) propyl adduct of F-PBN with 3-methyl butanal (compound 13)

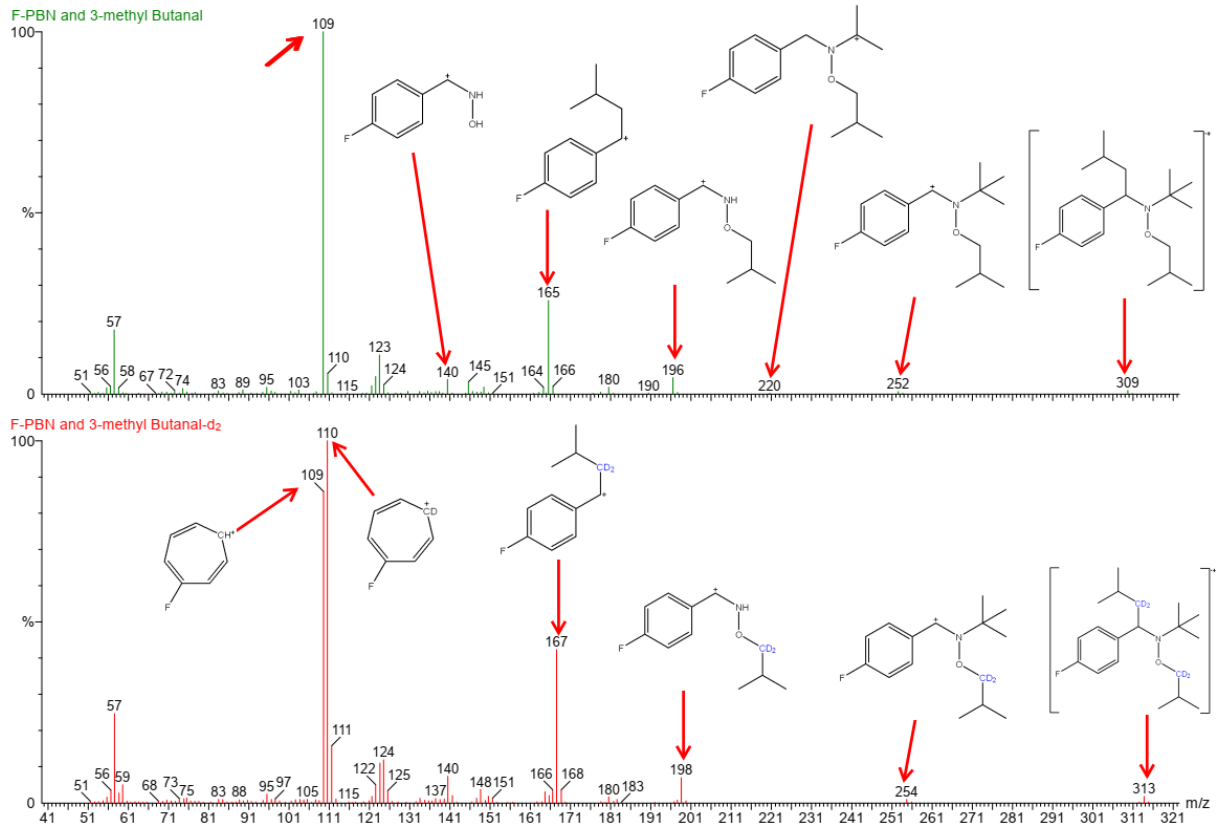

Figure 5.2.3 Electron Ionization mass spectra (EI-MS) corresponding to PBN adducts obtained from the analysis of the Fenton reaction mixture containing F-PBN, 3-methyl butanal (top) and deuterated 3-methyl butanal-d_2 (bottom) at rt 9.23 minutes

The EI Mass spectra in Figure 5.2.3Figure 5.2.1 correspond to a) the F-PBN di-isobutyl adduct {F-PBN-($CH_2CH(CH_3)CH_3)_2$} (top spectrum); and b) the di- F-PBN deuterated di-isobutyl adduct {F-PBN-($C\mathbf{D}_2CH(CH_3)_2)_2$} (bottom spectrum).

When the Fenton reaction was carried out in the presence of 3-methyl butanal as a secondary source of radicals, 2-methyl propyl radicals ($^{\bullet}CH_2CH(CH_3)_2$) are generated by the reaction of $^{\bullet}OH$ with 3-methyl butanal and then trapped by F-PBN. The peak at 309 *m/z* units corresponds to the molecular ion of F-PBN-isobut$_2$ di-adduct (one 2-methyl propyl radical adding to the alpha carbon atom of the C=N and the other adding to the oxygen). The loss of the 2-methyl propene from the alpha carbon (on the C=N bond) of the molecular ion results in *m/z* 252 The further loss of propyl from this fragment (from the nitrogen) leads to 198 *m/z*. The dissociation of the alpha carbon bond and the nitrogen gives *m/z* 165 and further

breakdown of this fragment results in *m/z* 140 N-fluorobenzyl hydroxylamine and the base peak at *m/z* 109, the fluorotropylium ion. *m/z* 57 is the tertiary butyl cation

Replacing 3-methyl butanal with its deuterated analogue in the Fenton-based reaction demonstrates the production of deuterated 2-methyl propyl radicals and subsequent incorporation by the spin trap. As shown by an increase on the molecular ion of 2 *m/z* when 3-methyl butanal-d_2 is used

When the Fenton reaction was carried out in the presence of 3-methyl butanal-2,2-d_2 as a secondary source of radicals (bottom spectrum), 2-methyl propyl radicals ($^{\bullet}C\mathbf{D}_2CH(CH_3)_2$) are generated by the reaction of $^{\bullet}OH$ with 3-methyl butanal and then trapped by F-PBN. Replacing 3-methyl butanal with 3-methyl butanal-2,2-d_2 in the Fenton-based reaction mixture increases the molecular ion by 4 *m/z* units. The peak at 313 *m/z* is the molecular ion. The loss of the 2-methyl propene from the alpha carbon (on the C=N bond) of the molecular ion results in *m/z* 254. The further loss of the 2-methyl propyl group from this subsequent fragment (from the nitrogen) leads to 198 *m/z*. The ion at *m/z* 167 is due to the C=N bond dissociation. This fragment provides clear evidence as to the position of the ($C\mathbf{D}_2CH(CH_3)_2$) group. *m/z* 122 is the N-benzyl hydroxylamine and the base peak at *m/z* 110 is the fluorotropylium-1-*d* ion. *m/z* 57 is the tertiary butyl cation

5.3 Detection of mono 2-methyl propyl {($^{\bullet}CH_2CH(CH_3)_2$)} radical (compound 14)

5.3.1 Mono-2-methyl propyl adduct of PBN with 3-methyl butanal (compound 14)

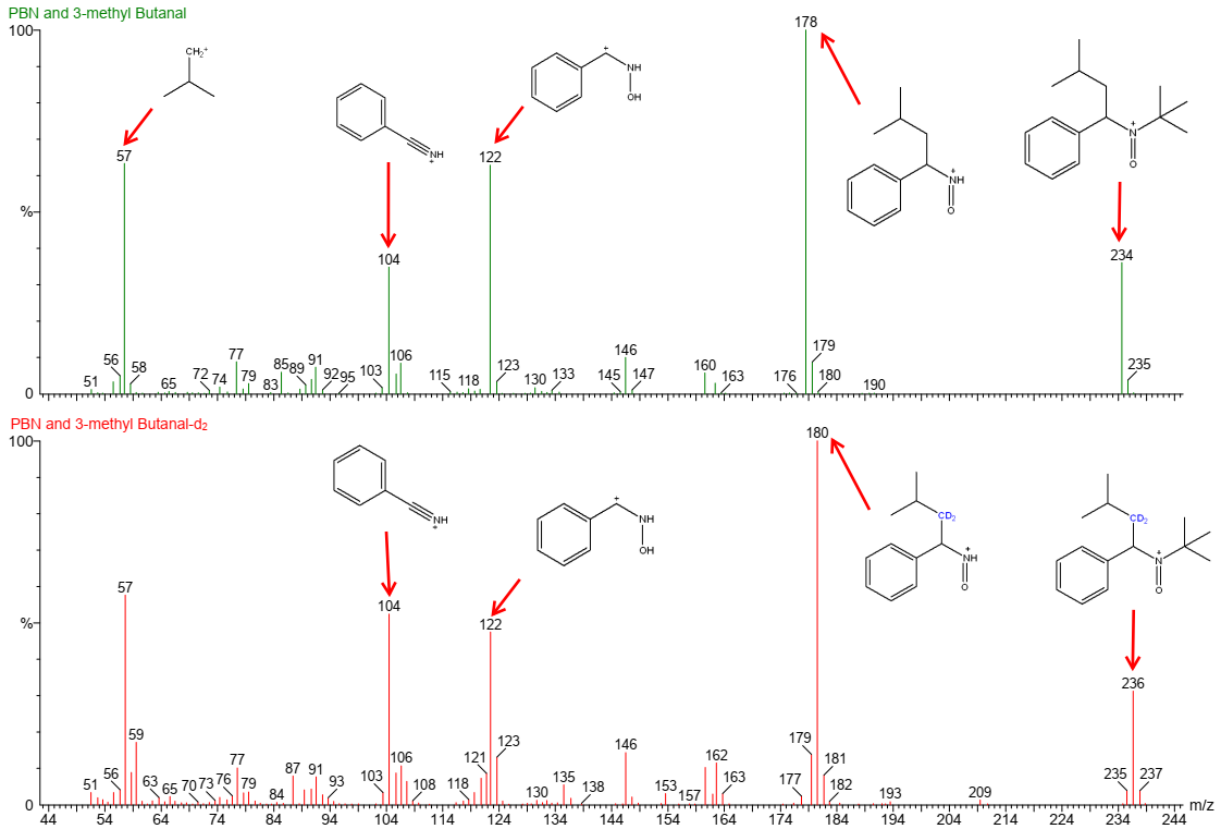

Figure 5.3.1 Electron Ionization mass spectra (EI-MS) corresponding to PBN adducts obtained from the analysis of the Fenton reaction mixture containing PBN, 3-methyl butanal (top) and deuterated 3-methyl butanal-d_2 (bottom) at rt 11.42 minutes

The EI mass spectra in Figure 5.3.1 correspond to the a) the PBN mono-(2-methyl) propyl adduct (top spectrum); b) the PBN dideuterated mono-(2-methyl) propyl adduct (bottom spectrum).

When the Fenton reaction was carried out in the presence of 3-methyl butanal as a secondary source of radicals, 2-methyl propyl radicals ($^{\bullet}CH_2CH(CH_3)_2$) are generated by the reaction of $^{\bullet}OH$ with 3-methyl butanal and then trapped by PBN. The peak at 234 *m/z* units corresponds to the molecular ion of PBN-2-methyl propyl (one 2-methyl propyl adding to the alpha carbon atom of the C=N). The loss of CH_2=CMe_2 results in base peak *m/z* 178 and the further loss of a 2-methyl propyl group from the molecular ion results in *m/z* 122 N-benzyl hydroxylamine cation. The peak at *m/z* 104 is the phenylmethanimine cation and

further breakdown of this fragment results in a tropylium cation at *m/z* 91. and the peak at *m/z* 57 is the characteristic tertiary butyl cation

Replacing 3-methyl butanal with its deuterated analogue in the Fenton-based reaction demonstrates the production of deuterated 2-methyl propyl radicals and subsequent incorporation by the spin trap. As shown by an increase on the molecular ion of 2 *m/z* when 3-methyl butanal-d_2 is used

When the Fenton reaction was carried out in the presence of 3-methyl butanal-2,2-d_2 as a secondary source of radicals, 2-methyl propyl radicals ($^{\bullet}C\mathbf{D}_2CH(CH_3)_2$) are generated by the reaction of $^{\bullet}OH$ with 3-methyl butanal and then trapped by PBN. The peak at 236 *m/z* units corresponds to the molecular ion of PBN-2-methyl propyl. The loss of $CH_2{=}CMe_2$ gives base peak *m/z* 180 and the loss of a dideuterated propyl group from this fragment results in *m/z* 122 N-benzyl hydroxylamine. The peak at *m/z* 104 is the phenylmethanimine cation and further breakdown of this fragment results in a tropylium cation peak at *m/z* 91. and the peak at *m/z* 57 is the tertiary butyl cation

5.3.2 Mono-2-methyl propyl adduct of PBN-d_6 with 3-methyl butanal (compound 14)

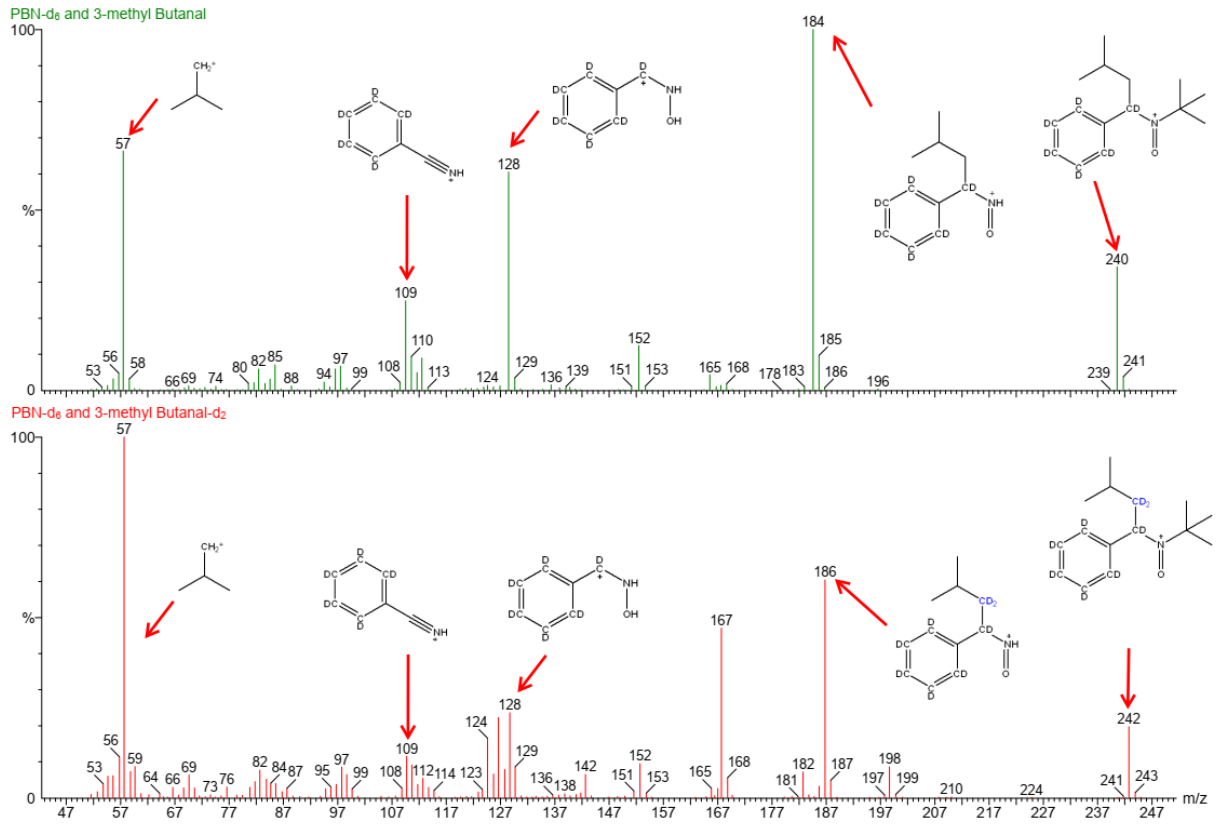

Figure 5.3.2 Electron Ionization mass spectra (EI-MS) corresponding to PBN-d_6 adducts obtained from the analysis of the Fenton reaction mixture containing PBN-d_6, 3-methyl butanal (top) and deuterated 3-methyl butanal-d_2 (bottom) at rt 11.42 minutes

The EI mass spectra in Figure 5.3.2 correspond to the a) the PBN-d_6 mono-(2-methyl) propyl adduct (top spectrum); b) the PBN-d_6 dideuterated mono-(2-methyl) propyl adduct (bottom spectrum)

When the Fenton reaction was carried out in the presence of 3-methyl butanal as a secondary source of radicals, 2-methyl propyl radicals ($^{\bullet}CH_2CH(CH_3)_2$) are generated by the reaction of $^{\bullet}OH$ with 3-methyl butanal and then trapped by PBN-d_6. The peak at 240 *m/z* units corresponds to the molecular ion of PBN-d_6-2-methyl propyl (one 2-methyl propyl adding to the alpha carbon atom of the C=N). The loss of CH_2=CMe_2 results in base peak *m/z* 184 and the further loss of a 2-methyl propyl group from the molecular ion results in *m/z* 128 N-benzyl hydroxylamine cation. The peak at *m/z* 109 is the phenyl-d_5 methanimine cation and further breakdown of this fragment results in a tropylium-d_6 cation at *m/z* 97. and the peak at *m/z* 57 is the characteristic tertiary butyl cation

Replacing 3-methyl butanal with its deuterated analogue in the Fenton-based reaction demonstrates the production of deuterated 2-methyl propyl radicals and subsequent incorporation by the spin trap. As shown by an increase on the molecular ion of 2 *m/z* when 3-methyl butanal-d_2 is used.

When the Fenton reaction was carried out in the presence of 3-methyl butanal-2,2-d_2 as a secondary source of radicals, 2-methyl propyl radicals ($^{\bullet}C\mathbf{D}_2CH(CH_3)_2$) are generated by the reaction of $^{\bullet}OH$ with 3-methyl butanal and then trapped by PBN. The peak at 236 *m/z* units corresponds to the molecular ion of PBN-2-methyl propyl. The loss of $CH_2{=}CMe_2$ gives base peak *m/z* 180 and the loss of a dideuterated propyl group from this fragment results in *m/z* 128 N-benzyl hydroxylamine cation. The peak at *m/z* 109 is the phenyl-d_5 methanimine cation and further breakdown of this fragment results in a tropylium-d_6 cation at *m/z* 97. and the peak at *m/z* 57 is the characteristic tertiary butyl cation

5.3.3 Mono-2-methyl propyl adduct of F-PBN with 3-methyl butanal (compound 14)

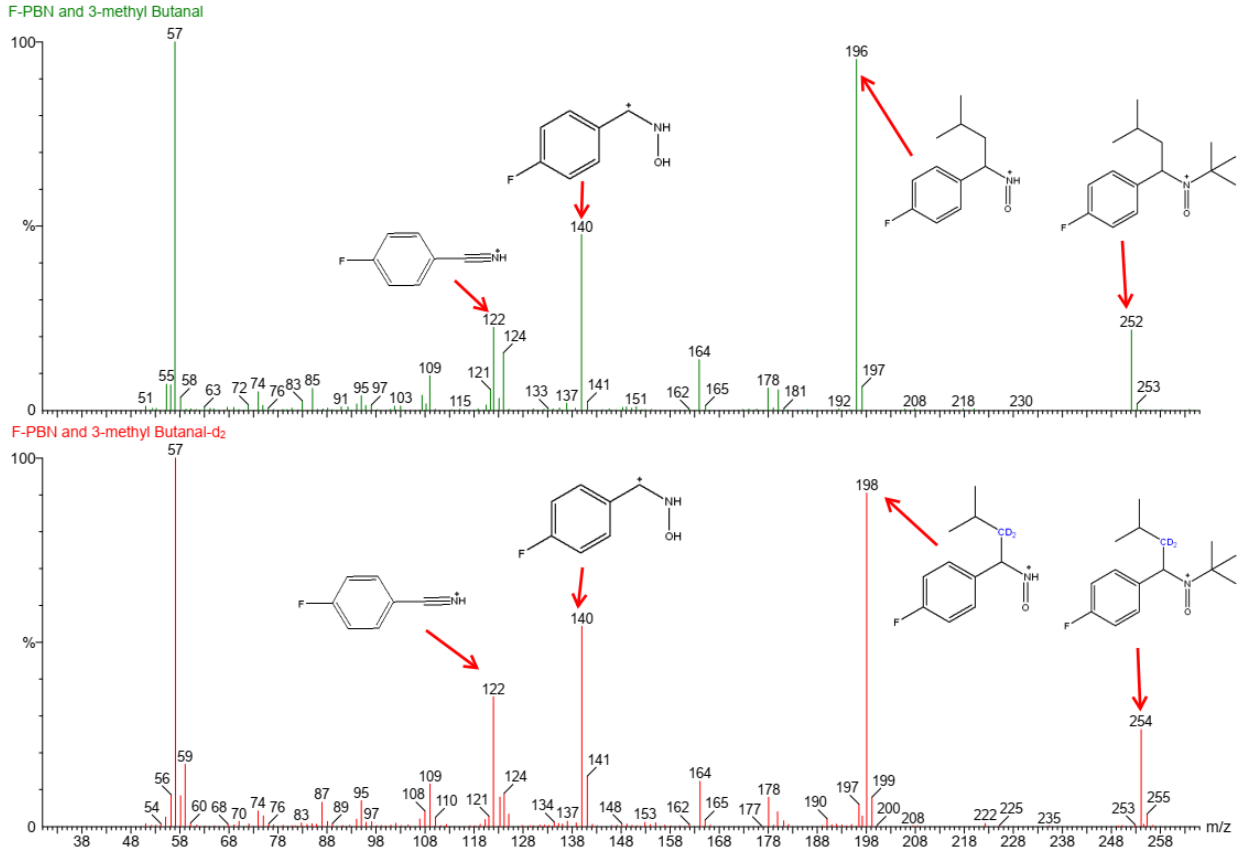

Figure 5.3.3 Electron Ionization mass spectra (EI-MS) corresponding to PBN adducts obtained from the analysis of the Fenton reaction mixture containing F-PBN, 3-methyl butanal (top) and deuterated 3-methyl butanal-d_2 (bottom) at rt 11.42 minutes

The EI mass spectra in Figure 5.3.3 correspond to the a) the F-PBN mono-(2-methyl) propyl adduct (top spectrum); b) the F-PBN dideuterated mono-(2-methyl) propyl adduct (bottom spectrum).

When the Fenton reaction was carried out in the presence of 3-methyl butanal as a secondary source of radicals, 2-methyl propyl radicals ($^{\bullet}CH_2CH(CH_3)_2$) are generated by the reaction of $^{\bullet}OH$ with 3-methyl butanal and then trapped by F-PBN. The peak at 252 *m/z* units corresponds to the molecular ion of F-PBN-2-methyl propyl (one 2-methyl propyl adding to the alpha carbon atom of the C=N). The loss of CH_2=CMe_2 results in base peak *m/z* 196 and the further loss of a 2-methyl propyl group from the molecular ion results in *m/z* 140 N-4-fluoro-benzyl hydroxylamine cation. The peak at *m/z* 122 is the 4-fluoro-phenylmethanimine cation and further breakdown of this fragment results in a fluorotropylium cation at *m/z* 109. and the peak at *m/z* 57 is the characteristic tertiary butyl cation

Replacing 3-methyl butanal with its deuterated analogue in the Fenton-based reaction demonstrates the production of deuterated 2-methyl propyl radicals and subsequent incorporation by the spin trap. As shown by an increase on the molecular ion of 2 *m/z* when 3-methyl butanal-d_2 is used

When the Fenton reaction was carried out in the presence of 3-methyl butanal-2,2-d_2 as a secondary source of radicals, 2-methyl propyl radicals ($^{\bullet}C\mathbf{D}_2CH(CH_3)_2$) are generated by the reaction of $^{\bullet}OH$ with 3-methyl butanal and then trapped by F-PBN. The peak at 254 *m/z* units corresponds to the molecular ion of F-PBN-2-methyl propyl. The loss of $CH_2{=}CMe_2$ gives base peak *m/z* 198 and the further loss of a 2-methyl propyl group from the molecular ion results in *m/z* 140 N-4-fluoro-benzyl hydroxylamine cation. The peak at *m/z* 122 is the 4-fluoro-phenylmethanimine cation and further breakdown of this fragment results in a fluorotropylium cation at *m/z* 109. and the peak at *m/z* 57 is the characteristic tertiary butyl cation

5.4 Detection of 3-methyl butanal radical and 2-methyl propyl radical adduct (compound 15)

5.4.1 3-methyl butanal radical and 2-methyl propyl radical adduct of PBN (compound 15)

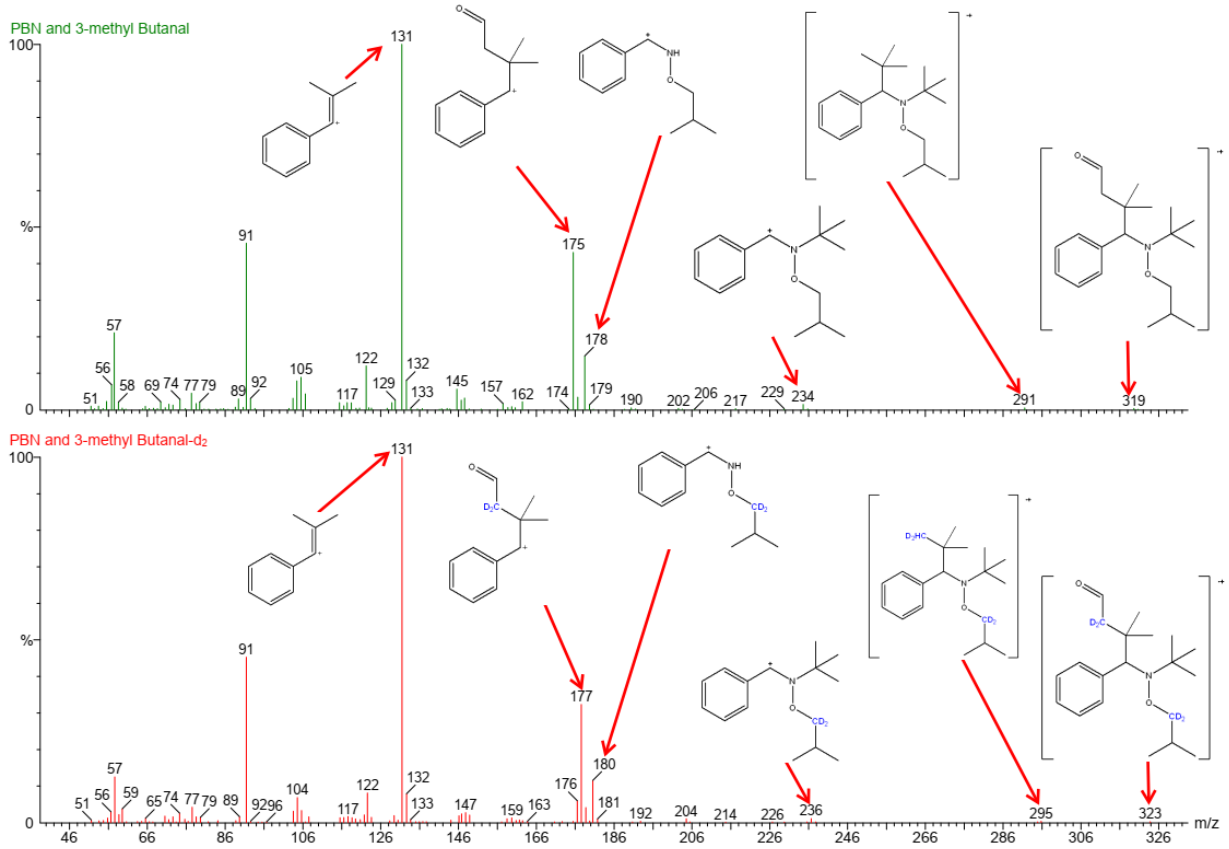

Figure 5.4.1 Electron Ionization mass spectra (EI-MS) corresponding to PBN adducts obtained from the analysis of the Fenton reaction mixture containing PBN, 3-methyl butanal (top) and deuterated 3-methyl butanal-d_2 (bottom) at rt 12.12 minutes

The EI mass spectra in Figure 5.4.1 correspond to a) the PBN-($CH_3^{\bullet}C(CH_3)CH_2CHO$)($^{\bullet}CH_2CH(CH_3)_2$) adduct, top (spectrum); and b) the di-deuterated PBN-($CH_3^{\bullet}C(CH_3)C\mathbf{D}_2CHO$)($^{\bullet}C\mathbf{D}_2CH(CH_3)_2$) (bottom spectrum).

When the Fenton reaction was carried out in the presence of 3-methyl butanal as a secondary source of radicals, 3-methyl butanal radicals ($CH_3^{\bullet}C(CH_3)CH_2CHO$) and 2-methyl propyl radicals ($^{\bullet}CH_2CH(CH_3)_2$) are generated by the reaction of $^{\bullet}OH$ with 3-methyl butanal and then trapped by PBN. The peak at 319 *m/z* units corresponds to the molecular ion of PBN-($CH_3^{\bullet}C(CH_3)CH_2CHO$)($^{\bullet}CH_2CH(CH_3)_2$) adduct (3-methyl butanal radical adding to the alpha carbon atom of the C=N and the 2-methyl propyl radical adding to the oxygen). The fragment at *m/z* 291 is due to the loss of C=O from the butanal radical group of the molecular

ion. The loss of the 3-methyl butanal radical from the alpha carbon (on the C=N bond) of the molecular ion results in *m/z* 234. The further loss of CH_2=CMe_2 from this subsequent fragment (from the nitrogen) leads to 178 *m/z*. The dissociation of the alpha carbon bond and the nitrogen gives *m/z* 175 and further breakdown of this fragment (loss of CH_2CHO) results in base peak *m/z* 131, the peak at *m/z* 91 is the tropylium cation and *m/z* 57 is the tertiary butyl cation

Replacing 3-methyl butanal with its deuterated analogue in the Fenton-based reaction demonstrates the production of deuterated 2-methyl propyl and deuterated 3-methyl butanal radicals and subsequent incorporation by the spin trap. As shown by an increase on the molecular ion of 4 *m/z* when 3-methyl butanal-d_2 is used

When the Fenton reaction was carried out in the presence of 3-methyl butanal-2,2-d_2 as a secondary source of radicals, 3-methyl butanal radicals ($CH_3^{\bullet}C(CH_3)C\mathbf{D}_2CHO$) and 2-methyl propyl radicals ($^{\bullet}C\mathbf{D}_2CH(CH_3)_2$) are generated by the reaction of $^{\bullet}OH$ with 3-methyl butanal and then trapped by PBN. The peak at 323 *m/z* units corresponds to the molecular ion of PBN-($CH_3^{\bullet}C(CH_3)C\mathbf{D}_2CHO$)($^{\bullet}C\mathbf{D}_2CH(CH_3)_2$) adduct (3-methyl butanal radical adding to the alpha carbon atom of the C=N and the 2-methyl propyl radical adding to the oxygen), demonstrating the deuterated radicals have been incorporated into the molecular ion owing to the 4 *m/z* unit increase. The fragment at *m/z* 295 is due to the loss of C=O from the butanal radical group of the molecular ion. The loss of the 3-methyl butanal radical from the alpha carbon (on the C=N bond) of the molecular ion results in *m/z* 236. The further loss of CH_2=CMe_2 from this subsequent fragment (from the nitrogen) leads to 180 *m/z*. The dissociation of the alpha carbon bond and the nitrogen gives *m/z* 177 and further breakdown of this fragment (loss of $C\mathbf{D}_2CHO$) results in base peak *m/z* 131, the peak at *m/z* 91 is the tropylium cation and *m/z* 57 is the tertiary butyl cation

5.4.2 3-methyl butanal radical and 2-methyl propyl radical adduct of PBN-d_6 (compound 15)

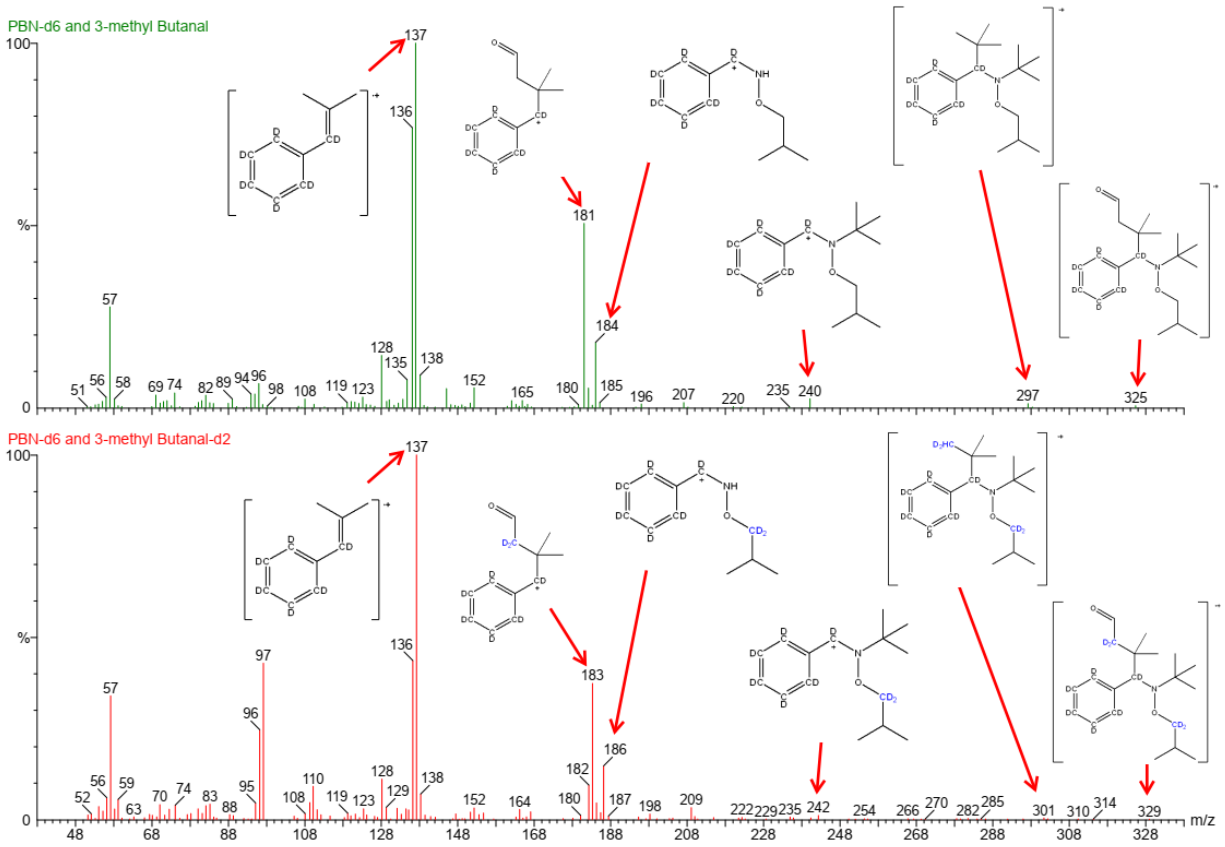

Figure 5.4.2 Electron Ionization mass spectra (EI-MS) corresponding to PBN-d_6 adducts obtained from the analysis of the Fenton reaction mixture containing PBN-d_6, 3-methyl butanal (top) and deuterated 3-methyl butanal-d_2 (bottom) at rt 12.12 minutes

The EI mass spectra in Figure 5.4.2 correspond to a) the PBN-d_6-(CH_3•$C(CH_3)CH_2CHO$)(•$CH_2CH(CH_3)_2$), top (spectrum); and b) the di-deuterated PBN-d_6-(CH_3•$C(CH_3)C\mathbf{D}_2CHO$)(•$C\mathbf{D}_2CH(CH_3)_2$) (bottom spectrum).

When the Fenton reaction was carried out in the presence of 3-methyl butanal as a secondary source of radicals, 3-methyl butanal radicals (CH_3•$C(CH_3)CH_2CHO$) and 2-methyl propyl radicals (•$CH_2CH(CH_3)_2$) are generated by the reaction of •OH with 3-methyl butanal and then trapped by PBN-d_6. The peak at 325 *m/z* units corresponds to the molecular ion of PBN-d_6-(CH_3•$C(CH_3)CH_2CHO$)(•$CH_2CH(CH_3)_2$) adduct (3-methyl butanal radical adding to the alpha carbon atom of the C=N and the 2-methyl propyl radical adding to the oxygen). The fragment at *m/z* 297 is due to the loss of C=O from the butanal radical group of the molecular ion. The loss of the 3-methyl butanal radical from the alpha carbon (on the C=N bond) of the molecular ion results in *m/z* 240. The further loss of CH_2=CMe_2 from this subsequent fragment (from the nitrogen)

leads to 184 *m/z*. The dissociation of the alpha carbon bond and the nitrogen gives *m/z* 181 and further breakdown of this fragment (loss of CH_2CHO) results in base peak *m/z* 137., the peak at *m/z* 96 is the tropylium-d_5 cation and *m/z* 57 is the tertiary butyl cation

Replacing 3-methyl butanal with its deuterated analogue in the Fenton-based reaction demonstrates the production of deuterated 2-methyl propyl radicals and deuterated 3-methyl butanal radicals and subsequent incorporation by the spin trap. As shown by an increase on the molecular ion of 4 *m/z* when 3-methyl butanal-d_2 is used

When the Fenton reaction was carried out in the presence of 3-methyl butanal-2,2-d_2 as a secondary source of radicals, 3-methyl butanal radicals ($CH_3^{\bullet}C(CH_3)C\mathbf{D}_2CHO$) and 2-methyl propyl radicals ($^{\bullet}C\mathbf{D}_2CH(CH_3)_2$) are generated by the reaction of $^{\bullet}OH$ with 3-methyl butanal and then trapped by PBN-d_6. The peak at 329 *m/z* units corresponds to the molecular ion of PBN-d_6-($CH_3^{\bullet}C(CH_3)C\mathbf{D}_2CHO$)($^{\bullet}C\mathbf{D}_2CH(CH_3)_2$) adduct (3-methyl butanal radical adding to the alpha carbon atom of the C=N and the 2-methyl propyl radical adding to the oxygen), demonstrating the deuterated radicals have been incorporated into the molecular ion owing to the 4 *m/z* unit increase. The fragment at *m/z* 301 is due to the loss of C=O from the butanal radical group of the molecular ion. The loss of the 3-methyl butanal radical from the alpha carbon (on the C=N bond) of the molecular ion results in *m/z* 242. The further loss of $CH_2{=}CMe_2$ from this subsequent fragment (from the nitrogen) leads to 186 *m/z*. The dissociation of the alpha carbon bond and the nitrogen gives *m/z* 183 and further breakdown of this fragment (loss of $C\mathbf{D}_2CHO$) results in base peak *m/z* 137., the peak at *m/z* 97 is the tropylium-d_6 cation and *m/z* 57 is the tertiary butyl cation

5.4.3 3-methyl butanal radical and 2-methyl propyl radical adduct of F-PBN (compound 15)

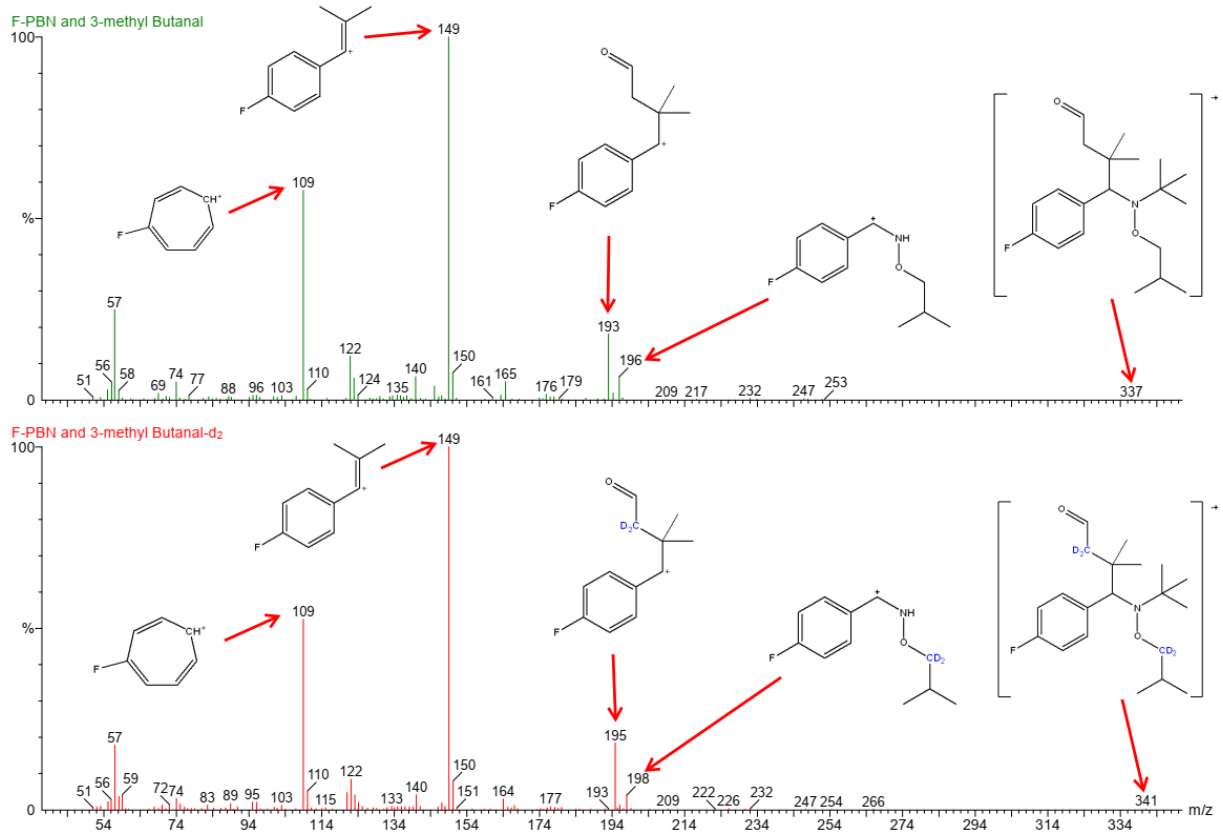

Figure 5.4.3 Electron Ionization mass spectra (EI-MS) corresponding to PBN adducts obtained from the analysis of the Fenton reaction mixture containing F-PBN, 3-methyl butanal (top) and deuterated 3-methyl butanal-d_2 (bottom) at rt 12.12 minutes

The EI mass spectra in Figure 5.4.3 correspond to a) the F-PBN-(CH_3•$C(CH_3)CH_2CHO$)(•$CH_2CH(CH_3)_2$) adduct, top (spectrum); and b) the F-PBN di-deuterated-(CH_3•$C(CH_3)C\mathbf{D}_2CHO$)(•$C\mathbf{D}_2CH(CH_3)_2$) (bottom spectrum).

When the Fenton reaction was carried out in the presence of 3-methyl butanal as a secondary source of radicals, 3-methyl butanal radicals (CH_3•$C(CH_3)CH_2CHO$) and 2-methyl propyl radicals (•$CH_2CH(CH_3)_2$) are generated by the reaction of •OH with 3-methyl butanal and then trapped by F-PBN. The peak at 337 *m/z* units corresponds to the molecular ion of F-PBN-(CH_3•$C(CH_3)CH_2CHO$)(•$CH_2CH(CH_3)_2$) adduct (3-methyl butanal radical adding to the alpha carbon atom of the C=N and the 2-methyl propyl radical adding to the oxygen). The loss of the 3-methyl butanal radical from the alpha carbon (on the C=N bond) of the molecular ion and further loss of CH_2=CMe_2 from this subsequent fragment (from the nitrogen) leads to 196 *m/z*. The dissociation of the alpha carbon bond and the nitrogen gives *m/z* 193 and further breakdown

of this fragment (loss of CH_2CHO) results in base peak *m/z* 149., the peak at *m/z* 109 is the tropylium cation and *m/z* 57 is the tertiary butyl cation

Replacing 3-methyl butanal with its deuterated analogue in the Fenton-based reaction demonstrates the production of deuterated 2-methyl propyl and deuterated 3-methyl butanal radicals and subsequent incorporation by the spin trap. As shown by an increase on the molecular ion of 4 *m/z* when 3-methyl butanal-d_2 is used

When the Fenton reaction was carried out in the presence of 3-methyl butanal-2,2-d_2 as a secondary source of radicals, 3-methyl butanal radicals ($CH_3^{\bullet}C(CH_3)C\mathbf{D}_2CHO$) and 2-methyl propyl radicals ($^{\bullet}C\mathbf{D}_2CH(CH_3)_2$) are generated by the reaction of $^{\bullet}OH$ with 3-methyl butanal and then trapped by F-PBN. The peak at 341 *m/z* units corresponds to the molecular ion of F-PBN-($CH_3^{\bullet}C(CH_3)C\mathbf{D}_2CHO$)($^{\bullet}C\mathbf{D}_2CH(CH_3)_2$) adduct (3-methyl butanal radical adding to the alpha carbon atom of the C=N and the 2-methyl propyl radical adding to the oxygen), demonstrating the deuterated radicals have been incorporated into the molecular ion owing to the 4 *m/z* unit increase. The loss of the 3-methyl butanal radical from the alpha carbon (on the C=N bond) of the molecular ion and further loss of $CH_2{=}CMe_2$ from this subsequent fragment (from the nitrogen) leads to 198 *m/z*. The dissociation of the alpha carbon bond and the nitrogen gives *m/z* 195 and further breakdown of this fragment (loss of $C\mathbf{D}_2CHO$) results in base peak *m/z* 149, the peak at *m/z* 109 is the tropylium cation and *m/z* 57 is the tertiary butyl cation

5.5 Detection of an additional 3-methyl butanal radical and 2-methyl propyl radical adduct (compound 16)

Compound 16 has essentially the same EI mass spectrum as that for compound 15. The structures are enantiomers of each other. It is impossible to deduce in what way they may differ due to the chiral nature of the alpha carbon and the chiral nature of the nitrogen as there is very significant similarities in the spectra therefore the structural arrangement has been kept the same for discussion purposes.

5.5.1 Additional 3-methyl butanal radical and 2-methyl propyl radical adduct of PBN (compound 16)

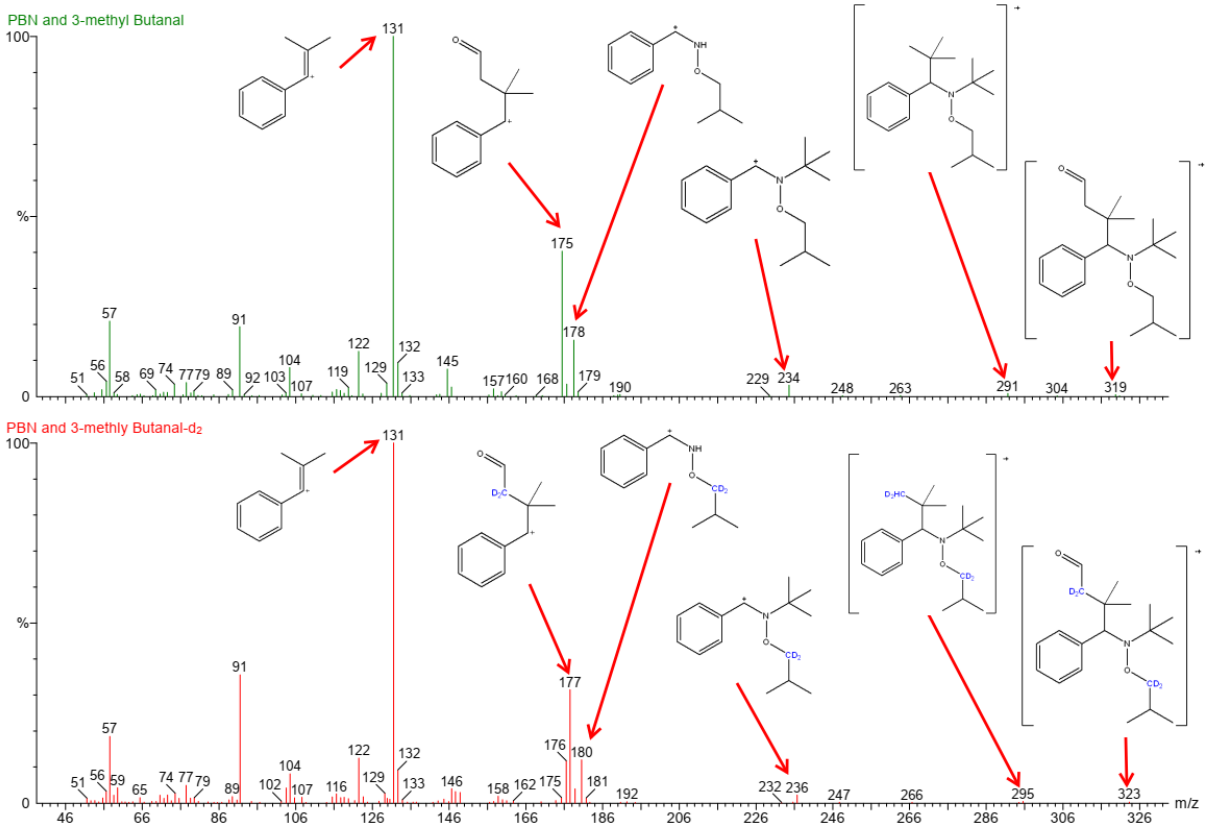

Figure 5.5.1 Electron Ionization mass spectra (EI-MS) corresponding to PBN adducts obtained from the analysis of the Fenton reaction mixture containing PBN, 3-methyl butanal (top) and deuterated 3-methyl butanal-d_2 (bottom) at rt 12.16 minutes

The EI mass spectra in Figure 5.5.1 correspond to a) the PBN-(CH_3•$C(CH_3)CH_2CHO$)(•$CH_2CH(CH_3)_2$) adduct, top (spectrum); and b) the di-deuterated PBN-(CH_3•$C(CH_3)C\mathbf{D}_2CHO$)(•$C\mathbf{D}_2CH(CH_3)_2$) (bottom spectrum).

When the Fenton reaction was carried out in the presence of 3-methyl butanal as a secondary source of radicals, 3-methyl butanal radicals ($CH_3^{\bullet}C(CH_3)CH_2CHO$) and 2-methyl propyl radicals ($^{\bullet}CH_2CH(CH_3)_2$) are generated by the reaction of $^{\bullet}OH$ with 3-methyl butanal and then trapped by PBN. The peak at 319 *m/z* units corresponds to the molecular ion of PBN-($CH_3^{\bullet}C(CH_3)CH_2CHO$)($^{\bullet}CH_2CH(CH_3)_2$) adduct (3-methyl butanal radical adding to the alpha carbon atom of the C=N and the 2-methyl propyl radical adding to the oxygen). The fragment at *m/z* 291 is due to the loss of C=O from the butanal radical group of the molecular ion. The loss of the 3-methyl butanal radical from the alpha carbon (on the C=N bond) of the molecular ion results in *m/z* 234. The further loss of CH_2=CMe_2 from this subsequent fragment (from the nitrogen) leads to 178 *m/z*. The dissociation of the alpha carbon bond and the nitrogen gives *m/z* 175 and further breakdown of this fragment (loss of CH_2CHO) results in base peak *m/z* 131., the peak at *m/z* 91 is the tropylium cation and *m/z* 57 is the tertiary butyl cation

Replacing 3-methyl butanal with its deuterated analogue in the Fenton-based reaction demonstrates the production of deuterated 2-methyl propyl radicals and deuterated 3-methyl butanal radicals and subsequent incorporation by the spin trap. As shown by an increase on the molecular ion of 4 *m/z* when 3-methyl butanal-d_2 is used

When the Fenton reaction was carried out in the presence of 3-methyl butanal-2,2-d_2 as a secondary source of radicals, 3-methyl butanal radicals ($CH_3^{\bullet}C(CH_3)C\mathbf{D}_2CHO$) and 2-methyl propyl radicals ($^{\bullet}C\mathbf{D}_2CH(CH_3)_2$) are generated by the reaction of $^{\bullet}OH$ with 3-methyl butanal and then trapped by PBN. The peak at 323 *m/z* units corresponds to the molecular ion of PBN-($CH_3^{\bullet}C(CH_3)C\mathbf{D}_2CHO$)($^{\bullet}C\mathbf{D}_2CH(CH_3)_2$) adduct (3-methyl butanal radical adding to the alpha carbon atom of the C=N and the 2-methyl propyl radical adding to the oxygen), demonstrating the deuterated radicals have been incorporated into the molecular ion owing to the 4 *m/z* unit increase. The fragment at *m/z* 295 is due to the loss of C=O from the butanal radical group of the molecular ion. The loss of the 3-methyl butanal radical from the alpha carbon (on the C=N bond) of the molecular ion results in *m/z* 236. The further loss of CH_2=CMe_2 from this subsequent fragment (from the nitrogen) leads to 180 *m/z*. The dissociation of the alpha carbon bond and the nitrogen gives *m/z* 177 and further breakdown of this fragment (loss of $C\mathbf{D}_2CHO$) results in base peak *m/z* 131, the peak at *m/z* 91 is the tropylium cation and *m/z* 57 is the tertiary butyl cation

5.5.3 Additional 3-methyl butanal radical and 2-methyl propyl radical adduct of PBN-d_6 adduct of PBN-d_6 (compound 16)

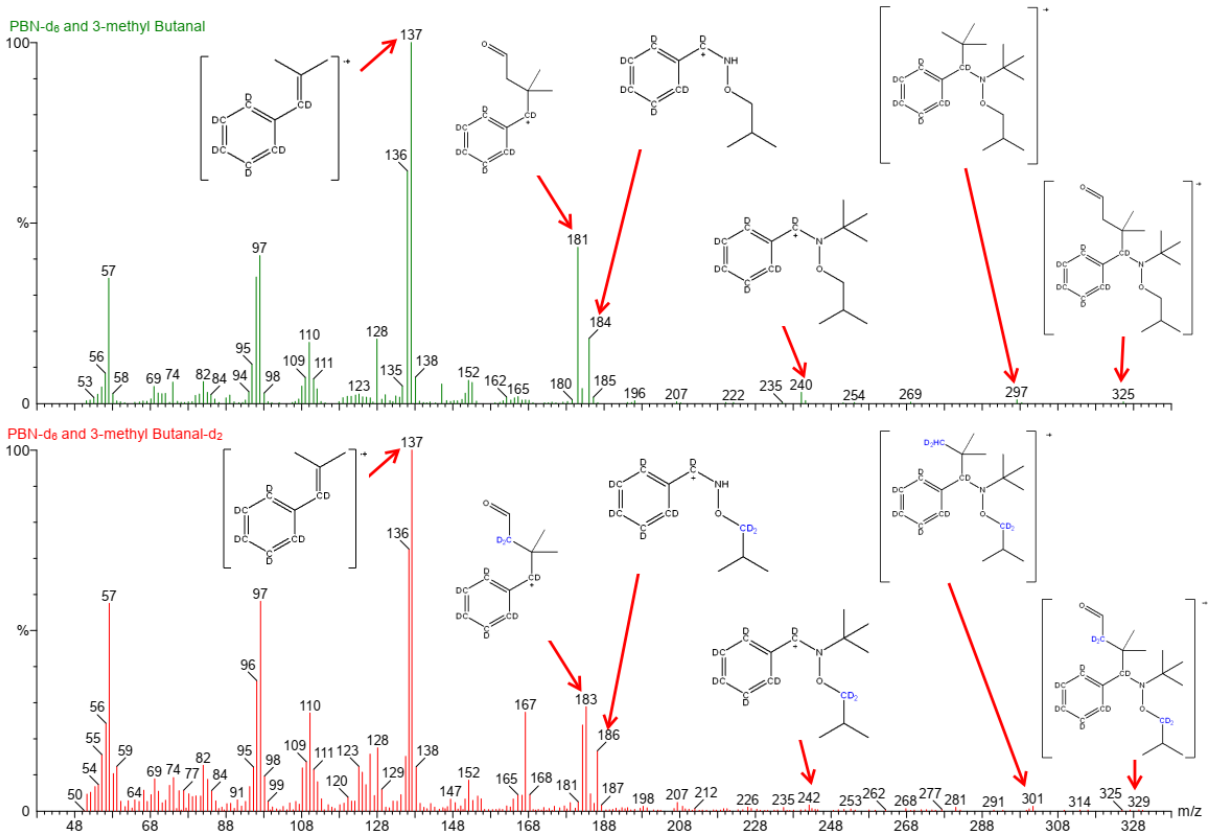

Figure 5.5.2 Electron Ionization mass spectra (EI-MS) corresponding to PBN-d_6 adducts obtained from the analysis of the Fenton reaction mixture containing PBN-d_6, 3-methyl butanal (top) and deuterated 3-methyl butanal-d_2 (bottom) at rt 12.16 minutes

The EI mass spectra in Figure 5.5.2 correspond to a) the PBN-d_6-(CH_3•$C(CH_3)CH_2CHO$)(•$CH_2CH(CH_3)_2$), top (spectrum); and b) the di-deuterated PBN-d_6-(CH_3•$C(CH_3)C\mathbf{D}_2CHO$)(•$C\mathbf{D}_2CH(CH_3)_2$) (bottom spectrum).

When the Fenton reaction was carried out in the presence of 3-methyl butanal as a secondary source of radicals, 3-methyl butanal radicals (CH_3•$C(CH_3)CH_2CHO$) and 2-methyl propyl radicals (•$CH_2CH(CH_3)_2$) are generated by the reaction of •OH with 3-methyl butanal and then trapped by PBN-d_6. The peak at 325 *m/z* units corresponds to the molecular ion of PBN-d_6-(CH_3•$C(CH_3)CH_2CHO$)(•$CH_2CH(CH_3)_2$) adduct (3-methyl butanal radical adding to the alpha carbon atom of the C=N and the 2-methyl propyl radical adding to the oxygen). The fragment at *m/z* 297 is due to the loss of C=O from the butanal radical group of the molecular ion. The loss of the 3-methyl butanal radical from the alpha carbon (on the C=N bond) of the molecular

ion results in *m/z* 240. The further loss of CH_2=CMe_2 from this subsequent fragment (from the nitrogen) leads to 184 *m/z*. The dissociation of the alpha carbon bond and the nitrogen gives *m/z* 181 and further breakdown of this fragment (loss of CH_2CHO) results in base peak *m/z* 137., the peak at *m/z* 96 is the tropylium-d_5 cation and *m/z* 57 is the tertiary butyl cation

Replacing 3-methyl butanal with its deuterated analogue in the Fenton-based reaction demonstrates the production of deuterated 2-methyl propyl radicals and deuterated 3-methyl butanal radicals and subsequent incorporation by the spin trap. As shown by an increase on the molecular ion of 4 *m/z* when 3-methyl butanal-d_2 is used

When the Fenton reaction was carried out in the presence of 3-methyl butanal-2,2-d_2 as a secondary source of radicals, 3-methyl butanal radicals ($CH_3^{\bullet}C(CH_3)C\mathbf{D}_2CHO$) and 2-methyl propyl radicals ($^{\bullet}C\mathbf{D}_2CH(CH_3)_2$) are generated by the reaction of $^{\bullet}OH$ with 3-methyl butanal and then trapped by PBN-d_6. The peak at 329 *m/z* units corresponds to the molecular ion of PBN-d_6-($CH_3^{\bullet}C(CH_3)C\mathbf{D}_2CHO$)($^{\bullet}C\mathbf{D}_2CH(CH_3)_2$) adduct (3-methyl butanal radical adding to the alpha carbon atom of the C=N and the 2-methyl propyl radical adding to the oxygen), demonstrating the deuterated radicals have been incorporated into the molecular ion owing to the 4 *m/z* unit increase. The fragment at *m/z* 301 is due to the loss of C=O from the butanal radical group of the molecular ion. The loss of the 3-methyl butanal radical from the alpha carbon (on the C=N bond) of the molecular ion results in *m/z* 242. The further loss of CH_2=CMe_2 from this subsequent fragment (from the nitrogen) leads to 186 *m/z*. The dissociation of the alpha carbon bond and the nitrogen gives *m/z* 183 and further breakdown of this fragment (loss of $C\mathbf{D}_2CHO$) results in base peak *m/z* 137., the peak at *m/z* 97 is the tropylium-d_6 cation and *m/z* 57 is the tertiary butyl cation

5.5.4 Additional 3-methyl butanal radical and 2-methyl propyl radical adduct of F-PBN (compound 16)

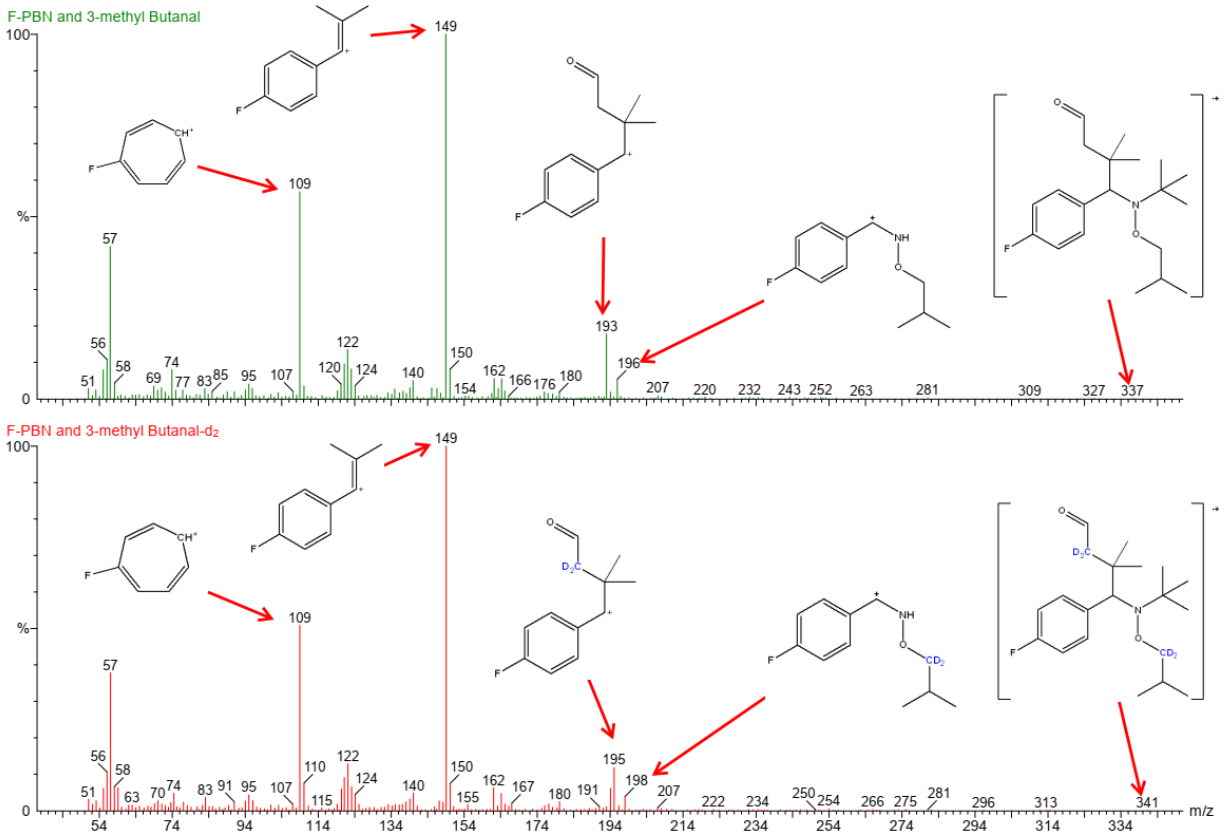

Figure 5.5.3 Electron Ionization mass spectra (EI-MS) corresponding to PBN adducts obtained from the analysis of the Fenton reaction mixture containing F-PBN, 3-methyl butanal (top) and deuterated 3-methyl butanal-d_2 (bottom) at rt 12.16 minutes

The EI mass spectra in Figure 5.5.3 correspond to a) the F-PBN-(CH_3•$C(CH_3)CH_2CHO$)(•$CH_2CH(CH_3)_2$) adduct, top (spectrum); and b) the F-PBN di-deuterated-(CH_3•$C(CH_3)C\mathbf{D}_2CHO$)(•$C\mathbf{D}_2CH(CH_3)_2$) (bottom spectrum).

When the Fenton reaction was carried out in the presence of 3-methyl butanal as a secondary source of radicals, 3-methyl butanal radicals (CH_3•$C(CH_3)CH_2CHO$) and 2-methyl propyl radicals (•$CH_2CH(CH_3)_2$) are generated by the reaction of •OH with 3-methyl butanal and then trapped by F-PBN. The peak at 337 *m/z* units corresponds to the molecular ion of F-PBN-(CH_3•$C(CH_3)CH_2CHO$)(•$CH_2CH(CH_3)_2$) adduct (3-methyl butanal radical adding to the alpha carbon atom of the C=N and the 2-methyl propyl radical adding to the oxygen). The loss of the 3-methyl butanal radical from the alpha carbon (on the C=N bond) of the molecular ion and further loss of CH_2=CMe_2 from this subsequent fragment (from the nitrogen) leads to

196 *m/z*. The dissociation of the alpha carbon bond and the nitrogen gives *m/z* 193 and further breakdown of this fragment (loss of CH_2CHO) results in base peak *m/z* 149., the peak at *m/z* 109 is the tropylium cation and *m/z* 57 is the tertiary butyl cation

Replacing 3-methyl butanal with its deuterated analogue in the Fenton-based reaction demonstrates the production of deuterated 2-methyl propyl radicals and deuterated 3-methyl butanal radicals and subsequent incorporation by the spin trap. As shown by an increase on the molecular ion of 4 *m/z* when 3-methyl butanal-d_2 is used

When the Fenton reaction was carried out in the presence of 3-methyl butanal-2,2-d_2 as a secondary source of radicals, 3-methyl butanal radicals ($CH_3^{\bullet}C(CH_3)C\mathbf{D}_2CHO$) and 2-methyl propyl radicals ($^{\bullet}C\mathbf{D}_2CH(CH_3)_2$) are generated by the reaction of $^{\bullet}OH$ with 3-methyl butanal and then trapped by F-PBN. The peak at 341 *m/z* units corresponds to the molecular ion of F-PBN-($CH_3^{\bullet}C(CH_3)C\mathbf{D}_2CHO$)($^{\bullet}C\mathbf{D}_2CH(CH_3)_2$) adduct (3-methyl butanal radical adding to the alpha carbon atom of the C=N and the 2-methyl propyl radical adding to the oxygen), demonstrating the deuterated radicals have been incorporated into the molecular ion owing to the 4 *m/z* unit increase. The loss of the 3-methyl butanal radical from the alpha carbon (on the C=N bond) of the molecular ion and further loss of $CH_2{=}CMe_2$ from this subsequent fragment (from the nitrogen) leads to 198 *m/z*. The dissociation of the alpha carbon bond and the nitrogen gives *m/z* 195 and further breakdown of this fragment (loss of $C\mathbf{D}_2CHO$) results in base peak *m/z* 149., the peak at *m/z* 109 is the tropylium cation and *m/z* 57 is the tertiary butyl cation

5.6 Detection of 2-methyl propyl and 3-methyl butanal radical adduct (compound 17)

5.6.1 2-methyl propyl radical and 3-methyl butanal radical adduct of PBN (compound 17)

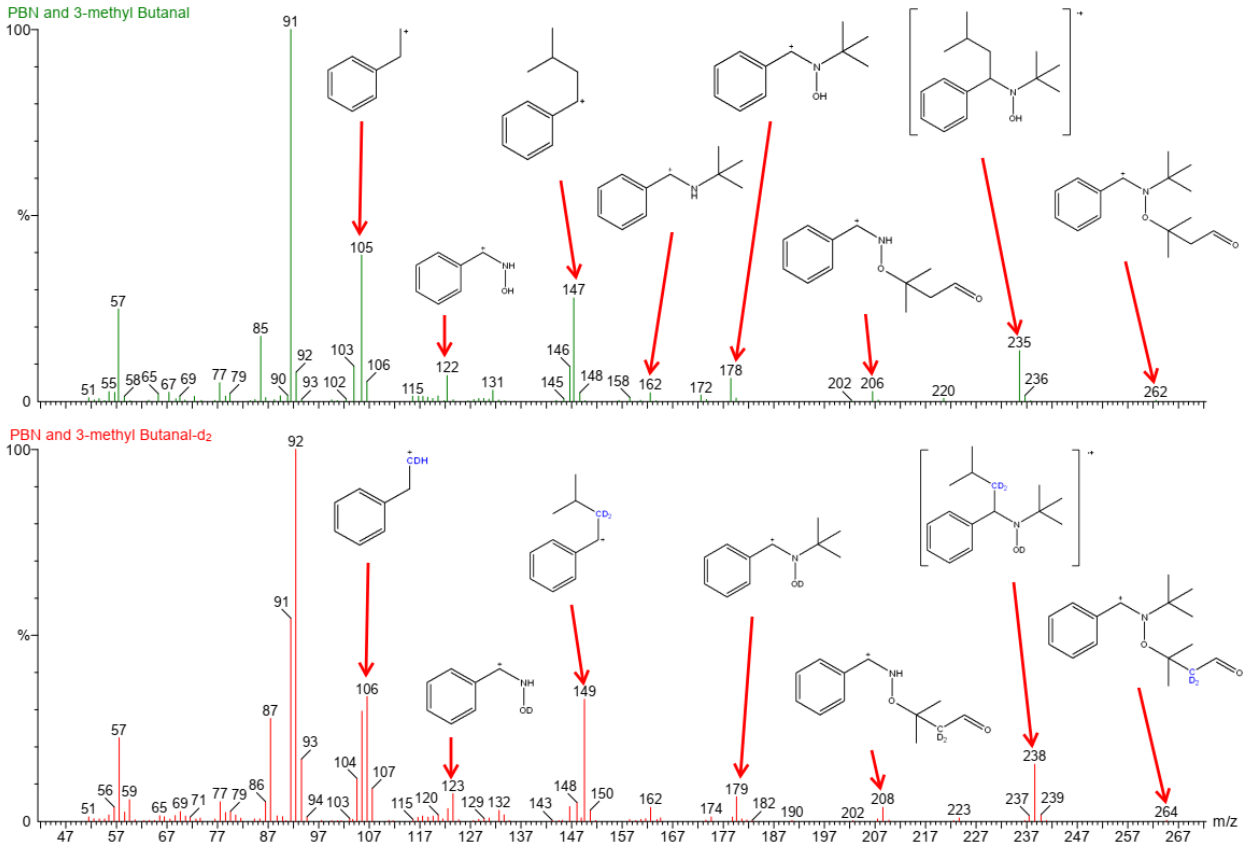

Figure 5.6.1 Electron Ionization mass spectra (EI-MS) corresponding to PBN adducts obtained from the analysis of the Fenton reaction mixture containing PBN, 3-methyl butanal (top) and deuterated 3-methyl butanal-d_2 (bottom) at rt 12.24 minutes

The EI mass spectra in Figure 5.6.1 correspond to a) the PBN-($CH_2CH(CH_3)_2$)($C(CH_3)_2CH_2CHO$) adduct, top (spectrum); and b) the di-deuterated PBN-($C\mathbf{D}_2CH(CH_3)_2$)($C(CH_3)_2C\mathbf{D}_2CHO$) (bottom spectrum).

When the Fenton reaction was carried out in the presence of 3-methyl butanal as a secondary source of radicals, 3-methyl butanal radicals ($CH_3^{\bullet}C(CH_3)CH_2CHO$) and 2-methyl propyl radicals ($^{\bullet}CH_2CH(CH_3)_2$) are generated by the reaction of $^{\bullet}OH$ with 3-methyl butanal and then trapped by PBN. The molecular ion of PBN-($^{\bullet}CH_2CH(CH_3)_2$)($^{\bullet}C(CH_3)_2CH_2CHO$) expected at 319 *m/z* units is too weak to be seen in the EI mass spectra. (2-methyl propyl radical adding to the alpha carbon atom of the C=N and the 3-methyl butanal radical adding to the oxygen). The fragment at *m/z* 262 is extremely weak and due to the loss of ($^{\bullet}CH_2CH(CH_3)_2$) from the alpha carbon of the molecular ion, further loss of $CH_2{=}CMe_2$ from this particular

fragment (from the nitrogen) leads to 206 *m/z* and dissociation of the nitrogen-oxygen bond leads to *m/z* 162. The loss of the 3-methyl butanal radical (from the oxygen site) of the molecular ion results in *m/z* 235 (replaced by hydrogen) subsequent loss of 2-methly propyl radical from the alpha carbon leads to *m/z* 178. The dissociation of the alpha carbon bond and the nitrogen gives *m/z* 147 and further breakdown of this fragment (loss of prop-2-yl radical) results in peak *m/z* 105., the base peak at *m/z* 91 is the tropylium cation and *m/z* 57 is the tertiary butyl cation

Replacing 3-methyl butanal with its deuterated analogue in the Fenton-based reaction demonstrates the production of deuterated 2-methyl propyl radicals and deuterated 3-methyl butanal radicals and subsequent incorporation by the spin trap. As shown by an increase on the molecular ion of 4 *m/z* when 3-methyl butanal-d_2 is used

When the Fenton reaction was carried out in the presence of 3-methyl butanal-2,2-d_2 as a secondary source of radicals, 3-methyl butanal radicals ($CH_3^{\bullet}C(CH_3)C\mathbf{D}_2CHO$) and 2-methyl propyl radicals ($^{\bullet}C\mathbf{D}_2CH(CH_3)_2$) are generated by the reaction of $^{\bullet}OH$ with 3-methyl butanal and then trapped by PBN. The molecular ion of PBN-($CH_3^{\bullet}C(CH_3)C\mathbf{D}_2CHO$)($^{\bullet}C\mathbf{D}_2CH(CH_3)_2$) expected at 323 *m/z* units is too weak to be seen in the EI mass spectra. (2-methyl propyl radical adding to the alpha carbon atom of the C=N and the 3-methyl butanal radical adding to the oxygen). The fragment at *m/z* 264 is due to the loss of ($^{\bullet}C\mathbf{D}_2CH(CH_3)_2$) from the alpha carbon of the molecular ion, further loss of $CH_2{=}CMe_2$ from this particular fragment (from the nitrogen) leads to 208 *m/z* and dissociation of the nitrogen-oxygen bond leads to *m/z* 162. The loss of the 3-methyl butanal radical (from the oxygen site) of the molecular ion results in *m/z* 238 (replaced by deuteron via rearrangement during fragmentation in the EI source) subsequent loss of 2-methly propyl radical from the alpha carbon leads to *m/z* 179. The dissociation of the alpha carbon bond and the nitrogen gives *m/z* 149 (demonstrating retention of deuterated radical) and further breakdown of this fragment (loss of prop-2-yl radical) results in peak *m/z* 106 (containing a remnant deuteron during fragmentation)., the base peak at *m/z* 92 is the tropylium-1-*d* cation and *m/z* 57 is the tertiary butyl cation

5.6.2 2-methyl propyl radical and 3-methyl butanal radical adduct of PBN-d_6 (compound 17)

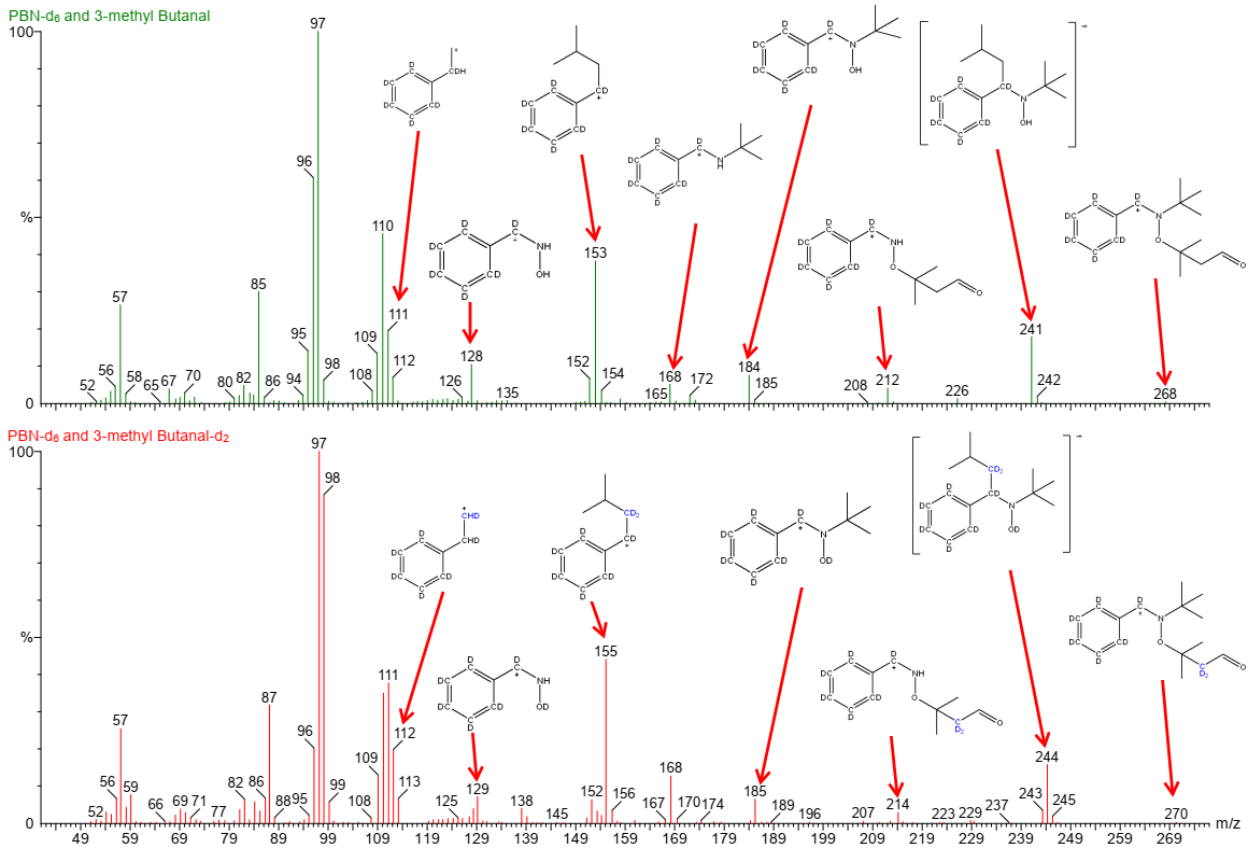

Figure 5.6.2 Electron Ionization mass spectra (EI-MS) corresponding to PBN-d_6 adducts obtained from the analysis of the Fenton reaction mixture containing PBN-d_6, 3-methyl butanal (top) and deuterated 3-methyl butanal-d_2 (bottom) at rt 12.24 minutes

The EI mass spectra in Figure 5.6.2 correspond to a) the PBN-d_6-$(CH_2CH(CH_3)_2)(C(CH_3)_2CH_2CHO)$ adduct, top (spectrum); and b) the di-deuterated PBN-d_6-$(C\mathbf{D}_2CH(CH_3)_2)(C(CH_3)_2C\mathbf{D}_2CHO)$ (bottom spectrum).

When the Fenton reaction was carried out in the presence of 3-methyl butanal as a secondary source of radicals, 3-methyl butanal radicals ($CH_3^{\bullet}C(CH_3)CH_2CHO$) and 2-methyl propyl radicals ($^{\bullet}CH_2CH(CH_3)_2$) are generated by the reaction of $^{\bullet}OH$ with 3-methyl butanal and then trapped by PBN-d_6. The molecular ion of PBN-$(CH_2CH(CH_3)_2)(C(CH_3)_2CH_2CHO)$ expected at 325 *m/z* units is too weak to be seen in the EI mass spectra. (2-methyl propyl radical adding to the alpha carbon atom of the C=N and the 3-methyl butanal radical adding to the oxygen). The fragment at *m/z* 268 is extremely weak and due to the loss of ($^{\bullet}CH_2CH(CH_3)_2$) from the alpha carbon of the molecular ion, further loss of CH_2=CMe_2 from this particular fragment (from the nitrogen) leads to 212 *m/z* and dissociation of the nitrogen-oxygen bond leads to *m/z*

168. The loss of the 3-methyl butanal radical (from the oxygen site) of the molecular ion results in *m/z* 241 (replaced by hydrogen) subsequent loss of 2-methly propyl radical from the alpha carbon leads to *m/z* 184. The dissociation of the alpha carbon bond and the nitrogen gives *m/z* 153 and further breakdown of this fragment (loss of prop-2-yl radical) results in peak *m/z* 110., the base peak at *m/z* 97 is the tropylium-d_6 cation and *m/z* 57 is the tertiary butyl cation

Replacing 3-methyl butanal with its deuterated analogue in the Fenton-based reaction demonstrates the production of deuterated 2-methyl propyl radicals and deuterated 3-methyl butanal radicals and subsequent incorporation by the spin trap. As shown by an increase on the molecular ion of 4 *m/z* when 3-methyl butanal-d_2 is used

When the Fenton reaction was carried out in the presence of 3-methyl butanal-2,2-d_2 as a secondary source of radicals, 3-methyl butanal radicals ($CH_3{}^{\bullet}C(CH_3)C\mathbf{D}_2CHO$) and 2-methyl propyl radicals (${}^{\bullet}C\mathbf{D}_2CH(CH_3)_2$) are generated by the reaction of ${}^{\bullet}OH$ with 3-methyl butanal and then trapped by PBN-d_6. The molecular ion of PBN-d_6-($CH_3{}^{\bullet}C(CH_3)C\mathbf{D}_2CHO$)(${}^{\bullet}C\mathbf{D}_2CH(CH_3)_2$) expected at 329 *m/z* units is too weak to be seen in the EI mass spectra. (2-methyl propyl radical adding to the alpha carbon atom of the C=N and the 3-methyl butanal radical adding to the oxygen). The fragment at *m/z* 270 is due to the loss of (${}^{\bullet}C\mathbf{D}_2CH(CH_3)_2$) from the alpha carbon of the molecular ion, further loss of $CH_2{=}CMe_2$ from this particular fragment (from the nitrogen) leads to 214 *m/z* and dissociation of the nitrogen-oxygen bond leads to *m/z* 168. The loss of the 3-methyl butanal radical (from the oxygen site) of the molecular ion results in *m/z* 244 (replaced by deuteron via rearrangement during fragmentation in the EI source) subsequent loss of 2-methly propyl radical from the alpha carbon leads to *m/z* 185. The dissociation of the alpha carbon bond and the nitrogen gives *m/z* 155 (demonstrating retention of deuterated radical) and further breakdown of this fragment (loss of prop-2-yl radical) results in peak *m/z* 112 (containing a remnant deuteron during fragmentation)., the base peak at *m/z* 97 is the tropylium-d_6 cation and *m/z* 57 is the tertiary butyl cation

5.6.3 2-methyl propyl radical and 3-methyl butanal radical adduct of F-PBN (compound 17)

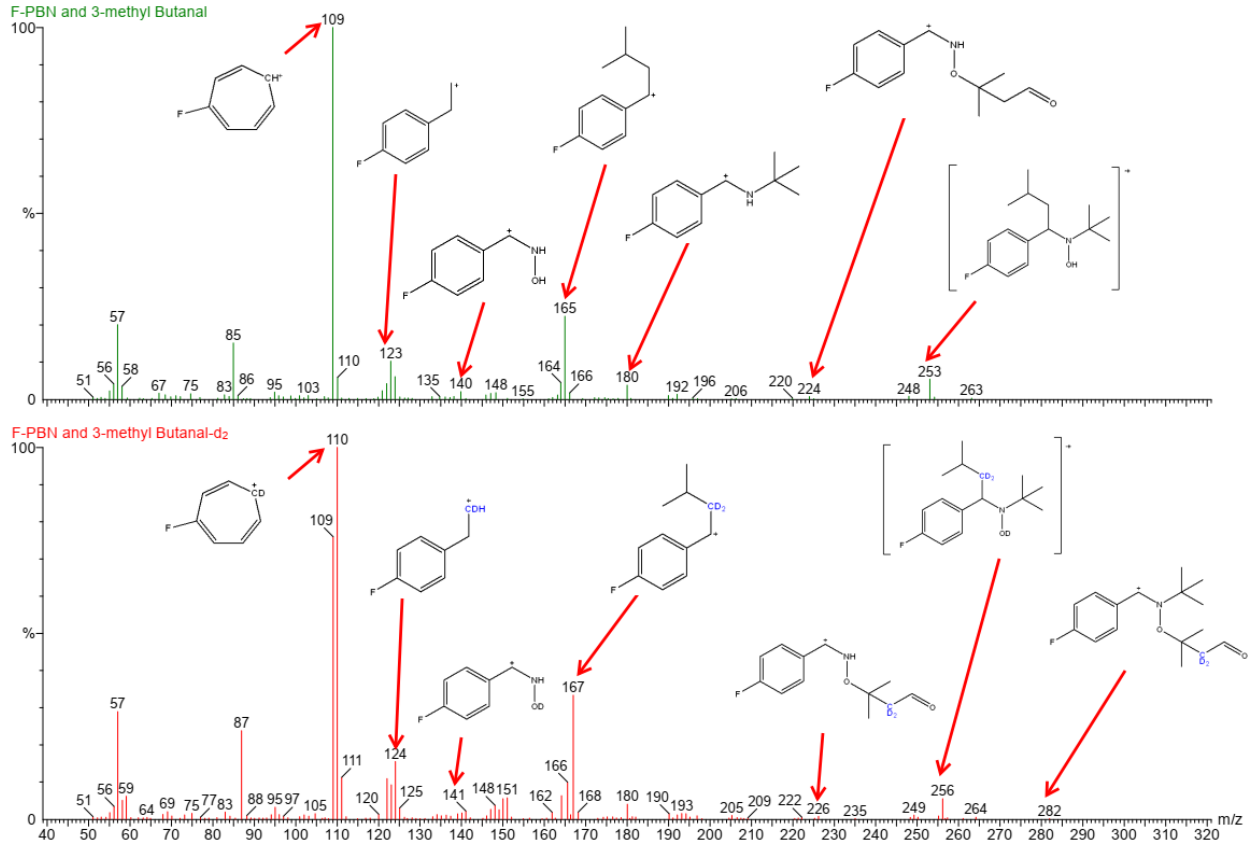

Figure 5.6.3 Electron Ionization mass spectra (EI-MS) corresponding to PBN adducts obtained from the analysis of the Fenton reaction mixture containing F-PBN, 3-methyl butanal (top) and deuterated 3-methyl butanal-d_2 (bottom) at rt 12.24 minutes

The EI mass spectra in Figure 5.6.3 correspond to a) the F-PBN-($CH_2CH(CH_3)_2$)($C(CH_3)_2CH_2CHO$) adduct, top (spectrum); and b) the di-deuterated F-PBN-($C\mathbf{D}_2CH(CH_3)_2$)($C(CH_3)_2C\mathbf{D}_2CHO$) (bottom spectrum).

When the Fenton reaction was carried out in the presence of 3-methyl butanal as a secondary source of radicals, 3-methyl butanal radicals ($CH_3^{\bullet}C(CH_3)CH_2CHO$) and 2-methyl propyl radicals ($^{\bullet}CH_2CH(CH_3)_2$) are generated by the reaction of $^{\bullet}OH$ with 3-methyl butanal and then trapped by F-PBN. The molecular ion of PBN-($CH_2CH(CH_3)_2$)($C(CH_3)_2CH_2CHO$) expected at 337 *m/z* units is too weak to be seen in the EI mass spectra. (2-methyl propyl radical adding to the alpha carbon atom of the C=N and the 3-methyl butanal radical adding to the oxygen). The fragment at *m/z* 280 is also not visible on the spectrum due to the loss of ($^{\bullet}CH_2CH(CH_3)_2$) from the alpha carbon of the molecular ion (however seen when using PBN and PBN-d_6), further loss of CH_2=CMe_2 from this particular fragment (from the nitrogen) leads to 224 *m/z* and

dissociation of the nitrogen-oxygen bond leads to *m/z* 180. The loss of the 3-methyl butanal radical (from the oxygen site) of the molecular ion results in *m/z* 253 (replaced by hydrogen) subsequent loss of 2-methly propyl radical from the alpha carbon leads to *m/z* 196. The dissociation of the alpha carbon bond and the nitrogen gives *m/z* 165 and further breakdown of this fragment (loss of prop-2-yl radical) results in peak *m/z* 123., the base peak at *m/z* 109 is the fluoro-tropylium cation and *m/z* 57 is the tertiary butyl cation

Replacing 3-methyl butanal with its deuterated analogue in the Fenton-based reaction demonstrates the production of deuterated 2-methyl propyl radicals and deuterated 3-methyl butanal radicals and subsequent incorporation by the spin trap. As shown by an increase on the molecular ion of 4 *m/z* when 3-methyl butanal-d_2 is used

When the Fenton reaction was carried out in the presence of 3-methyl butanal-2,2-d_2 as a secondary source of radicals, 3-methyl butanal radicals ($CH_3^{\bullet}C(CH_3)C\mathbf{D}_2CHO$) and 2-methyl propyl radicals ($^{\bullet}C\mathbf{D}_2CH(CH_3)_2$) are generated by the reaction of $^{\bullet}OH$ with 3-methyl butanal and then trapped by PBN. The molecular ion of PBN-($CH_3^{\bullet}C(CH_3)C\mathbf{D}_2CHO$)($^{\bullet}C\mathbf{D}_2CH(CH_3)_2$) expected at 341 *m/z* units is too weak to be seen in the EI mass spectra. (2-methyl propyl radical adding to the alpha carbon atom of the C=N and the 3-methyl butanal radical adding to the oxygen). The fragment at *m/z* 282 is weak yet visible due to the loss of ($^{\bullet}C\mathbf{D}_2CH(CH_3)_2$) from the alpha carbon of the molecular ion, further loss of CH_2=CMe_2 from this particular fragment (from the nitrogen) leads to 226 *m/z* and dissociation of the nitrogen-oxygen bond leads to *m/z* 180. The loss of the 3-methyl butanal radical (from the oxygen site) of the molecular ion results in *m/z* 256 (replaced by deuteron via rearrangement during fragmentation in the EI source). The dissociation of the alpha carbon bond and the nitrogen gives *m/z* 167 (demonstrating retention of deuterated radical) and further breakdown of this fragment (loss of prop-2-yl radical) results in peak *m/z* 124 (containing a remnant deuteron during fragmentation)., the base peak at *m/z* 110 is the fluorotropylium-1-*d* cation and *m/z* 57 is the tertiary butyl cation

5.7 Chromatogram of Spin trapping PBN derivatives and 3-methyl butanal and DMSO as a competing source of secondary radicals forming DMSO radicals

To understand the orientation of the adducts formed a secondary competing source of radicals was introduced in the form of methyl radicals derived from DMSO. It was hypothesised that alkyl/alkoxy and methyl hybrid adducts would form and show as new peaks on the TIC

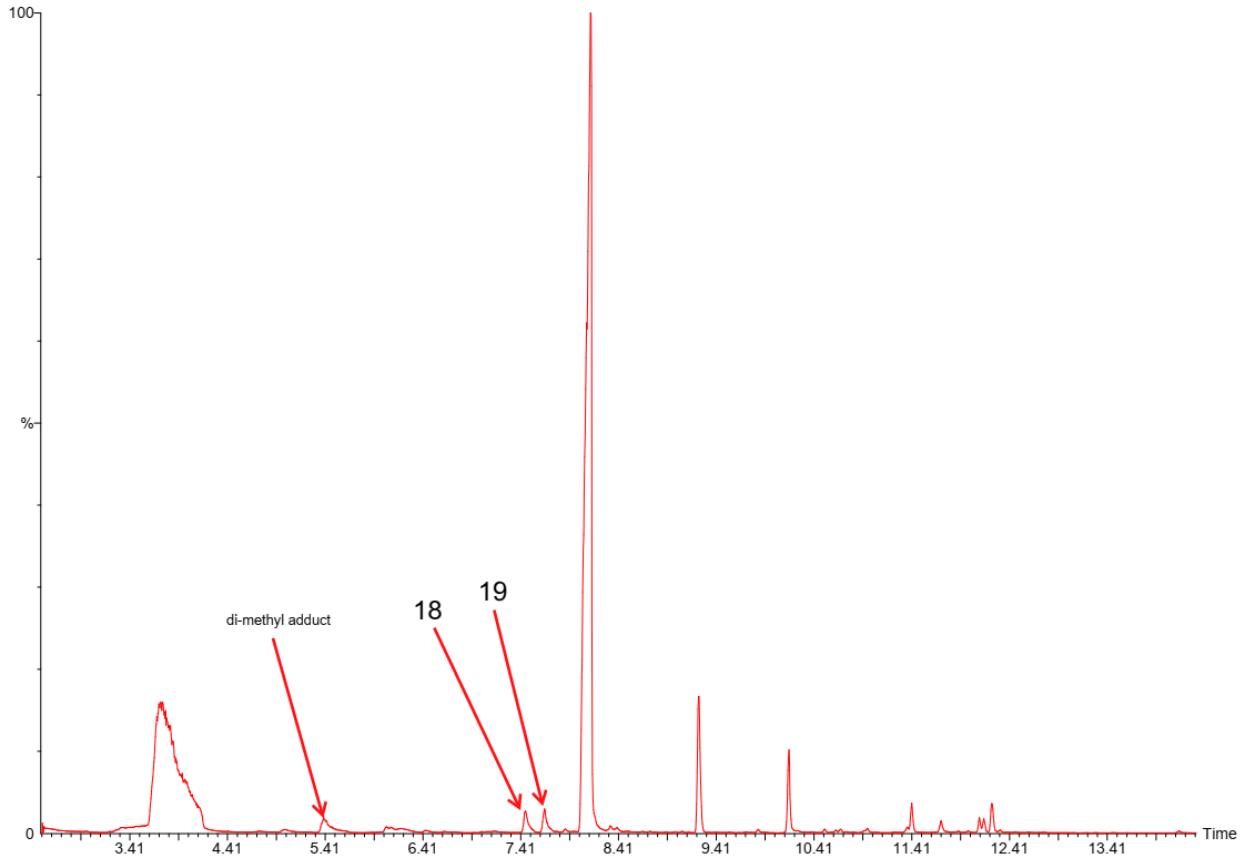

Figure 5.7.1 The total ion chromatogram obtained from the GC-MS analysis of the Fenton system with PBN in the presence of 3-methyl butanal and DMSO

The TIC shown in Figure 5.7.1 was obtained from the Fenton-based reaction containing PBN as the spin trap and 3-methyl butanal as a secondary source of free radicals however DMSO was added as a competing secondary source of radicals to produce methyl radicals ($^{\bullet}CH_3$). Three more significant peaks at rt 5.41 minutes, rt 7.46 minutes and rt 7.62 minutes have appeared. The peak at 5.41 minutes corresponds to the PBN-$(CH_3)_2$ adduct, the peak at rt 7.46 minutes (compound 18) corresponds to the PBN-$(CH_2CH(CH_3)_2)(CH_3)$, the peak at 7.62 minutes (Compound 19) corresponds to PBN-$(CH_3)(CH_2CH(CH_3)_2)$.

For the di methyl adduct please refer to section 4.9 Detection of Methyl ($^{\bullet}CH_3$) radical from DMSO

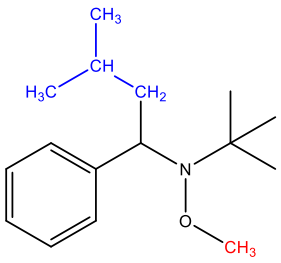

Compound 18 (peak 18)

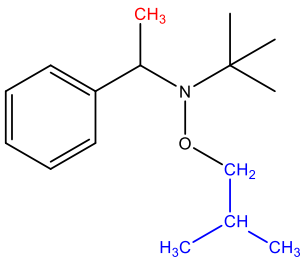

Compound 19 (peak 19)

Figure 5.7.2 The structures of additional compounds identified by GC-MS analysis of a Fenton based reaction mixture containing PBN, butanal and DMSO. The atoms in red are believed to be derived from DMSO and the blue from 3-methyl butanal

5.8 Detection of C-2-methyl propyl {$(CH_3)_2CH^{\bullet}CH_2$} radical and O-Methyl ($^{\bullet}CH_3$) radical from DMSO (peak/compound 18)

5.8.1 Mono-2-methyl propyl monomethyl adduct of PBN with 3-methylbutanal and DMSO (compound 18)

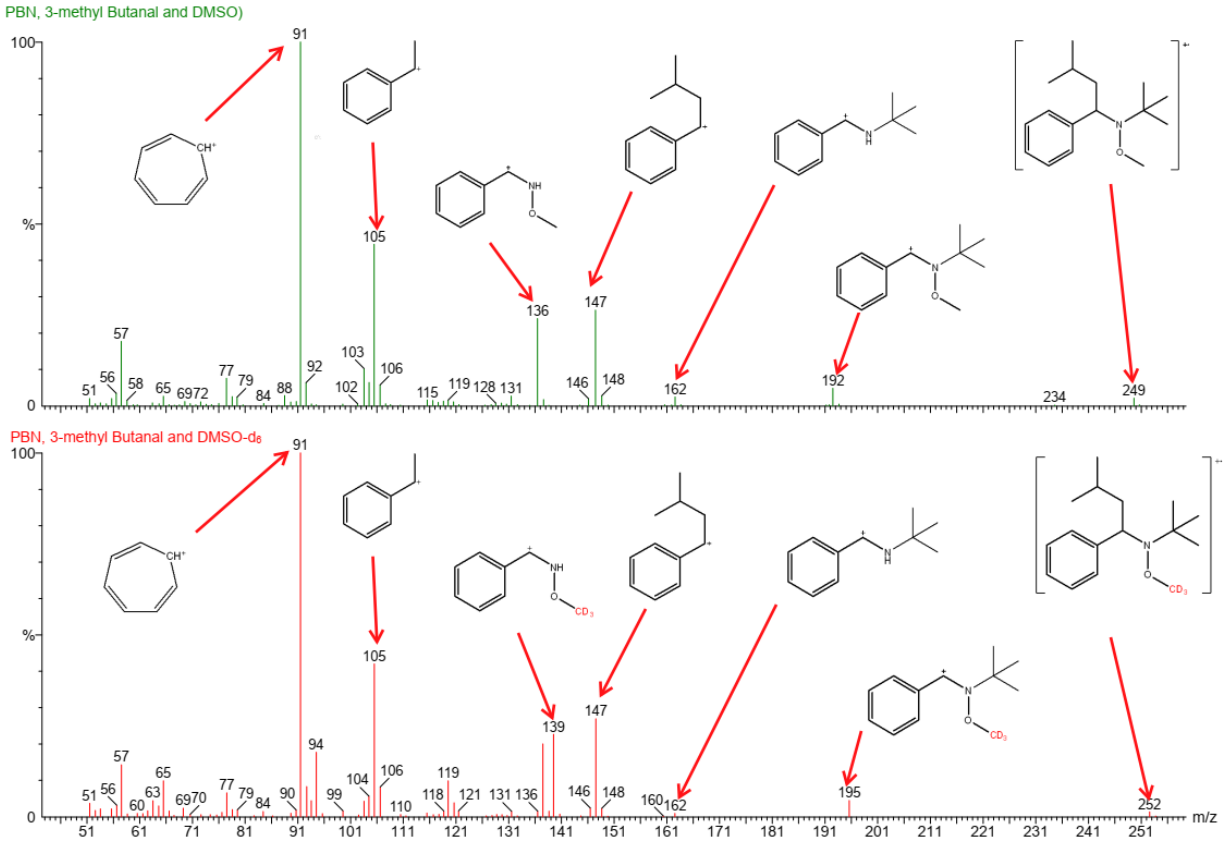

Figure 5.8.1 Electron Ionization mass spectra (EI-MS) corresponding to PBN adduct obtained from the analysis of the Fenton reaction mixture containing PBN, 3-methylbutanal and DMSO or DMSO-d_6 at rt 7.46 minutes

The EI mass spectra shown in Figure 5.8.1 correspond to the a) PBN-$(CH_2CH(CH_3)_2)(CH_3)$ (top spectra), and b) the deuterated methyl group PBN-$(CH_2CH(CH_3)_2)(C\mathbf{D}_3)$ (bottom spectra).

When the Fenton reaction was carried out in the presence of 3-methyl butanal and DMSO as a competing secondary source of radicals, methyl radicals ($^{\bullet}CH_3$) were also generated by the reaction of $^{\bullet}OH$ with DMSO and were then trapped by PBN. The peak at *m/z* 249 units corresponds to the molecular ion of PBN-$(CH_2CH(CH_3)_2)(CH_3)$. The fragment at *m/z* 234 is the loss of a methyl group from the molecular ion (from

the tBu group). The loss from the molecular ion of the 2-methyl propyl group from the alpha carbon position results in *m/z* 192 and further loss of (CH_3O) from this fragment results in *m/z* 162 .The dissociation of the alpha carbon bond and the nitrogen gives the isopentyl benzene cation at *m/z* 147. Further breakdown of this fragment results in the ethyl benzene cation at *m/z* 105 and the base peak *m/z* 91 tropylium cation and a phenyl cation at *m/z* 77. The peak at *m/z* 136 is N-benzyl-O-methyl hydroxylamine. The peak at *m/z* 57 is the tertiary butyl cation

When the Fenton reaction was carried out in the presence of butanal and deuterated DMSO as a competing secondary source of radicals deuterated methyl radicals ($^{\bullet}CD_3$) were also generated by the reaction of $^{\bullet}OH$ with DMSO and were then trapped by PBN. Replacing DMSO with d_6-DMSO in the Fenton-based reaction mixture gives rise to an increase in the *m/z* value of the molecular ion of 3 *m/z* units. The peak at *m/z* 252 units corresponds to the molecular ion of PBN-($CH_2CH(CH_3)_2$)($C\mathbf{D}_3$). The loss from the molecular ion of the 2-methyl propyl group from the alpha carbon position results in *m/z* 195 and further loss of ($C\mathbf{D}_3O$)from this fragment results in *m/z* 162. The dissociation of the alpha carbon bond and the nitrogen gives the isopentyl benzene cation at *m/z* 147. Further breakdown of this fragment results in the results in the ethyl benzene cation at *m/z* 105 and base peak *m/z* 91 tropylium cation and a phenyl cation at *m/z* 77. The peak at *m/z* 139 is N-benzyl-O-(methyl-d_3)hydroxylamine with an increase of 3 *m/z* units. The peak at *m/z* 57 is the tertiary butyl cation

5.8.2 Mono-2-methyl propyl monomethyl adduct of PBN with 3-methylbutanal-d_2 and DMSO (compound 18)

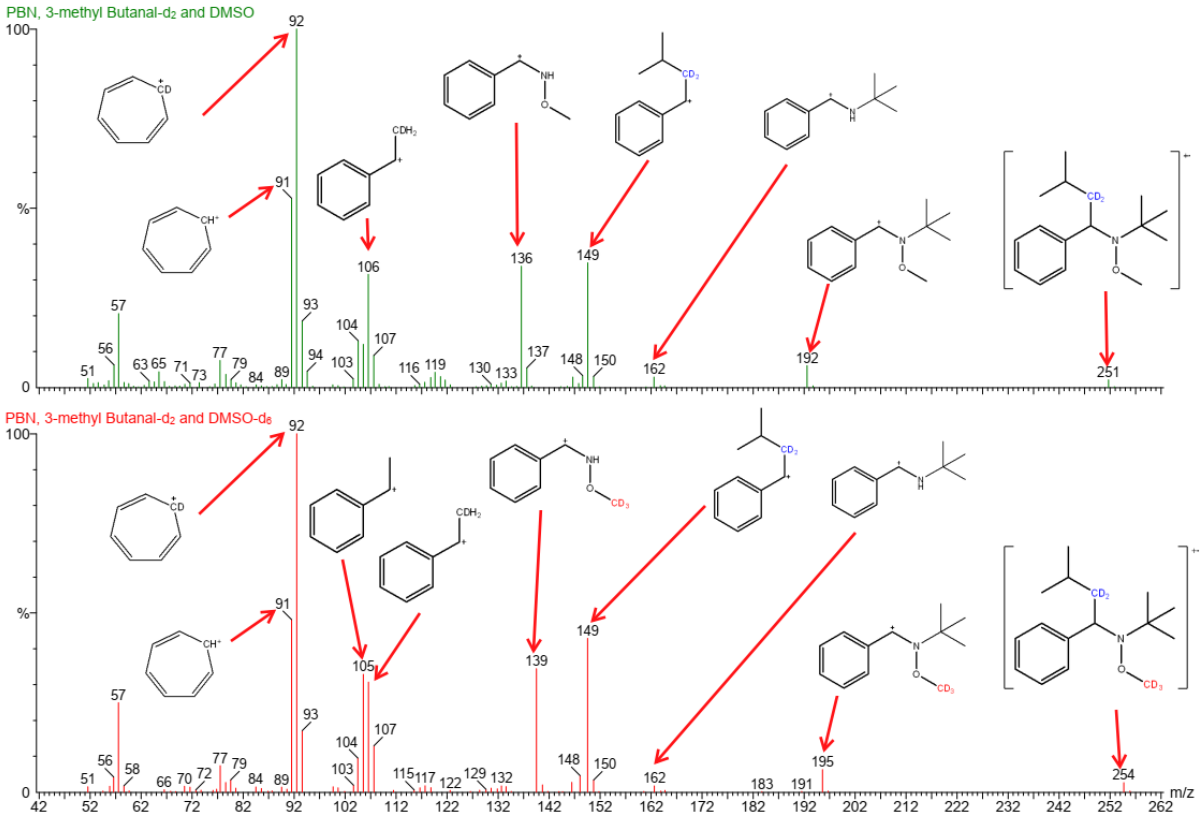

Figure 5.8.2 Electron Ionization mass spectra (EI-MS) corresponding to PBN adduct obtained from the analysis of the Fenton reaction mixture containing PBN, 3-methylbutanal-d_2 and DMSO or DMSO-d_6 at rt 7.46 minutes

The EI mass spectra shown in Figure 5.8.2 correspond to the a) PBN-(C**D**$_2$CH(CH$_3$)$_2$)(CH$_3$) (top spectra), and b) the deuterated methyl group PBN-(C**D**$_2$CH(CH$_3$)$_2$)(C**D**$_3$) (bottom spectra).

Replacing 3-methyl butanal with its deuterated analogue in the Fenton-based reaction demonstrates the production of deuterated 2-methyl propyl radicals and subsequent incorporation by the spin trap. As shown by an increase on the molecular ion of 2 *m/z* when 3-methyl butanal-d_2 is used

When the Fenton reaction was carried out in the presence of 3-methyl butanal and DMSO as a competing secondary source of radicals, methyl radicals (•CH$_3$) were also generated by the reaction of •OH with DMSO and were then trapped by PBN. The peak at *m/z* 251 units corresponds to the molecular ion of PBN-(CH$_2$CH(CH$_3$)$_2$)(CH$_3$) 2 *m/z* unit increase. The loss from the molecular ion of the 2-methyl propyl group from

the alpha carbon position results in *m/z* 192 and further loss of (CH_3O) from this fragment results in *m/z* 162 .The dissociation of the alpha carbon bond and the nitrogen gives the isopentyl benzene cation at *m/z* 149 (retaining 2 deuterium). Further breakdown of this fragment results in the ethyl benzene cation at *m/z* 106 (deuteron has been retained when rearranging post fragmentation) and the base peak *m/z* 92 tropylium1-d cation and a phenyl cation at *m/z* 77. The peak at *m/z* 136 is N-benzyl-O-methyl hydroxylamine. The peak at *m/z* 57 is the tertiary butyl cation

When the Fenton reaction was carried out in the presence of butanal and deuterated DMSO as a competing secondary source of radicals deuterated methyl radicals ($^{\bullet}CD_3$) were also generated by the reaction of $^{\bullet}OH$ with DMSO and were then trapped by PBN. Replacing DMSO with d_6-DMSO in the Fenton-based reaction mixture gives rise to an increase in the *m/z* value of the molecular ion of 3 *m/z* units. The peak at *m/z* 254 units corresponds to the molecular ion of PBN-($CH_2CH(CH_3)_2$)($C\mathbf{D}_3$) with a 2 *m/z* unit increase demonstrating the incorporation of two deuterium. The loss from the molecular ion of the 2-methyl propyl group from the alpha carbon position results in *m/z* 195 and further loss of ($C\mathbf{D}_3O$)from this fragment results in *m/z* 162 .The dissociation of the alpha carbon bond and the nitrogen gives the isopentyl benzene cation at *m/z* 149 (retaining 2 deuterium). Further breakdown of this fragment results in the results in the ethyl benzene-1-d cation at *m/z* 106 and base peak *m/z* 91 tropylium cation and a phenyl cation at *m/z* 77. The peak at *m/z* 139 is N-benzyl-O-(methyl-d_3)hydroxylamine with an increase of 3 *m/z* units. The peak at *m/z* 57 is the tertiary butyl cation

5.8.3 Mono-2-methyl propyl monomethyl adduct of PBN-d_6 with 3-methylbutanal and DMSO (compound 18)

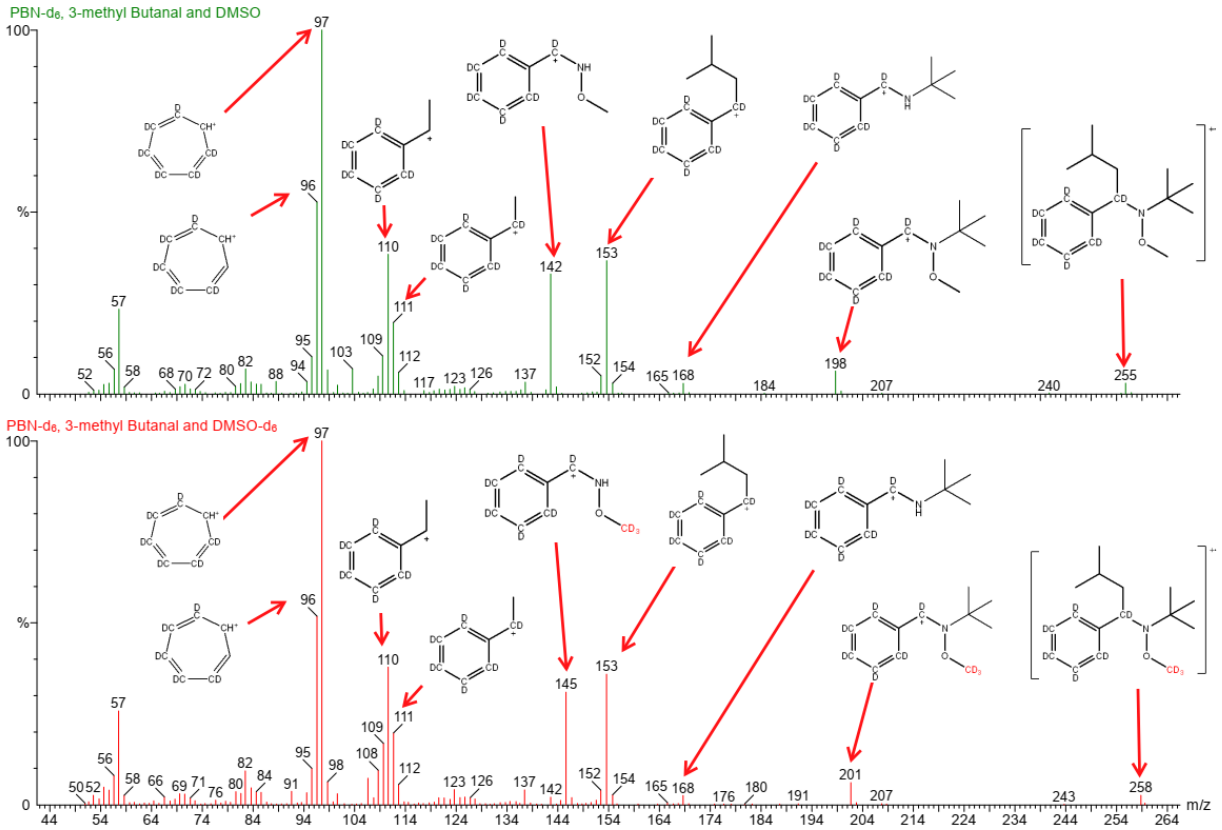

Figure 5.8.3 Electron Ionization mass spectra (EI-MS) corresponding to PBN adduct obtained from the analysis of the Fenton reaction mixture containing PBN-d_6, 3-methyl-butanal and DMSO or DMSO-d_6 at rt 7.46 minutes

The EI mass spectra shown in Figure 5.8.3 correspond to the a) PBN-d_6-$(CH_2CH(CH_3)_2)(CH_3)$ (top spectra), and b) the deuterated methyl group PBN-d_6-$(CH_2CH(CH_3)_2)(C\mathbf{D}_3)$ (bottom spectra).

When the Fenton reaction was carried out in the presence of 3-methyl butanal and DMSO as a competing secondary source of radicals, methyl radicals ($^{\bullet}CH_3$) were also generated by the reaction of $^{\bullet}OH$ with DMSO and were then trapped by PBN-d_6. The peak at *m/z* 255 units corresponds to the molecular ion of PBN-d_6-$(CH_2CH(CH_3)_2)(CH_3)$. The fragment at *m/z* 240 is the loss of a methyl group from the molecular ion (from the tBu group). The loss from the molecular ion of the 2-methyl propyl group from the alpha carbon position results in *m/z* 198 and further loss of (CH_3O) from this fragment results in *m/z* 168 .The dissociation of the alpha carbon bond and the nitrogen gives the isopentyl benzene cation at *m/z* 153.

Further breakdown of this fragment results in ethyl-1-d benzene-d_5 cation at *m/z* 111 and ethyl benzene-d_5 cation at *m/z* 110 and the base peak *m/z* 97 tropylium-d_6 cation and a phenyl-d_5 cation at *m/z* 82. The peak at *m/z* 142 is N-benzyl-d_5-O-methyl hydroxylamine-1-d. The peak at *m/z* 57 is the tertiary butyl cation

When the Fenton reaction was carried out in the presence of butanal and deuterated DMSO as a competing secondary source of radicals deuterated methyl radicals ($^{\bullet}CD_3$) were also generated by the reaction of $^{\bullet}OH$ with DMSO and were then trapped by PBN-d_6. Replacing DMSO with d_6-DMSO in the Fenton-based reaction mixture gives rise to an increase in the *m/z* value of the molecular ion of 3 *m/z* units. The peak at *m/z* 258 units corresponds to the molecular ion of PBN-d_6-($CH_2CH(CH_3)_2$)($C\mathbf{D}_3$). The fragment at *m/z* 243 is the loss of a methyl group from the molecular ion (from the tBu group) The loss from the molecular ion of the 2-methyl propyl group from the alpha carbon position results in *m/z* 201 and further loss of ($C\mathbf{D}_3O$)from this fragment results in *m/z* 168. The dissociation of the alpha carbon bond and the nitrogen gives the isopent-1-yl benzene-d_5 cation at *m/z* 153. Further breakdown of this fragment results in ethyl-1-d benzene-d_5 cation at *m/z* 111 and ethyl benzene-d_5 cation at *m/z* 110 and the base peak *m/z* 97 tropylium-d_6 cation and a phenyl-d_5 cation at *m/z* 82.The peak at *m/z* 145 is N-benzyl-d_6-O-(methyl-d_3)hydroxylamine with an increase of 3 *m/z* units. The peak at *m/z* 57 is the tertiary butyl cation

5.8.4 Mono-2-methyl propyl monomethyl adduct of PBN-d_6 with 3-methylbutanal-d_2 and DMSO (compound 18)

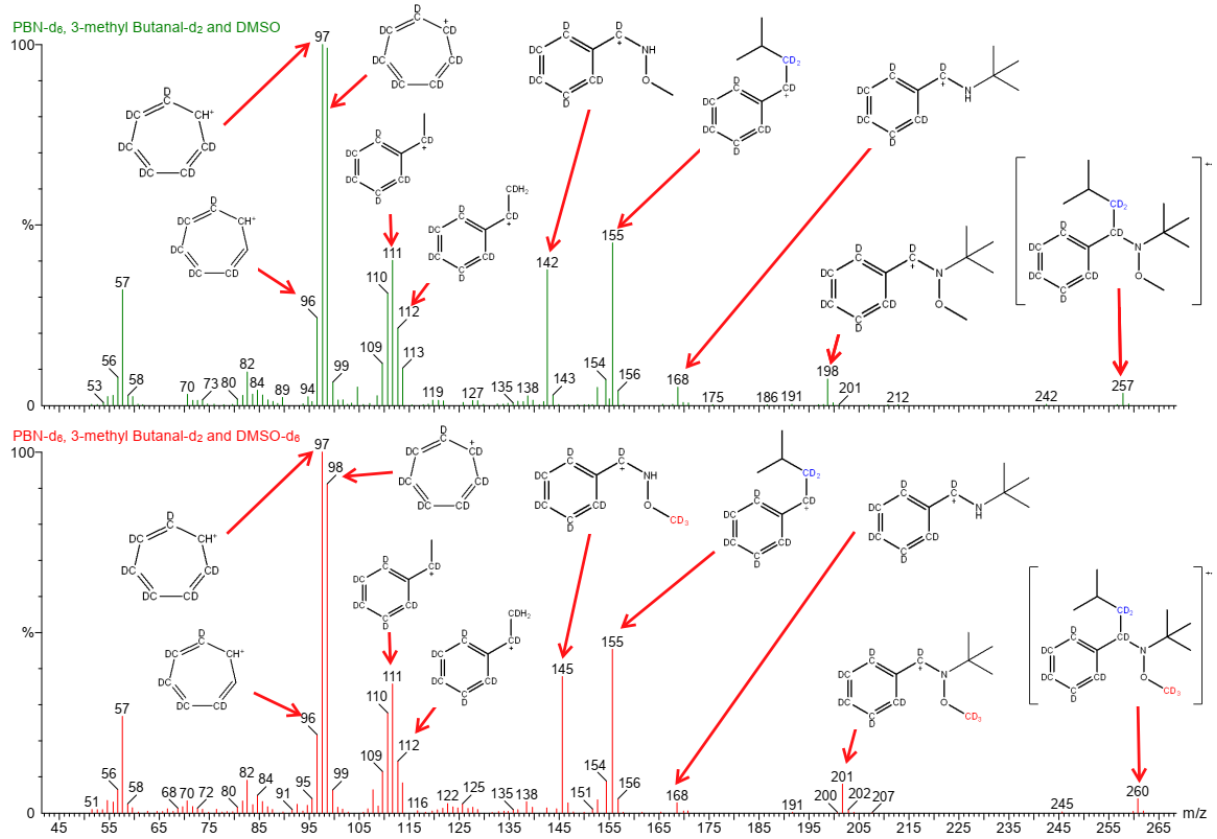

Figure 5.8.4 Electron Ionization mass spectra (EI-MS) corresponding to PBN-d_6 adduct obtained from the analysis of the Fenton reaction mixture containing PBN-d_6, 3-methyl-butanal-d_2 and DMSO (top) or DMSO-d_6 (bottom)at rt 7.46 minutes

The EI mass spectra shown in Figure 5.8.4 correspond to the a) PBN-d_6-($CH_2CH(CH_3)_2$)(CH_3) (top spectra), and b) the deuterated methyl group PBN-d_6-($^{\bullet}C\mathbf{D}_2CH(CH_3)_2$)($C\mathbf{D}_3$) (bottom spectra).

Replacing 3-methyl butanal with its deuterated analogue in the Fenton-based reaction demonstrates the production of deuterated 2-methyl propyl radicals and subsequent incorporation by the spin trap. As shown by an increase on the molecular ion of 2 *m/z* when 3-methyl butanal-d_2 is used

When the Fenton reaction was carried out in the presence of 3-methyl butanal and DMSO as a competing secondary source of radicals, methyl radicals ($^{\bullet}CH_3$) were also generated by the reaction of $^{\bullet}OH$ with DMSO and were then trapped by PBN-d_6. The peak at *m/z* 257 units corresponds to the molecular ion of PBN-d_6-($C\mathbf{D}_2CH(CH_3)_2$)(CH_3). The fragment at *m/z* 242 is the loss of a methyl group from the molecular ion (from

the tBu group). The loss from the molecular ion of the 2-methyl propyl group from the alpha carbon position results in *m/z* 198 and further loss of (CH_3O) from this fragment results in *m/z* 168 .The dissociation of the alpha carbon bond and the nitrogen gives the isopentyl benzene cation at *m/z* 155. Further breakdown of this fragment results in ethyl-1-d benzene-d_5 cation at *m/z* 111 and ethyl benzene-d_5 cation at *m/z* 110 and the base peak *m/z* 97 tropylium-d_6 cation and a phenyl-d_5 cation at *m/z* 82. The peak at *m/z* 142 is N-benzyl-d_5-O-methyl hydroxylamine-1-d. The peak at *m/z* 57 is the tertiary butyl cation

When the Fenton reaction was carried out in the presence of butanal and deuterated DMSO as a competing secondary source of radicals deuterated methyl radicals ($^{\bullet}CD_3$) were also generated by the reaction of $^{\bullet}OH$ with DMSO and were then trapped by PBN-d_6. Replacing DMSO with d_6-DMSO in the Fenton-based reaction mixture gives rise to an increase in the *m/z* value of the molecular ion of 3 *m/z* units. The peak at *m/z* 260 units corresponds to the molecular ion of PBN-d_6-(C**D**$_2$CH(CH_3)$_2$)(C**D**$_3$). The fragment at *m/z* 245 is the loss of a methyl group from the molecular ion (from the tBu group) The loss from the molecular ion of the 2-methyl propyl group from the alpha carbon position results in *m/z* 201 and further loss of (C**D**$_3$O)from this fragment results in *m/z* 168. The dissociation of the alpha carbon bond and the nitrogen gives the isopent-1-yl benzene-d_5 cation at *m/z* 155. Further breakdown of this fragment results in ethyl-1-d benzene-d_5 cation at *m/z* 111 and ethyl benzene-d_5 cation at *m/z* 110 and the base peak *m/z* 97 tropylium-d_6 cation and a phenyl-d_5 cation at *m/z* 82.The peak at *m/z* 145 is N-benzyl-O-(methyl-d_3)hydroxylamine with an increase of 3 *m/z* units. The peak at *m/z* 57 is the tertiary butyl cation

5.9 Detection of Methyl ($^{\bullet}CH_3$) radical and O-Isobutyl/2-methyl propyl { $(CH_3)_2CH^{\bullet}CH_2$} radical from DMSO (peak/compound 19)

5.9.1 Methyl radical and 2-methyl propyl adduct of PBN with 3-methylbutanal and DMSO (compound 19)

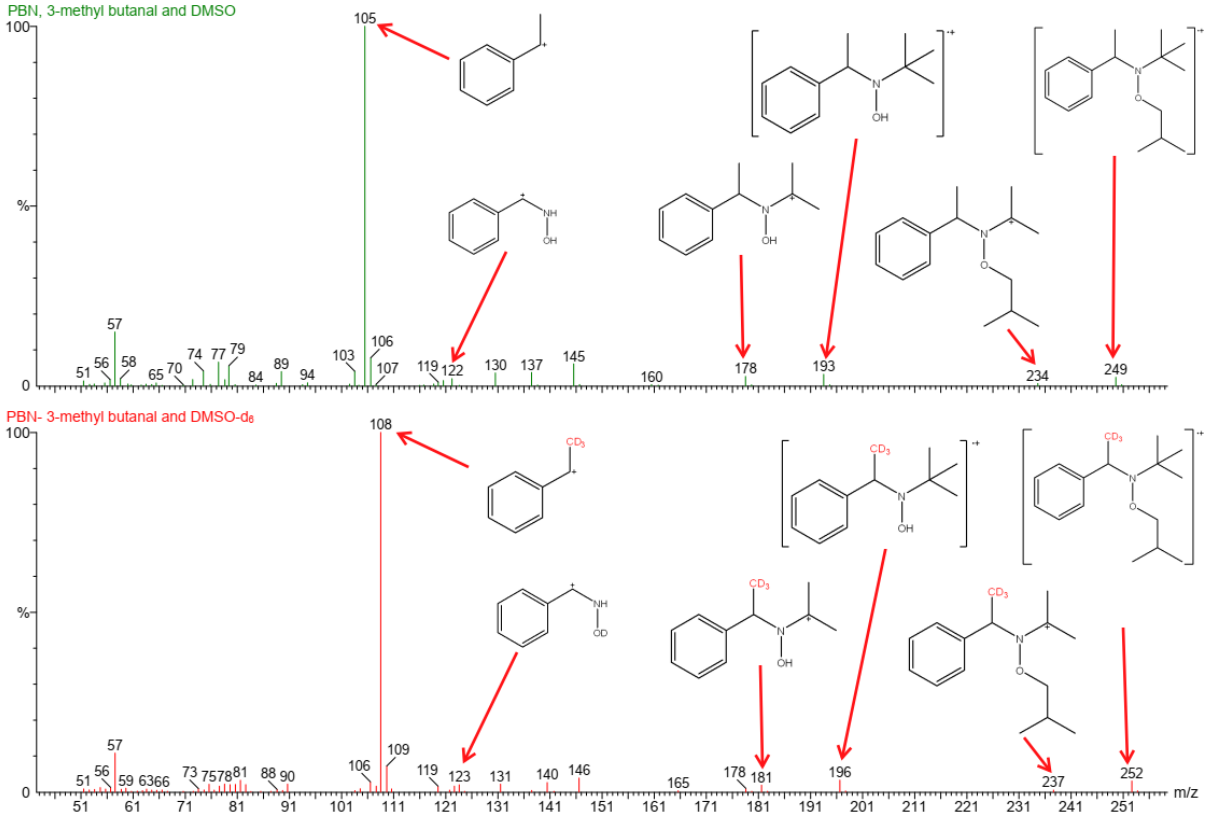

Figure 5.9.1 Electron Ionization mass spectra (EI-MS) corresponding to PBN adduct obtained from the analysis of the Fenton reaction mixture containing PBN, 3-methylbutanal and DMSO or DMSO-d_6 at rt 7.66 minutes

The EI mass spectra shown in Figure 5.9.1 correspond to the a) PBN-$(CH_3)(CH_2CH(CH_3)_2)$ (top spectra), and b) the deuterated methyl group PBN $(C\mathbf{D}_3)(CH_2CH(CH_3)_2)$ (bottom spectra).

When the Fenton reaction was carried out in the presence of 3-methyl butanal and DMSO as a competing secondary source of radicals, methyl radicals ($^{\bullet}CH_3$) were also generated by the reaction of $^{\bullet}OH$ with DMSO and were then trapped by PBN. The peak at *m/z* 249 units corresponds to the molecular ion of PBN-$(CH_3)(CH_2CH(CH_3)_2)$ The fragment at *m/z* 234 is the loss of a methyl group from the molecular ion (from the tBu group). The loss from the molecular ion of the 2-methyl propyl group from the oxygen (substituted

with hydrogen) results in *m/z* 193 and further loss of a methyl group from the tBu group results in *m/z* 178 .The dissociation of the alpha carbon bond and the nitrogen results in the base peak ethyl benzene cation at *m/z* 105 and. The peak at *m/z* 122 is N-benzyl-hydroxylamine. The peak at *m/z* 57 is the tertiary butyl cation

When the Fenton reaction was carried out in the presence of butanal and deuterated DMSO as a competing secondary source of radicals deuterated methyl radicals ($^{\bullet}CD_3$) were also generated by the reaction of $^{\bullet}OH$ with DMSO and were then trapped by PBN. Replacing DMSO with d_6-DMSO in the Fenton-based reaction mixture gives rise to an increase in the *m/z* value of the molecular ion of 3 *m/z* units. The peak at *m/z* 252 units corresponds to the molecular ion of PBN-(C**D**$_3$)($CH_2CH(CH_3)_2$) The fragment at *m/z* 237 is the loss of a methyl group from the molecular ion (from the tBu group). The loss from the molecular ion of the 2-methyl propyl group from the oxygen (substituted with hydrogen) results in *m/z* 196 and further loss of a methyl group from the tBu group results in *m/z* 178 .The dissociation of the alpha carbon bond and the nitrogen results in the base peak (ethyl-2,2,2,-d_3) benzene cation at *m/z* 108 and. The peak at *m/z* 123 is N-benzyl-hydroxylamine-O-d. The peak at *m/z* 57 is the tertiary butyl cation

5.9.2 Methyl radical and 2-methyl propyl adduct of PBN with 3-methylbutanal-d_2 and DMSO (compound 19)

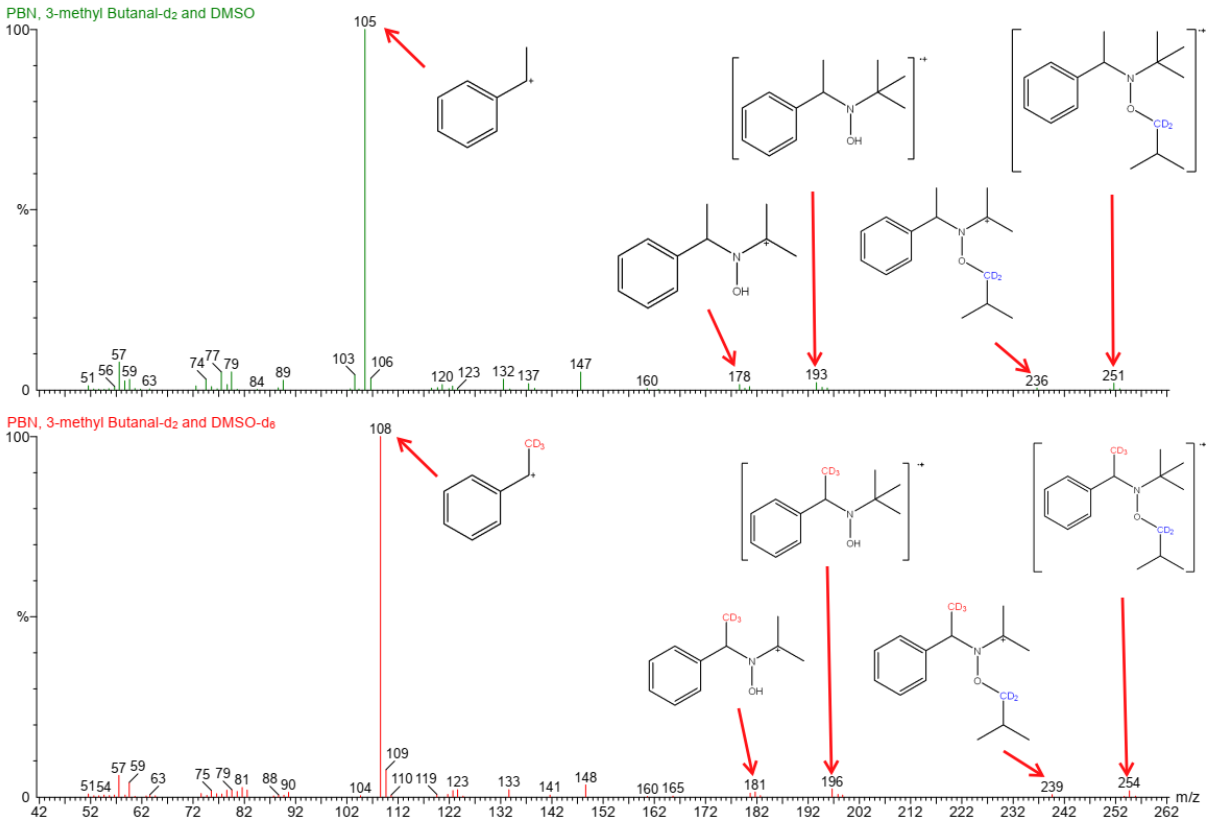

Figure 5.9.2 Electron Ionization mass spectra (EI-MS) corresponding to PBN adduct obtained from the analysis of the Fenton reaction mixture containing PBN, 3-methylbutanal-d_2 and DMSO or DMSO-d_6 at rt 7.66 minutes

The EI mass spectra shown in Figure 5.9.2 correspond to the a) PBN-$(CH_3)(CH_2CH(CH_3)_2)$ (top spectra), and b) the deuterated methyl group PBN $(C\mathbf{D}_3)(CH_2CH(CH_3)_2)$ (bottom spectra).

Replacing 3-methyl butanal with its deuterated analogue in the Fenton-based reaction demonstrates the production of deuterated 2-methyl propyl radicals and subsequent incorporation by the spin trap. As shown by an increase on the molecular ion of 2 *m/z* when 3-methyl butanal-d_2 is used

When the Fenton reaction was carried out in the presence of 3-methyl butanal and DMSO as a competing secondary source of radicals, methyl radicals ($^{\bullet}CH_3$) were also generated by the reaction of $^{\bullet}OH$ with DMSO and were then trapped by PBN. The peak at *m/z* 249 units corresponds to the molecular ion of PBN-$(CH_3)(CH_2CH(CH_3)_2)$ The fragment at *m/z* 234 is the loss of a methyl group from the molecular ion (from

the tBu group). The loss from the molecular ion of the 2-methyl propyl group from the oxygen (substituted with hydrogen) results in *m/z* 193 and further loss of a methyl group from the tBu group results in *m/z* 178 .The dissociation of the alpha carbon bond and the nitrogen results in the base peak ethyl benzene cation at *m/z* 105 and. The peak at *m/z* 122 is N-benzyl-hydroxylamine. The peak at *m/z* 57 is the tertiary butyl cation

When the Fenton reaction was carried out in the presence of butanal and deuterated DMSO as a competing secondary source of radicals deuterated methyl radicals ($^{\bullet}CD_3$) were also generated by the reaction of $^{\bullet}OH$ with DMSO and were then trapped by PBN. Replacing DMSO with d_6-DMSO in the Fenton-based reaction mixture gives rise to an increase in the *m/z* value of the molecular ion of 3 *m/z* units. The peak at *m/z* 252 units corresponds to the molecular ion of PBN-(C**D**$_3$)($CH_2CH(CH_3)_2$) The fragment at *m/z* 237 is the loss of a methyl group from the molecular ion (from the tBu group). The loss from the molecular ion of the 2-methyl propyl group from the oxygen (substituted with hydrogen) results in *m/z* 196 and further loss of a methyl group from the tBu group results in *m/z* 178 .The dissociation of the alpha carbon bond and the nitrogen results in the base peak (ethyl-2,2,2,-d_3) benzene cation at *m/z* 108 and. The peak at *m/z* 123 is N-benzyl-hydroxylamine-O-d. The peak at *m/z* 57 is the tertiary butyl cation

5.9.3 Methyl radical and 2-methyl propyl adduct of PBN-d_6 with 3-methylbutanal and DMSO (compound 19)

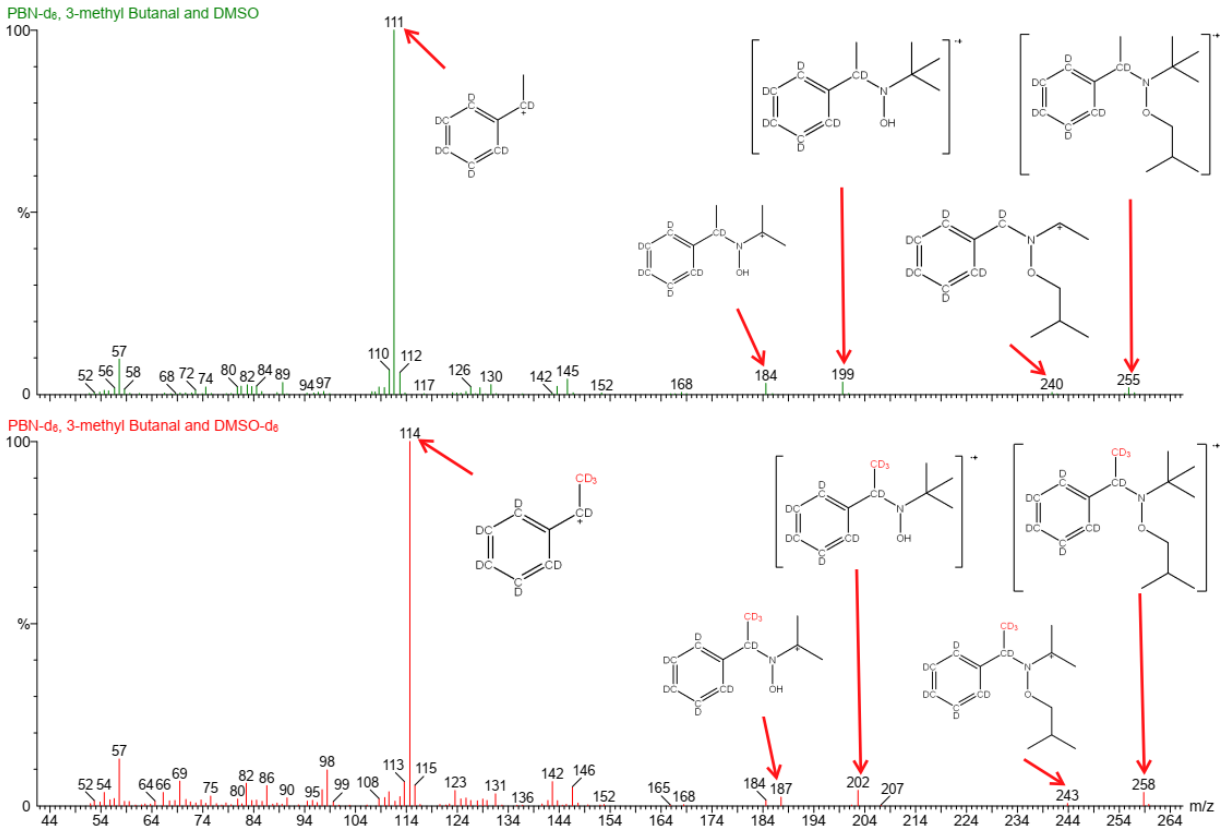

Figure 5.9.3 Electron Ionization mass spectra (EI-MS) corresponding to PBN-d_6 adduct obtained from the analysis of the Fenton reaction mixture containing PBN-d_6, 3-methylbutanal and DMSO or DMSO-d_6 at rt 7.66 minutes

The EI mass spectra shown in Figure 5.9.3 correspond to the a) PBN-d_6-$(CH_3)(CH_2CH(CH_3)_2)$ (top spectra), and b) the deuterated methyl group PBN-d_6 $(C\mathbf{D}_3)(CH_2CH(CH_3)_2)$ (bottom spectra).

When the Fenton reaction was carried out in the presence of 3-methyl butanal and DMSO as a competing secondary source of radicals, methyl radicals ($^{\bullet}CH_3$) were also generated by the reaction of $^{\bullet}OH$ with DMSO and were then trapped by PBN-d_6. The peak at *m/z* 255 units corresponds to the molecular ion of PBN-d_6-$(CH_3)(CH_2CH(CH_3)_2)$ The fragment at *m/z* 240 is the loss of a methyl group from the molecular ion (from the tBu group). The loss from the molecular ion of the 2-methyl propyl group from the oxygen (substituted with hydrogen) results in *m/z* 199 and further loss of a methyl group from the tBu group results in *m/z*

184 .The dissociation of the alpha carbon bond and the nitrogen results in the base peak ethyl-1-d benzene-d_5 cation at *m/z* 111. The peak at *m/z* 57 is the tertiary butyl cation

When the Fenton reaction was carried out in the presence of butanal and deuterated DMSO as a competing secondary source of radicals deuterated methyl radicals ($^{\bullet}CD_3$) were also generated by the reaction of $^{\bullet}OH$ with DMSO and were then trapped by PBN-d_6. Replacing DMSO with d_6-DMSO in the Fenton-based reaction mixture gives rise to an increase in the *m/z* value of the molecular ion of 3 *m/z* units. The peak at *m/z* 258 units corresponds to the molecular ion of PBN-d_6-(C**D**$_3$)($CH_2CH(CH_3)_2$) The fragment at *m/z* 243 is the loss of a methyl group from the molecular ion (from the tBu group). The loss from the molecular ion of the 2-methyl propyl group from the oxygen (substituted with hydrogen) results in *m/z* 202 and further loss of a methyl group from the tBu group results in *m/z* 184 .The dissociation of the alpha carbon bond and the nitrogen results in the base peak (ethyl-1,2,2,2,-d_4) benzene-d_5 cation at *m/z* 114 and. The peak at *m/z* 57 is the tertiary butyl cation

5.9.4 Methyl radical and 2-methyl propyl adduct of PBN-d_6 with 3-methylbutanal-d_2 and DMSO (compound 19)

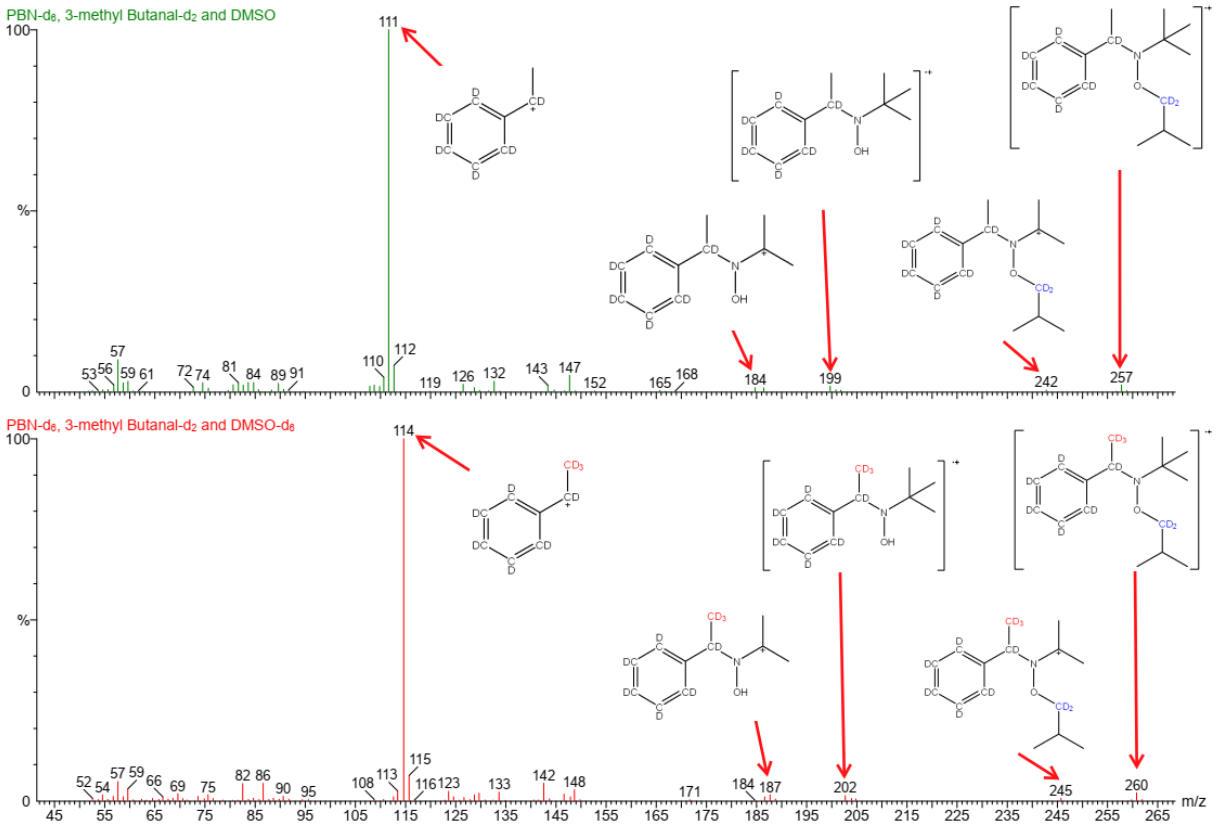

Figure 5.9.4 Electron Ionization mass spectra (EI-MS) corresponding to PBN-d_6 adduct obtained from the analysis of the Fenton reaction mixture containing PBN-d_6, 3-methylbutanal-d_2 and DMSO (top) or DMSO-d_6 (bottom)at rt 7.66 minutes

The EI mass spectra shown in Figure 5.9.4 correspond to the a) PBN-d_6-$(CH_3)(C\mathbf{D}_2CH(CH_3)_2)$ (top spectra), and b) the deuterated methyl group PBN-d_6 $(C\mathbf{D}_3)(C\mathbf{D}_2CH(CH_3)_2)$ (bottom spectra).

When the Fenton reaction was carried out in the presence of 3-methylbutanal and DMSO as a competing secondary source of radicals, methyl radicals ($^{\bullet}CH_3$) were also generated by the reaction of $^{\bullet}OH$ with DMSO and were then trapped by PBN-d_6. The peak at *m/z* 257 units corresponds to the molecular ion of PBN-d_6-$(CH_3)(C\mathbf{D}_2CH(CH_3)_2)$ The fragment at *m/z* 242 is the loss of a methyl group from the molecular ion (from the tBu group). The loss from the molecular ion of the 2-methyl propyl group from the oxygen (substituted with hydrogen) results in *m/z* 199 and further loss of a methyl group from the tBu group results in *m/z*

184 .The dissociation of the alpha carbon bond and the nitrogen results in the base peak ethyl-1-d benzene-d_5 cation at *m/z* 111. The peak at *m/z* 57 is the tertiary butyl cation

When the Fenton reaction was carried out in the presence of butanal and deuterated DMSO as a competing secondary source of radicals deuterated methyl radicals ($^{\bullet}CD_3$) were also generated by the reaction of $^{\bullet}OH$ with DMSO and were then trapped by PBN-d_6. Replacing DMSO with d_6-DMSO in the Fenton-based reaction mixture gives rise to an increase in the *m/z* value of the molecular ion of 3 *m/z* units. The peak at *m/z* 260 units corresponds to the molecular ion of PBN-d_6-(C**D**$_3$)(C**D**$_2$CH(CH$_3$)$_2$) The fragment at *m/z* 245 is the loss of a methyl group from the molecular ion (from the tBu group). The loss from the molecular ion of the 2-methyl propyl group from the oxygen (substituted with hydrogen) results in *m/z* 202 and further loss of a methyl group from the tBu group results in *m/z* 187 .The dissociation of the alpha carbon bond and the nitrogen results in the base peak (ethyl-1,2,2,2,-d_4) benzene-d_5 cation at *m/z* 114 and. The peak at *m/z* 57 is the tertiary butyl cation

5.10 Discussion

The main aim of this chapter was to trap, analyse and identify radicals generated from the reaction of hydroxyl radicals with 3-methyl butanal and PBN and its derivatives.

Five new peaks were observed when the Fenton reaction was run in the presence of 3-methyl butanal as a secondary source of radicals (Figure 5.1.1) compared to control reactions, and three additional peaks were observed when DMSO was added as a competitive secondary source of radicals (Figure 5.7.1) (one previously identified dimethyl adduct peak discussed in section 4.9, and two new peaks). The resulting adducts have been identified in the previous sections.

The Fenton reactions were carried out in the presence of phosphate buffer (pH 7.0), EDTA, hydrogen peroxide(H_2O_2), ascorbic acid, spin-trap (PBN, PBN-d_6 or 4-fluoro-PBN), Fe(II) and 3-methyl butanal to generate PBN-$(CH_2CH(CH_3)_2)_2$ which was extracted using liquid-liquid extraction (chloroform solvent extraction). The Fe(II) reacts with H_2O_2 to form hydroxyl radicals, hydroxyl ions and Fe(III). The hydroxyl radical reactions with 3-methyl butanal formed 2-methyl propyl radicals (isobutyl radicals) and two possible enantiomers of 3-methyl butanal radicals (see Figure 5.10.1) however at least 4 variations are possible based on where the hydrogen is abstracted from. The resulting spin trap adducts were extracted and analysed via GC/MS. Figure 5.1.1 shows multiple peaks that were not present in control experiments (Figure 3.1.1) where 3-methyl butanal was absent, confirming that these peaks originated from 3-methyl butanal. Conclusively compounds 3, 5, 7, 8 and 9 originated from 3-methyl butanal.

5.10.2 Discussing the di-2-methyl propyl adduct of PBN

The peak detected at 9.23 minutes (Figure 5.1.1) can be unequivocally identified as the di adduct of PBN and 2-methyl propyl radicals where they have added to the alpha carbon and the oxygen. The is largely proven using the deuterated analogue, 3-methyl butanal-2,2,-d_2 resulting in two additional deuterons per radical formed. It is assumed the hydroxyl radical attacks the carbonyl site of the aldehyde leaving the deuterons intact on the radical that is formed. Table 5.1 shows the di-isobutyl adducts formed and key fragments formed.

Table 5.1 di-2-methyl propyl adducts from different PBN derivatives and 3-methylbutanal isotopic isoforms

Fenton system	Compound name or formula	$M^{+\bullet}$ (*m/z*)	other significant ions (*m/z*)
PBN + 3-methylbutanal	PBN-$(CH_2CH(CH_3)_2)_2$	**291**	276, 234, 220, 178, 147, 122, 105, 91 (bp), 77, 57
PBN + 3-methylbutanal-d_2	PBN-$(CD_2CH(CH_3)_2)_2$	**295**	280, 236, 222, 180, 149, 122, 105, 91 (bp), 77, 57
PBN-d_6+ 3-methylbutanal	PBN-d_6-$(CH_2CH(CH_3)_2)_2$	**297**	282, 240, 226, 184, 153, 128, 110, 97 (bp), 82, 57
PBN-d_6+ 3-methylbutanal-d_2	PBN-d_6-$(CD_2CH(CH_3)_2)_3$	**301**	286, 242, 228, 186, 155, 128, 111, 97 (bp), 82, 57
F-PBN + 3-methylbutanal	F-PBN-$(CH_2CH(CH_3)_2)_2$	**309**	252, 220, 196, 165, 140, 123, 109 (bp), 95, 57
F-PBN + 3-methylbutanal-d_2	F-PBN-$(CD_2CH(CH_3)_2)_3$	**313**	254, 222, 198, 167, 140, 124, 110 (bp), 95, 57

The mass spectrum (Figure 5.2.1) shows the molecular ion is *m/z* 291 where 3-methyl butanal is used, *m/z* 295 where 3-methyl butanal-d_2 is used (an increase of 4 *m/z* units). The identity of the adduct is clearly demonstrated by use of the deuterated analogue to generate deuterated isobutyl radicals that have added to PBN. The fragment pattern of the molecular ion also demonstrates where the adducts have added. The peak at *m/z* 147 where 3-methylbutanal is used identified as an isopentylbenzene cation, has retained one of the isobutyl adducts on the alpha carbon, thus *m/z* 147 becomes *m/z* 149 where 3-methylbutanal-d_2 is used (showing 2 deuterium are retained).

5.10.3 Discussion the secondary oxoallylic radical

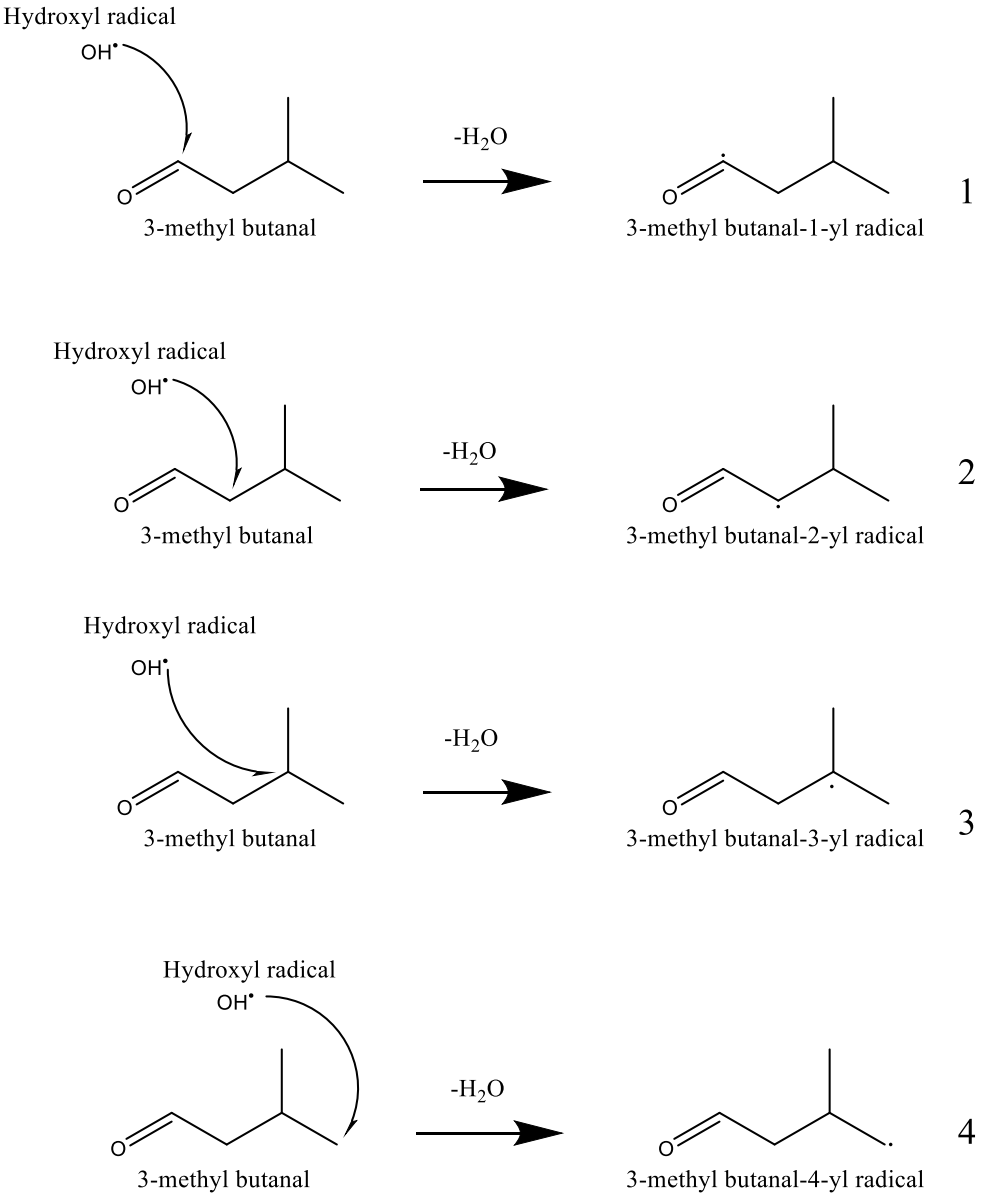

Figure 5.10.1 schematic showing the variations of 3-methyl butanal radicals formed when subjected to hydroxyl radical attack

The 3-methyl-butanal radicals (oxoallylic radicals) have four possible radical conformations reflected by the possible hydrogens abstracted when attacked by the hydroxyl radical. However, the most likely radical formed is the secondary radical (see Figure 5.10.1, number 3) as this is the most stable (Papajak *et al*., 2012).

Viskolcz *et al*., (1996) investigated propyl, butyl and pentyl radicals and found 1,2 and 1,3 H atom-transfer reactions were feasible. Further work on the subject, in a study by Hayes and Burgess, (2009) they investigated the H-atom transfers (migrations) for several alkyl and oxoallylic radicals in general paying attention to the thermodynamics and kinetics of these reactions. The activation energies and enthalpies of reactions were modelled, and it was found that increased alkyl substitution reduced barriers to isomerization by about 10 and 20 kJ mol^{-1} for secondary and tertiary radical formation, respectively, relative to primary radical reactions favouring hydrogen atom transfers and radical isomerisation reactions. The formation of secondary radicals from primary radicals (e.g., 1-propyl to 2-propyl) was demonstrated and the formation of branched radicals such as tertiary alkyl radicals via β-scission was investigated. For instance, the β scission of tertiary butyl radical to yield isobutene and a H atom. It was found isomerisation producing tertiary alkyl radicals occur preferentially to those producing secondary and primary alkyl radicals and that tertiary alkyl radicals are more stable than secondary or primary alkyl radicals respectively. Barriers to isomerization were significantly influenced by the presence of adjacent chemical functionalities such as double bonds or carbonyl groups

This leads to a conclusion that for 3-methyl butanal, the probable radical, irrespective of the primary radical formed is 3-methyl butanal-3-yl formed via internal isomerisation radical reactions and is independent of where the hydroxyl radical initially attacked the aldehyde.

5.10.4 Discussing the mono-2-methyl propyl monomethyl adduct of PBN

The peaks retained at 7.46 and 7.62 minutes are diastereomers of one another with the identity of PBN(C-2-methyl propyl-O-methyl) and PBN(C-methyl-O-2-methyl propyl), respectively.

An important point to note is that both peaks are not sharp relative to other peaks such as the PBN unreacted peak. There seems to be a “shoulder” that demonstrates there may be multiple enantiomers of the adducts in their various conformations. This is evidenced by the fact that the 1,3-adducts of PBN are double chiral molecules allowing multiple conformations of adducts.

5.10.5 Miscellaneous discussion

An interesting observation can be made when paying attention to the tropylium cations formed in the various reactions involving the deuterated isotopologues. Since the tropylium cation structure is a product of the resonance between a seven membered ring (see Figure 5.10.2 , A) and a six-membered ring with a methyl (toluene) an interesting rearrangement takes place at the point of fragmentation in the ionising chamber of the mass spectrometer (Siegel, 1970). The movement of deuterons from the deuterated adducts on the tropylium is observed and evidenced by the presence of m/z 96, m/z 97 and m/z 98

fragments dependent upon the level of deuteration on the radical being studied. For example when 2-methylpropyl-d_0 radicals are used with deuterated PBN-d_6, the resulting tropylium cation profile is *m/z* 96 and *m/z* 97, however when propyl-d_2 or propyl d_7 is used, the resulting tropylium is *m/z* 97 and *m/z* 98 , alluding to the fact that a deuteron has internally transferred onto the seven membered ring (see Figure 5.8.3 and Figure 5.8.4).

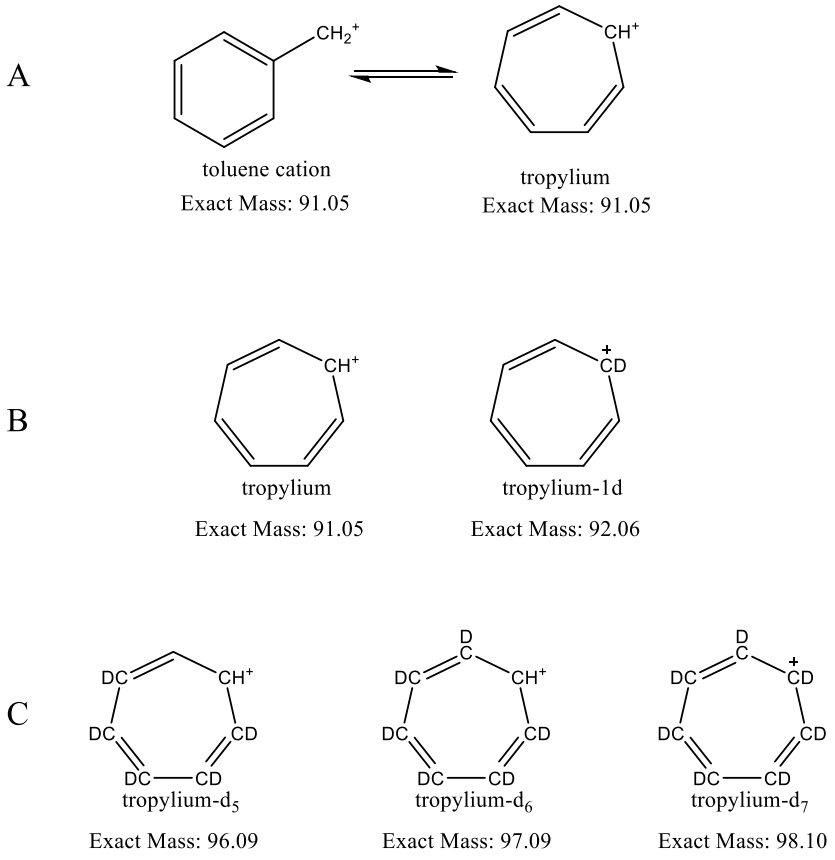

Figure 5.10.2 A) the resonance between the toluene cation and tropylium cation, B) tropylium and troylium-1d, C) tropylium-d_5, tropylium-d_6 and tropylium-d_7

6 Summary and future work

The Fenton reaction is one of the most studied biochemical reactions to date. The resulting hydroxyl radicals are vastly important in countless reactions. They are particularly important in the cells of animals where they place a crucial role in disease pathogenesis. Hydroxyl radicals can react with a many different organic compounds triggering chain reactions. Hydroxyl radicals are difficult to detect and to neutralise meaning their field of damage can far extend their site of origin. Spin trapping is a technique which can be used to indirectly measure free radicals such as the hydroxyl radical. The advantages of spin-trapping mean their application can be beyond solely using GC-MS and could be used in combination with EPR, LCMS HPLC and functional studies *in vitro*.

In chapter 3, it was shown that hydroxyl radical adducts on the aromatic ring of PBN can be formed. Compound A was shown to be a mono-hydroxyl radical adduct of either the ortho or meta position of the aromatic ring of PBN, compound B was shown to be a mono-hydroxyl radical adduct of the para position of the aromatic ring of PBN, compound C was shown to be a dihydroxyl radical adduct of the para position and either the ortho or meta position of the aromatic ring of PBN, and finally compound D was shown to be a mono-hydroxyl radical adduct of either the ortho or meta position of the aromatic ring of 4-fluoro-PBN. It is impossible to discern between the ortho and meta attack by the hydroxyl radical and more investigation is needed in this regard.

In chapter 4, it was shown that alkyl, acyl/oxoallylic and combined adducts of PBN could be formed. The hydroxyl radicals attacked the butanal and formed propyl radicals which subsequently were trapped by PBN and its derivatives to form the PBN dipropyl adduct made up of two propyl radicals. The hydroxyl radicals also abstracted hydrogens from various sites on the butanal to form butanoyl and oxobutyl (oxoallylic) radicals (also classed as acyl radicals). As well as diadducts of alkyls and acyls there were combination adducts formed of the two classes of radicals. It was also shown that due to the hydrogen abstraction at various sites when forming the radicals diastereomers of the diadducts were formed

In chapter 5 it was shown how alkyl, acyl/oxoallylic and combined adducts of PBN could be formed in a similar fashion to chapter 4 however the proof of concept was tested on longer chain radicals showing that the methodology has applicability and validity when testing other aliphatic aldehydes.

An interesting direction of study involves extending the scope of this thesis and investigating applications of this technology in *in vivo* environments or *in vitro* studies using cell culture and analysing the volatiles produced. The development of an aldehyde radical assay is feasible based on the principles established in

this thesis. Various biological aldehydes could be analysed and identified. Based on other areas not in the scope of this thesis, omega 6 fatty acids have been found to decompose when attacked by hydroxyl radicals into pentyl radicals. In a study by (Iwahashi *et al*., 2002) they digested 13-hydroperoxide octadecadienoic acid (13-HPODE) with cytochrome C and spin trap to form pentyl radicals and octadecadienoic radicals demonstrating that other radicals can be analysed

An interesting approach for analysing other radicals could be the headspace analysis of carbonyl radicals as previously demonstrated by Manzoor, (2018) where ethyl radicals were identified and characterised using headspace combined with thermal desorption GCMS techniques. Further analysis could look into whether these stable radicals species could be trapped in the headspace of oxidatively stressed cells.

Future work could investigate using chiral separation in GC utilising special techniques for separating out the enantiomers and chiral molecules from one another. One of the limitations of conventional GC is that it cannot be used to separate enantiomers. Enantiomers are nonsuperimposable mirror-image molecules and since they have identical properties they elute at the same time in non-chiral GC. Diastereomers, on the other hand, can be separated using chromatography as they have different chromatographic properties and different retention times. Enantiomers can be separated using derivatization to form diastereomer complexes which can then be separated using GC (Schurig, 2002; Morrison, 2012).

Interestingly the use of triadducts is also a possibility for the characterisation and identification of radical carbonyl adducts. Wang et al., (2005) used nitric oxide as a nitroxide spin trap to trap acyl and alkyl radicals however as they were using EPR, the limitations of this analytical method in the study meant diadducts could only analysed. Utilising GCMS as the analytical method and nitric oxide, as the spin trap, triadducts could easily be identified

7 References

- Abuarrah, M., Setianto, B. Y., Faisal, A. and Sadewa, A. H. (**2021**) '8-hydroxy-2-deoxyguanosine as oxidative dna damage biomarker of medical ionizing radiation: A scoping review.' *Journal of Biomedical Physics and Engineering*. Shiraz University of Medical Sciences, 11(3) pp. 389–402.
- Alahmar, A. T. (**2019**) 'Role of Oxidative Stress in Male Infertility: An Updated Review.' *Journal of Human Reproductive Sciences*. Wolters Kluwer -- Medknow Publications, 12(1) p. 4.
- Alkadi, H. (**2020**) 'A Review on Free Radicals and Antioxidants.' *Infectious Disorders - Drug Targets*. Bentham Science Publishers Ltd., 20(1) pp. 16–26.
- Amann, A., Costello, B. de L., Miekisch, W., Schubert, J., Buszewski, B., Pleil, J., Ratcliffe, N. and Risby, T. (**2014**) 'The human volatilome: Volatile organic compounds (VOCs) in exhaled breath, skin emanations, urine, feces and saliva.' *Journal of Breath Research*. IOP Publishing p. 034001.
- Asano, T., Komatsu, M., Yamaguchi-Iwai, Y., Ishikawa, F., Mizushima, N. and Iwai, K. (**2011**) 'Distinct Mechanisms of Ferritin Delivery to Lysosomes in Iron-Depleted and Iron-Replete Cells.' *Molecular and Cellular Biology*. American Society for Microbiology (ASM), 31(10) pp. 2040–2052.
- Bartolazzi, A., Santonico, M., Pennazza, G., Martinelli, E., Paolesse, R., D'Amico, A. and Di Natale, C. (**2010**) 'A sensor array and GC study about VOCs and cancer cells.' *Sensors and Actuators, B: Chemical*, 146(2) pp. 483–488.
- Beck, O., Olin, A. C. and Mirgorodskaya, E. (**2016**) 'Potential of mass spectrometry in developing clinical laboratory biomarkers of nonvolatiles in exhaled breath.' *Clinical Chemistry* pp. 84–91.
- Benham, A. M., van Lith, M., Sitia, R. and Braakman, I. (**2013**) 'Ero1-PDI interactions, the response to redox flux and the implications for disulfide bond formation in the mammalian endoplasmic reticulum.' *Philosophical Transactions of the Royal Society B: Biological Sciences*. The Royal Society, 368(1617) pp. 1–9.

- Berliner, L. (**2012**) 'History of the Use of Nitroxides (Aminoxyl Radicals) in Biochemistry: Past, Present and Future of Spin Label and Probe Method.' *Nitroxides - Theory, Experiment and Applicaitons* pp. 3–24.
- Bhatt, S., Nagappa, A. N. and Patil, C. R. (**2020**) 'Role of oxidative stress in depression.' *Drug Discovery Today*, 25(7).
- Boyd, S. L. and Boyd, R. J. (**1994**) 'A Theoretical Study of Spin Trapping by Nitrone: Trapping of Hydrogen, Methyl, Hydroxyl, and Peroxyl Radicals.' *J. Phys. Chem*, 98 pp. 11705–11713.
- Bulugahapitiya, V. P. (**2020**) *Isomerism in Organic Chemistry*. Digital resource.
- Burns, J. L., Nakamura, M. T. and Ma, D. W. L. (**2018**) 'Differentiating the biological effects of linoleic acid from arachidonic acid in health and disease.' *Prostaglandins, Leukotrienes and Essential Fatty Acids*. Churchill Livingstone, 135, August, pp. 1–4.
- Cadet, J. and Wagner, J. (**2013**) 'DNA base damage by reactive oxygen species, oxidizing agents, and UV radiation.' *Cold Spring Harbor Perspectives in Biology*. Cold Spring Harb Perspect Biol, 5(2).
- Calenic, B., Miricescu, D., Greabu, M., Kuznetsov, A. V., Troppmair, J., Ruzsanyi, V. and Amann, A. (**2015**) 'Oxidative stress and volatile organic compounds: Interplay in pulmonary, cardio-vascular, digestive tract systems and cancer.' *Open Chemistry*, 13(1) pp. 1020–1030.
- Cao, Y., Chu, Q. and Ye, J. (**2003**) 'Determination of hydroxyl radical by capillary electrophoresis and studies on hydroxyl radical scavenging activities of Chinese herbs.' *Analytical and Bioanalytical Chemistry*. Springer, 376(5) pp. 691–695.
- Castro, G. D., Delgado De Layño, A. M. A. and Castro, J. A. (**1997**) 'Hydroxyl and 1-hydroxyethyl free radical detection using spin traps followed by derivatization and gas chromatography-mass spectrometry.' *Redox Report*, 3(5–6) pp. 343–347.
- Castro, G. D., Delgado De Layño, A. M. A. and Castro, J. A. (**1998**) 'Liver nuclear ethanol

metabolizing systems (NEMS) producing acetaldehyde and 1-hydroxyethyl free radicals.' *Toxicology*, 129(2–3) pp. 137–144.

- Catapano, M. C., Protti, M., Fontana, T., Mandrioli, R., Mladěnka, P. and Mercolini, L. (**2019**) 'An original HPLC method with coulometric detection to monitor hydroxyl radical generation via fenton chemistry.' *Molecules*. Multidisciplinary Digital Publishing Institute (MDPI), 24(17).
- Cheng, F. C., Jen, J. F. and Tsai, T. H. (**2002**) 'Hydroxyl radical in living systems and its separation methods.' *Journal of Chromatography B: Analytical Technologies in the Biomedical and Life Sciences* pp. 481–496.
- Cooke, M. S., Evans, M. D., Dizdaroglu, M. and Lunec, J. (**2003**) 'Oxidative DNA damage: mechanisms, mutation, and disease.' *The FASEB Journal*. Wiley, 17(10) pp. 1195–1214.
- Coolen, S. A. J., Everaerts, F. M. and Huf, F. A. (**1997**) 'Characterization of 60Co γ-radiation induced radical products of antipyrine by means of high-performance liquid chromatography, mass spectrometry, capillary zone electrophoresis, micellar electrokinetic capillary chromatography and nuclear magnetic resona.' *Journal of Chromatography A*, 788(1–2) pp. 95–103.
- Dai, Y., Shao, C., Piao, Y., Hu, H., Lu, K., Zhang, T., Zhang, X., Jia, S., Wang, M. and Man, S. (**2017**) 'The mechanism for cleavage of three typical glucosidic bonds induced by hydroxyl free radical.' *Carbohydrate Polymers*. Elsevier, 178, December, pp. 34–40.
- Dalle-Donne, I., Scaloni, A., Giustarini, D., Cavarra, E., Tell, G., Lungarella, G., Colombo, R., Rossi, R. and Milzani, A. (**2005**) 'Proteins as biomarkers of oxidative/nitrosative stress in diseases: The contribution of redox proteomics.' *Mass Spectrometry Reviews*. John Wiley & Sons, Ltd, 24(1) pp. 55–99.
- Das, T. K., Wati, M. R. and Fatima-Shad, K. (**2015**) 'Oxidative Stress Gated by Fenton and Haber Weiss Reactions and Its Association With Alzheimer's Disease.' *Archives of Neuroscience 2015*

2:2. Briefland, 2(2).

- Das, U. (**2006**) 'Essential Fatty Acids - A Review.' *Current Pharmaceutical Biotechnology*, 7(6) pp. 467–482.
- Davis, R. and Frearson, M. (**1987**) *Mass Spectrometry - Analytical chemistry*. London: John Wiley & Sons, Ltd.
- Englander, S. W., Mayne, L., Bai, Y. and Sosnick, T. R. (**1997**) 'Hydrogen exchange: The modem legacy of Linderstrom-Lang.' *Protein Science*. John Wiley & Sons, Ltd, 6(5) pp. 1101–1109.
- Evans, S. E. and Kasprzyk-Hordern, B. (**2014**) 'Applications of chiral chromatography coupled with mass spectrometry in the analysis of chiral pharmaceuticals in the environment.' *Trends in Environmental Analytical Chemistry*. Elsevier pp. e34–e51.
- Fenton, H. J. H. (**1894**) 'LXXIII. - Oxidation of tartaric acid in presence of iron.' *Journal of the Chemical Society, Transactions*. The Royal Society of Chemistry pp. 899–910.
- Finkel, T. and Holbrook, N. J. (**2000**) 'Oxidants, oxidative stress and the biology of ageing.' *Nature*. Nature pp. 239–247.
- Fransen, M., Nordgren, M., Wang, B. and Apanasets, O. (**2012**) 'Role of peroxisomes in ROS/RNS-metabolism: Implications for human disease.' *Biochimica et Biophysica Acta - Molecular Basis of Disease*. Biochim Biophys Acta pp. 1363–1373.
- Fu, P. P., Xia, Q., Sun, X. and Yu, H. (**2012**) 'Phototoxicity and environmental transformation of polycyclic aromatic hydrocarbons (PAHs)-light-induced reactive oxygen species, lipid peroxidation, and DNA damage.' *Journal of Environmental Science and Health - Part C Environmental Carcinogenesis and Ecotoxicology Reviews*. J Environ Sci Health C Environ Carcinog Ecotoxicol Rev, 30(1) pp. 1–41.
- Furuhashi, T. and Okuda, K. (**2017**) 'Application of GC/MS Soft Ionization for Isomeric Biological Compound Analysis.' *Critical Reviews in Analytical Chemistry*, 47(5) pp. 438–453.

References

- Garcia-Alcega, S., Nasir, Z. A., Ferguson, R., Whitby, C., Dumbrell, A. J., Colbeck, I., Gomes, D., Tyrrel, S. and Coulon, F. (**2017**) 'Fingerprinting outdoor air environment using microbial volatile organic compounds (MVOCs) – A review.' *TrAC - Trends in Analytical Chemistry* pp. 75–83.
- Gariboldi, M. B., Rimoldi, V., Supino, R., Favini, E. and Monti, E. (**2000**) 'The nitroxide tempol induces oxidative stress, p21(WAF1/CIP1), and cell death in HL60 cells.' *Free Radical Biology and Medicine*. Free Radic Biol Med, 29(7) pp. 633–641.
- Gerber, P. A. and Rutter, G. A. (**2017**) 'The Role of Oxidative Stress and Hypoxia in Pancreatic Beta-Cell Dysfunction in Diabetes Mellitus.' *Antioxidants and Redox Signaling*. Mary Ann Liebert, Inc. 140 Huguenot Street, 3rd Floor New Rochelle, NY 10801 USA pp. 501–518.
- Glorieux, C. and Calderon, P. B. (**2017**) 'Catalase, a remarkable enzyme: Targeting the oldest antioxidant enzyme to find a new cancer treatment approach.' *Biological Chemistry*. De Gruyter pp. 1095–1108.
- Gogus, U. and Smith, C. (**2010**) 'n-3 Omega fatty acids: a review of current knowledge.' *International Journal of Food Science & Technology*. John Wiley & Sons, Ltd (10.1111), 45(3) pp. 417–436.
- Gupta, P. and Rajakumar, B. (**2020**) 'Reaction of phenyl radicals towards propionaldehyde and butyraldehyde over the temperature range of 200–2000 K.' *Chemical Physics Letters*. North-Holland, 758, November, p. 137915.
- Halliwell, B. (**2015**) 'Free Radicals and Other Reactive Species in Disease.' *In eLS*. Chichester, UK: John Wiley & Sons, Ltd, pp. 1–9.
- Halliwell, B. and Whiteman, M. (**2004**) 'Measuring reactive species and oxidative damage in vivo and in cell culture: how should you do it and what do the results mean?' *British Journal of Pharmacology*, 142 pp. 231–255.
- Hamer, J. and Macaluso, A. (**1964**) 'Nitrones.' *Chemical Reviews*, 64(4) pp. 473–495.

References

- Hayes, C. J. and Burgess, D. R. (**2009**) 'Kinetic barriers of H-atom transfer reactions in alkyl, allylic, and oxoallylic radicals as calculated by composite ab initio methods.' *Journal of Physical Chemistry A*, 113(11) pp. 2473–2482.
- Hinton, R. D. and Janzen, E. G. (**1992**) 'Synthesis and Characterization of Phenyl-Substituted C-Phenyl-N-tert -butylnitrones and Some of Their Radical Adducts.' *Advances*, 57(13) pp. 2646–2651.
- Iwahashi, H., Nishizaki, K. and Takagi, I. (**2002**) 'Cytochrome c catalyses the formation of pentyl radical and octanoic acid radical from linoleic acid hydroperoxide.' *Biochemical Journal*. Portland Press, 361(1) pp. 57–66.
- Iwamura, M. and Inamoto, N. (**1967**) 'Novel Radical 1,3-Addition to Nitrones.' *Bulletin of the Chemical Society of Japan*. The Chemical Society of Japan 公益社団法人 日本化学会, 40(3) pp. 702–702.
- Janzen, E. G. and DuBose, C. M. (**1993**) 'Electron Impact Mass Spectra of Some Substituted C-Phenyl N-Tert-Butyl Nitrones (Pbn's).' *Analytical Letters*, 26(12).
- Janzen, E. G., Krygsman, P. H., Larry Haire, D. and Lindsay, D. A. (**1990**) 'Detection of Alkyl, Alkoxyl, and Alkyperoxyl Radicals from the Thermolysis of Azobis(isobutyronitrile) by ESR/Spin Trapping. Evidence for Double Spin Adducts from Liquid-Phase Chromatography and Mass Spectroscopy.' *Journal of the American Chemical Society*, 112(23) pp. 8279–8284.
- Janzen, E. G. and Lopp, I. G. (**1972**) 'Detection and identification of gas phase free radicals by electron spin resonance spin trapping [1].' *Journal of Physical Chemistry* pp. 2056–2058.
- Janzen, E. G., Sang, H., Kotake, Y., DuBose, C. M., Poyer, J. L. and Arimura, M. (**1995**) 'Tandem mass spectrometry study of C-phenyl-N-tert-butyl nitrone spin adducts from in vitro rat liver microsomal metabolism of bromotrichloromethane and carbon tetrachloride.' *Journal of the American Society for Mass Spectrometry*, 6(9).

References

- Janzen, E. G., Weber, J. R., Haire, D. L. and Fung, D. M. (**1985**) 'Gas Chromatography - Mass Spectroscopy (GC/MS) of Single and Double Spin Adducts of PBN and the Hydroxylamines of Corresponding Structure.' *Analytical Letters*. Taylor & Francis Group, 18(14) pp. 1749–1757.
- Jerzykiewicz, M., Ćwieląg-Piasecka, I., Witwicki, M. and Jezierski, A. (**2011**) 'α-Tocopherol impact on oxy-radical induced free radical decomposition of DMSO: Spin trapping EPR and theoretical studies.' *Chemical Physics*, 383(1–3) pp. 27–34.
- Karoui, H., Clément, J.-L., Rockenbauer, A., Siri, D. and Tordo, P. (**2004**) 'Synthesis and structure of 5,5-diethoxycarbonyl-1-pyrroline N-oxide (DECPO). Application to superoxide radical trapping.' *Tetrahedron Letters*. Pergamon, 45(1) pp. 149–152.
- Khan, N., Wilmot, C. M., Rosen, G. M., Demidenko, E., Sun, J., Joseph, J., O'Hara, J., Kalyanaraman, B. and Swartz, H. M. (**2003**) 'Spin traps: in vitro toxicity and stability of radical adducts.' *Free Radical Biology and Medicine*. Pergamon, 34(11) pp. 1473–1481.
- Kim, I. Y., Suh, S. H., Lee, I. K. and Wolfe, R. R. (**2016**) 'Applications of stable, nonradioactive isotope tracers in in vivo human metabolic research.' *Experimental and Molecular Medicine*. Nature Publishing Group, 48(1) pp. e203-10.
- Konermann, L., Pan, J. and Liu, Y. H. (**2011**) 'Hydrogen exchange mass spectrometry for studying protein structure and dynamics.' *Chemical Society Reviews*. The Royal Society of Chemistry, 40(3) pp. 1224–1234.
- Kotake, Y. and Janzen, E. G. (**1991**) 'Decay and Fate of the Hydroxyl Radical Adduct of α-Phenyl-N-tert-butylnitrone in Aqueous Media.' *Journal of the American Chemical Society*. American Chemical Society, 113(25) pp. 9503–9506.
- Krutmann, J., Schikowski, T., Morita, A. and Berneburg, M. (**2021**) 'Environmentally-Induced (Extrinsic) Skin Aging: Exposomal Factors and Underlying Mechanisms.' *Journal of Investigative Dermatology*. Elsevier, 141(4) pp. 1096–1103.

- Krygsman, P. H., Janzen, E. G., Towner, R. A. and Haire, D. L. (**1989**) 'Enhanced recognition of spin trapped radicals in complex mixtures: Deuterated nitronyl adducts provide a gas chromatographic/mass spectrometric marker.' *Analytical Letters*. Taylor & Francis Group, 22(4) pp. 1009–1020.
- Lachlan, D. (**2014**) *Uncovering the Energetics and Reactivity of Aminoxyl Radicals by Mass Spectroscopy*.
- De Lacy Costello, B., Amann, A., Al-Kateb, H., Flynn, C., Filipiak, W., Khalid, T., Osborne, D. and Ratcliffe, N. M. (**2014**) 'A review of the volatiles from the healthy human body.' *Journal of Breath Research*.
- Lavra, L., Catini, A., Ulivieri, A., Capuano, R., Baghernajad Salehi, L., Sciacchitano, S., Bartolazzi, A., Nardis, S., Paolesse, R., Martinelli, E. and Di Natale, C. (**2015**) 'Investigation of VOCs associated with different characteristics of breast cancer cells.' *Scientific Reports*, 5(1).
- Lewandowski, M. and Gwozdzinski, K. (**2017**) 'Nitroxides as antioxidants and anticancer drugs.' *International Journal of Molecular Sciences*. MDPI AG, 18(11).
- Li, Z., Chen, X., Teng, X. and Lu, C. (**2019**) 'Chemiluminescence as a New Indicator for Monitoring Hydroxylated Intermediates in Persulfate-Based Advanced Oxidation Processes.' *Journal of Physical Chemistry C*. American Chemical Society, 123(35) pp. 21704–21712.
- Lobo, V., Patil, A., Phatak, A. and Chandra, N. (**2010**) 'Free radicals, antioxidants and functional foods: Impact on human health.' *Pharmacognosy Reviews*. Wolters Kluwer -- Medknow Publications pp. 118–126.
- LoPachin, R. M. and Gavin, T. (**2014**) 'Molecular Mechanisms of Aldehyde Toxicity: A Chemical Perspective.' *Chemical Research in Toxicology*. American Chemical Society, 27(7) pp. 1081–1091.
- Mallet, A. and Down, S. (**2009**) *Dictionary of Mass Spectrometry*.
- Mantovani, A. C. G., Chendynski, L. T., Salviato, A., Borsato, D., Santana, V. T., Di Mauro, E. and

Mauro, E. Di (**2018**) 'Monitoring free radicals formation in the biodiesel oxidation reaction via electronic paramagnetic resonance.' *Fuel*. Elsevier Ltd, 224, July, pp. 255–260.

- Manzoor, K. (**2018**) *Detection and analysis of spin trapped radical adducts using thermal desorption gas chromatography mass spectrometry*. *Unpublished*.
- Manzoor, K., Mishra, S. and Podmore, I. D. (**2020**) 'Detection and identification of ethanal-derived spin-trapped free radicals using headspace thermal desorption gas chromatography-mass spectrometry (TD-GC-MS).' *Free Radical Research*. Informa UK Limited, October, pp. 1–26.
- Marcheggiani, F., Kordes, S., Cirilli, I., Orlando, P., Silvestri, S., Vogelsang, A., Möller, N., Blatt, T., Weise, J. M., Damiani, E. and Tiano, L. (**2021**) 'Anti-ageing effects of ubiquinone and ubiquinol in a senescence model of human dermal fibroblasts.' *Free Radical Biology and Medicine*, 165 pp. 282–288.
- Masson, G. R., Burke, J. E., Ahn, N. G., Anand, G. S., Borchers, C., Brier, S., Bou-Assaf, G. M., Engen, J. R., Englander, S. W., Faber, J., Garlish, R., Griffin, P. R., Gross, M. L., Guttman, M., Hamuro, Y., Heck, A. J. R., Houde, D., Iacob, R. E., Jørgensen, T. J. D., Kaltashov, I. A., Klinman, J. P., Konermann, L., Man, P., Mayne, L., Pascal, B. D., Reichmann, D., Skehel, M., Snijder, J., Strutzenberg, T. S., Underbakke, E. S., Wagner, C., Wales, T. E., Walters, B. T., Weis, D. D., Wilson, D. J., Wintrode, P. L., Zhang, Z., Zheng, J., Schriemer, D. C. and Rand, K. D. (**2019**) 'Recommendations for performing, interpreting and reporting hydrogen deuterium exchange mass spectrometry (HDX-MS) experiments.' *Nature Methods 2019 16:7*. Nature Publishing Group, 16(7) pp. 595–602.
- Mistry, P., Najim, N., Purdie, A. and Podmore, I. (**2008**) 'Indirect detection of hydroxyl radicals using spin trapping and gas chromatography-mass spectrometry.' *Journal of Chemical Research*, (7) pp. 395–397.
- Mordi, R. C., Ademosun, O. T., Ajanaku, C. O., Olanrewaju, I. O. and Walton, J. C. (**2020**) 'Free

radical mediated oxidative degradation of carotenes and xanthophylls.' *Molecules*. Multidisciplinary Digital Publishing Institute (MDPI).

- Morrison, C. (**2012**) 'Chromatographic Separations and Analysis: Chiral Gas Chromatography.' *In Comprehensive Chirality*. Elsevier Ltd, pp. 333–353.
- Nelson, K. J., Knutson, S. T., Soito, L., Klomsiri, C., Poole, L. B. and Fetrow, J. S. (**2011**) 'Analysis of the peroxiredoxin family: Using active-site structure and sequence information for global classification and residue analysis.' *Proteins: Structure, Function and Bioinformatics*. Proteins, 79(3) pp. 947–964.
- Nicolussi, A., D'Inzeo, S., Capalbo, C., Giannini, G. and Coppa, A. (**2017**) 'The role of peroxiredoxins in cancer.' *Molecular and Clinical Oncology*, 6(2) pp. 139–153.
- Niki, E. (**2015**) 'Evidence for beneficial effects of vitamin E.' *Korean Journal of Internal Medicine*. Korean Association of Internal Medicine pp. 571–579.
- Nishikawa, T., Edelstein, D., Du, X. L., Yamagishi, S., Matsumura, T., Kaneda, Y., Yorek, M. A., Beebe, D., Oates, P. J., Hammes, H.-P., Giardino, I. and Brownlee, M. (**2000**) 'Normalizing mitochondrial superoxide production blocks three pathways of hyperglycaemic damage.' *Nature*, 404(6779) pp. 787–790.
- O'Brien, P., Siraki, A. and Shangari, N. (**2005**) 'Aldehyde sources, metabolism, molecular toxicity mechanisms, and possible effects on human health.' *Critical Reviews in Toxicology* pp. 609–662.
- Papajak, E., Seal, P., Xu, X. and Truhlar, D. G. (**2012**) 'Thermochemistry of radicals formed by hydrogen abstraction from 1-butanol, 2-methyl-1-propanol, and butanal.' *Journal of Chemical Physics*. American Institute of PhysicsAIP, 137(10) p. 104314.
- Pattison, D. I. and Davies, M. J. (**2006**) 'Actions of ultraviolet light on cellular structures.' *EXS*. Birkhäuser Basel pp. 131–157.
- Phaniendra, A., Jestadi, D. B. and Periyasamy, L. (**2015**) 'Free Radicals: Properties, Sources,

Targets, and Their Implication in Various Diseases.' *Indian Journal of Clinical Biochemistry* pp. 11–26.

- Phillips, M., Cataneo, R. N., Cummin, A. R. C., Gagliardi, A. J., Gleeson, K., Greenberg, J., Maxfield, R. A. and Rom, W. N. (**2003**) 'Detection of lung cancer with volatile markers in the breath.' *Chest*. The American College of Chest Physicians, 123(6) pp. 2115–2123.
- Phillips, M., Gleeson, K., Hughes, J. M. B., Greenberg, J., Cataneo, R. N., Baker, L. and McVay, W. P. (**1999**) 'Volatile organic compounds in breath as markers of lung cancer: A cross-sectional study.' *Lancet*, 353(9168) pp. 1930–1933.
- Reeves Huie, W. (**1987**) 'Nitrone Spin Traps for Biological Studies.' *LSU Historical Dissertations and Theses*, 1(4451).
- Reinke, L. A., Moore, D. R., Sang, H., Janzen, E. G. and Kotake, Y. (**2000**) 'Aromatic hydroxylation in PBN spin trapping by hydroxyl radicals and cytochrome P-450.' *Free Radical Biology and Medicine*. Pergamon, 28(3) pp. 345–350.
- Rinnerthaler, M., Bischof, J., Streubel, M. K., Trost, A. and Richter, K. (**2015**) 'Oxidative stress in aging human skin.' *Biomolecules*, 5(2) pp. 545–589.
- Rösen, P., Nawroth, P. P., King, G., Möller, W., Tritschler, H. J. and Packer, L. (**2001**) 'The role of oxidative stress in the onset and progression of diabetes and its complications: A summary of a congress series sponsored by UNESCO-MCBN, the American diabetes association and the German diabetes society.' *Diabetes/Metabolism Research and Reviews* pp. 189–212.
- Sandmann, G. (**2019**) 'Antioxidant protection from UV-and light-stress related to carotenoid structures.' *Antioxidants*. Multidisciplinary Digital Publishing Institute p. 219.
- Schallschmidt, K., Becker, R., Zwaka, H., Menzel, R., Johnen, D., Fischer-Tenhagen, C., Rolff, J. and Nehls, I. (**2015**) 'In vitro cultured lung cancer cells are not suitable for animal-based breath biomarker detection.' *Journal of Breath Research*, 9(2).

- Schmidt, K. and Podmore, I. (**2015**) 'Current Challenges in Volatile Organic Compounds Analysis as Potential Biomarkers of Cancer.' *Journal of Biomarkers*, 2015 pp. 1–16.
- Schoenmakers, P. J., Oomen, J. L. M. M., Blomberg, J., Genuit, W. and van Velzen, G. (**2000**) 'Comparison of comprehensive two-dimensional gas chromatography and gas chromatography – mass spectrometry for the characterization of complex hydrocarbon mixtures.' *Journal of Chromatography A*. Elsevier, 892(1–2) pp. 29–46.
- Schuppe, H. C., Meinhardt, A., Allam, J. P., Bergmann, M., Weidner, W. and Haidl, G. (**2008**) 'Chronic orchitis: A neglected cause of male infertility?' *Andrologia*. Andrologia, 40(2) pp. 84–91.
- Schurig, V. (**2002**) 'Chiral separations using gas chromatography.' *Trends in Analytical Chemistry*. Elsevier, 21(9–10) pp. 647–661.
- Shoeb, M., Ansari, N., Srivastava, S. and Ramana, K. (**2014**) '4-Hydroxynonenal in the Pathogenesis and Progression of Human Diseases.' *Current Medicinal Chemistry*. Bentham Science Publishers Ltd., 21(2) pp. 230–237.
- Siegel, A. S. (**1970**) 'Rearrangement ions. III. Tropylium ion in the mass spectrum of toluene-2,6-13C2.' *Journal of the American Chemical Society*. Academic Press, 92(17) pp. 5277–5278.
- Sies, H. (**2017**) 'Hydrogen peroxide as a central redox signaling molecule in physiological oxidative stress: Oxidative eustress.' *Redox Biology*. Redox Biol pp. 613–619.
- Song, Y., Tang, L., Han, J., Gao, Y., Tang, B., Shao, M., Yuan, W., Ge, W., Huang, X., Yao, T., Bian, X., Li, S., Cao, W. and Zhang, H. (**2019**) 'Uric Acid Provides Protective Role in Red Blood Cells by Antioxidant Defense: A Hypothetical Analysis.' *Oxidative Medicine and Cellular Longevity*. Hindawi Limited, 2019.
- Stadtman, E. R. (**2006**) 'Protein oxidation and aging.' *Free Radical Research*. Taylor & Francis, 40(12) pp. 1250–1258.
- Stolze, K., Udilova, N., Rosenau, T., Hofinger, A. and Nohl, H. (**2003**) 'Spin trapping of superoxide,

alkyl- and lipid-derived radicals with derivatives of the spin trap EPPN.' *Biochemical Pharmacology*. Elsevier, 66(9) pp. 1717–1726.

- Uchida, K. (**2000**) 'Role of reactive aldehyde in cardiovascular diseases.' *Free Radical Biology and Medicine*, 28(12) pp. 1685–1696.
- Vaks, V. L., Domracheva, E. G., Sobakinskaya, E. A. and Chernyaeva, M. B. (**2014**) 'Exhaled breath analysis: physical methods, instruments and medical diagnostics.' *Uspekhi Fizicheskih Nauk*, 184(7) pp. 739–758.
- Valko, M., Morris, H. and Cronin, M. (**2005**) 'Metals, Toxicity and Oxidative Stress.' *Current Medicinal Chemistry*. Bentham Science Publishers Ltd., 12(10) pp. 1161–1208.
- Vanhees, I., Van den Bergh, V., Schildermans, R., De Boer, R., Compernolle, F. and Vinckier, C. (**2001**) 'Determination of the oxidation products of the reaction between α-pinene and hydroxyl radicals by high-performance liquid chromatography.' *Journal of Chromatography A*. J Chromatogr A, 915(1–2) pp. 75–83.
- De Vietro, N., Aresta, A., Teresa Rotelli, M., Zambonin, C., Lippolis, C., Picciariello, A. and Francesco Altomare, D. (**2020**) 'Relationship between cancer tissue derived and exhaled volatile organic compound from colorectal cancer patients. Preliminary results.' *Journal of Pharmaceutical and Biomedical Analysis*, 180 p. 113055.
- Viskolcz, B., Lendvay, G., Körtvélyesi, T. and Seres, L. (**1996**) 'Intramolecular H atom transfer reactions in alkyl radicals and the ring strain energy in the transition structure.' *Journal of the American Chemical Society*, 118(12) pp. 3006–3009.
- Wang, F., Lei, L. and Wu, L. (**2005**) 'NO spin trapping and EPR studies on the photochemistry of aliphatic aldehydes.' *Magnetic Resonance in Chemistry*, 43(2) pp. 156–165.
- Whitaker, A. M., Schaich, M. A., Smith, M. R., Flynn, T. S. and Freudenthal, B. D. (**2017**) 'Base excision repair of oxidative DNA damage: from mechanism to disease .' *Frontiers In Bioscience*,

22 pp. 1493–1522.

- Winterbourn, C. C. (**1995**) 'Toxicity of iron and hydrogen peroxide: the Fenton reaction.' *Toxicology Letters*, 82–83(C) pp. 969–974.
- Zhong, H. and Yin, H. (**2015**) 'Role of lipid peroxidation derived 4-hydroxynonenal (4-HNE) in cancer: Focusing on mitochondria.' *Redox Biology*. Elsevier, 4(55) pp. 193–199.

Appendix

Miscellaneous peaks

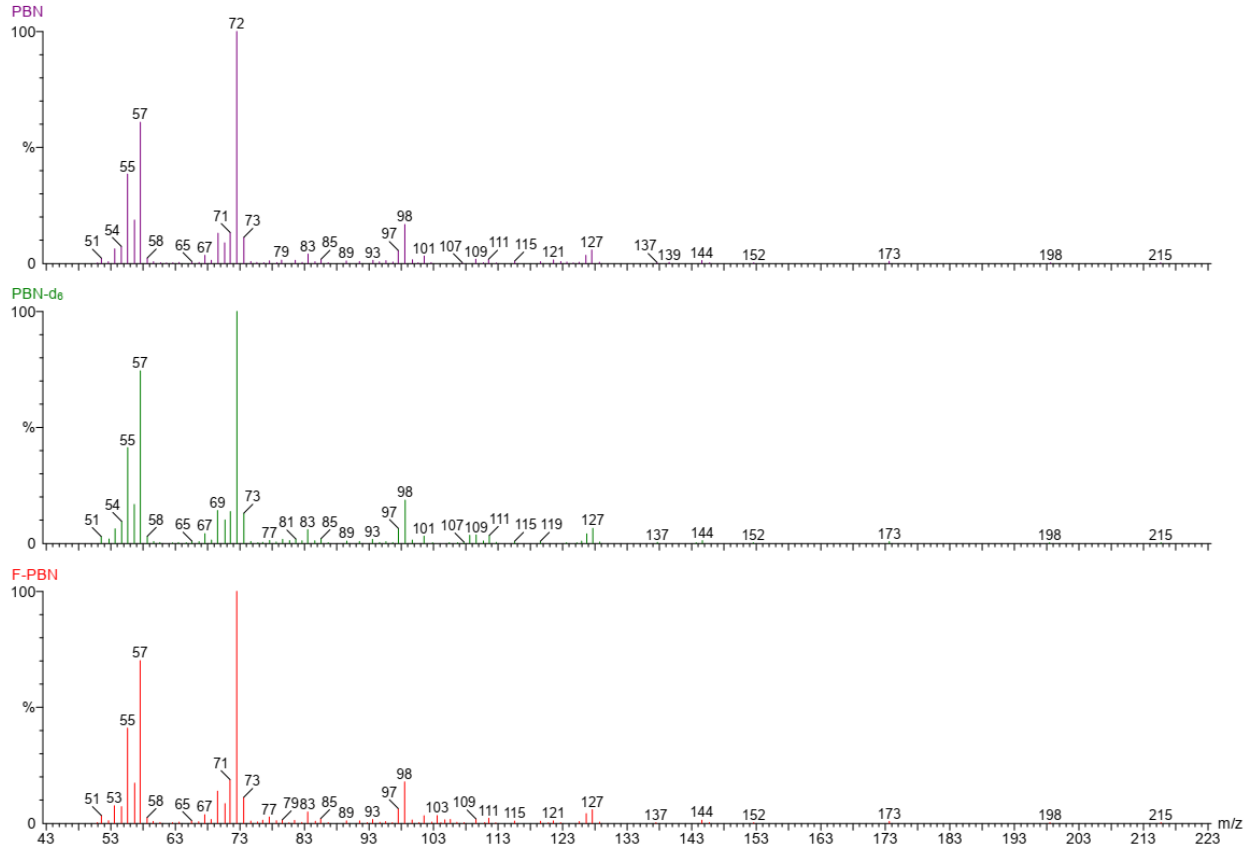

Figure 5.10.1 Electron Ionization mass spectra (EI-MS) corresponding to products obtained from the analysis of the Fenton reaction mixture without iron/EDTA containing PBN (top), PBN-d_6 (middle) and F-PBN (bottom) at rt 6.72 minutes.

The Figure 5.10.1 shows the peak retained at 6.72 minutes for the control reaction without iron/EDTA (Figure 2.7.1).The spectra are identical in their fragmentation patterns. The molecular ion retained is *m/z* 215, and a strong base peak at *m/z* 72 units. This peak has no association with PBN or its derivatives as the molecular ion is the same regardless of the spin trap used. This indicates this may be a product of the degradation of the column or otherwise. It is also noteworthy that peak is retained in many of the TIC analysed in this thesis.

lCompound 9

Fluoro dimethyl adducts

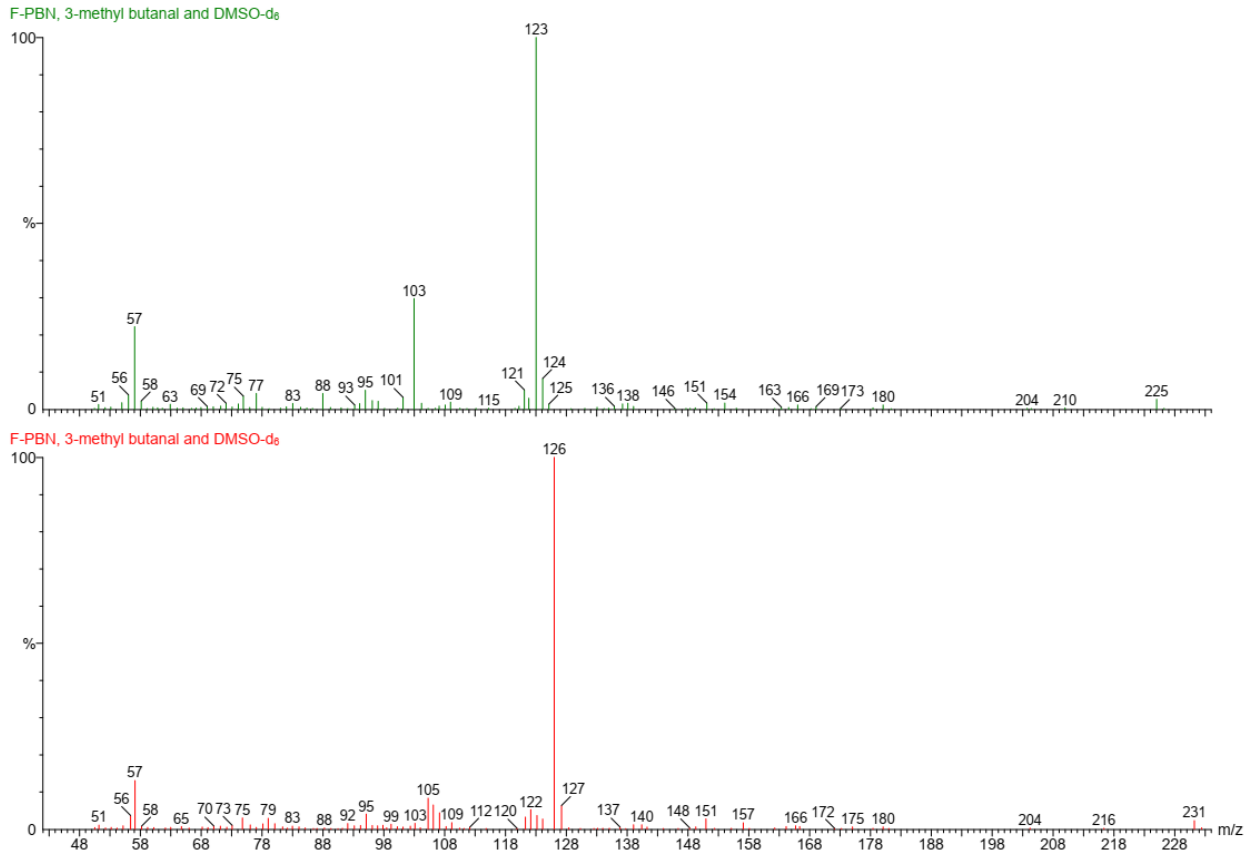

Figure 5.10.2 Electron Ionization mass spectra (EI-MS) corresponding to F-PBN adduct obtained from the analysis of the Fenton reaction mixture containing F-PBN, butanal and DMSO or DMSO-d_6 at rt 5.4 minutes

Compound 10 monomethyl monopropyl adduct of F-PBN with butanal and DMSO

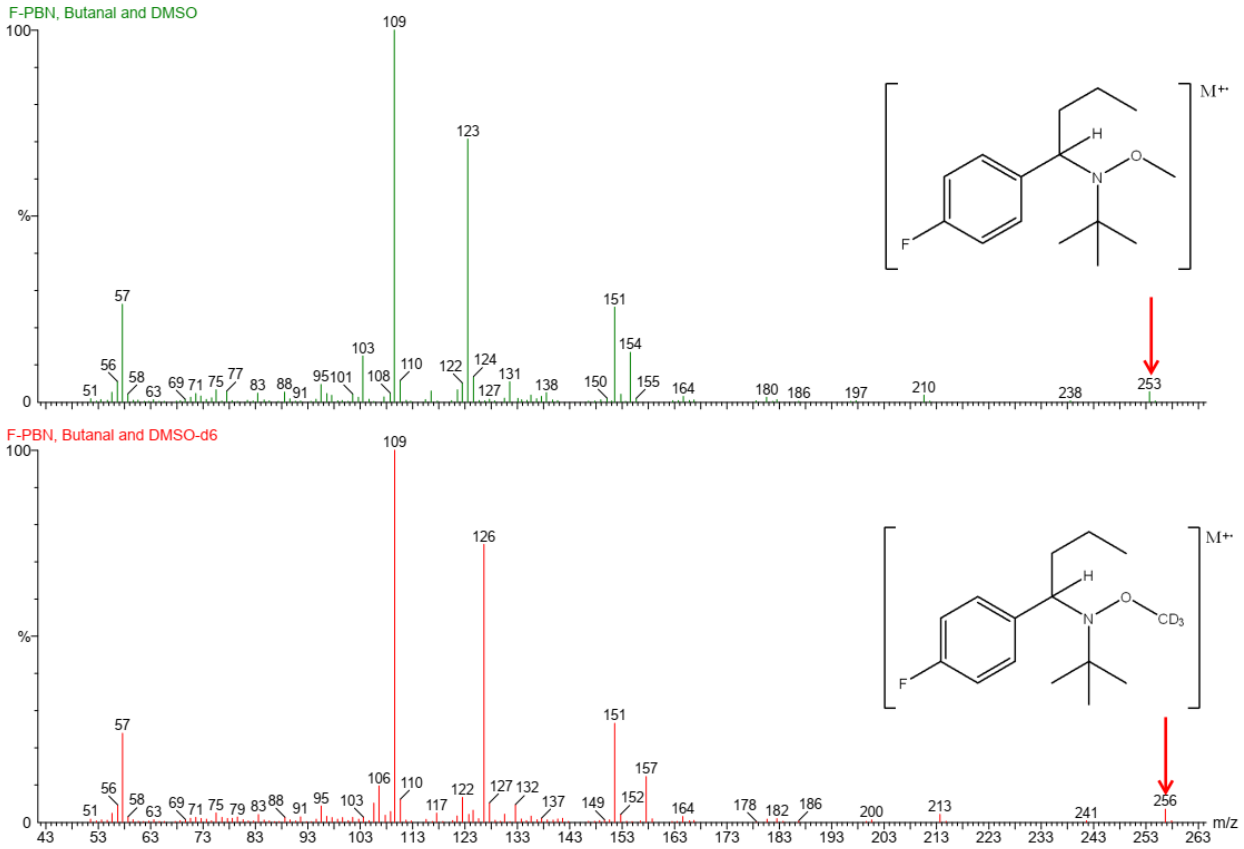

Figure 5.10.3 Electron Ionization mass spectra (EI-MS) corresponding to F-PBN adduct obtained from the analysis of the Fenton reaction mixture containing F-PBN, butanal and DMSO or DMSO-d_6 at rt 7.09 minutes

Compound 10 monomethyl monopropyl adduct of F-PBN with butanal d_2 and DMSO

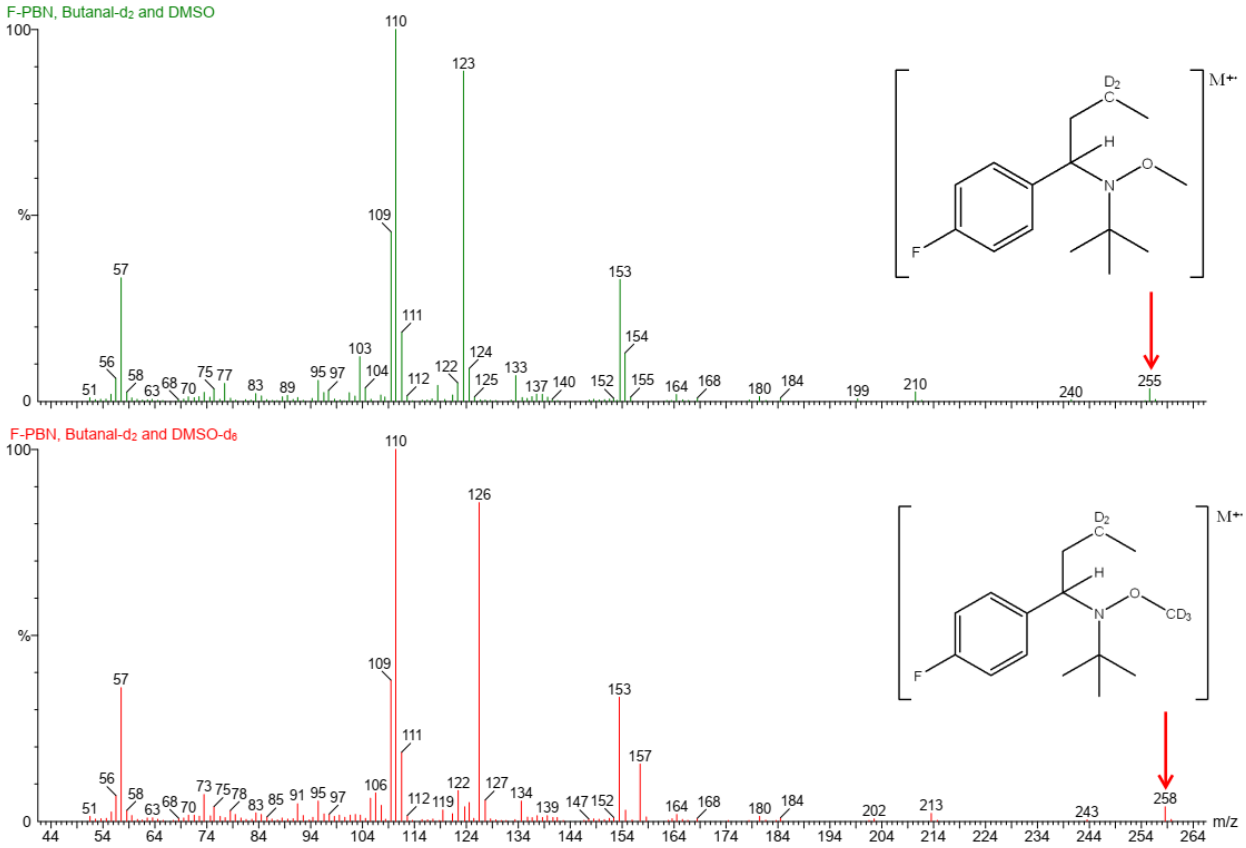

Figure 5.10.4 Electron Ionization mass spectra (EI-MS) corresponding to F-PBN adduct obtained from the analysis of the Fenton reaction mixture containing F-PBN, butanal-d_2 and DMSO or DMSO-d_6 at rt 7.09 minutes

Compound 10 monomethyl monopropyl adduct of F-PBN with butanal d_7 and DMSO

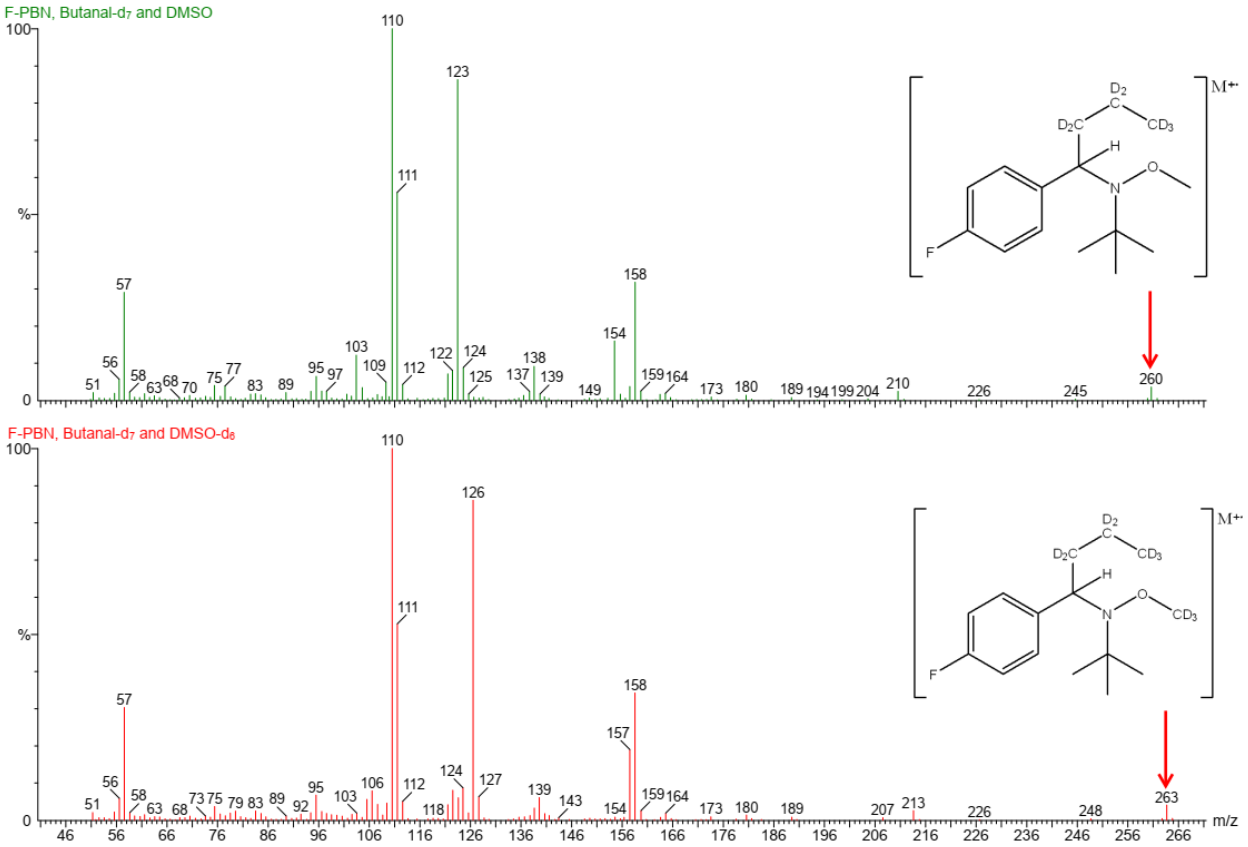

Figure 5.10.5 Electron Ionization mass spectra (EI-MS) corresponding to PBN adduct obtained from the analysis of the Fenton reaction mixture containing F-PBN, butanal-d_7 and DMSO or DMSO-d_6 at rt 7.09 minutes

Compound 11 Monopropyl monomethyl adduct of F-PBN with butanal and DMSO

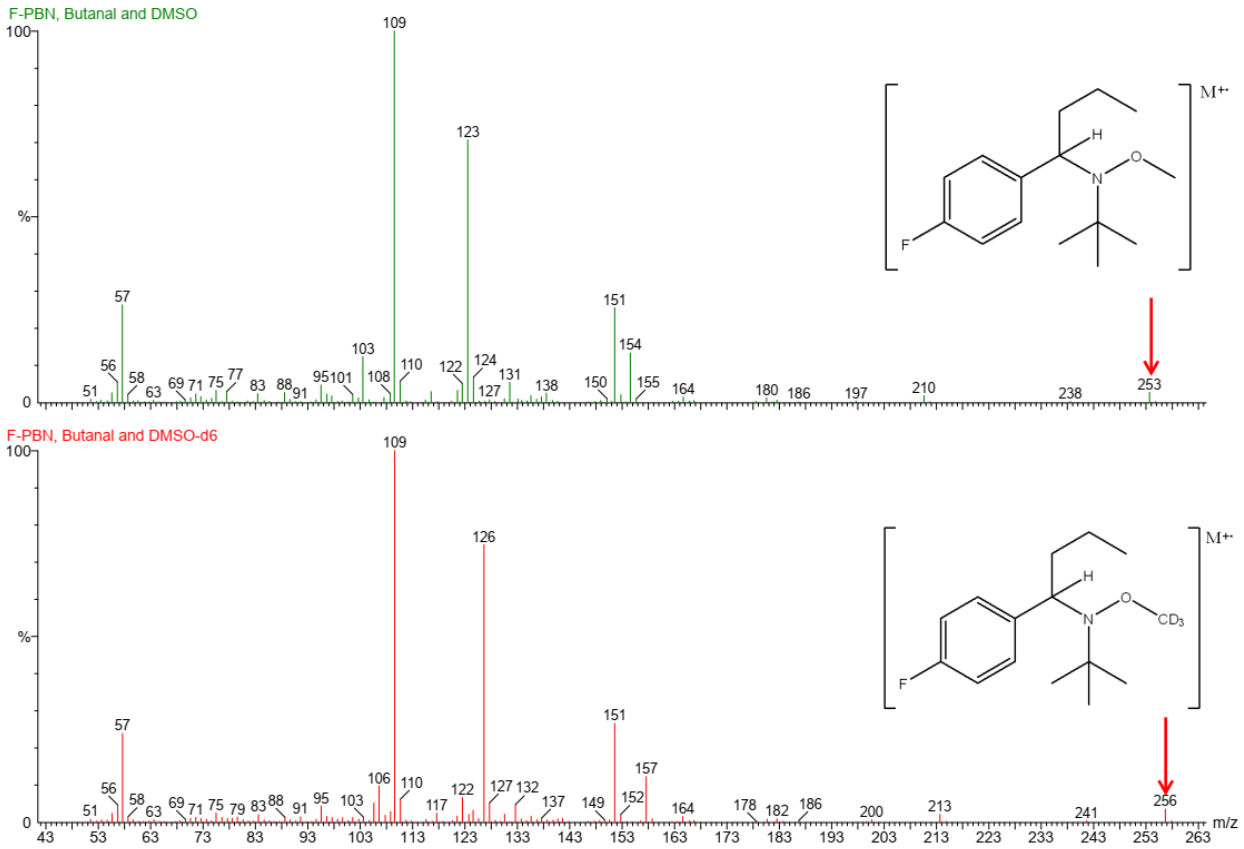

Figure 5.10.6 Electron Ionization mass spectra (EI-MS) corresponding to PBN adduct obtained from the analysis of the Fenton reaction mixture containing F-PBN, butanal and DMSO or DMSO-d_6 at rt 7.09 minutes

Compound 11 Monopropyl monomethyl adduct of F-PBN with butanal d_2 and DMSO

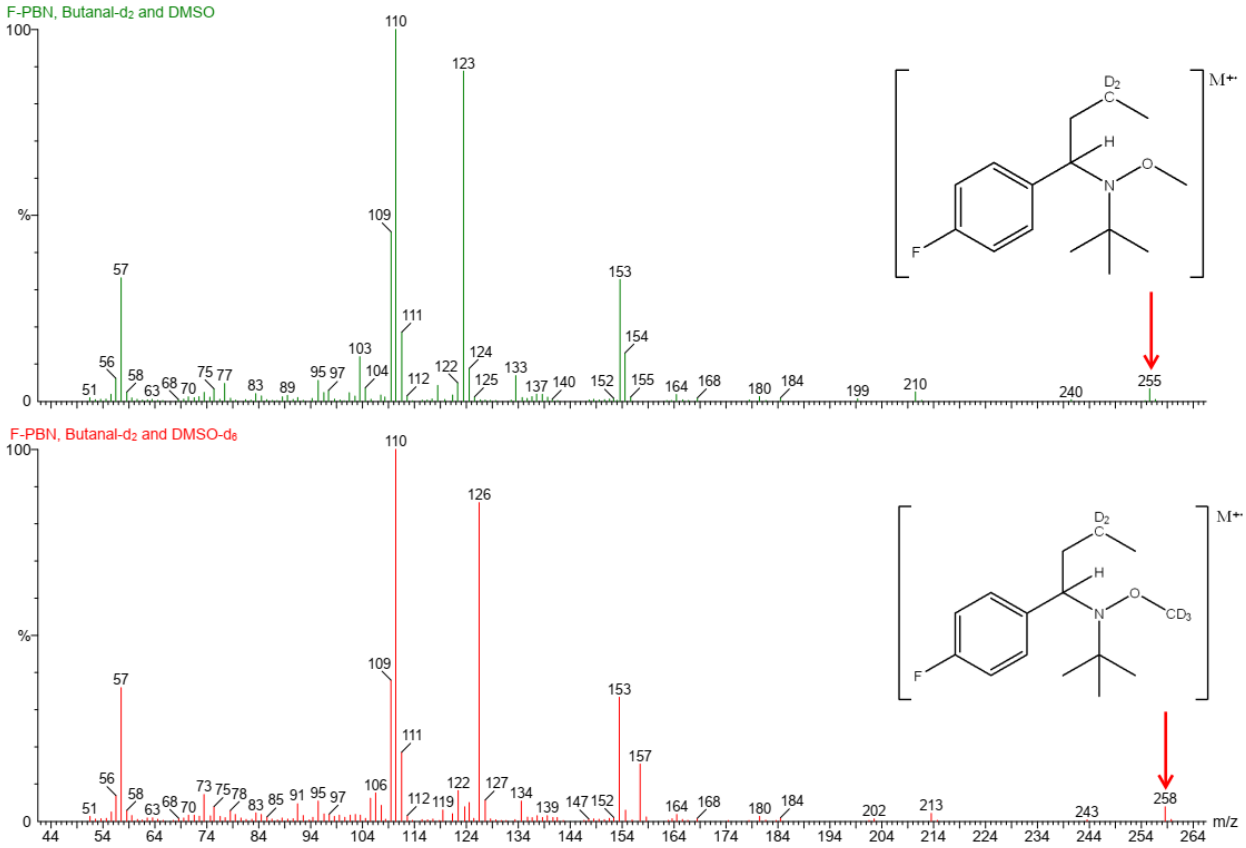

Figure 5.10.7 Electron Ionization mass spectra (EI-MS) corresponding to PBN adduct obtained from the analysis of the Fenton reaction mixture containing F-PBN, butanal-d_2 and DMSO or DMSO-d_6 at rt 7.09 minutes

Compound 11 Monopropyl monomethyl adduct of F-PBN with butanal d_7 and DMSO

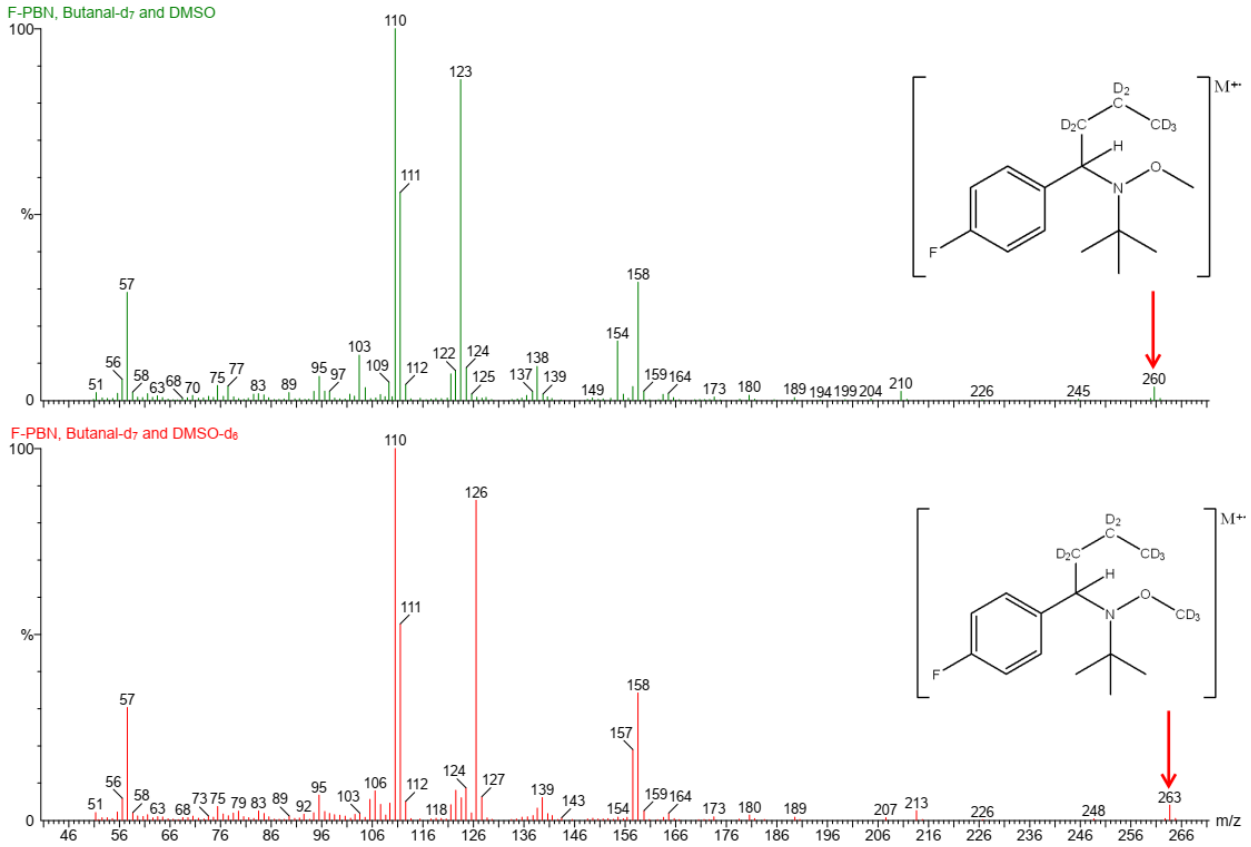

Figure 5.10.8 Electron Ionization mass spectra (EI-MS) corresponding to PBN adduct obtained from the analysis of the Fenton reaction mixture containing F-PBN, butanal-d_7 and DMSO or DMSO-d_6 at rt 7.09 minutes

compound 12 Mono oxybutyl monomethyl adduct of F-PBN with butanal and DMSO

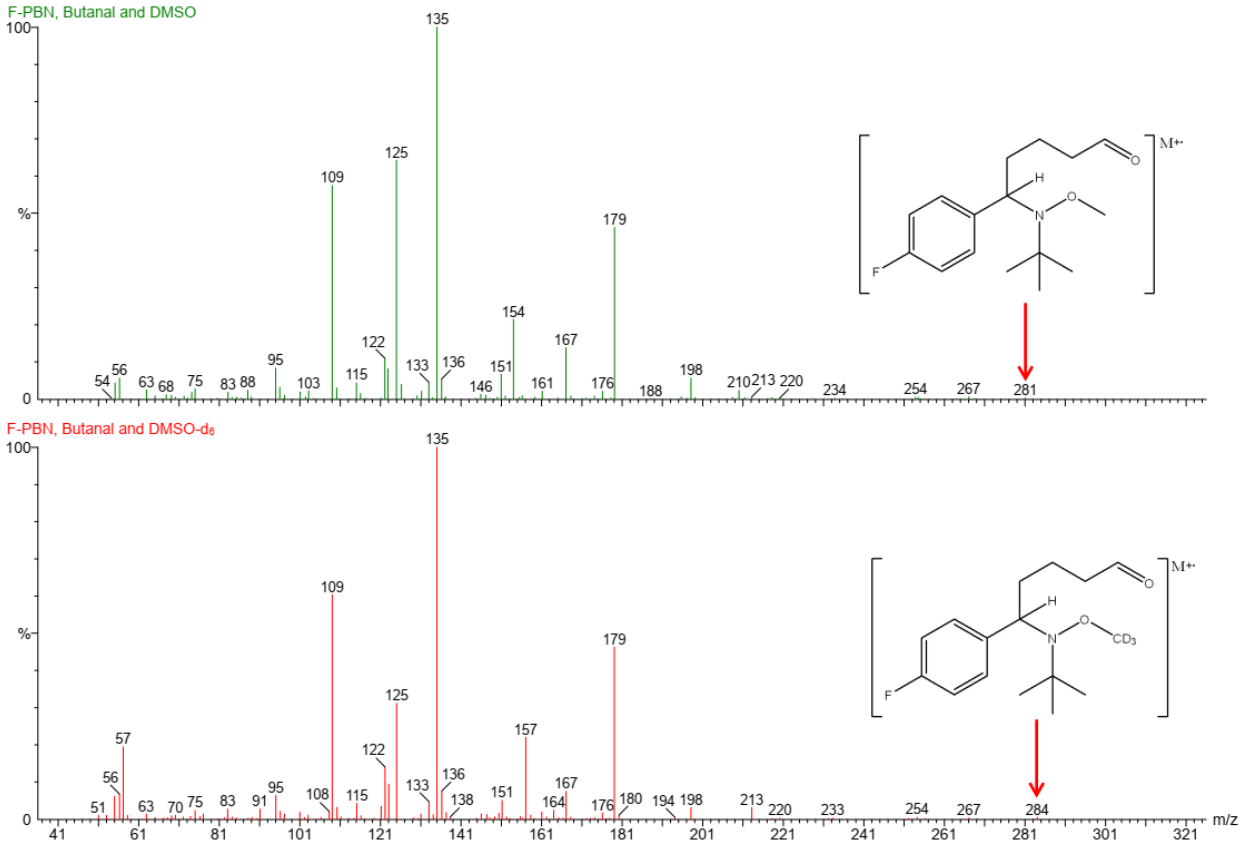

Figure 5.10.9 Electron Ionization mass spectra (EI-MS) corresponding to PBN adduct obtained from the analysis of the Fenton reaction mixture containing F-PBN, butanal and DMSO or DMSO-d_6 at rt 10.47 minutes

Compound 12 Mono oxybutyl monomethyl adduct of F-PBN with butanal-d_2 and DMSO

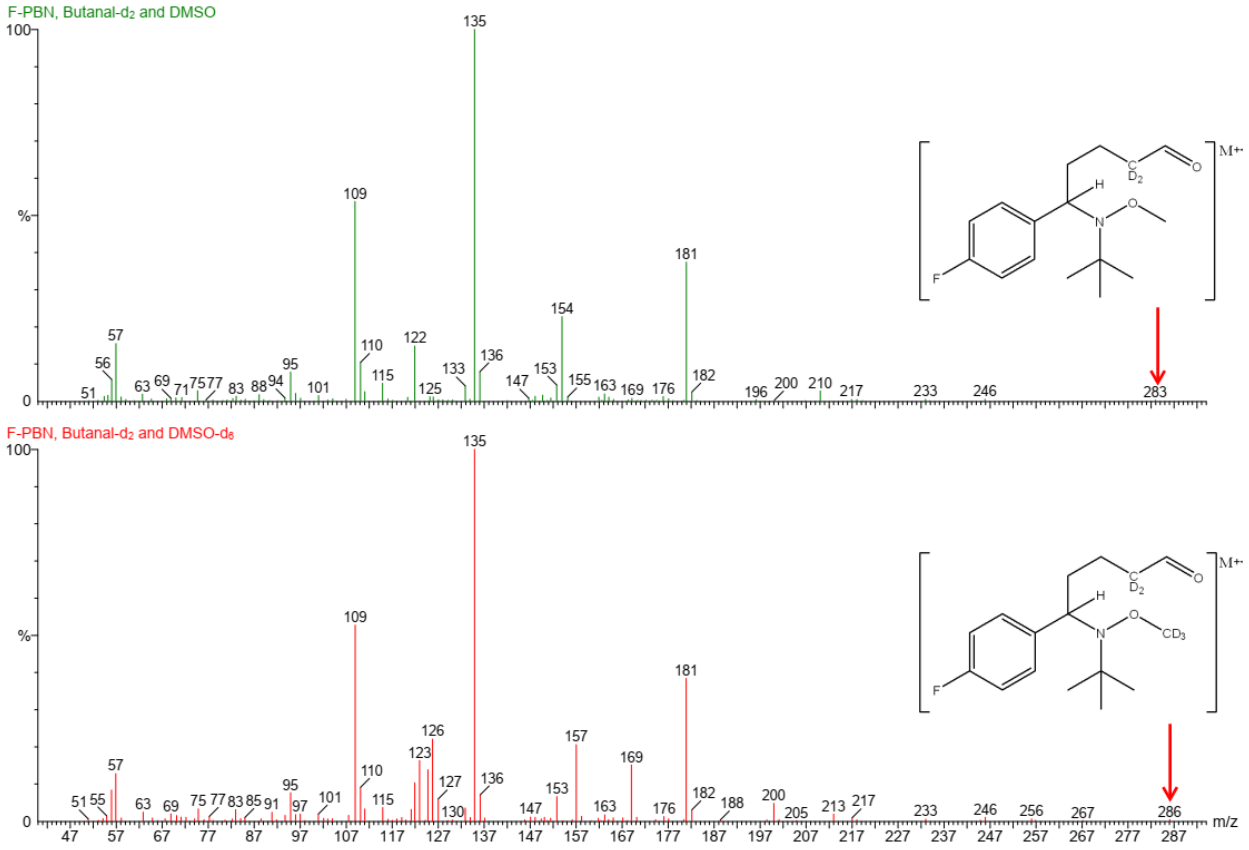

Figure 5.10.10 Electron Ionization mass spectra (EI-MS) corresponding to PBN adduct obtained from the analysis of the Fenton reaction mixture containing F-PBN, butanal-d_2 and DMSO or DMSO-d_6 at rt 10.47 minutes

Compound 12 Mono oxybutyl monomethyl adduct of F-PBN with butanal-d_7 and DMSO

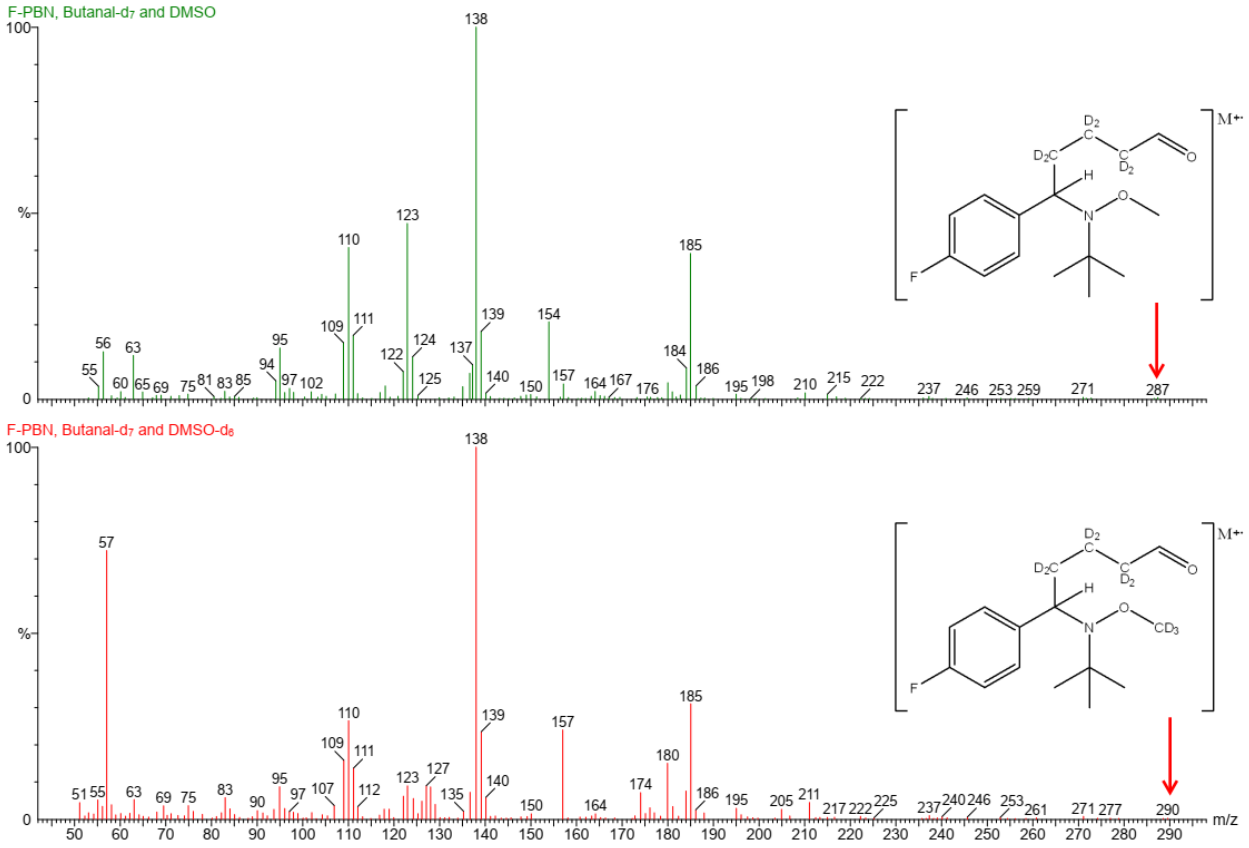

Figure 5.10.11 Electron Ionization mass spectra (EI-MS) corresponding to PBN adduct obtained from the analysis of the Fenton reaction mixture containing F-PBN, butanal-d_7 and DMSO or DMSO-d_6 at rt 10.47 minutes

Compound 18 Mono-2-methyl propyl monomethyl adduct of F-PBN with 3-methylbutanal and DMSO

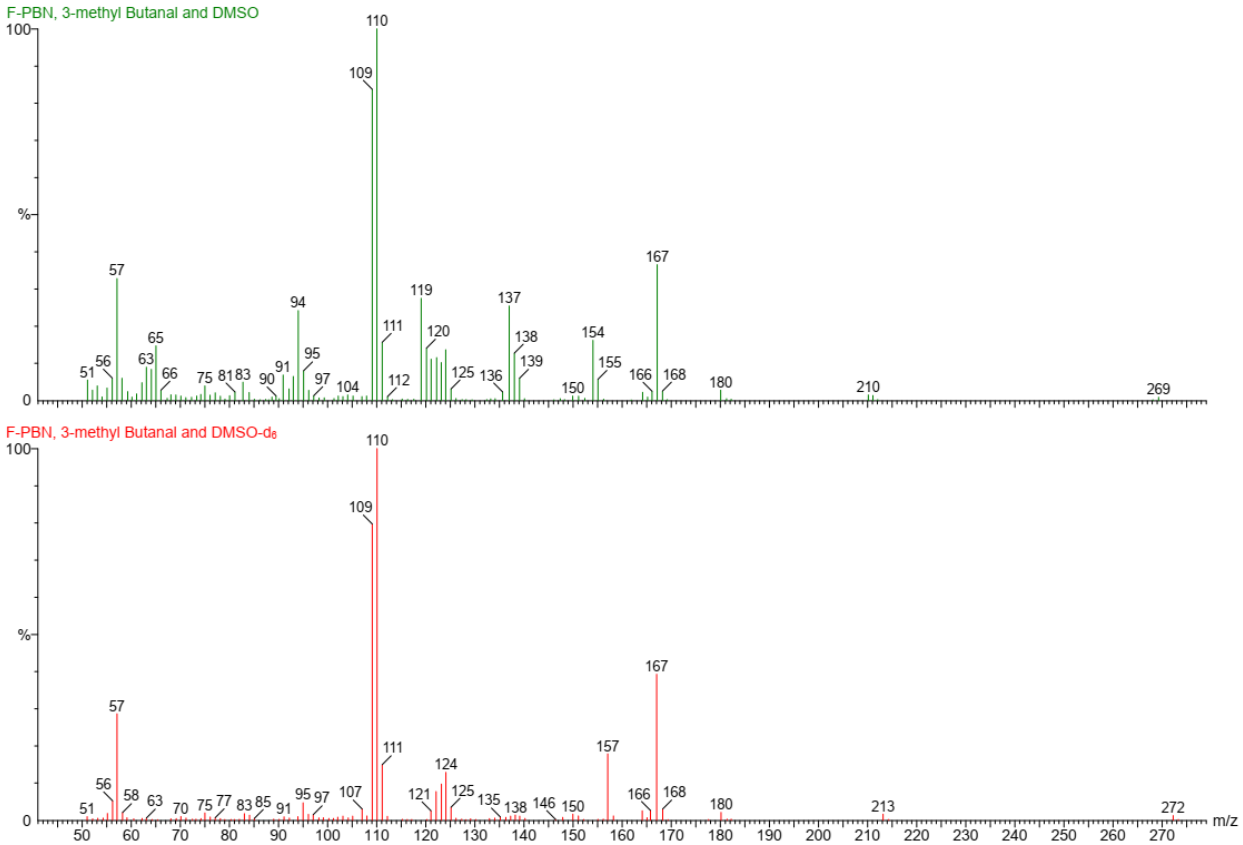

Figure 5.10.12 Electron Ionization mass spectra (EI-MS) corresponding to F-PBN adduct obtained from the analysis of the Fenton reaction mixture containing PBN, 3-methylbutanal and DMSO or DMSO-d_6 at rt 7.46 minutes

Compound 18 Mono-2-methyl propyl monomethyl adduct of F-PBN with 3-methylbutanal-d_2 and DMSO

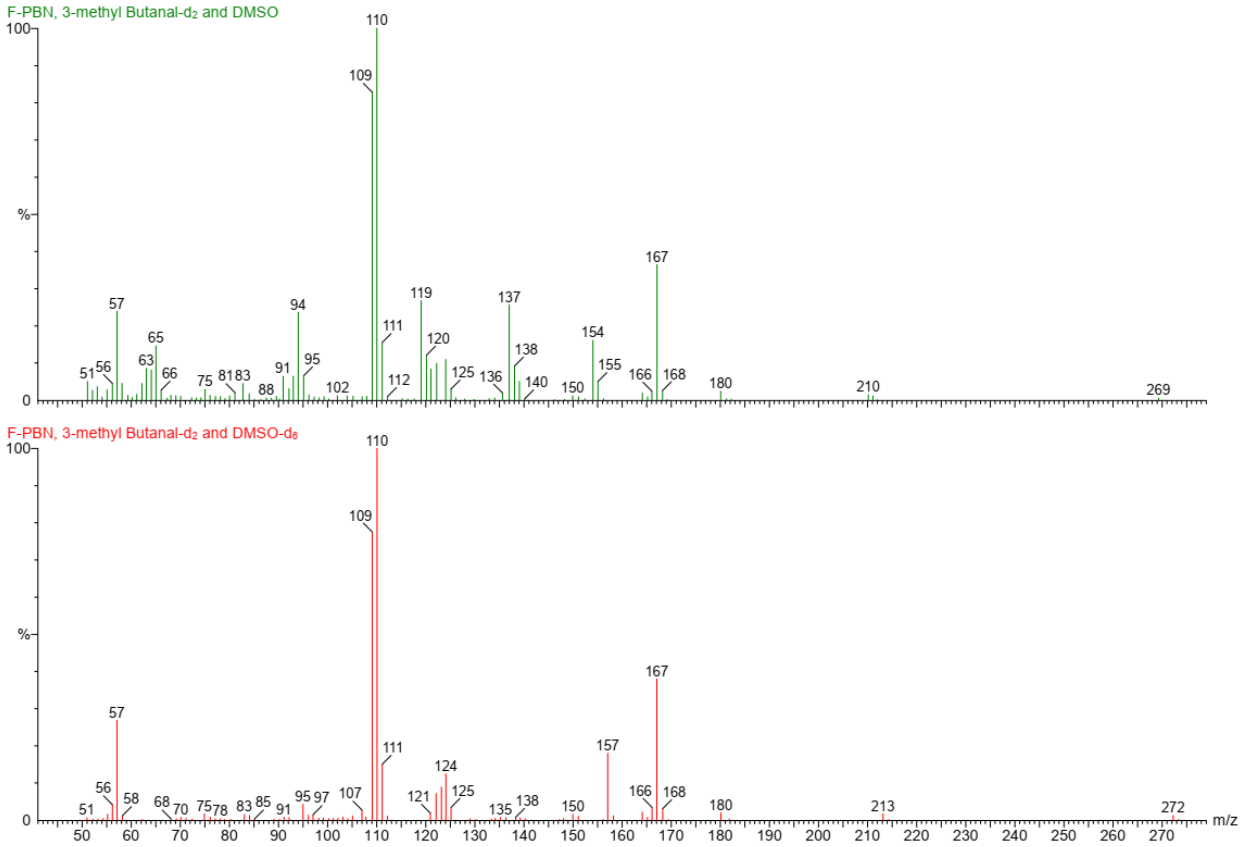

Figure 5.10.13 Electron Ionization mass spectra (EI-MS) corresponding to F-PBN adduct obtained from the analysis of the Fenton reaction mixture containing PBN, 3-methylbutanal-d_2 and DMSO or DMSO-d_6 at rt 7.46 minutes

compound 19 Methyl radical and 2-methyl propyl adduct of F-PBN with 3-methylbutanal and DMSO

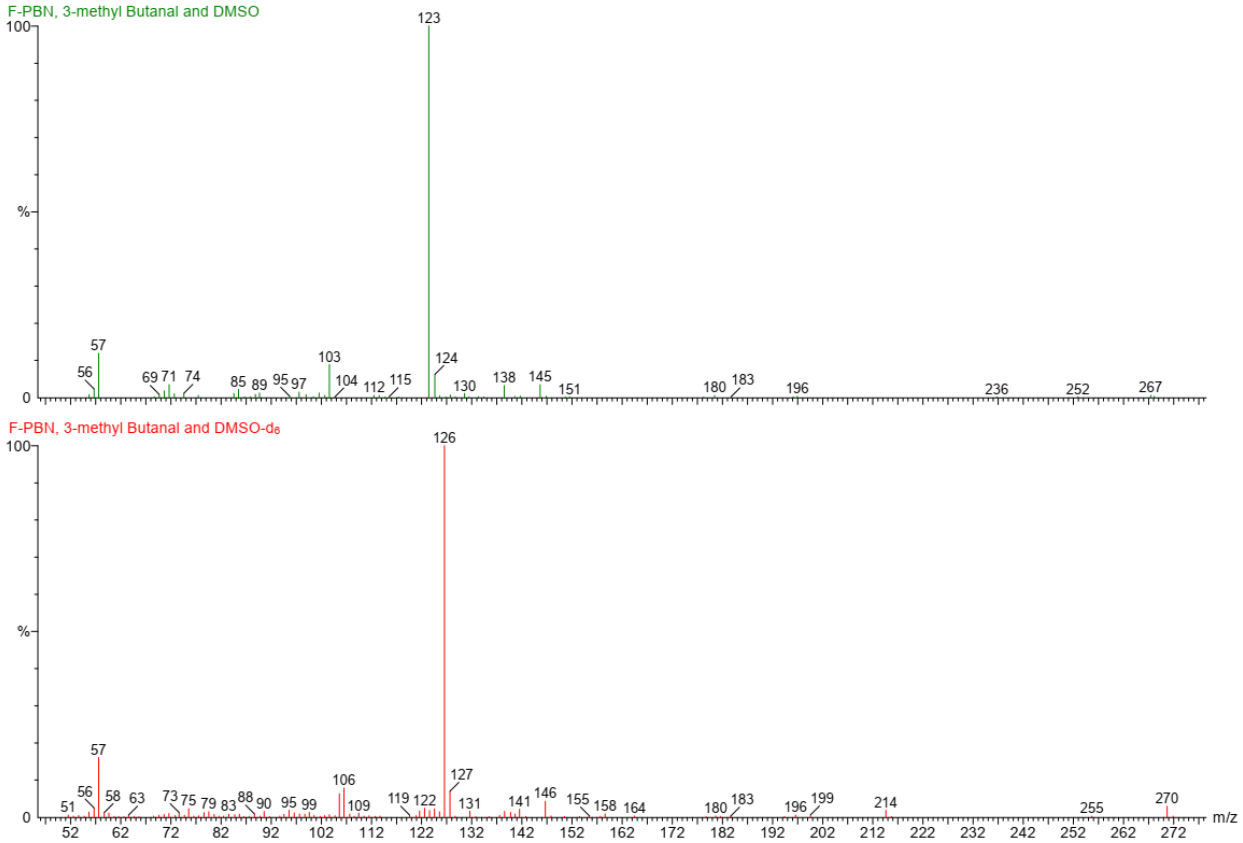

Figure 5.10.14 Electron Ionization mass spectra (EI-MS) corresponding to F-PBN adduct obtained from the analysis of the Fenton reaction mixture containing PBN, 3-methylbutanal and DMSO or DMSO-d_6 at rt 7.66 minutes

Compound 19 Methyl radical and 2-methyl propyl adduct of F-PBN with 3-methylbutanal-d_2 and DMSO

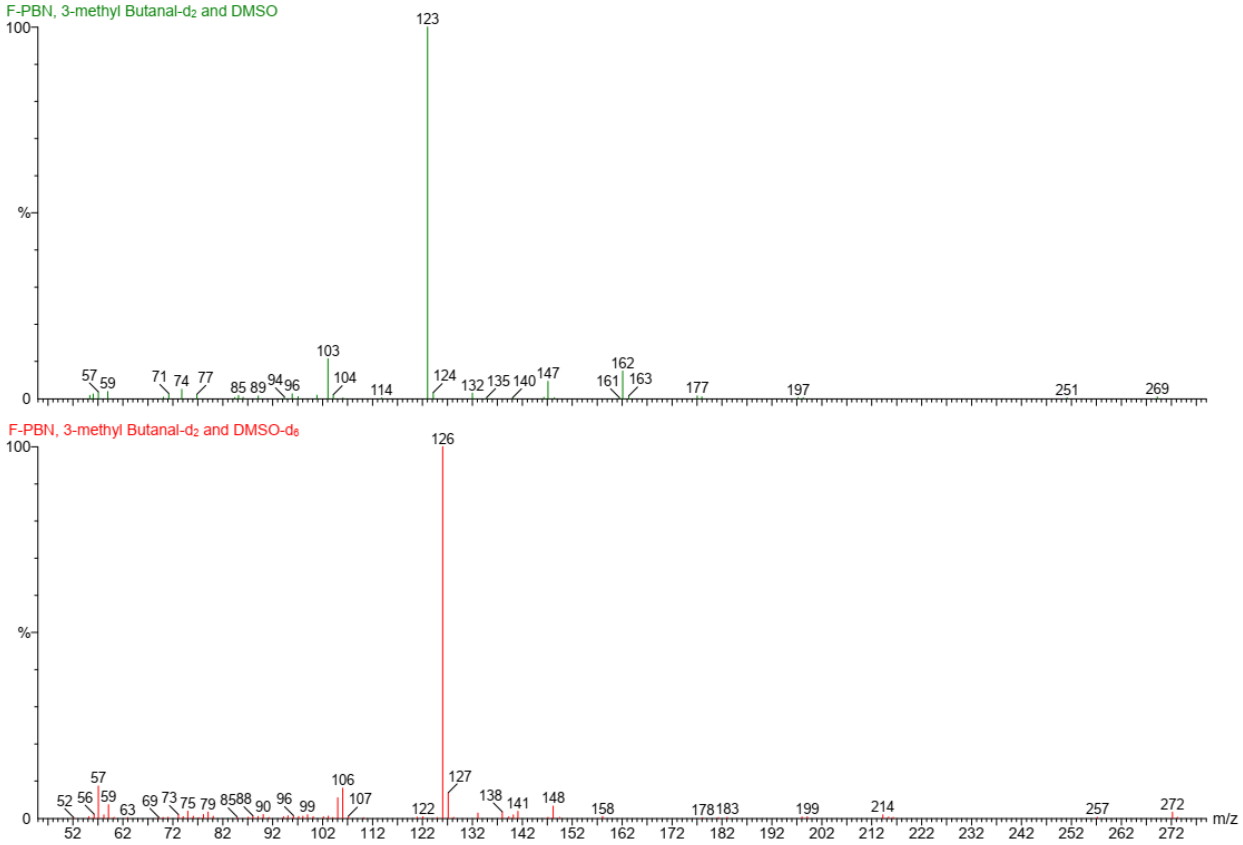

Figure 5.10.15 Electron Ionization mass spectra (EI-MS) corresponding to F-PBN adduct obtained from the analysis of the Fenton reaction mixture containing PBN, 3-methylbutanal and DMSO or DMSO-d_6 at rt 7.66 minutes